Synthetic studies toward the four invariant stereogenic centres of the left side of the backbone of the fumonisins and AAL toxins

by

STEPHEN THOMPSON

Submitted in partial fulfilment of the requirements for the degree

MAGISTER SCIENTIAE

In the Faculty of Natural & Agricultural Sciences

UNIVERSITY OF PRETORIA

PRETORIA

Supervisor: Prof. R. Vleggaar

September 2011

DECLARATION

I, Stephen Thompson, declare that this dissertation, which I hereby submit for the degree Magister Scientiae at the University of Pretoria is my own work and has not been previously submitted by me for a degree at this or any other tertiary institution.

Signature: ……. Date: …….

ACKNOWLEDGEMENTS

I would like to express my thanks to the following people, for their help, guidance and assistance throughout this project:

My supervisor, **Professor Robert Vleggaar**, thank you for your continuous assistance and guidance. I have learned so much from you over the past three years. Your mentorship will always be remembered and greatly valued.

To my family, thank you for always being there to assist me when I needed it most. You were a pillar of strength throughout my studies. I will always appreciate what you have done for me.

To **Eric Palmer**, thanks you for always being willing to run NMR samples, but more than that, thank you for being a great friend and mentor. Our long conversations will always be fondly remembered.

Thank you to the rest of the Organic group over the past two years: **Karl, Samson, Cara, Chantal, René, Marion, Hanlie, Reinardt** and **Rohen** – you will forever be friends, and it was you who often assisted during the most trying times.

Finally, I would like to thank the **University of Pretoria** and the **National Research Foundation** for financial assistance throughout this project.

SUMMARY

The fumonisins are a class of polyketide mycotoxins produced by *Fusarium verticilliodes* (formerly *Fusarium monoliforme*) which commonly affects maize. Ingestion of these toxins has been associated with leukoencephalomalacia in equine species, pulmonary oedema in swine, hepatocarcinogenesis in rats and have been linked to oesophageal cancer in humans. The structurally related AAL toxins are host specific mycotoxins produced by *Alternaria alternata* f. sp. *lycopersici*, producing stem canker disease in susceptible tomato cultivars.

Examination of the C-11–C-20 fragment of the fumonisin B_1 backbone [(2*S*,3*S*,5*R*,10*R*,12*S*,14*S*, 15*R*,16*R*)-2-amino-3,5,10,14,15-hydroxy-12,16-dimethyleicosane] and the C-10–C-17 fragment of the AAL toxin TA backbone [(2*S*,4*S*,5*R*,11*S*,13*S*,14*R*,15*R*)-1-amino-2,4,5,13,14-hydroxy-11,15-dimethylheptadecane], reveals four common stereogenic centres, with the only difference between the two fragments being the length of the alkyl chain. It is thought that the position and configuration of these four stereogenic centres is conserved among all members of the fumonisin and AAL classes of toxins. Retrosynthetic analysis of the backbones reveals a common intermediate aldehyde, which can be synthesised from methyl (*S*)-3-hydroxy-2-methylpropionate. A simple synthetic route to access the C-11–C-20 fragment for the fumonisins and the C-10–C-17 fragment of the AAL toxins was devised utilising Sharpless asymmetric epoxidation and an Evans aldol reaction as key transformations.

In practice, it was found that although the Sharpless asymmetric epoxidation produced the desired epoxide in low enantiomeric excess, the two diastereomers produced could be separated by two consecutive flash chromatography silica gel columns. In pursuit of a more efficient method for introduction of the stereogenic centre in the target, other synthetic routes and key transformations were considered. Jacobsen's kinetic resolution of terminal racemic epoxides was explored, requiring a terminal alkene from which the racemic epoxide was synthesised. An attempt to synthesise the terminal alkene from the appropriate tosylate and vinyl-MgBr, mediated by copper (I) iodide, failed. The synthetic route was redesigned, and the terminal alkene was synthesised by two one-carbon additions: the first a nucleophilic substitution with cyanide, and the second a Wittig olefination. The resolution of the terminal epoxide was also unsuccessful with no significant kinetic resolution occurring. Sharpless asymmetric dihydroxylation was also investigated; however, this reaction too failed to produce products of high diastereomeric excess. As a consequence, it was decided to pursue the asymmetric epoxidation route as the diastereomeric products could at least be separated.

The second key transformation, the Evans aldol reaction, also provided an interesting result. When the aldol reaction was attempted with benzaldehyde and enolates derived from (4*R*,5*S*)-3-butanoyl-4-methyl-5-phenyl-oxazolidin-2-one and (4*R*,5*S*)-3-hexanoyl-4-methyl-5-phenyl-oxazolidin-2-one, the

butanoyl derivative was found to give the expected Evans *syn* product, while the hexanoyl derivative was found to give the non-Evans *syn* product, with proof provided by single crystal X-ray diffraction analysis. It is proposed that the aldol reaction with the hexanoyl derivative does not proceed through the expected Zimmerman-Traxler-type transition state, but rather through an open chain transition state similar to that seen for asymmetric alkylation reactions. Synthesis of the pentanoyl derivative, and subjecting it to the same aldol reaction gave the expected *syn* Evans product, as deduced from spectroscopic properties.

When the aldol reaction was attempted with the appropriate aldehyde intermediate, it was found that the dibutylboron triflate in the reaction medium caused the cleavage of the *O*-TBS ether protection, resulting in the formation of (3*S*,5*R*)-3-(4-methoxybenzyloxy)-5-methyl-tetrahydropyran-2-ol, before the aldehyde could undergo the aldol reaction. In order to avoid this problem, it is suggested that an alternative protecting group strategy using a more robust protecting group, such as a benzyl group which is stable to Lewis acids, could be substituted for the *O*-TBS group.

LIST OF ABBREVIATIONS

AIBN	Azobisisobutyronitrile
9-BBN	9-Borabicyclo(3.3.1)nonane
BH_3.DMS	Borane-dimethyl sulfide complex
COSY	Correlation spectroscopy
CSA	Camphorsulfonic acid
DCM	Dichloromethane
DEAD	Diethyl azodicarboxylate
DET	Diethyl tartrate
DHQ	Dihydroquinine
DHQD	Dihydroquinidine
$(DHQ)_2PHAL$	Dihydroquinine 1,4-phthalazinediyl diether
$(DHQ)_2PYR$	Dihydroquinine 2,5-diphenyl-4,6-pyrimidinediyl diether
DIAD	Diisopropyl azodicarboxylate
DIBALH	Diisobutylaluminium hydride
DIPT	Diisopropyl tartrate
DMAP	4-Dimethylaminopyridine
DMF	Dimethylformamide
DMSO	Dimethyl sulfoxide
EDCI	1-Ethyl-3-(3-dimethylaminopropyl)carbodiimide
EI-IT-MS	Electron impact ion trap mass spectrometry
ESI-IT-MS	Electrospray ionization ion trap mass spectrometry
ESI-TOF-MS	Electrospray ionization time-of-flight mass spectrometry
$Eu(hfc)_3$	Europium tris[3-(heptafluoropropylhydroxymethylene)-(+)-camphorate]
$Eu(fod)_3$	Europium tris(1,1,1,2,2,3,3-heptafluoro-7,7-dimethyl-4,6-octanedionate)
HETCOR	Heteronuclear correlation spectroscopy
HO	Higher order
HPLC	High performance liquid chromatography
HSQC	Heteronuclear single-quantum correlation spectroscopy
HWE	Horner-Wadsworth-Emmons
IBX	2-Iodoxybenzoic acid
Icp_2B-allyl	*B*-allyldiisopinocampheylborane
IR	Infrared
LAH	Lithium aluminium hydride
LEM	Leucoencephalomalacia
LiHDMS	Lithium bis(trimethylsilyl)amide
MCPBA	*meta*-Chloroperbenzoic acid
MS	Mass spectrometry
NMO	*N*-morpholine oxide
NMR	Nuclear magnetic resonance

NOE	Nuclear Overhauser effect
PMB	*p*-Methoxybenzyl
PMP	*p*-Methoxyphenyl
PPL	Porcine pancreatic lipase
PPTS	Pyridinium *p*-toluenesulfonate
Red-Al	Sodium bis(2-methoxyethoxy)aluminumhydride
RP-HPLC	Reversed phase high performance liquid chromatography
SAE	Sharpless asymmetric epoxidation
SAR	Structure-activity relationship
TBAF	Tetrabutylammonium fluoride
TBAI	Tetrabutylammonium iodide
TBDPS	*tert*-Butyldiphenylsilyl
TBDPSCl	*tert*-Butyldiphenylsilyl chloride
TBHP	*tert*-Butylhydroperoxide
TBS	*tert*-Butyldimethylsilyl
TBSCl	*tert*-Butyldimethylsilyl chloride
TCA	Tricarballylic acid
TFA	Trifluoroacetic acid
THF	Tetrahydrofuran
TIPSCl	Triisopropylsilyl chloride
TLC	Thin layer chromatography
$TMSCHN_2$	Trimethylsislyldiazomethane
TMSOTf	Trimethylsilyl triflate
(*R*)-Tol-BINAP	(*R*)-2,2′-Bis(di-p-tolylphosphino)-1,1′-binaphthyl
$VO(acac)_2$	Vanadyl acetylacetonate
XRD	X-ray diffraction

TABLE OF CONTENTS

1. INTRODUCTION……..……..……..1

1.1. The Fumonisins……3

1.1.1. Discovery and Structure Elucidation……...……...3

1.1.2. Synthetic Studies……...…16

1.1.3. Biological Effects ……..…….....25

1.1.4. Biosynthesis…….……..……..……32

1.2. The AAL Toxins…….……..……..……34

1.2.1. Discovery and Structure Elucidation…….……..……34

1.2.2. Synthetic Studies…….……..……..…37

1.2.3. Biological Effects……..……..……...…...40

1.3. Conclusion……..……..……...…..41

2. RETROSYNTHESIS ……...……43

2.1. Retrosynthetic Analysis of Fumonisins ……...……44

2.1.1. Disconnection of the Tricarballylic Fragment and Backbone…….……44

2.1.2. Retrosynthetic Analysis of the Left Synthon……..…….……..……45

2.2. Retrosynthetic Analysis of AAL-Toxins……..……..…….....…48

2.2.1. Disconnection of the Tricarballylic Acid Fragment and Backbone……..…..…48

2.2.1. Retrosynthetic Analysis of the Left Synthon……..……...…49

3. SYNTHETIC DISCUSSION……,,,,,……..…50

3.1. Protecting Group Strategy……..……..…..50

3.1.1. Silyl Ethers…….……..……..……..…52

3.1.2. Benzylidene Acetal Derivatives…….……..……..…...54

3.1.3. Benzyl Ethers……..……..……..…55

3.2. Sharpless Asymmetric Epoxidation Route……..……..……..57

3.2.1. Theoretical Aspects…….……..……..……..57

3.2.2. Experimental Aspects……62

3.3. Vinyl Addition Route……69

3.3.1. Theoretical Aspects……69

3.3.2. Experimental Aspects……73

3.3.3. Alternative Experimental Approach……75

3.4. Jacobsen Route……77

3.4.1. Theoretical Aspects……77

3.4.2. Experimental Aspects……82

3.5. Sharpless Asymmetric Dihydroxylation Route……84

3.5.1. Theoretical Aspects……84

3.5.2. Experimental Aspects……88

3.6. Evans Auxiliary Route……91

3.6.1. Theoretical Aspects……91

3.6.2. Experimental Aspects……95

3.7. Future Work……104

4. EXPERIMENTAL……107

4.1. General……107

4.2. Preparation of Reagents……108

4.2.1. Visualising Reagents……108

Ammonium heptamolybdate……108

Anisaldehyde – sulfuric acid……108

Ceric sulfate – sulfuric acid……108

4.2.2. General Reagents……108

Methyltriphenylphosphonium iodide……108

Ethyl diisopropylphosphonoacetate……109

Anisaldehyde dimethylacetal……109

(4*R*,5*S*)-4-Methyl-5-phenyl-oxazolidin-2-one (**125**)……109

(4*R*,5*S*)-3-Butanoyl-4-methyl-5-phenyl-oxazolidin-2-one (**145**)……110

(4*R*,5*S*)-4-Methyl-3-pentanoyl-5-phenyl-oxazolidin-2-one (**259**)……111

(4*R*,5*S*)-3-Hexanoyl-4-methyl-5-phenyl-oxazolidin-2-one (**123**)……112

4.3. Procedures……113

4.3.1. Sharpless Asymmetric Epoxidation Route……113

Methyl (*S*)-3-(*tert*-Butyldimethylsilanyloxy)-2-methylpropionate (**148**) ……113

(*R*)-3-(*tert*-Butyldimethylsilanyloxy)-2-methylpropan-1-ol (**149**)……114

(*S*)-3-(*tert*-Butyldimethylsilanyloxy)-2-methylpropanal (**150**)……114

Ethyl (2*E*,4*R*)-5-(*tert*-butyldimethylsilanyloxy)-4-methylpent-2-enoate (**151**)……115

(2*E*,4*R*)-5-(*tert*-Butyldimethylsilanyloxy)-4-methylpent-2-en-1-ol (**152**)……116

(2*R*,3*R*,4*S*)-5-(*tert*-Butyldimethylsilanyloxy)-2,3-epoxy-4-methylpentan-1-ol (**153**)... 116

(2*RS*,3*RS*)-5-(*tert*-Butyldimethylsilanyloxy)-2,3-epoxy-4-methylpentan-1-ol (**153**)….117

4.3.2. Vinyl Addition Route……118

(*S*)-3-(*tert*-Butyldimethylsilanyloxy)-2-methylpropan-1-ol tosylate (**185**)..……118

(*S*)-3-(*tert*-Butyldimethylsilanyloxy)-1-iodo-2-methylpropane (**187**)……119

4.3.3. Jacobsen Route……119

Methyl (*S*)-3-benzyloxy-2-methylpropionate (**201**)……119

(*R*)-3-Benzyloxy-2-methylpropan-1-ol (**202**)……120

(*S*)-3-Benzyloxy-2-methylpropan-1-ol tosylate (**203**)……120

(*R*)-4-Benzyloxy-3-methylbutanenitrile (**204**)……121

(*R*)-4-Benzyloxy-3-methylbutanal (**205**)……122

(4*R*)-5-Benzyloxy-4-methylpent-1-ene (**206**)……122

(2*RS*,4*R*)-5-Benzyloxy-1,2-epoxy-4-methylpentane (**207**)……123

(2*S*,4*R*)-5-Benzyloxy-4-methylpentane-1,2-diol (**208**)……124

4.3.4. Sharpless Asymmetric Dihydroxylation Route……124

Methyl (*S*)-3-(*tert*-butyldiphenylsilanyloxy)-2-methylpropionate (**222**)……124

(2*R*)-3-(*tert*-Butyldiphenylsilanyloxy)-2-methylpropan-1-ol (**223**)……125

(*S*)-3-(*tert*-Butyldiphenylsilanyloxy)-2-methylpropan-1-ol tosylate (**224**)...……126

(3*R*)-4-(*tert*-Butyldiphenylsilanyloxy)-3-methylbutanenitrile (**225**) ……126

(3*R*)-4-(*tert*-Butyldiphenylsilanyloxy)-3-methylbutanal (**226**) ……127

(4*R*)-5-(*tert*-Butyldiphenylsilanyloxy)-4-methylpent-1-ene (**227**)……128

(2*S*,4*R*)-5-(*tert*-Butyldiphenylsilanyloxy)-4-methylpentane-1,2-diol (**228**)……128

4.3.5. Evans Auxiliary Route……129

(2*S*,4*R*)-5-(*tert*-Butyldimethylsilanyloxy)-4-methylpentane-1,2-diol (**154**) ……129

(2*S*,4*R*)-5-(*tert*-Butyldimethylsilanyloxy)-1,2-*O*-*p*-methoxybenzylidine-4-methyl-pentane-1,2-diol (**155**)……130

(2*S*,4*R*)-5-(*tert*-Butyldimethylsilanyloxy)-2-(4-methoxybenzyloxy)-4-methylpentan-1-ol (**156**)……131

(2*S*,4*R*)-5-(*tert*-Butyldimethylsilanyloxy)-2-(4-methoxybenzyloxy)-4-methylpentanal (**157**)……131

(2′*R*,3′*R*,4*R*,5*S*)-3-(2′-Ethyl-3′-hydroxy-3′-phenylpropanoyl)-4-methyl-5-phenyl-oxazolidin-2-one (**258**)……132

(2′*S*,3′*S*,4*R*,5*S*)-3-(2′-Butyl-3′-hydroxy-3′-phenylpropanoyl)-4-methyl-5-phenyl-oxazolidin-2-one (**257**)……133

(2′*R*,3′*R*,4*R*,5*S*)-3-(3′-Hydroxy-3′-phenyl-2′-propylpropanoyl)-4-methyl-5-phenyl-oxazolidin-2-one (**260**)……134

(3*S*,5*R*)-3-(4-Methoxybenzyloxy)-5-methyl-tetrahydropyran-2-ol (**265**)……134

Addendum 1: Structure Tables for (2′*R*,3′*R*,4*R*,5*S*)-3-(2′-Ethyl-3′-hydroxy-3′-phenylpropanoyl)-4-methyl-5-phenyl-oxazolidin-2-one (**258**)……136

Addendum 2: Structure Tables for (2′*S*,3′*S*,4*R*,5*S*)-3-(2′-Butyl-3′-hydroxy-3′-phenylpropanoyl)-4-methyl-5-phenyl-oxazolidin-2-one (**257**)……143

1. INTRODUCTION

Mycotoxins are fungal secondary metabolites which produce toxic effects in plants and animals. They are synthesised by filamentous fungi which readily colonise crops such as wheat, maize, rye and rice, amongst others.[1] Mycotoxins have been shown to play a role in a number of pathologies affecting plants, animals and humans, and as a result, these mycotoxins often attract considerable attention.[2]

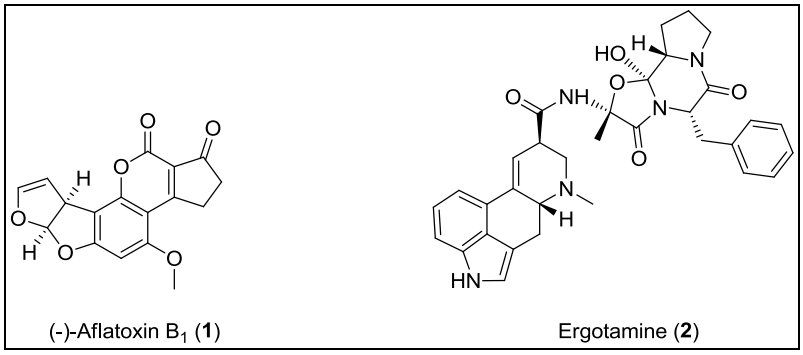

Figure 1:Aflatoxin B_1 and Ergotamine.

The term "mycotoxin" was first coined after an outbreak of "Turkey X Disease" around London in 1962.[1] Over 100 000 turkey poults died of the disease whose cause was unknown. It was found that the disease was caused by the consumption of peanut meal contaminated by toxic secondary metabolites of the fungus *Aspergillus flavus*, named aflatoxins.[3] The aflatoxins have since been shown to be carcinogenic to many species, including humans,[4] with aflatoxin B_1 (**1**) as shown in **Figure 1**, being the most potent natural carcinogen known.[5] Though this was the first use of the term "mycotoxin", it is thought that the earliest recorded reference to a mycotoxin is from an Assyrian tablet dated to 600 BC, which refers to a "noxious pustule in the ear of grain".[6] It is believed that this refers to the sclerotia of a fungus known as ergot (*Claviceps* spp), which have since been found to produce a number of toxic

[1] Bennett, J.W.; Klich, M. *Clin. Microbiol. Rev*. **2003**, *16*, 497.
[2] Bennet, J.W. *Mycopathologia* **1987**, *100*, 3.
[3] Forgacs, J. *Feedstuffs* **1962**, *34*, 124.
[4] Peers, F.G.; Linsell, C.A. *Br. J. Cancer* **1973**, *27*, 473.
[5] Hsu, I.C.; Metcalf, R.A.; Sun, T.; Welsh, J.A.; Wang, N.J.; Harris, C.C. *Nature* **1991**, *350*, 377.
[6] Hofmann, A. Ergot - A rich source of pharmacologically active substances. In *Plants in the development of modern medicine*. T. Swain (ed.). Harvard University Press, Cambridge, p. 236.

alkaloids [such as ergotamine (**2**)] causing ergotism. Ergot alkaloids affect the circulatory system and the nervous system, producing gangrenous ergotism or convulsive ergotism, respectively.[7] These diseases have, however, been mostly eliminated in humans by modern grain processing techniques.The ergot alkaloids were the basis for the discovery of the semi-synthetic hallucinogenic lysergic acid diethylamide (LSD), which was discovered in the attempt to synthesise derivatives of ergot alkaloids.[6]

The trichothecenes are another class of mycotoxins which have received considerable attention. These toxins have been shown to be secondary metabolites of a number of genera of fungi, including, *Myrothecium*, *Phomopsis*, *Stachybotrys*, *Trichoderma*, *Trichothecium* and *Fusarium*.[8] There are over sixty toxins in the class, which affect the gastrointestinal, dermatological and neurological[9] systems in humans and livestock via their ability to inhibit protein synthesis by the action of a ubiquitous 12,13-epoxy moiety.[10] The trichothecene-producing *Stachybotrys* has been associated with a number of "toxic mould" lawsuits, in which the presence of the fungus in moist cellulose-based building material has been associated with a pulmonary bleeding disorder in infants.[11] It is still debated whether the fungus, and the macrocyclic trichothecenes it produces, are the direct cause of the disorder.[12]

Though the *Fusarium* genus produces trichothecenes, the genus is most well-known as the major producer of the fumonisin mycotoxins. The fumonisins were first isolated and characterised in South Africa in 1988, and were shown to be the cause of leucoencephalo-malacia (LEM) in equine species and to be hepatocarcinogenic in rats.[13] It was known that *Fusarium verticillioides* (formerly *Fusarium moniliforme*) was the cause of the pathologies, though the specific agent was unknown. Fusarin C was isolated and characterised and thought to be the culprit, but was found not to cause carcinogenesis in rats.[14] After further separation, assays and characterisation, four fumonisins (named A_1, A_2, B_1 and B_2) were isolated from *F.*

[7] Bennett, J.W.; Bentley, R. *Perspect. Biol. Med*. **1999**, *42*, 333.
[8] Cole, R.J.; Cox, R.H. *Handbook of toxic fungal metabolites*. Academic Press: New York, **1981**.
[9] Trenholm, H.L.; Friend, D.; Hamilton, R.M.G.; Prelusky, D.B.; Foster, B.C. Lethal toxicity and nonspecific effects. In *Trichothecene mycotoxicosis: pathophysiologic effects, vol. 1*. Beasley, V.L. (ed.), CRC Press: Boca Raton, **1989**, p. 107.
[10] McLaughlin, C.S.; Vaughan, M.H.; Campbell, I.M.; Wei, C.M.; Stafford, M.E.; Hansen, B.S. Inhibition of protein synthesis by trichothecenes. In *Mycotoxins in human and animal health*. Rodricks, J.V.; Hesseltine, C.W.; Mehlman, M.A. (eds.) Pathotox Publications: Park Forest South, **1977**, p. 261.
[11] Etzel, R.A.; Montana, E.; Sorenson, W.G.; Kullman, G.J.; Allan, T.M.; Dearborn, D.G. *Arch. Pediatr. Adolesc. Med.* **1998**, *152*, 757.
[12] Johanning, J. *J. Toxicol. Clin. Toxicol.* **1998**, *36*, 629.
[13] Bezuidenhout, S.C.; Gelderblom, W.C.A.; Gorst-Allman, C.P.; Horak, R.M.; Marasas, W.F.O.; Spiteller, G.; Vleggaar, R. *J. Chem. Soc. Chem. Comm*. **1988**, 743.
[14] Gelderblom, W.C.A.; Thiel, P.G.; Jaskiewicz, K.; Marasas, W.F.O. *Carcinogenesis* **1986**, *7*, 1899.

verticillioides cultures and they were found to reproduce the pathologies. After structure elucidation, the fumonisins were found to resemble the phytotoxins known as the AAL-toxins, produced by *Alternaria alternata*, a host-specific fungus affecting susceptible tomato cultivars.[15,16]

More detail regarding the fumonisins and AAL-toxins is discussed in the following sections.

1.1. THE FUMONISINS

The fungus *Fusarium verticillioides* is one of the most common fungal contaminants of maize (*Zea mays*).[17] Maize is one of the bases of the food chain, both as a food staple and as feed for livestock. Consumption of maize infected with the *F. verticillioides* was associated with LEM in equines, pulmonary oedema in swine and high rates of oesophageal cancer in humans, in the Transkei region of South Africa, and in China.[18,19] A strong correlation between the presence of the *F. verticillioides* and oesophageal cancer was shown to exist, while there was no correlation between oesophageal cancer risk and other *Fusarium* species also associated with maize.[20] This made *F. verticilliodes* an attractive target for study due to its potential implications to a number of parties, including maize and livestock farmers, governmental regulators and those interested in and affected by food safety. This then led to an extensive search for the causal agent of LEM, pulmonary oedema and oesophageal cancer that was associated with cultures and extracts of *F. verticilliodes*.

1.1.1. Discovery and Structure Elucidation

In 1988, a previously unknown class of mycotoxins was isolated from cultures of *F. verticillioides* by a process of extensive fractionation of an aqueous methanolic extract of *F. verticillioides*.[13] The fractionation process was guided by rat liver histopathology and rat liver cancer initiation and promotion bioassays, leading to the isolation of four novel compounds showing the desired biological activity.[21] These compounds were named fumonisin A_1, fumonisin A_2, fumonisin B_1 and fumonisin B_2. The structure of the tetramethyl ester of fumonisin A_1 was elucidated by means of liquid secondary ion mass spectrometry, ^{1}H and ^{13}C

[15] Bottini, A.T.; Gilchrist, D.G. *Tetrahedron Lett.* **1981**, *22*, 2719.
[16] Bottini, A.T.; Bowen, J.R.; Gilchrist, D.G. *Tetrahedron Lett.* **1981**, *22*, 2723.
[17] Booth, C. *The Genus Fusarium.* Commonwealth Mycological Institute: Kew, **1971**, p. 237.
[18] Van Rensburg, S.J. *S. Afr. Cancer Bull.* **1985**, *29*, 22.
[19] Yang, C.S. *Cancer Res*. **1980**, *40*, 2633.
[20] Marasas, W.F.O.; Jaskiewicz, K.; Venter, F.S.; Van Schalkwyk, D.J. *S. Afr. Med. J*. **1988**, *74*, 110.
[21] Gelderblom, W.; Jaskiewicz, K.; Marasas, W.; Thiel, P.G.; Horak, R.M.; Vleggaar, R.; Kriek, N. *Appl. Environ. Microbiol.* **1988**, *54*, 1806.

NMR spectroscopy, and chemical derivatization.[13] The ^{13}C NMR spectrum, accompanied by analysis of results from mass spectrometry led to an empirical formula of $C_{40}H_{69}NO_{16}$, while derivatization with *N*-methyl-*N*-trimethylsilyl trifluoroacetamide and acetylation indicated the presence of three hydroxyl groups. Base hydrolysis of the tetramethyl ester of fumonisin A_1, and subsequent methylation of the salt obtained gave trimethyl propane-1,2,3-tricarboxylate as a product, indicating the presence of 2 esters with the core propane-1,2,3-tricarboxylic acid moiety. This conclusion was supported by ^{1}H-^{1}H and ^{1}H-^{13}C NMR correlation experiments. The NMR spectral data also showed the presence and location of methyl groups in the compound. The fragmentation pattern in the electron impact mass spectra led to the deduction of **3** as the structure for fumonisin A_1, as shown in **Figure 2.**

The structure of the tetramethyl ester of fumonisin A_2 was elucidated by comparison of its electron impact mass spectrum fragmentation pattern with that of the tetramethyl ester of fumonisin A_1, which led to the conclusion that the C-10 hydroxyl group was absent giving **4** as the structure for fumonisin A_2. Comparison of ^{13}C NMR spectral data of fumonisin B_1 and fumonisin B_2 showed a similar pattern to that of the A-class, in that the C-10 hydroxyl group is absent in fumonisin B_2. ^{1}H and ^{13}C NMR data also showed the absence of the *N*-acetyl group in the B class, giving **5** and **6** as the structures of fumonisin B_1 and fumonisin B_2, respectively.[13]

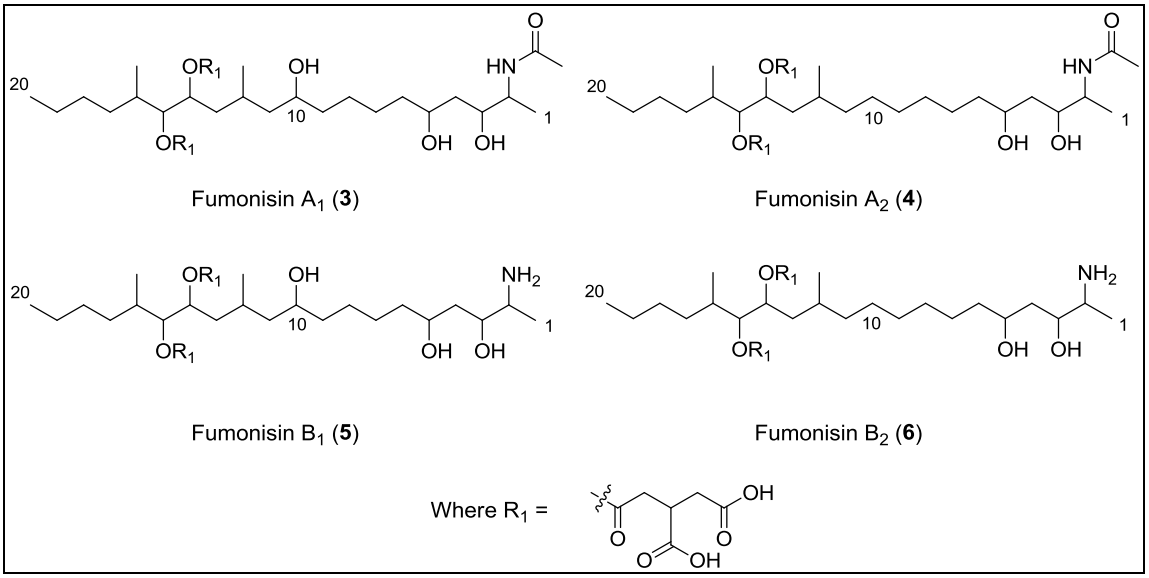

Figure 2: The 2-D structure of the first four fumonisins isolated and characterised.[13]

The tricarballylic fragment could be esterified to the backbone of the fumonisins either through one of the terminal carboxyl groups, or via the central carboxyl group of the propane-1,2,3-tricarboxylate moiety. The mode of linkage was investigated by Boer, and it was found that the linkage to the backbone is through one of the terminal carboxyl groups of the

tricarballylic acid fragment.[22] The strategy made use of the selective reduction of the ester function to the alcohol in the presence of the carboxyl groups, generating a hydroxydicarboxylate species, which could potentially undergo spontaneous lactone formation. If the tricarballylic acid fragment was bound via the central carboxyl group, an achiral reduction product would be expected, which could undergo lactonization to give 4-oxotetrahydrofuran-4-acetic acid. If the tricarballylic acid fragment was bound via a terminal carboxyl group, a chiral reduction product would be expected, which could undergo lactonization to give the five-membered lactone (2-oxotetrahydrofuran-3-acetic acid), or the six-membered lactone (2-oxotetrahydropyran-4-carboxylic acid).

The reduction was achieved using sodium borohydride in *t*-BuOH-MeOH, and IR an MS data indicated that a lactone had indeed formed. NMR spectral data, and specifically the connectivity pattern observed in the HETCOR and COSY experiments and the vicinal coupling constants showed that 2-oxotetrahydrofuran-3-acetic acid was the product, and led to the conclusion that the tricarballylic fragment was indeed bound by a terminal carboxyl group, and that the tricarballylic fragment contains an additional stereocentre, whose configuration was not known at the time.

After isolation and characterisation, fumonisin B_1 was shown to be a carcinogen and a hepatotoxin in rats,[21] providing evidence that the fumonisins were responsible for the carcinogenic and hepatotoxic effects observed after consumption of maize contaminated by *F. verticillioides*. Fumonisin B_1 was also shown to cause LEM in horses when dosed intravenously[23] and orally,[24] and pulmonary oedema in pigs when dosed intravenously,[25] conclusively pointing to the fumonisins as the culprits for the numerous adverse biological effects associated with consumption of maize contaminated with *F. verticillioides*.

Although the 2-dimensional structures had been elucidated, the relative and absolute configuration of the multiple stereocentres remained to be solved, and an investigation into the stereochemistry of the toxin was performed by Boer.[22] It was immediately noticed that the basic structure of the fumonisins was strikingly similar to that of the AAL toxins (as shown in

[22] Boer, A. Stereochemical studies on the fumonisins, metabolites of *Fusarium moniliforme*. M.Sc. Dissertation, University of Pretoria, Pretoria, May 1992.
[23] Marasas, W.F.O.; Kellerman, T.S.; Gelderblom, W.C.A.; Coetzer, J.A.W.; Thiel, P.G.; van der Lugt, J.J. *Onderstepoort J. Vet. Res*. **1988**, *55*, 197.
[24] Kellerman, T.S.; Marasas, W.F.O.; Thiel, P.G.; Gelderblom, W.C.A.; Cawood, M.; Coetzer, J.A.W. *Onderstepoort J. Vet. Res.* **1990**, *57*, 269.
[25] Harrison, L.R.; Colvin, B.M.; Greene, J.T.; Newman, L.E.; Cole, J.R. *J. Vet. Diagn. Invest.* **1990**, *2*, 217.

Figure 3) and the structure and absolute stereochemistry of AAL-toxin TA had previously been described.[26] Due to this resemblance, it was likely that the two classes of toxins were biosynthesised via similar pathways, and it was suggested that there would be a relationship between the stereochemistry of the backbones.

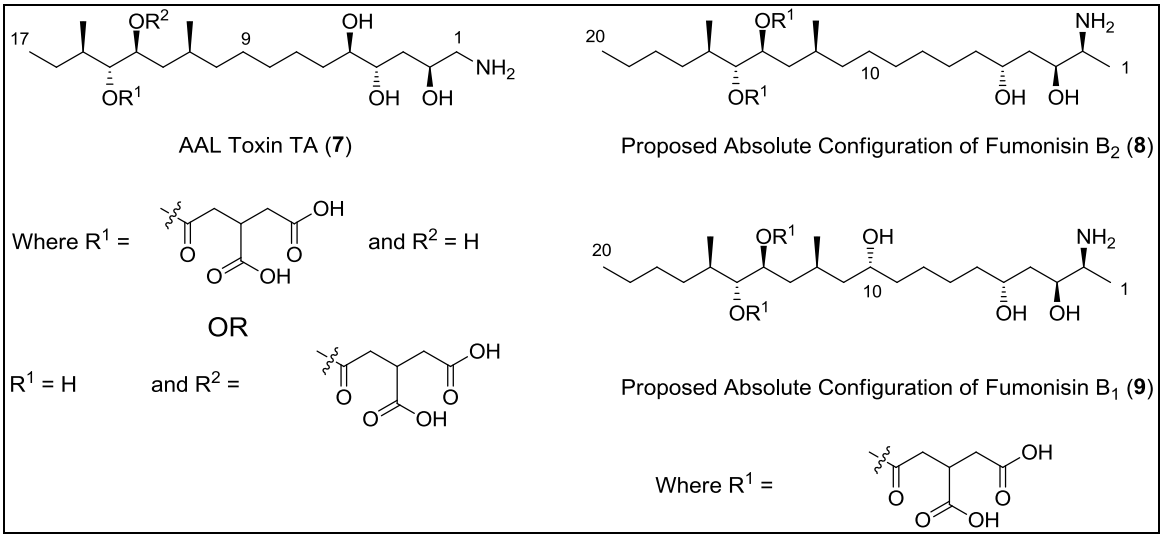

Figure 3: Similarity between AAL Toxin TA and fumonisin B_1, showing the proposed stereochemistry for fumonisin B_1[22] and fumonisin B_2.[27]

Boer proposed the structure shown in **Figure 3** to possess the stereochemistry of the backbone of fumonisin B_1 (**9**).[22] This conclusion was reached using a systematic approach in the study of the relative configuration of the stereocentres on the right half and left half of the fumonisin toxins, followed by the determination of the absolute configuration of a single stereocentre on each half.

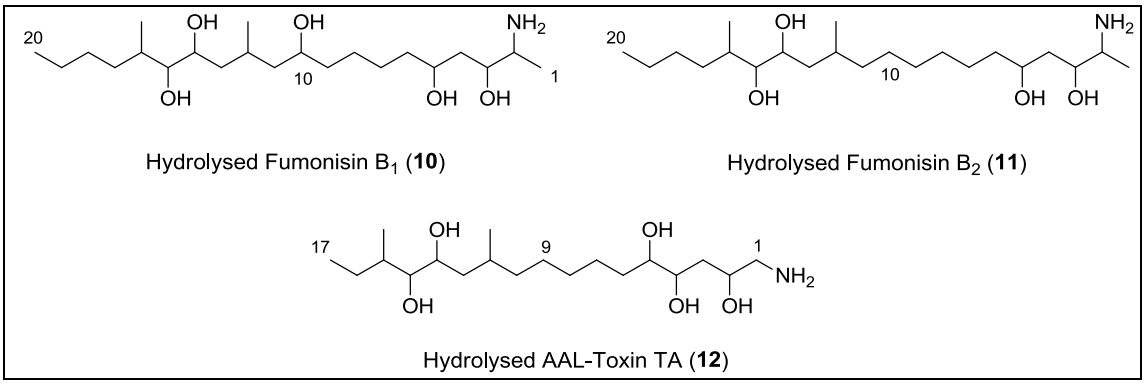

Figure 4: Hydrolysed fumonisin and AAL toxins used in the determination of the configuration of the backbone.

[26] Boyle, C.D.; Harmange, J.C.; Kishi, Y. *J. Am. Chem. Soc.* **1994**, *116*, 4995.
[27] Harmange, J.C.; Boyle, C.D.; Kishi, Y. *Tetrahedron Lett.* **1994**, *35*, 6819.

The relative configuration of the stereocentres at C-2 and C-3 of the right half was determined by synthesising the oxazolidinone derivatives of hydrolysed fumonisin B_2 (**11**) (as shown in **Figure 4**), at the amino group at C-2 and the hydroxyl group at C-3. The conformationally rigid oxazolidinone ring was then analysed by NMR spectroscopy and specifically by nuclear Overhauser effect (NOE) experiments, which showed a strong NOE between the protons of C-1 and C-3, but not for the protons of C-4. From this, it could be concluded that C-1 and C-4 were *trans* in the oxazolidinone ring, and consequently, that the stereocentres at C-2 and C-3 had a *syn* configuration.

The relative configuration between C-3 and C-5 was determined by synthesis of the formylal derivative at the hydroxyl groups at C-3 and C-5 of the tetramethyl ester of fumonisin A_1. NOE experiments showed that the proton on C-5 and the C_2 chain on C-3 were *syn* in the 6-membered ring (due to a strong NOE observed between the axial formylal proton and protons on C-2 and C-5), and from this, it was determined that the hydroxyl groups at C-3 and C-5 had an *anti* relationship.

The absolute configuration of C-5 was determined using the method of Horeau, which makes use of partial kinetic resolution with excess racemic α-phenylbutyric anhydride to determine the stereochemistry of secondary alcohols.[28] One enantiomer of the α-phenylbutyric anhydride is expected to react more rapidly with the chiral secondary alcohol in a predictable fashion, due to differences in energy of the transition states, and after hydrolysis of excess anhydride after the reaction is complete, the optical rotation of the acid can be determined to establish which enantiomer of α-phenylbutyric acid remains, and consequently the stereochemistry of the secondary alcohol.

The absolute configuration at C-5 was determined using derivative **11**, after protection of the other hydroxyl groups on the backbone. The oxazolidinone was prepared between the amino group at C-2 and the hydroxyl group at C-3 and the 14,15-diol was protected as the isopropylidene acetal, leaving the hydroxyl group at C-5 as the only free hydroxyl group. The protected compound was allowed to react with excess racemic α-phenylbutyric anhydride, with both diastereomers of the α-phenylbutyric ester forming in a ratio of 1:2. After recovery and hydrolysis of the excess α-phenylbutyric anhydride, the remaining α-phenylbutyric acid showed a specific rotation of +1.0, which corresponds to the *S* configuration of the C-5 ester according to Horeau's method, and 5*R* configuration in the hydrolysed fumonisin. This in

[28] Horeau, A. *Tetrahedron Lett.* **1961**, 506.

conjunction with the results of the relative configuration determination suggests that the absolute configuration of the right side of the fumonisins' backbone was 2*S*,3*S*,5*R*.

N-Acetyl **10** was protected as the 3,5:14,15-bis-isopropylidene and the protected compound subjected to Horeau's method to determine the absolute stereochemistry of C-10. The ester was shown to have the *S* configuration due to a positive optical rotation, implying that the absolute configuration at C-10 was *R*.

The absolute configuration at C-16 was determined by oxidative cleavage of the 14,15-diol by Kiliani's reagent, giving 2-methylhexanoic acid, which was derivatised as the (*S*)-α-methyl-*p*-nitrobenzylamide. HPLC analysis of the product, and comparison of elution times of standards led to the conclusion that the absolute configuration at C-16 was *R*. In the study, no determination of the configuration of the stereocentre at C-12 was performed; however, it was suggested that since enzymatic methylation of polyketides probably follows the same course, that the stereocentre at C-12 had the *S* configuration.

The relative configuration of the 14,15-diol moiety was determined by comparison of the magnitude of the coupling constant between protons on C-14 and C-15 of various derivatives of the fumonisins, which showed values indicating a *cis* relationship when compared to literature values.

The absolute configuration of the 14,15-acetonide was determined by examination of the magnitude of the coupling constant between protons on C-14 and C-15 (found to be 9.7 Hz), which were found to exist in either an anti- or synperiplanar arrangement according to the Karplus equation. NOE studies of the acetonide derivative showed a strong effect between protons on C-14 and C-15 (amongst others), which by conformational analysis indicated that the absolute configuration was 14*S*,15*R*, giving **9** as the proposed structure of fumonisin B_1.

Harmange *et al.*[27] proposed the absolute configuration for the fumonisin B_2 (**8**) backbone based on comparison of NMR data of AAL-toxin TA and fumonisin B_2, and their proposed structure matched that of Boer.[22] Their approach involved the synthesis of a number of diastereomers of **11** and acetate derivatives thereof,[27] and comparison of the NMR spectroscopic data for the compounds. They compared ^{1}H NMR spectral data for the C-11–C-15 fragment of the peracetate derivative of **12** to that of the C-12–C-16 fragment of the tetramethyl ester of *N*-acetyl **8**. The spectra had a high degree of similarity indicating that there was a relationship between the stereochemistry of the left half of AAL-toxin TA and fumonisin B_2. Similar analysis of the ^{13}C NMR spectra of the C-1–C-4 fragment of the tetramethyl ester of *N*-acetyl **8** and acetates of 2-aminotetradeca-5,7-dien-3-ols indicated the relative stereochemistry at C-2 and C-3 as *syn* by comparison of the chemical shift values for

C-1 for the various derivatives. Comparison of chemical shift values at C-2 and C-4 of AAL-toxin TA and C-3 and C-5 of fumonisin B_2 indicated that these two stereocentres have the *anti* relative configuration, though this remained to be proved.

Based on the above analysis, it was proposed that the backbone **11** had one of three possible configurations (**13**, **14** and **15** in **Figure 5**), or enantiomers thereof, and these compounds were synthesised by a fragment-based approach, involving the coupling of the desired fragments using Wittig methodology to prove their proposed structure. The relative stereochemistry of the two halves was established by comparison of the ^{1}H NMR spectra of the hydrochloride salts of **13** and **14** with the hydrochloride salt derived from **11**, which then proved that the stereochemical relationship between C-2, C-3 and C-5 was as shown in **13**. Pentaacetate derivatives were then synthesised to establish the stereochemical relationship between the two halves as **11**, **13** and **15** all give indistinguishable ^{1}H NMR spectra due to the distance between the two groups of functionality on the backbone. The response of each of these compounds to an achiral shift reagent [Eu(fod)$_3$] was investigated, with pentaacetate **15** behaving differently to the pentaacetate of **11**, while the pentaacetate of **13** behaved identically. This established **13** as the relative stereochemistry of the backbone. The absolute stereochemistry was deduced by investigating the response of the pentaacetates of **13** and **11** to a chiral shift reagent [(+)-Eu(hfc)$_3$]. The two compounds behaved differently in this chiral environment, implying that the natural fumonisin derivative was the enantiomer of **13**, giving **8** as the absolute configuration of the backbone of fumonisin B_2, which corresponded to the proposed structure based solely on comparison with data from AAL-toxin TA, and confirmed the result of Boer.[22]

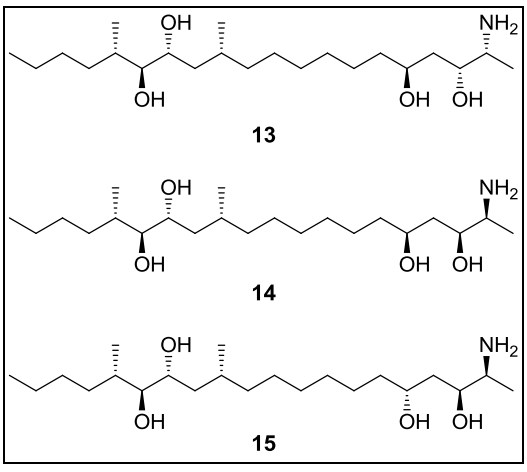

Figure 5: Diastereomers synthesised for absolute configuration assignment of fumonisin B_2.[27]

The absolute configuration of fumonisin B_1 was proven shortly after that of fumonisin B_2,

though by a different approach. The approach used by Hoye *et al.*[29] was based on chemical derivatization of **10**, and the analysis of the properties of the products obtained using NMR spectroscopy, gas chromatography and molecular modelling, in a manner similar to Boer.[22]

The absolute configuration of C-10 was assigned as *R* based on (*R*)- and (*S*)-Mosher ester analysis. The free hydroxyl group on C-10 was obtained by first peracetylating**10**, followed by pentaester cleavage, giving the *N*-acetyl derivative of **10**. The bisacetonide was then prepared, giving the dioxolane incorporating C-14 and C-15 and the dioxane incorporating C-3 and C-5 and leaving the free hydroxyl group on C-10. Analysis of the ^{1}H NMR spectroscopic data of the Mosher esters of the C-10 hydroxyl group showed positive δΔ [where $\delta\Delta = (\delta_S - \delta_R)$] values for protons at C-9 and C-5, and negative Δδ values for protons at C-11 and C-12 giving the *R* configuration at C-10 using the Mosher method. Analysis of the ^{1}H NMR spectral data of the peracetylated derivative indicated the relative configuration between C-3 and C-5 as *anti*, due to the similar chemical shifts of both diastereotopic protons at C-4. The conclusion of an *anti* relationship is supported by the ^{13}C chemical shift of the acetal carbon in the dioxane, which was found to be 100.4 ppm, which is indicative of a 4,6-*anti* relationship at C-3 and C-5.[30]

Monte Carlo conformational analysis of four model compounds (*syn* and *anti* models of C-2 and C-3, and C14 and C-15) was used to predict coupling constants between protons on C-14 and C-15, as well as C-2 and C-3, which were then compared to the experimental values. This data indicated an *anti* relationship between the hydroxyl groups of C-14 and C-15, and a *syn* relationship between the amino group on C-2 and the hydroxyl group on C-3. The absolute configuration at C-2 was determined using **10** by Cbz protection of the primary amine, followed again by bisacetonide formation, and subsequent hydrogenolysis of the Cbz group giving the free amine. The (*R*)- and (*S*)-Mosher amides were synthesised, and by comparison of^{1}H NMR spectral data and δΔ values, the absolute configuration was assigned as *S* for C-2. Sodium periodate cleavage of **10**, and subsequent chiral GC analysis of the mixture showed the cleavage product was (*R*)-2-methylhexanal by comparison with racemic and enantiomerically enriched samples of 2-methylhexanal. From this it was concluded that the absolute configuration of C-16 was *R*. The final stereocentres' configurations were determined from the bisacetonide of *N*-acetylated **10**. The acetonides were cleaved after mesylation of the free C-10 hydroxyl group, allowing for the generation of a pyran ring upon

[29] Hoye, T.R.; Jimenez, J.I.; Shier, W.T. *J. Am. Chem. Soc.* **1994**, *116*, 9409.
[30] Grindley, T.B.; Gulasekharam, V. *Carbohyd. Res*. **1979**, *74*, 7.

addition of NaH, with assumed inversion at C-10. The remaining three hydroxyl groups were converted to the tris-(*R*) and tris-(*S*) Mosher esters. The coupling constants of the resultant pyran indicated that the protons at C-10 and C-14 were axial, while that of C-12 was equatorial meaning the absolute configuration of both C-12 and C-14 was *S*. Conformational analysis of model pyrans and their calculated coupling constants supported this conclusion, giving **16** as the structure of the backbone of fumonisin B_1, as shown in **Figure 6**.

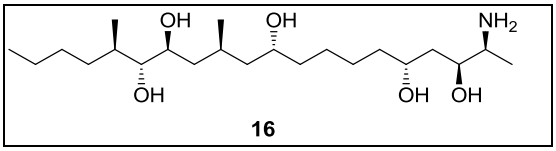

Figure 6: The proposed stereochemistry of the backbone of fumonisin B_1 as determined by Hoye *et al.*[29]

The relative stereochemistry of the C-1–C-5 fragment was confirmed by two other studies of that side of the backbone of fumonisin B_1, using different methods. In the first of these studies,[31] the 2,3-carbamate of **10** was prepared using triphosgene. Analysis of the coupling constants of the resultant ring system showed that the amino group on C-2 and hydroxyl group on C-3 were *cis*, due to the protons on C-2 and C-3 having a coupling constant of 6.5 Hz. Using the Karplus equation, it can be determined that the dihedral angle between these protons is either 60° or 110°. The observed NOE effect between the protons on C-1 and C-3 proved that the angle was 110°. The *N*-*p*-bromobenzoate 3,5-carbonate of **10** was also prepared, and the coupling constants in this ring system were compared to those of a series of model 2-oxo-1,3-dioxanes, which indicated a *trans* relationship between the two hydroxyl groups on C-3 and C-5.

In the second study,[32] oxazoline derivatives of **10** were prepared with methylbenzimidate.HCl and analysed by comparison to oxazolines of the model compound 2-amino-3-hydroxyeicosane. The *cis* and *trans* diastereomers of the oxazoline derivative of 2-amino-3-hydroxyeicosane were then separated by reversed phase HPLC, and their relative stereochemistry assigned by comparison of chemical shift and coupling constant values to those of known compounds. By the same method, the oxazoline of **10** was assigned as *trans*, meaning the two functionalities are *syn*, confirming the result of the other two studies.[22,27]

The only feature of the fumonisins which remained unsolved was the stereochemistry of the

[31] ApSimon, J.W.; Blackwell, B.A.; Edwards, O.E.; Fruchier, A. *Tetrahedron Lett*. **1994**, *35*, 7703.
[32] Poch, G.K.; Powell, R.G.; Plattner, R.D.; Weisleder, D. *Tetrahedron Lett.* **1994**, *35*, 7707.

propane-1,2,3-tricarboxyllic acid (tricarballylic acid) side-chains of the toxins. The challenge lay in that free tricarballylic acid is symmetrical, and therefore not chiral, meaning the analysis of the stereochemistry needed to occur either before cleavage of the ester, or after derivatization to differentiate the unesterified carboxylic acid moieties. These two methods were attempted, and gave a different result for the absolute configuration of the tricarballylic acid moiety. Shier *et al.*[33] used the derivatization method, and concluded by chiral GC analysis, that the configuration at the stereocentre was *S* for fumonisin B_1. Fumonisin B_1 was *N*-acetylated before the carboxylic acid functionalities were reduced with diborane in THF, followed by immediate tosylation of the resultant alcohols. $LiAlH_4$ reduction of the intermediate gave 3-methylpentan-1-ol as the product. Neither this product, nor its acetate derivative was resolvable on a chiral column, so the alcohol was oxidised to the acid, which was methylated to give the resolvable methyl 3-methylpentanoate. The retention time of the ester obtained from fumonisin B_1 was compared to that of L-isoleucine derived (*S*)-methyl 3-methylpentanoate, and they were found to be identical, indicating that the tricarballylic side-chain had the *S* absolute configuration.

Boyle and Kishi[34] used an alternative approach involving NMR spectroscopic analysis of a protected tetramethyl tricarballylic ester of fumonisin B_1, and comparison to synthetic (*R*)-, (*S*)- and racemic tetramethyl tricarballylic esters of fumonisin B_1. All four possible diastereomers were distinguishable by ^1H NMR spectroscopy and the spectrum of the tetramethylfumonisin B_1 correlated with that of the synthetic (*R*)-tetramethyl tricarballylic esters, implying that the absolute configuration is *R* at the tricarballylic moiety. They had previously used the same method to establish the *R* configuration in the tricarballylic acid moiety of fumonisin B_2 as well.[35]

Edwards *et al.*[36] confirmed that the stereochemistry of the tricarballylic ester moiety of fumonisin B_1 was indeed *R* using chemical derivatization to give the benzoyl-protected γ-lactone of partially reduced tricarballylic acid. The properties ($[\alpha]_D^{25}$, IR, MS, ^1H and ^{13}C NMR spectral data) of this lactone were compared to that of a synthetically prepared standard with known absolute configuration, and were found to be identical.

This result completed the 3-dimensonal structure elucidation of the most prevalent

[33] Shier, W.T.; Abbas, H.K.; Badria, F.A. *Tetrahedron Lett.* **1995**, *36*, 1571.
[34] Boyle, C.D.; Kishi, Y. *Tetrahedron Lett.* **1995**, *36*, 5695.
[35] Boyle, C.D.; Kishi, Y. *Tetrahedron Lett*. **1995**, *36*, 4579.
[36] Edwards, O.E.; Blackwell, B.A.; Driega, A.B.; Bensimon, C.; ApSimon, J.W. *Tetrahedron Lett*. **1999**, *40*, 4515.

fumonisins. To date, numerous other analogues of fumonisin B_1 and fumonisin B_2 produced by *Fusarium* and other fungi, including *Aspergillus niger*,[37] have been described. The complete set of fumonisins is classified into four series, namely A, B, C, and P. Only fumonisins A_1, A_2, B_1, B_2, B_3, B_4, C_1 and C_4 have been fully described. The members of these series are summarised below.

The A series are characterised by a C_{20} backbone, with an acetylated amino group on C-2, with varying degrees and sites of hydroxylation, as shown in **Figure 7** and **Table 1**. Some members of the class exist as monoesters of tricarballylic acid (TCA), while others are not esterified to TCA at all. Varying degrees of oxidation have also been observed, with the hydroxyl group on C-15 (which is usually esterified to TCA) oxidised to a ketone.

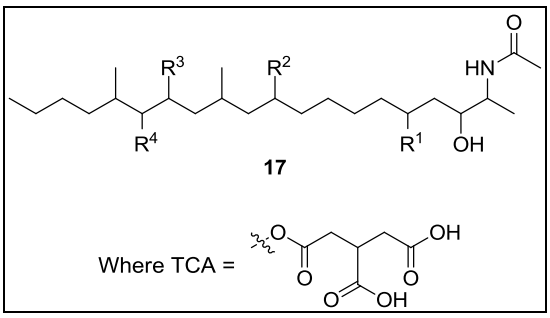

Figure 7: Basic structure of fumonisins of the A series.

Table 1: Substitution pattern of the fumonisins of the A series.

Analogue	R^1	R^2	R^3	R^4
FA_1	OH	OH	TCA	TCA
FA_2	OH	H	TCA	TCA
FA_3	H	OH	TCA	TCA
FA_4	H	H	TCA	TCA
$PHFA_{3a}$	H	OH	OH	TCA
$PHFA_{3b}$	H	OH	TCA	OH
HFA_3	H	OH	OH	OH
FAK_1	OH	OH	TCA	=O

Fumonisins of the B series also have C_{20} backbones as shown in **Figure 8**, but the amino group is not acetylated. Like the A series, some members exist as monoesters of tricarballylic acid (TCA), while others are not esterified to TCA at all. Varying degrees of oxidation have also been observed, with the hydroxyl group at C-15 oxidised to the ketone. Epimers at C-3 of

[37] Nielsen, K.F.; Mogensen, J.; Johansen, M.; Larson, T.O.; Frisvad, J.C. *Anal. Bioanal. Chem.* **2008**, *395*, 1225.

FB_3 and FB_4 have also been identified, with all known structures described in **Table 2**.[38]

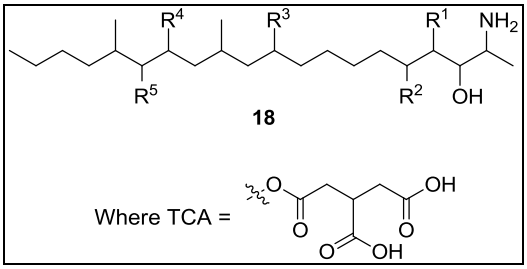

Figure 8: Basic structure of fumonisins of the B series.

Table 2: Substitution pattern of the fumonisins of the B series.

Analogue	R^1	R^2	R^3	R^4	R^5
FB_1	H	OH	OH	TCA	TCA
Iso-FB_1	OH	H	OH	TCA	TCA
$PHFB_{1a}$	H	OH	OH	OH	TCA
$PHFB_{1b}$	H	OH	OH	TCA	OH
HFB_1	H	OH	OH	OH	OH
FBK_1	H	OH	OH	TCA	=O
FB_2	H	OH	H	TCA	TCA
FB_3	H	H	OH	TCA	TCA
FB_4	H	H	H	TCA	TCA
FB_5	Known to have a hexahydroxyl backbone				
FB_6	OH	OH	H	TCA	TCA

Fumonisins of the C series have C_{19} backbones as shown in **Figure 9**, with the methyl group at the amino end of the molecule absent. To date, all characterised members of this series exist as diesters of TCA, with the individual members described in **Table 3**.

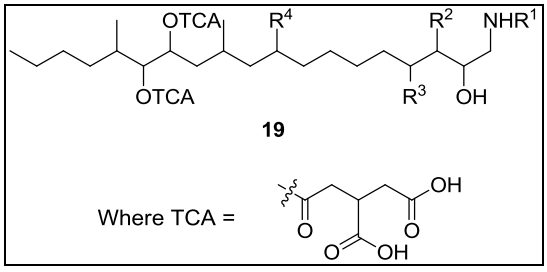

Figure 9: Basic structure of fumonisins of the C series.

[38] Gelderblom, W.C.A., Sewram, V., Shephard, G.S., Snijman, P.W., Tenza, K., van der Westhuizen, L., Vleggaar, R. *J. Agric. Food Chem*. **2007**, *55*, 4388.

Table 3: Substitution pattern of the fumonisins of the C series.

Analogue	R^1	R^2	R^3	R^4
FC_1	H	H	OH	OH
***N*-acetyl-FC_1**	$COCH_3$	H	OH	OH
Iso-FC_1	H	OH	H	OH
***N*-acetyl-iso-FC_1**	$COCH_3$	OH	H	OH
OH-FC_1	H	OH	OH	OH
***N*-acetyl-OH-FC_1**	$COCH_3$	OH	OH	OH
FC_3	H	H	H	OH
FC_4	H	H	H	H

Fumonisins of the P series have C_{20} backbones, and resemble the B series; however, their amino group has been converted into the biologically rare 3-hydroxypyridinium moiety (**Figure 10**). To date, all characterised members of this series exist as diesters of TCA, and are described in **Table 4**.

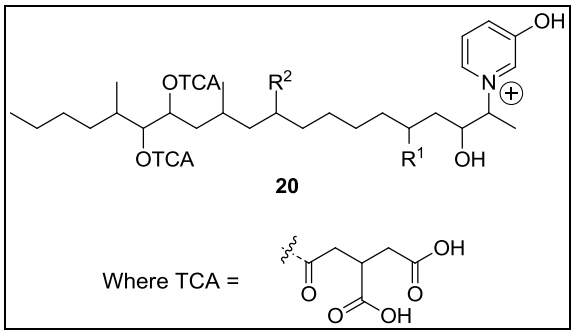

Figure 10: Basic structure of fumonisins of the P series.

Table 4: Substitution pattern of the fumonisins of the P series.

Analogue	R^1	R^2
FP_1	OH	OH
FP_2	OH	H
FP_3	H	OH

The above lists all fumonisins discovered to date whose 2-dimensional structures are known, though recently it has been shown that there are likely many more. Using reversed phase high performance liquid chromatography/electrospray ionisation ion trap mass spectrometry (RP-HPLC/ EI-IT-MS), thirty seven fumonisin and fumonisin-like compounds were isolated from a crude extract of a rice culture of *F. verticillioides* by Bartok.[39] Structures were tentatively assigned to some of these compounds based on distinctive fragmentation patterns, masses of

[39] Bartok, T. *Rapid Comm. Mass Spectrom*. **2006**, *20*, 2447.

protonated ions and retention times on a C_{18} HPLC column. The results of the above investigation seemed to show that the tricarballylic acid moiety is not always bound at C-14 and C-15, and in some cases, the esterified acid is not tricarballylic acid, but other common carboxylic acids, including *cis*-aconitic acid, oxalylsuccinic acid and oxalylfumaric acid. Numerous isomers of known fumonisins were also detected. These structures are still to be confirmed by other techniques such as NMR spectroscopy and X-ray crystallography.

In a second study Bartok *et al.*[40] detected twenty eight isomers of fumonisin B_1 including the single known iso-FB_1 shown above using reversed phase high performance liquid chromatography/electrospray ionisation time-of-flight mass spectrometry (RP-HPLC/ ESI-TOF-MS) and RP-HPLC/ ESI-IT-MS. No indication of the structures of these isomers was given, though was postulated that these isomers may be the result of variations in stereochemistry and site of esterification of the TCA moiety.

Though the number of fumonisins continues to grow, fumonisins B_1, B_2, and B_3 remain the most significant due to them being the predominant fumonisin isolates from rice and maize cultures, accounting for 70-80%, 15-25% and 3-8% of total fumonisins, respectively.[41]

1.1.2. Synthetic Studies

Fumonisin B_1 and fumonisin B_2 were attractive targets for synthesis after their structure elucidation was complete. The presence of eight and seven stereocentres on the backbone of fumonisin B_1 and B_2, respectively, as well as the single stereocentre and site of esterification of the tricarballylic acid on the polyhydroxyl backbone offered a unique challenge to synthetic chemists. Synthesis of the toxins would also allow for confirmation of the assigned stereochemistry by comparison of spectroscopic data and physical properties. A simple synthetic route could also offer access to other diastereomers or analogs, allowing for investigation of structure-activity relationships to establish the mechanism of action of the fumonisin toxins.

The first published synthesis of a fumonisin was the enantioselective total synthesis of fumonisin B_2 by Shi *et al.*,[42] which, without the hydroxyl group on C-10, was a simpler target than fumonisin B_1. To determine the synthetic targets, the toxin was divided into two distinct

[40] Bartok, T.; Tölgyesi, L.; Szekeres, A.; Varga, M.; Bartha, R.; Szécsi, Á.; Bartok, M.; Mesterházy, Á. *Rapid Comm. Mass Spectrom.* **2010**, *24*, 35.
[41] Rheeder, J.P.; Marasas, W.F.O.; Vismer, H.F. *Appl. Environ. Microbiol.* **2002**, *68*, 2101.
[42] Shi, Y.; Peng, L.; Kishi, Y. *J. Org. Chem.* **1997**, *62*, 5666.

halves: the left half composed of C-10–C-20, and the right half composed of C-1–C-9, which the researchers hypothesised were involved in separate biological events. The researchers therefore designed their synthetic pathway in a way that would allow them to test this hypothesis. The design involved the convergent synthesis of the two halves (**21** and **22**) and the tricarballylic acid moiety (**23**), shown in **Figure 11**, which were coupled at a late stage of the synthesis. This would, in theory, allow access to various analogues to test their hypothesis.

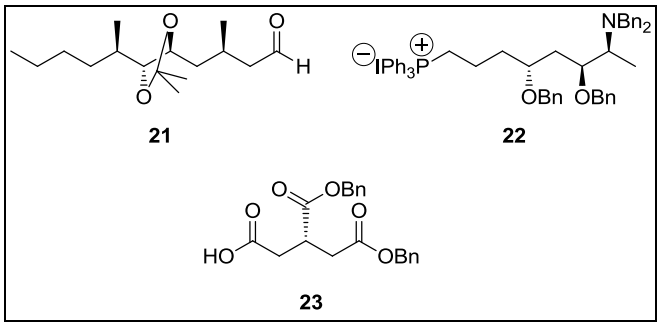

Figure 11: Targets for synthesis of fumonisin B_2 by Shi *et al.*[42]

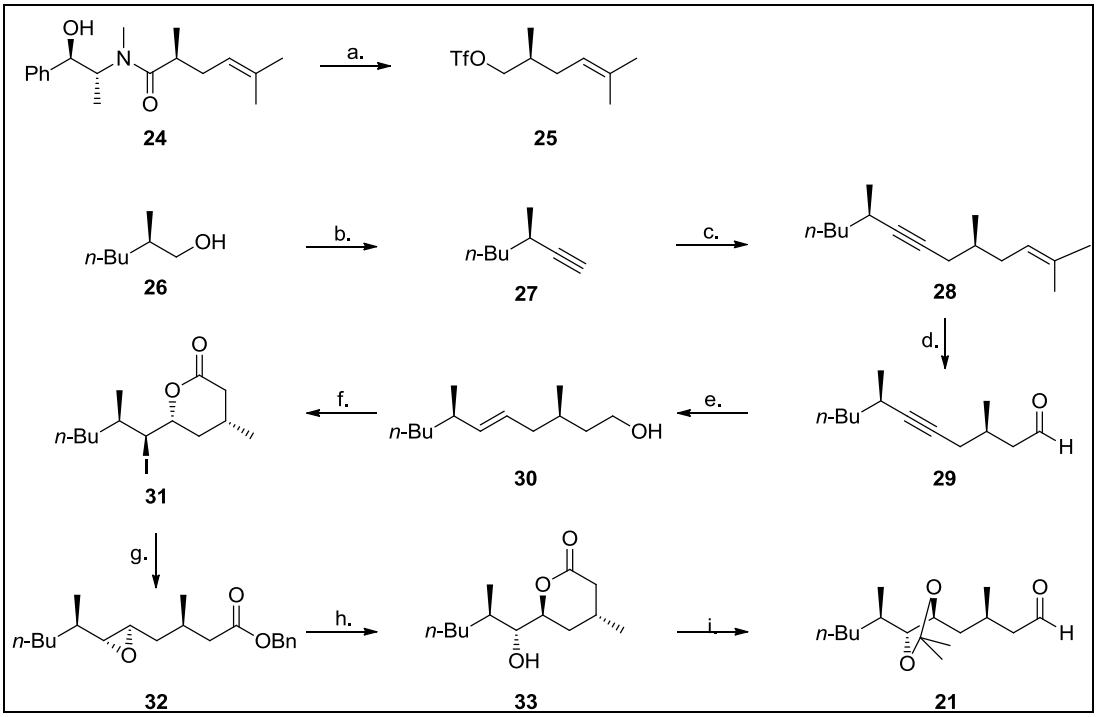

Scheme 1: Synthesis of the C-10–C-20 fragment by Shi *et al.*[42]

Reagents: a. i). Pyrrolidine, BH_3, *n*-BuLi, ii). Tf_2O; b. i). $(COCl)_2$, DMSO, Et_3N, ii). CBr_4, PPh_3, *n*-BuLi, H_2O; c. i). *n*-BuLi, **25**, ii). $K_2OsO_4.2H_2O$; d. $Pb(OAc)_4$; e. i). $NaBH_4$ ii). Na/NH_3; f. i). $(COCl)_2$, DMSO, Et_3N, ii). $NaClO_2$, iii). I_2, $NaHCO_3$; g. BnONa; h. i). H_2, Pd/C, ii). TsOH; i. i). $LiAlH_4$, ii).TsOH, acetone, iii). $(COCl)_2$, DMSO, Et_3N.

The synthesis of the left unit (shown in **Scheme 1**) began by oxidation of (*R*)-2-methylhexan-1-ol (**26**) using the Swern protocol, followed by a Corey-Fuchs procedure to generate alkyne

(**27**). Asymmetric alkylation of the *N*-propionyl derivative of (–)-pseudoephedrine with 1-bromo-3-methylbut-2-ene gave **24**, which, after reduction with pyrrolidine/BH_3/*n*-BuLi and triflation of the subsequent alcohol gave **25**, which was coupled to the lithiated alkyne giving enyne (**28**) in 70% yield. Osmylation generated the vicinal diol, which was cleaved with lead(IV) acetate to give aldehyde (**29**) as the product. The aldehyde was reduced to the alcohol, which was followed by a stereoselective reduction of the alkyne to the *trans*-alkene (**30**) with sodium in liquid ammonia. The primary alcohol group in **30** was then oxidised to the acid via the aldehyde. Iodolactonization generated iodolactone (**31**) in >20:1 diastereomeric ratio. **31** was then cleaved with sodium phenylmethoxide giving the epoxy benzyl ester (**32**) via an intramolecular S_N2 reaction. Deprotection of the benzyl ester by hydrogenolysis gave a product which underwent spontaneous lactone formation to give **33** which contained all the desired functionality. The lactone was converted into target aldehyde (**21**) by $LiAlH_4$ reduction of the lactone, protection of the vicinal diol as the acetonide and oxidation of the primary alcohol using the Swern protocol.

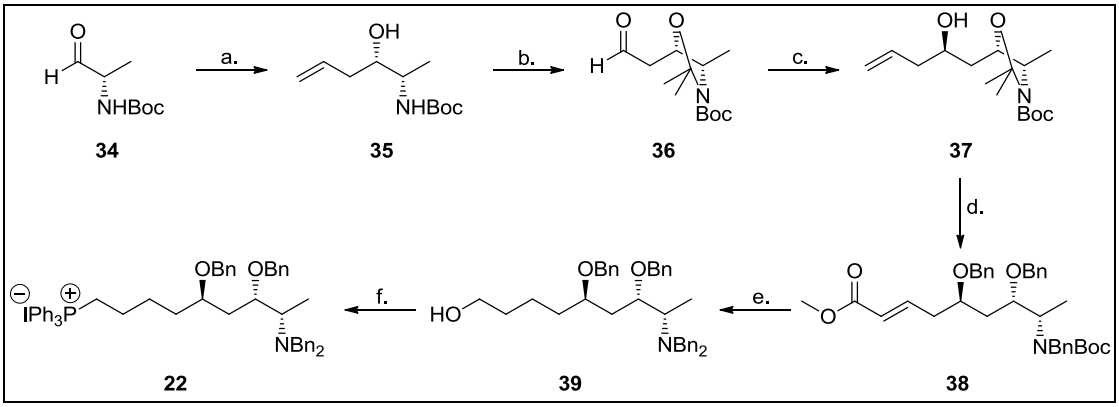

Scheme 2: Synthesis of the C-1–C-9 fragment by Shi *et al*.[42]

> *Reagents*: a. (–)-Icp_2B-allyl; b. i). TsOH, acetone, ii). O_3, Me_2S; c. (+)-Icp_2B-allyl; d. i). TsOH, ii). NaH, BnBr, TBAI, iii). O_3, Me_2S, iv). NaH, $(MeO)_2POCH_2COOMe$; e. i). H_2/Lindlar, ii). TFA, iii). BnBr, K_2CO_3, iv). DIBALH; f. i). I_2, PPh_3, imidazole, ii). PPh_3.

Synthesis of the C-1–C-9 fragment (**Scheme 2**) began with protected α-amino aldehyde (**34**) which was prepared from L-alanine.[43] The aldehyde was subjected to stereoselective allylation using the α-pinene-derived (–)-*B*-allyldiisopinocampheylborane to give *syn* amino alcohol (**35**) with 94% diastereoselectivity. The amino alcohol was protected as the acetonide, before the alkene underwent ozonolysis with reductive work-up to give **36** which was again

[43] Fehrentz, J-A.; Castro, B. *Synthesis* **1983**, 676.

stereoselectively allylated, but with (+)-*B*-allyldiisopinocampheylborane, to give the *anti* alcohol (**37**) with 91% diastereoselectivity. The acetonide was cleaved with TsOH, and the product tribenzylated with sodium hydride and benzyl bromide. Ozonolysis and reductive work-up of the alkene, followed by a two-carbon addition by Horner-Wadsworth-Emmons reaction gave the α,β-unsaturated ester (**38**). The resultant alkene was selectively hydrogenated over Lindlar catalyst, before the Boc protection of the amine was cleaved with trifluoroacetic acid in dichloromethane, and the dibenzyl protected amine was prepared with benzyl bromide and potassium carbonate. The ester was reduced with DIBALH giving primary alcohol (**39**), which was converted into the iodide with triphenylphosphine, iodine and imidazole. The target phosphonium salt (**22**) was then made by addition of triphenylphosphine in acetonitrile.

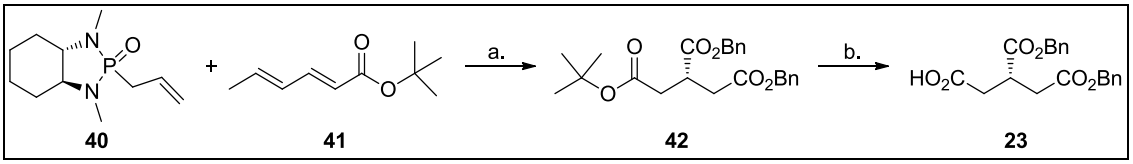

Scheme 3: Preparation of the tricarballylic fragment.

Reagents: a. i). *n*-BuLi,. ii). O_3, Me_2S, iii). CrO_3, H_2SO_4, iv). BnOH, EDCI, DMAP; b. TFA.

The tricarballylic fragment was prepared by an asymmetric Michael addition of allylphosphonamide (**40**) to the ester (**41**) (**Scheme 3**). Ozonolysis of the product, followed by Jones oxidation and benzyl ester formation with BnOH mediated by EDCI gave tri-ester (**42**). Selective cleavage of the *t*-butyl ester by trifluoroacetic acid gave target fragment **23**.

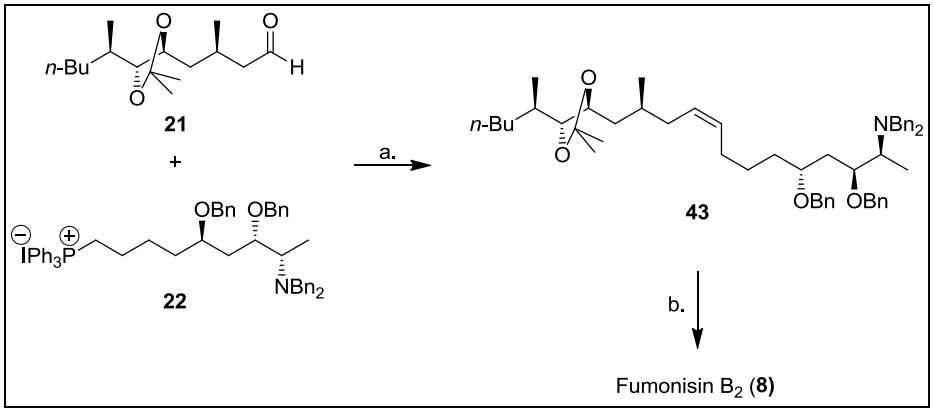

Scheme 4: Coupling of targets to give fumonisin B_2.

Reagents: a. *n*-BuLi; b. i). TFA, ii). **23**, EDCI, DMAP, iii). H_2, Pearlman's catalyst, HCl.

Coupling of the fragments was achieved by treatment of **22** with *n*-BuLi to generate the ylid, and its reaction with aldehyde (**21**) gave *cis* alkene (**43**) as product, as shown in **Scheme 4**.

The acetonide group protecting the 14,15-diol was removed by treatment with trifluoroacetic acid, before the free hydroxyl groups were esterified to **23** by addition of EDCI and DMAP. Global hydrogenation with Pearlman's catalyst in the presence of HCl removed the benzyl protection and reduced the alkene to give fumonisin B_2 (**8**) as product in 60% yield. The synthetic fumonisin B_2 was compared to a natural standard and found to be identical in spectroscopic and chromatographic properties.

After the total synthesis of fumonisin B_2, fumonisin B_1 became the next target for synthetic chemists due to its predominance in fumonisin extracts from infected maize. The first attempt at the synthesis of fumonisin B_1 was by Gurjar *et al.*[44] who synthesised a hexaacetate derivativeof **10** from D-glucose and D-glucosamine. Their synthetic scheme also divided the toxin into a left- and right-half, though their disconnection was between C-6 and C-7, in contrast to a disconnection at C-9 and C-10 as was done by Shi *et al.*[42] The synthesis is summarised in **Scheme 5**.

Synthesis of the C-7–C-20 fragment began with the conversion of D-glucose (**44**) to ketone (**45**).[45] A Wittig reaction with the triphenylphosphonium bromide derived from *n*-butyl bromide gave the alkene (**46**), which on catalytic hydrogenation over Pd-C gave a diastereomeric mixture of the reduced product, which was successfully separated by chromatography with chemical correlation studies confirming the desired stereochemistry. The stereochemistry of the benzyl protected alcohol was inverted by reduction with calcium in liquid ammonia, oxidation of the hydroxyl group with IBX, followed by reduction of the ketone by $NaBH_4$ and benzylation, before the acetonide was removed in 70% acetic acid to give vicinal diol (**47**). The diol was oxidatively cleaved with sodium periodate, and the product underwent a Horner-Wadsworth-Emmons reaction with the appropriate phosphonate ester giving **48** as product. Lactonization of the product by addition of potassium carbonate, followed by a stereoselective reduction of the lactone with DIBALH gave lactol (**49**) as product, from which the isopropyl glycoside was prepared by reaction with isopropanol and camphorsulfonic acid. It was thought that the isopropyl glycoside would induce greater stereoselectivity in the reduction of the alkene over rhodium on alumina, and this is what was observed, as **50** was obtained as the sole product, proven by the 3.0 Hz coupling constant between the proton on the anomeric carbon and the proton on the carbon bearing the methyl group. Hydrolysis of the glycosidic bond by acetic acid, a one-carbon Wittig reaction and

[44] Gurjar, M.K.; Rajendran, V.; Rao, B.V. *Tetrahedron Lett*. **1998**, *39*, 3803.
[45] Araki, Y.; Arai, Y.; Endo, T.; Ishido, Y. *Chem. Lett.* **1989**, 1.

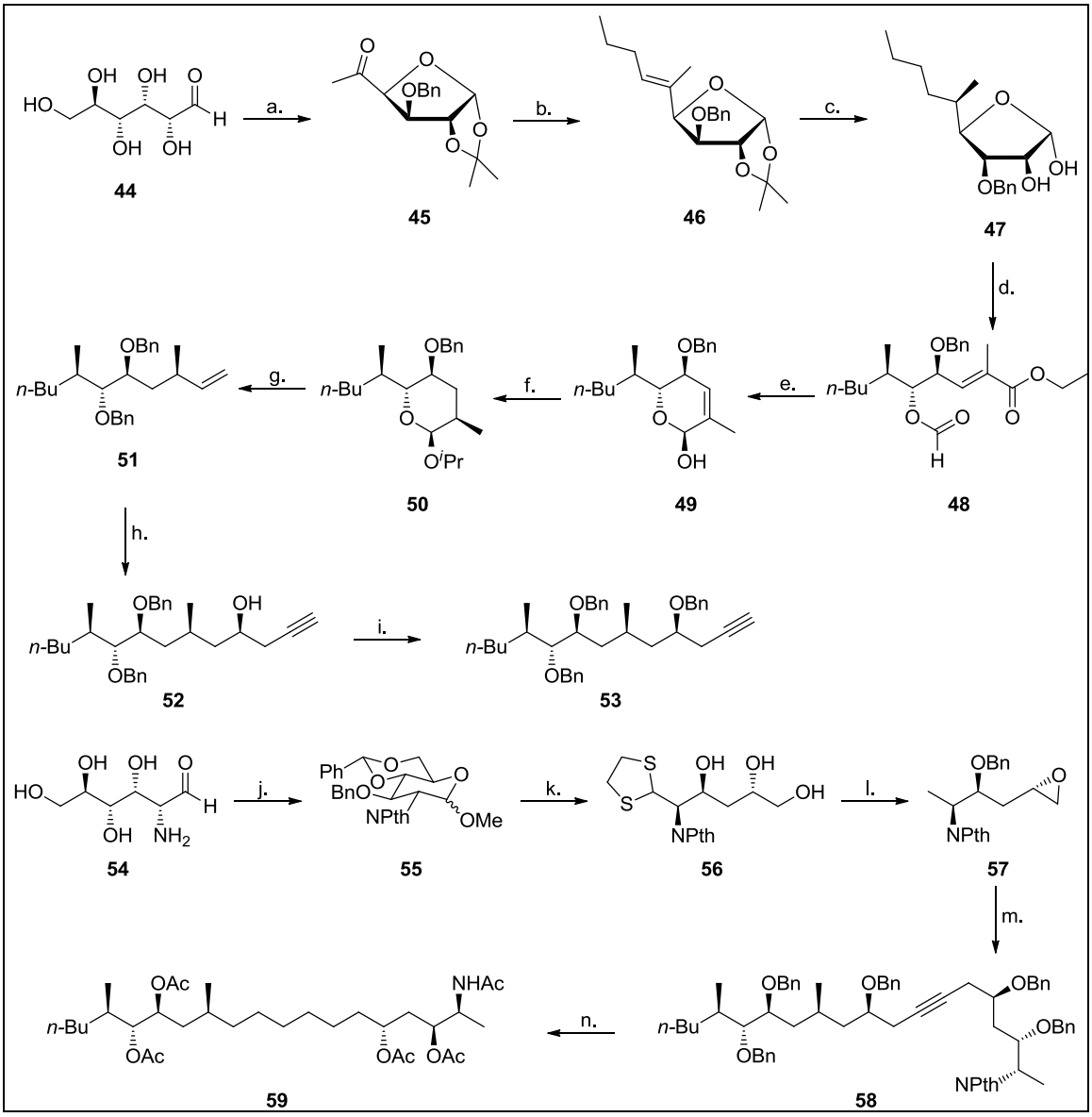

Scheme 5: Synthetic approach to a hexaacetyl derivative of hydrolysed fumonisin B_1.

Reagents: a. Ref. 45; b. $CH_3(CH_2)_2CH_2PPh_3Br$, *n*-BuLi; c. i). H_2Pd/C, separation, ii). Ca/NH_3, iii). IBX, DMSO, iv). $NaBH_4$, v). BnBr, NaH, vi). CH_3COOH, H_2SO_4; d. i). $NaIO_4$, ii). $(MeO)_2POCH(CH_3)COOEt$, NaH; e. i). K_2CO_3, ii). DIBALH; f. i). ^{i}PrOH, CSA, ii). Rh/Al_2O_3, H_2; g. i). CH_3COOH, H_2SO_4 ii). CH_3PPh_3I, *n*-BuLi, iii). BnBr, NaH; h. i). 9-BBN, NaOH, H_2O_2, ii). $(COCl)_2$, DMSO, Et_3N, iii). Propargyl bromide, Zn, NH_4Cl, separation, i. BnBr, NaH, j. Ref 46; k. i). CH_3COOH, ii). TBSCl, imidazole, iii). NaH, CS_2, MeI, iv). Bu_3SnH, AIBN, v). TsOHvi). $BF_3.Et_2O$, $HS(CH_2)_2SH$; l. i). Raney Ni, ii). pentan-3-one, CSA, iv). BnBr, NaH, v).TsOH, vi). TsCl, pyridine, vi). NaH; m. **53**, *n*-BuLi, $BF_3.Et_2O$; n. i). $MeNH_2$-MeOH, ii). Ac_2O, Et_3N, iii). $Pd(OH)_2$, H_2, iii). Ac_2O, Et_3N.

benzylation with BnBr and NaH gave alkene (**51**) as product. The alkene was subjected to hydroboration-oxidation in the presence of 9-BBN, NaOH and H_2O_2, and the alcohol oxidised by a Swern protocol giving the aldehyde which was alkylated with propargyl bromide in the presence of zinc and aqueous ammonium chloride. The product was a diastereomeric mixture

of alcohol (**52**), which was separated by column chromatography to give diastereomerically pure **52**, confirmed by the Mosher ester method.The hydroxyl group was protected as the benzyl ether by addition of BnBr and NaH, giving the C-7–C-20 target (**53**).

D-Glucosamine (**54**) was converted to glycoside (**55**) by the protection of the amino group as the phthalimide, benzylidene formation and methylation.[46] The benzylidene was hydrolysed by addition of acetic acid, before selective protection of the primary alcohol by TBSCl with imidazole. The free secondary alcohol was reduced by Barton-McCombie radical deoxygenation, and the glycosidic bond cleaved by addition of *p*-TsOH in methanol. Dithiolane (**56**) was prepared by addition of ethane-1,2-dithiol and boron trifluoride diethyl etherate, and desulfurised over Raney-Ni. The triol was regioselectivly protected by addition of pentan-3-one and camphorsulfonic acid, giving the dioxolane in 92% yield. The secondary alcohol was protected as the benzyl ether by addition of BnBr and NaH, and the acetal was cleaved by *p*-TsOH. The primary alcohol was selectively tosylated, and the secondary hydroxyl group deprotonated by addition of NaH, allowing for stereospecific nucleophilic substitution generating epoxide (**57**), the target for the right-side of the hexaacetate derivative of **10**.

The acetylene (**53**) and epoxide (**57**) were coupled by deprotonation of the alkyne by *n*-BuLi in the presence of boron trifluoride diethyl etherate, and addition of the epoxide to give adduct **58** by nucleophilic substitution. Removal of the phthalimide group by refluxing with methylamine in methanol, followed by acetylation, hydrogenation of the product over $Pd(OH)_2$ on carbon and acetylation of the deprotected hydroxyl groups gave target molecule **59** in 95% yield.

The reason for the synthesis of the hexaacetate derivative rather than the complete fumonisin B_1 toxin is unclear. With a modification of protecting group strategy, and synthesis and coupling of the tricarballylic acid moiety in a similar fashion to that of Shi *et al.*,[42] fumonisin B_1 could be synthesised. With the hydroxyl groups on C-14 and C-15 protected as benzyl ethers, instead of protecting the newly generated hydroxyl group on C-10 also as the benzyl ether (**53**), an orthogonal protecting group could be used, such as the silyl protecting group. **56** could be protected as a silyl ether as well (after acetonide formation), and the acetonide removed using Dowex 50W-X8,[47] which is known to cleave terminal acetonides in the presence of other acid-sensitive groups. The same method could then be followed, and the

[46] Shigehrio, H. *Carbohydr Res.* **1971**, *6*, 229.
[47] Park, K.H.; Yoon, Y.; Lee, S.G. *Tetrahedron Lett.* **1994**, *35*, 9737.

two modified fragments coupled in the same manner, and the newly generated hydroxyl group on C-5 could also be protected as a silyl ether. Removal of the phthalimide protection of the amino group followed by hydrogenation would give a product with free hydroxyl groups on C-14 and C-15, which could then be esterified to **23**. Hydrogenation and fluoride-based removal of the silyl protection would yield fumonisin B_1 (**9**).

In 2009, the first total synthesis of fumonisin B_1 was reported by Pereira *et al.*[48](**Scheme 6**). Again, the backbone of the toxin was divided into right- and left-halves (C-1–C-9 and C-10–C-20), and after synthesis of the halves, they were coupled and esterified to the tricarballylic acid moiety giving fumonisin B_1.

The C-1–C-9 segment was synthesised from pent-4-yn-1-ol (**60**) by the protection of the acetylene as the triisopropylsilyl ether with TIPSCl and ethyl magnesium bromide. Oxidation of the primary alcohol with Dess-Martin periodinane gave aldehyde (**61**) which was subjected to a stereoselective allyl transfer reaction with the camphor-derived chiral auxiliary (**62**) in the presence of catalytic camphorsulfonic acid, giving exclusively *cis* homoallylic alcohol (**63**) in 90% ee. The alkene was epoxidised by a directed, vanadium-catalysed epoxidation, and the hydroxyl group subjected to Mitsunobu inversion, before a regioselective epoxide opening with $Ti(O^iPr)_2(N_3)_2$ giving azide (**64**) in 47% yield. Cleavage of the silyl ether in the presence of TBAF, and protection of the hydroxyl groups by NaH and BnBr gave **65** as the target for the right-side of fumonisin B_1.

The C-10–C-20 fragment of fumonisin B_1 was synthesised from two smaller fragments which were linked by a second allylic transfer, followed by a spontaneous *in situ* 2-oxonia-Cope rearrangement. The first of these fragments (**68**) was synthesised from hept-2-en-1-ol (**66**). Sharpless asymmetric epoxidation gave (2*S*,3*S*)-2,3-epoxyheptan-1-ol, which was regioselectively opened with trimethylaluminium to give diol (**67**). The benzylidene acetal was prepared by addition of benzaldehyde dimethylacetal and camphorsulfonic acid as a catalyst and the acetal was regioselectively opened to give the primary alcohol, which was oxidised by IBX to aldehyde (**68**), the first target for the key allyl transfer reaction. The second target for the allyl transfer reaction was synthesised from butane-1,4-diol (**69**). Monoprotection of the diol with TBSCl and Et_3N, and oxidation of the free hydroxyl group by Swern protocol gave aldehyde (**70**). The imide (**73**) was prepared from the appropriate Evans chiral auxiliary (**71**) and (*E*)-but-2-enyl chloride (**72**), and the stereoselective aldol reaction

[48] Pereira, C.L., Chen, Y.H., McDonald, F.E. *J. Am. Chem. Soc*. **2009**, *131*, 6066.

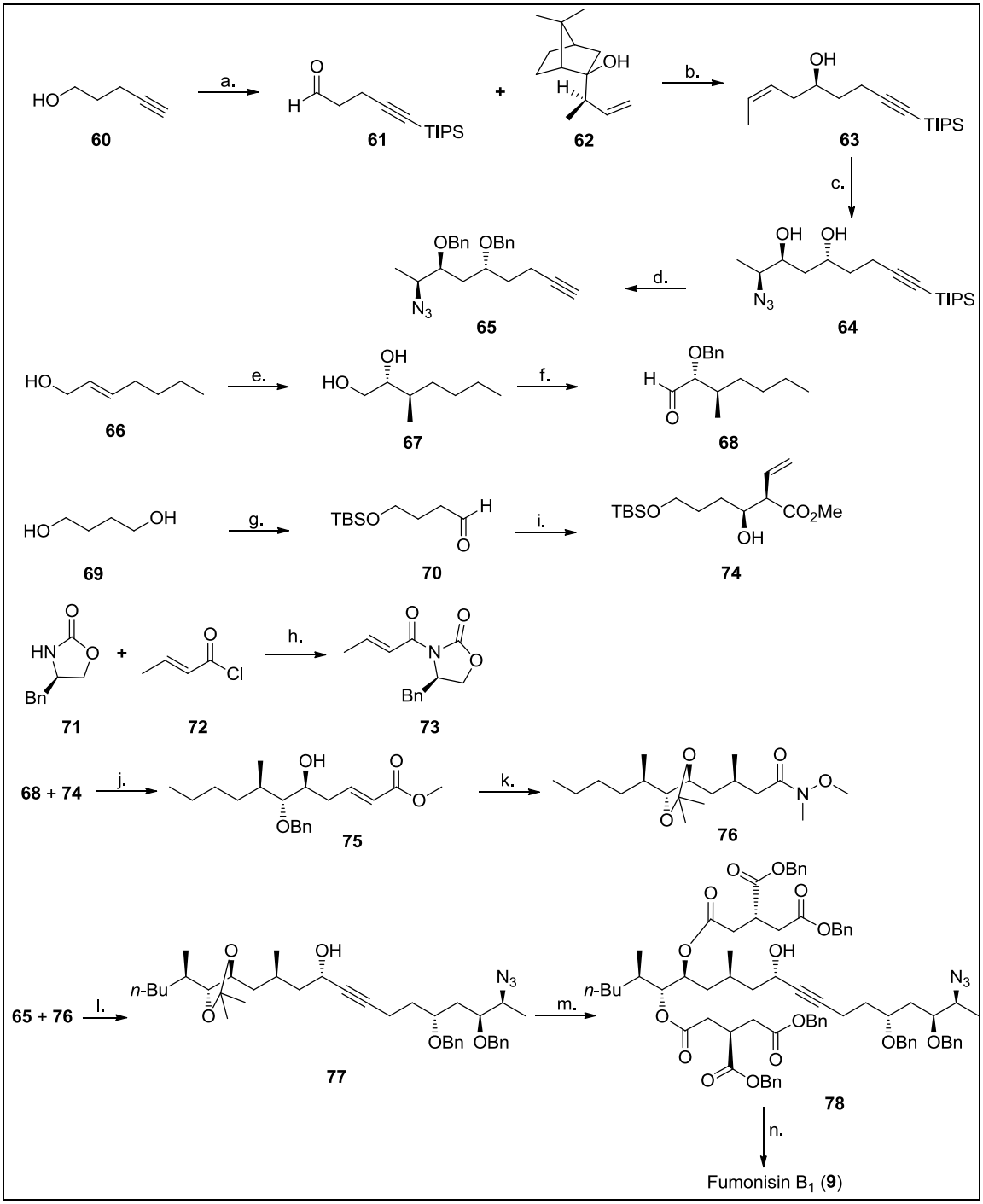

Scheme 6: Synthesis of fumonisin B_1 by Pereira *et al.*[48]

Reagents: a. i). EtMgBr, TIPSCl, ii). Dess-Martin periodinane; b). CSA; c. i). $VO(acac)_2$, *t*-BuOOH, ii). PPh_3, DIAD, AcOH, K_2CO_3 iii). $Ti(O^iPr)_2(N_3)_2$; d. i). TBAF, ii). NaH, BnBr; e. i). $Ti(O^iPr)_4$, (*R*,*R*)-DIPT, *t*-BuOOH, ii). Me_3Al; f. i). $PhCH(OMe)_2$, TsOH, ii). DIBALH, iii). IBX, DMSO; g. i.) Et_3N, TBSCl, ii). $(COCl_2)$, DMSO, Et_3N; h. *n*-BuLi; i. i). Bu_2BOTf, Et_3N, **73**, ii). LiOH, iii). $TMSCHN_2$; j. TMSOTf; k. i). 2-benzyloxy-*N*-methylpyridinium triflate, MgO, $PhCF_3$, ii). MeMgBr, CuI, (*R*)-Tol-BINAP, iii). BCl_3, iv). $Me_2C(OMe)_2$, TsOH, v). Me(MeO)NH.HCl, ^{i}PrMgCl; l. i). *n*-BuLi, ii). (*R*)-CBS, catecholborane; m. i). NaH, BnBr, ii). Amberlite-120 (H^+), iii). **20**, EDCI, DMAP; n. H_2, $Pd(OH)_2$, HCl.

between the imide and aldehyde (**70**), and subsequent basic cleavage of the auxiliary and methylation of the acid gave target **74**. The allyl transfer reaction between aldehyde (**65**) and aldol product (**74**) in the presence of trimethylsilyl triflate, and a 2-oxonia-Cope rearrangement gave α,β-unsaturated ester (**75**) as the product. Benzylation of the hydroxyl group under neutral conditions using Dudley's reagent,[49] followed by an asymmetric conjugate addition of methyl magnesium bromide catalysed by CuI and (*R*)-Tol-BINAP and replacement of the benzyl groups with an acetonide by cleavage with boron trichloride and reaction with 2,2-dimethoxypropane in the presence of *p*-TsOH gave the acetonide. The ester was converted into the Weinreb amide by addition to a mixture of Me(MeO)NH.HCl and ^{i}PrMgCl, giving **76** as the target for the C-10–C-20 fragment of fumonisin B_1.

Pereira *et al.*[48] used the same tricarballylic fragment (**23**) as Shi *et al.*,[42] though they synthesised the dibenzyl ester derivative by a different method. Their method involved the asymmetric alkylation of 3-(pent-5-enoyl)-4-methyl-5-phenyloxazolidin-2-one (derived from (+)-norephedrine) with benzyl bromoacetate in the presence of lithium bis(trimethylsilyl)-amide. Simultaneous cleavage of the chiral auxiliary and benzylation with *n*-BuLi and benzyl alcohol, followed by sodium periodate oxidation of the alkene in the presence of ruthenium(III) chloride gave **23**, the target for the tricarballylic fragment of the toxin.

The alkyne (**65**) and the Weinreb amide (**76**) were coupled by lithiation of the alkyne with *n*-BuLi, and addition of the Weinreb amide. Stereoselective Corey-Bakshi-Shibata reduction of the ketone gave **77**, which was benzylated with BnBr and NaH, before the acetonide was removed by stirring with Amberlite-120(H^+) resin. Esterification with the tricarballylic fragment (**23**) in the presence of EDCI and DMAP gave **78**, which was subjected to hydrogenation over $Pd(OH)_2$ to give fumonisin B_1 (**9**).

The synthesis of fumonisin B_1 completed the total synthesis of arguably the two most important fumonisins; however, with the 3-dimensional structures of most of the fumonisins still to be confirmed, there is still much room for research into the structure and synthesis of the remaining fumonisins.

1.1.3. Biological Effects

The biological effects of consumption of products contaminated by the *Fusarium* fungus were well known before the causal agent itself was established. After Gelderblom *et al.*[21]

[49] Poon, K.W.C.; Dudley, G.B. *J. Org. Chem.* **2006**, *71*, 3923.

established that the fumonisins were responsible for the most prevalent effects, their simultaneous structure elucidation hinted at their possible mechanism of action, in that the fumonisins resemble a subclass of lipids known as the sphingolipids in their two-dimensional structure.

The sphingolipids are a class of lipids with a wide variety of functions within biological systems. Sphingolipids consist of a characteristic structural unit, which may be linked to other biological molecules giving the functional sphingolipids. This characteristic structural unit is sphingosine (**79**) in animals, and phytosphingosine (**80**) in plants, with the structures of these components shown in **Figure 12**.[50] The fumonisins resemble these structural units and their actions are thought to be as a result of this resemblance.

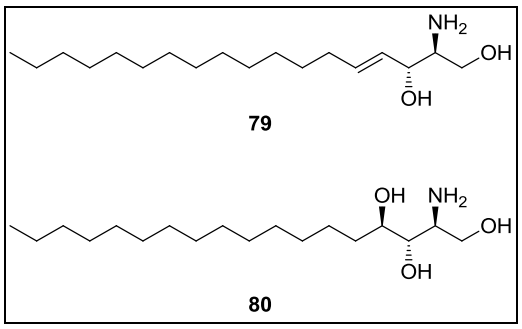

Figure 12: Structure of sphingosine and phytosphingosine.

Sphingolipids have two broad roles within cells. They play an important role in the structure of membranes, and are also involved in the regulation of cellular activities.[47] The regulatory sphingolipids include sphingosine itself and derivatives thereof. Sphingosine and sphingosine-1-phosphate affect cell growth,[51] differentiationand motility,[52,53] calcium storage[54] and the activity of numerous enzymes, including protein kinase C (an important regulatory enzyme).[55] *N*-acyl sphingosine (where the acyl portion is a fatty acid such as stearic acid, $CH_3(CH_2)_{14}COOH$), known as a ceramide (**81**), is thought to be a secondary messenger and anti-proliferation agent within the cell.[56] Glycosylated ceramide derivatives (**82**), such as

[50] Shier, W.T.; Shier, A.C. *Toxin Rev*. **2000**, *19*, 189.
[51] Olivera, A.; Spiegel, S. *Nature* **1993**, *365*, 557.
[52] Merril, A.H.; Sereni, A.M.; Stevens, V.L.; Hannun, Y.A.; Bell, R.M.; Kinkade, J.M. *J. Biol. Chem.* **1986**, *261*, 12610.
[53] Igarashi, Y.; Sadahira, Y.; Yamamura, S.; Hakomori, S. Inhibition of Mouse B16 Melanoma Cell Motility by Sphingosine-1-Phosphate Eicosanoids and Other Bioactive Lipids. In *Cancer, Inflammation, and Radiation Injury.* Honn, K.V. (Ed.), Plenum Press: New York, **1997**, p. 693.
[54] Gosh, T.K.; Bian, J.; Gill, D.L. *Science* **1990**, *248*, 1653.
[55] Ogawa, T.; Hakomori, S. *J. Biol. Chem.* **1990**, *265*, 5385.
[56] Olivera, A.; Spiegel, S. *J. Biol. Chem*. **1992**, *267*, 26121.

cerebrosides and gangliosides as shown in **Figure 13** also play regulatory roles, and are thought to be involved in a diverse array of functions within the cell including cell adhesion,[57] transmembrane signalling,[58] and transmembrane transport.[59] The predominant structural sphingolipids, known as sphingomyelins (**83**), consist of ceramides bound to choline by a phosphodiester bond at the primary hydroxyl group.[50] Evidence of the importance of sphingolipids in the structural integrity of membranes is provided by treatment of cells with sphingomyelinase enzymes (which are components of some bacterial toxins and arachnid venoms), producing cytolysis and membrane disruption due to their hydrolytic action at the phosphodiester bond of the sphingomyelins.[60]

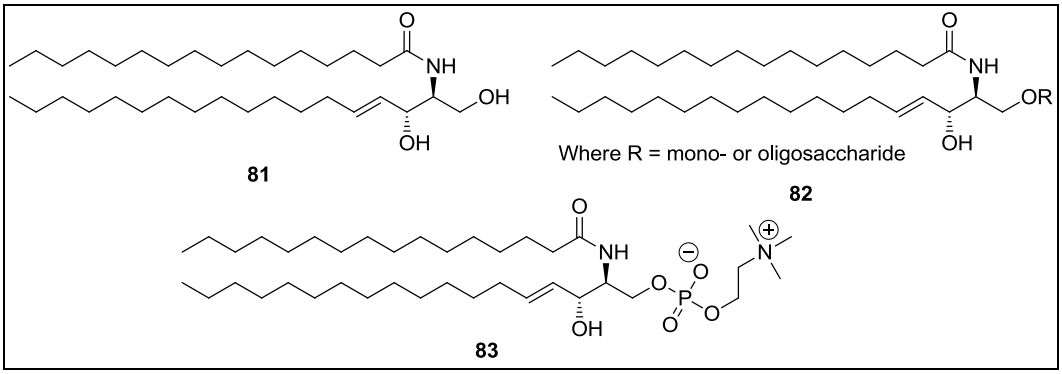

Figure 13: A ceramide, glycosylated ceramide and sphingomyelin.

The biochemical pathways of sphingolipid production and breakdown have been thoroughly studied, and is shown in **Scheme 7**.[61,62,63] *De novo* sphingolipid biosynthesis begins with the transferase catalysed condensation of palmitoyl-coenzyme A (**84**) with serine (**85**) giving 3-ketosphinganine (**86**), which undergoes an enzymatic stereoselective reduction to dihydrosphingosine (**87**) (also known as sphinganine). Dihydrosphingosine is then acylated by ceramide synthase (also known as sphingosine *N*-acyl transferase), giving a dihydro-

[57] Shayman, J.A.; Deshmukh, G.D.; Mahdiyoun, S.; Thomas, T.P.; Barcelon, F.S.; Radin, N.S. *J. Biol. Chem*. **1991**, *266*, 22968.
[58] Hakamori, S.I. *Perspectives in Cancer Res.* **1996**, *56*, 5309.
[59] Sandvig, K.; Dubinina, E.; Garred, O.; Prydz, K.; Kozlov, J.V.; Hansen, S.H.; van Deurs, B. *Biochem. Soc. Trans*. **1992**, *20*, 724.
[60] Harvey, A.L. Cytolytic Toxins. In *Handbook of Toxinology*. Shier, W.T., Mebs, D. (eds.), Marcel Dekker, Inc.: New York, **1990**, p. 1.
[61] Merrill, A.H.; Schmelz, E-M.; Dillehay, D.L.; Spiegel, S.; Shayman, J.A.; Schroeder, J.J.; Riley, R.T.; Voss, K.A.; Wang, E. *Toxicol. Appl. Pharmacol*. **1997**, *142*, 208.
[62] Merrill, A.H.; Sullards, M.C.; Wang, E.; Voss, K.A.; Riley, R.T. *Environ. Health Perspect*. **2001**, *109*, 283.
[63] WHO. Fumonisin B1 (Environmental Health Criteria 219). *International programme on chemical safety*. World Health Organization: Geneva, **2000**.

ceramide (**88**), which undergoes enzymatic desaturation to give a ceramide (**81**). Interestingly, the regulating sphingolipid sphingosine is not an intermediate in the *de novo* synthesis of sphingolipids, but is produced by the hydrolysis of ceramides by ceramidase. Sphingosine is also a substrate for ceramide synthase and can be acylated giving a ceramide, allowing for a constant turnover of sphingolipids, without the need for complete *de novo* synthesis.[60] Ceramides produced by this pathwaycan then be modified by glycosylation or phosphorylation to give to give various other structural and regulatory sphingolipids.

Due to the structural resemblance between dihydrosphingosine (sphinganine) and the backbone of the fumonisins, it was thought that the fumonisins may affect the biosynthesis of sphingolipids in some way. Soon after the elucidation of the two-dimensional structure of the fumonisins, the first studies into the mechanism of action of the fumonisins were published, and the expected result was confirmed.

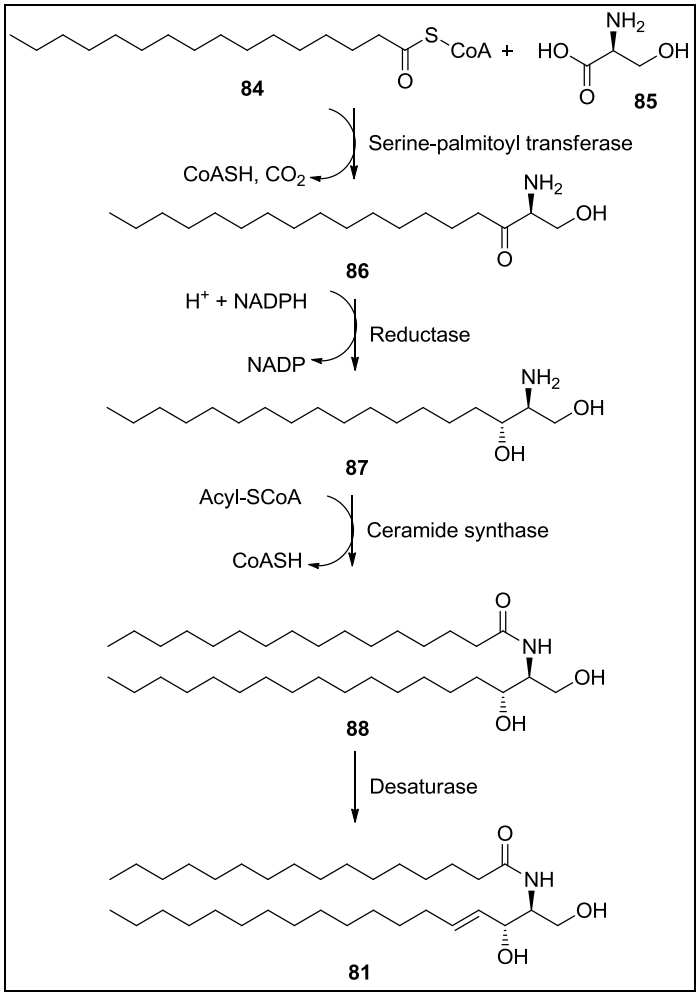

Scheme 7: Biosynthesis of ceramides.

The first indication of the effect of fumonisins on sphingolipid biosynthesis was in a study on

the effect fumonisins B_1 and B_2 had on the incorporation of [^{14}C]-serine into sphingolipids.[64] The incorporation was measured by hydrolysing the lipid extract of two groups of rat hepatocytes, one which had been exposed to fumonisins, and the other not. The hepatocytes were incubated in the presence of [^{14}C]-serine, and after lipid extraction and hydrolysis, gave the free long-chain bases. The hydrolysed lipid extracts were then separated by thin layer chromatography, which indicated that the hepatocytes which had been exposed to fumonisins contained significantly less [^{14}C]-sphingosine than the control group, while synthesis of other serine-containing biosynthetic products was not affected. It was also found that the amount of [^{14}C]-sphinganine present in hepatocytes was significantly elevated in fumonisin-exposed samples.

Since ceramide synthase converts sphinganine to a ceramide, and sphinganine was found to accumulate in fumonisin-exposed cells, it was possible that ceramide synthetase was being inhibited by fumonisins. In the same study, *in vitro* studies of activity of the enzyme in intact rat liver microsomes in the presence of fumonisins showed that the enzyme is indeed inhibited, with an IC_{50} of 0.1μM. This result was confirmed in two similar experiments, one in renal cells[65] and another in mouse cerebellar neurons,[66] which found the IC_{50} value to be 0.075μM, while also showing that concentrations of complex sphingolipids in the culture decreased while that of sphingosine/sphinganine and other bioactive derivatives thereof increased.

The accepted mechanism of action of the fumonisins on ceramide synthase involves the various substituents on the backbone of the fumonisin toxin. It is thought that the sphingoid-like backbone competes with sphingoid bases for binding to ceramide synthase, while the anionic tricarballylic acid moiety interferes with the binding of acyl-CoA to the enzyme.[58] Evidence of this comes from experiments showing that hydrolysis of the tricarballylic acid fragment decreases the potency of the fumonisins, and allows for the hydrolysed backbone to be acylated,[67] and that the inhibition is dependent on the concentration of the natural substrates for the enzyme.[64] It is also widely accepted that the free amine group plays a vital role in the toxicity of the fumonisins.[68] Evidence of this comes from studies of the toxicity of

[64] Wang, E.; Norred, W.P.; Bacon, C.W.; Riley, R.T.; Merril, A.H. *J. Biol. Chem.* **1991**, *266*, 14486.
[65] Yoo, H.; Norred, W.P.; Wang, E.; Merrill, A.H.; Riley, R.T. *Toxicol. Appl. Pharmacol.* **1992**, *114*, 9.
[66] Merrill, A.; Van Echten, G.; Wang, E.; Sandhoff, K. *J. Biol. Chem.* **1993**, *268*, 27299.
[67] Humpf, H.U.; Schmelz, E.M.; Meredith, F.I.; Vesper, H.; Vales, T.R.; Menaldino, D.S.; Liotta, D.C.; Merrill, A.H. *J. Biol. Chem.* **1998**, *273*, 19060.
[68] Gelderblom, W.C.; Cawood, M.E.; Snyman, S.D.; Vleggaar, R; Marasas, W.F.O. *Food Chem. Toxicol.* **1993**, *31*, 407.

N-acylated fumonisins (fumonisin A_1 and fumonisin A_2), which have been found to have as little as 2% of the ability of fumonisin B_1 in inhibiting ceramide synthase.[69]

The observed cellular and macroscopic pathologies associated with ingestion of the toxins is thought to be related to the disruption of sphingolipid biosynthesis. The mechanism of the induction of these effects is not clear, though there is evidence that some pathways involved in these biological events are mediated or affected by sphingolipids, and a disruption of biosynthesis of sphingolipids would be expected to affect these pathways. Before the elucidation of the structure of the fumonisins and their mechanism of action, the mascroscopic effects that were associated with the fumonisins appeared to be unrelated.

The consumption of *Fusarium*-contaminated maize was associated with four pathologies-namely, equine leukoencephalomalacia (LEM), pulmonary oedema and hydrothorax in swine, oesophageal cancer in humans and rat liver cancer, before the causal agent was determined.[70] Due to fumonisin B_1 being the major fumonisin found in most samples of affected maize, most subsequent studies on animals have involved fumonisin B_1, which has been proven to be the causal agent of all of the above pathologies, amongst others.

Fumonisin B_1 is known to cause LEM in horses, a disease characterised by necrotic lesions predominantly in the white matter of the cerebrum, which is usually fatal.[24] Both oral and intravenous dosing of fumonisin B_1 has been shown to cause the disease, with the dose required to produce symptoms being quite low, at around 0.125 mg/kg body weight/day for 7 days for intravenous dosing[23] and 44.3 mg/kg over 29 days by oral dosing.[24] The neurological symptoms are often accompanied by pathology of liver cells.[71]

Pulmonary oedema and hydrothorax are also associated with consumption of maize contaminated with fumonisin B_1 by pigs.[72] The main symptoms observed include massive fluid build-up in the thoracic cavity, with marked swelling of lung tissue. An intravenous dose of 0.4 mg/kg body weight/day was found to be fatal after five days, showing that small doses of the toxin are sufficient to produce the pathology. These symptoms were accompanied by pathological changes in both the liver (cell enlargement, fibrosis) and pancreas (necrosis,

[69] Merrill, A.H.; Wang, E; Vales, T.R.; Smith, E.R.; Schroeder, J.J.; Menaldino, D.S. *Adv. Exp. Med. Biol.* **1996**, *392*, 297.
[70] Marasas, W.F.O. *Environ. Health Perspect.* **2001**, *109* (Suppl. 2), 239.
[71] Ross, P.F.; Ledet, A.E.; Owens, D.L.; Rice, L.G.; Nelson, H.A.; Osweiler, G.D.; Wilson, T.M. *J. Vet. Diagn. Invest.* **1993**, *5*, 69.
[72] Harrison, L.R.; Colvin, B.M.; Greene, J.T.; Newman, L.E.; Cole, J.R. *J. Vet. Diagn. Invest.* **1990**, *2*, 217.

morphology changes). The oedema is thought to be caused by reduced mechanical efficiency of the left ventricle,[73] caused by disruption of sphingolipid metabolism.

Epidemiological studies have found a link between the consumption of fumonisin-contaminated maize and increased risk for neural tube defects in human populations in China,[74] southern Africa[75] and the United States of America.[76] Neural tube defects in mouse studies have been directly linked to folate uptake, where the gene coding for the folate receptor (*Folbp1*) has been disrupted.[77] The folate receptor is known to be a glycophosphatidylinositol (GPI) anchored receptor, which is anchored in lipid rafts, whose structure is stabilised by the presence of complex glycosphingolipids.[78] It has been shown in mouse embryo models that the fumonisins disrupt folate uptake, and that the disruption can be reduced by introducing glycosphingolipids, indicating that the disruption of sphingolipid metabolism by fumonisins likely affects folate uptake, causing the observed neural tube defects.[79]

Consumption of fumonisin-containing maize has also been associated with high incidences of oesophageal cancer in humans in studies in southern Africa,[80] Italy,[81] Iran[82] and the USA,[83] while studies in China seemed to indicate a link between fumonisins and promotion of primary liver cancer.[84,85] Evidence of the carcinogenicity of the fumonisins has been found in animal models, with the kidney and liver appearing to be the main sites of carcinogenesis. Fumonisin B_1 has been shown to be a tumour promoter,[21] and not a tumour initiator[86] in rats, with different strains and sexes showing different targets. As a result of these studies, the

[73] Constable, P.D.; Smith, G.W.; Rottinghaus, G.E.; Haschek, W.M. *Toxicol. Appl. Pharmacol.* **2000**, *162*, 151.
[74] Melnick, M.; Marazita, M.L. *J. Craniofac. Genet. Dev. Biol.* **1998**, *18*, 233.
[75] Ncayiyana, D.J. *S. Afr. Med. J.* **1986**, *69*, 618.
[76] Hendricks, K. *Epidemiology* **1999**, *10*, 198.
[77] Piedrahita, J.A.; Oetama, B.; Bennett, G.D. *Nat. Genet.* **1999**, *23*, 228.
[78] Elortza, F.; Nuhse, T.S.; Foster, L.J. *Mol. Cell Proteomics* **2003**, *2*, 1261.
[79] Gelineau-van Waes, J.; Starr, L.; Maddox, J.; Aleman, F.; Voss, K.A.; Wilberding, J.; Riley, R.T. *Birth Defects Res., Part A.* **2005**, *73*, 487.
[80] Sydenham, E.W.; Thiel, P.G.; Marasas, W.F.O.; Shephard, G.S.; Van Schalkwyk, D.J.; Koch, K.R. *J. Agric. Food Chem.* **1990**, *38*, 1900.
[81] Franceschi, S.; Bidoli, E.; Baron, A.E.; La Vecchia, C. *J. Natl. Cancer I.* **1990**, *82*, 1407.
[82] Shephard, G.S.; Marasas, W.F.O.; Leggott, N.L.; Yazdanpanah, H.; Rahimian, H.; Safavi, N. *J. Agr. Food Chem.* **2000**, *48*, 1860.
[83] Gelderblom, W.C.; Marasas, W.F.O.; Vleggaar, R.; Thiel, P.G.; Cawood, M.E. *Mycopathologia* **1992**, *117*, 11.
[84] Chu, F.S.; Li, G.Y. *Appl. Environ. Microbiol.* **1994**, *60*, 847.
[85] Li, F.Q.; Yoshizawa, T.; Kawamura, O.; Luo, X.Y.; Li, Y.W. *J. Agric. Food. Chem.* **2001**, *49*, 4122.
[86] Gelderblom, W.C.A.; Semple, E.; Marasas, W.F.O.; Farber, E. *Carcinogenesis* **1992**, *13*, 433.

International Agency for Research on Cancer has classified fumonisin B_1 as "possibly carcinogenic to humans".[87]

Along with the above effects which manifest as distinct pathologies, the fumonisins have been shown to cause apoptosis,[88] oxidative stress,[89] along with being cytotoxic.[90] Most of these studies have been conducted on distinct cell lines, so generalization of the effects of ingestion of fumonisins is still not possible.

The fumonisins have also been shown to be toxic to a number of plant species including jimsonweed[91] and duckweed[92] causing necrosis and other cellular changes at the site of administration, thought to be produced as a result of disruption in sphingolipid metabolism.

1.1.4. Biosynthesis

Studies on the biosynthesis have revealed the molecular origins of most of the atoms making up the fumonisin B_1. C-3–C-20 were found to be derived from acetate in an experiment where *Fusarium verticilliodes* was grown in a medium enriched with [^{13}C]-acetate, which gave rise to ^{13}C-enriched fumonisin B_1.[93] L-Alanine was found to be the source of C-1, C2 and the amino group on C-2 in a similar experiment where the fungus was grown in the presence of [^{2}H,^{13}C]-L-alanine.[94] The methyl groups on C-12 and C-16 were shown to be derived from L-methionine in experiments where cultures were grown in a medium enriched with [*methyl*-d_3]-L-methionine, from which fumonisin B_1 with ^{2}H incorporated into these methyl groups of the toxin was isolated. The oxygen atoms of the hydroxyl groups on C-5, C-10, C-14 and C-15 were found to be derived from molecular oxygen in a culture study in the presence of $^{18}O_2$,

[87] WHO. IARC monographs on the evaluation of carcinogenic risk to humans. Some naturally occurring substances: food items and constituents, heterocyclic aromatic amines and mycotoxins, vol. 56. Lyon: IARC; **1993**, p. 445.
[88] Tolleson, W.H.; Dooley, K.L.; Sheldon, W.G.; Thurman, J.D.; Bucci, T.J.; Howard, P.C. The mycotoxin fumonisin induces apoptosis in cultured human cells and in livers and kidneys of rats. In *Advances in experimental and medical biology*. Jackson, L.S., DeVries, J.W., Bullerman, L.B. (eds). Plenum Press: New York, **1996**, p. 237.
[89] Stockmann-Juvala, H.; Mikkola, J.; Naarala, J.; Loikkanen, J.; Elovaara, E.; Savolainen, K. *Free Radic. Res.* **2004**, *38*, 933.
[90] Tolleson, W.H.; Melchior, W.B.; Morris, S.M.; McGarrity, L.J.; Domon, O.E.; Muskhelishvili, L. *Carcinogenesis* **1996**, *17*, 239.
[91] Abbas, H.K.; Gelderblom, W.C.; Cawood, M.E.; Shier, W.T. *Toxicon* **1993**, *31*, 345.
[92] Abbas, H.; Shier, W.; Seo, J.; Lee, Y.; Musser, S. *Toxicon* **1998**, *36*, 2033.
[93] Blackwell, B.A.; Edwards, O.E.; Fruchier, A.; ApSimon, J.W.; Miller, J.D. *Adv. Exp. Med. Bio.* **1996**, *392*, 75.
[94] Branham, B.E.; Plattner, R.D. *Mycopathologia* **1993**, *124*, 99.

while the oxygen atom of the hydroxyl group at C-3 was found to be derived from acetate.[95] The origin of the tricarballylic ester moiety is still unclear, though it is thought that it originates from the citric acid (Krebs) cycle.[93]

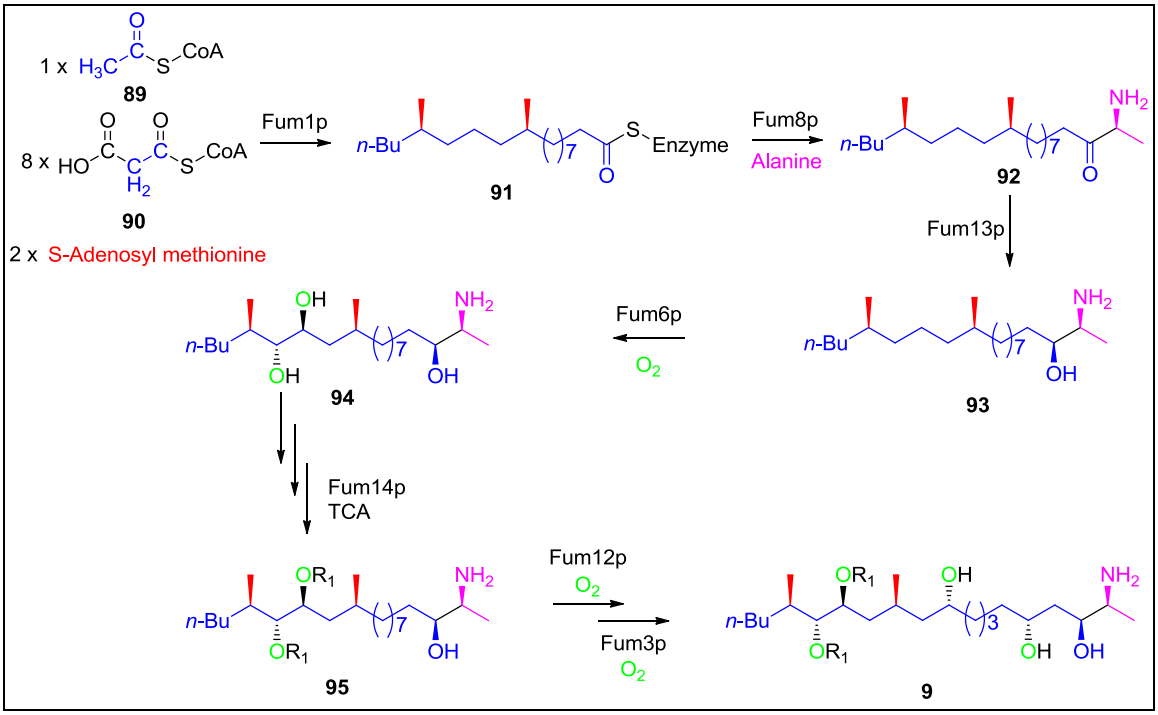

Scheme 8: Biosynthesis of fumonisin B_1, showing the origin of each of the components.[97]

The acetate derived backbone of the fumonisins could be derived from two possible biosynthetic routes, one via fatty acid biosynthesis, and the other polyketide biosynthesis, with both pathways known to use acetate as a C_2 building block. It was shown that fumonisins are most likely produced by a polyketide synthesis pathway in a study where disruption of the *FUM1* (previously *FUM5*) gene resulted in a 99% reduction in fumonisin production.[96] The carbon backbone of the fumonisins is synthesised by a highly reducing polyketide synthase (Fum1p), coded for by the *FUM1* gene located within the *FUM* gene cluster. The synthase is responsible for producing a highly reduced, dimethylated C_{18} alkyl chain, through the action of a set of seven individual functional domains within the synthase.[97] The product of the *FUM8* gene (Fum8p) is thought to be responsible for condensing the highly reduced polyketide with L-alanine, while simultaneously offloading the newly synthesised alkyl chain

[95] Caldas, E.D.; Sadilkova, K.; Ward, B.L.; Jones, A.D.; Winter, C.K.; Gilchrist, D.G. *J. Agric. Food Chem.* **1998**, *46*, 4734.
[96] Proctor, R.H.; Desjardins, A.E.; Plattner, R.D.; Hohn, T.M. *Fungal Genet. Biol.* **1999**, *27*, 100.
[97] Gerber, R.; Lou, L.; Du, L. *J. Am. Chem. Soc.* **2009**, *131*, 3148.

from the synthase[97] giving a 3-keto intermediate. *FUM13* produces a ketoreductase (Fum13p), which stereoselectively reduces the ketone to the hydroxyl group on C-3.[98] The subsequent hydroxylations and esterifications have been less well studied.[99] It is thought that hydroxyls at C-14 and C-15 are introduced by a P450 oxygenase (Fum6p) coded for by *FUM6*, while the hydroxyl at C-10 is introduced by a similar oxygenase (Fum12p), coded for by *FUM12*.[100] The product of *FUM14* (Fum14p) is thought to be responsible for esterification of C-14 and C-15 with tricarballylic acid,[101] and the product of *FUM3* (Fum3p) introduces the hydroxyl at C-5, giving fumonisin B_1.[102] The biosynthesis is summarised in **Scheme 8**.

1.2. THE AAL TOXINS

The AAL toxins are a class of host specific phytotoxins affecting tomato plants, produced by the fungus *Alternaria alternata* f. sp. *lycopersici*.[15] The toxins are known to produce stem canker disease in susceptible tomato varieties (such as *Lycopersicon esculentum* Mill), giving rise to cankerous spots on the stem, and necrosis of leaves around the midrib.[103]

1.2.1. Discovery and Structure Elucidation

In 1976 a host specific toxin was isolated from *Alternaria alternata* and chemically characterised.[104] This toxin was chemically distinct from other toxins previously isolated from *Alternaria alternata*, and was found to reproduce the symptoms of stem canker disease in certain cultivars of tomato plants while other varieties of tomatoes as well as representatives from sixteen genera of nine plant families were found to be unaffected significantly by the toxin. The disease and symptoms were indistinguishable from those caused by infection of *Alternaria alternata* f. sp. *lycopersici*, leading to the conclusion that the new isolate was indeed a host-specific toxin.

Five years after the toxin was first identified, more detail began to emerge about the chemical nature of the toxins. It was found that the toxin as isolated in 1976 actually contained two fractions which were separable by isoelectric focussing, or by thin layer chromatography.

[98] Yi, H.; Bojja, R.S.; Fu, J.; Du, L. *J. Agric. Food Chem.* **2005,** *53*, 5456.
[99] Du, L.; Zhu, X.; Gerber, R.; Huffman, J.; Lou, L.; Jorgenson, J.; Yu, F.; Zaleta-Rivera, K.; Wang, Q. *J. Indust. Microbiol. Biotech.* **2008**, *35*, 455.
[100] Bojja, R.S.; Cerny, R.L.; Procter, R.H.; Du, L. *J. Agric. Food Chem.* **2004**, *52*, 2855.
[101] Zaleta-Rivera, K.; Xu, C.; Yu, F.; Butchko, R.A.; Proctor, R.H.; Hidalgo-Lara, M.E.; Raza, A.; Dussault, P.H.; Du, L. *Biochem.* **2006**, 45, 2561.
[102] Ding,Y.; Bojja, R.S.; Du, L. *Appl. Environ. Microbiol.* **2004**, *70*, 1931.
[103] Grogan, R.G.; Kimble, K.A.; Mishagi, I. *Phytopathology* **1975**, *65*, 880.
[104] Gilchrist, D.; Grogan, R. *Phytopathology* **1976**, *66*, 165.

These fractions were named AAL-toxin TA and AAL-toxin TB, and both were found to induce stem canker in susceptible tomato cultivars.[16] A detailed study into the structure of AAL-toxin TA was undertaken, using mass spectrometry, chemical derivatization and NMR spectroscopy. Base hydrolysis of AAL-toxin TA gave propane-1,2,3-tricarboxylic acid (**96**) and an aminopentol (**12**) as shown in **Figure 14**, whose molecular formula was determined to be $C_{19}H_{41}NO_5$ by high resolution mass spectrometry of the methylated and deuteriomethylated aminopentol. Subsequent analysis of the daughter ions produced by fragmentation led to the deduction of the molecular formula, and consequently structure of some of the fragments. Proton-coupled ^{13}C NMR spectroscopy (chemical shift values and coupling pattern) established the connectivity of some of the identified fragments. By comparing the chemical shift values obtained in the experiment with those calculated by the Lindeman-Adams rule and parameters from Wehrli and Wirthlin, the location of the two methyl groups was established. Proton NMR spectroscopy confirmed the above conclusions, and analysis of the coupling constants between protons on the left side of the aminopentol led to the conclusion that the absolute configuration at the stereocentres at C-2, C-4 and C-5 were all either *R* or *S*.

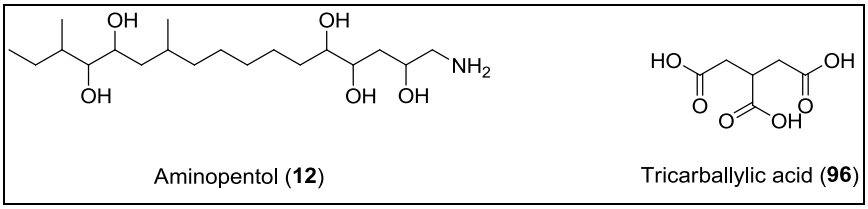

Figure 14: Structure of aminopentol and tricarballylic acid as derived from AAL-toxin TA.

The AAL-toxin TA was found to have both a major and minor component on the ^{13}C NMR spectrum, and after examination of chemical shifts in the ^{13}C and ^{1}H NMR spectra, it was found that these components differed by the site of esterification of the tricarballylic acid, with the major component (AAL-toxin TA_1) being the ester of the terminal carboxyl of the tricarballylic acid and the hydroxyl on C-13, and the minor component (AAL-toxin TA_2) to be the ester at C-14.[16] It was also speculated in the same paper, that the AAL-toxin TB fraction had the same carbon skeleton, but lacked the hydroxyl group at C-5, and was thought to have different absolute configuration at the right side of the backbone.

The fumonisins were discovered before any further reports on the structure of the AAL toxins were published. The 2-D structure elucidation of the fumonisins showed that they bore resemblance to the 2-D structure of the AAL-toxins, though differences were apparent. The fumonisins had an additional carbon at the amino end, and two additional carbons at the other end, while the remaining functionality on the backbone remained the same. As a result, much of the investigation into the structure of the fumonisins (which had a wider range of biological effects, therefore attracting more attention) was accompanied by simultaneous study of the

structure of the AAL toxins. The absolute stereochemistry of the backbone of AAL-toxin TA was established by Boyle *et al.* in a manner nearly identical to that of their determination of the absolute configuration of fumonisin B_2.[26] A number of diastereomers of the left and right halves were synthesised separately, and their ^{1}H NMR spectra were compared to that of **12**. This allowed them to establish the relative stereochemistry of the two halves, and also showed that only the spectrum of one diastereomer of each half matched that of the natural product. Coupling of the appropriate halves by a Wittig reaction, followed by peracetylation of the product and NMR spectroscopic studies in the presence of both an achiral and a chiral shift reagent led to the conclusion that **97** was the 3-D structure of the backbone of AAL-toxin TA (**Figure 15**).

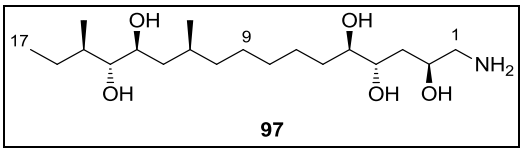

97

Figure 15: Absolute configuration of the backbone of AAL-toxin TA.

The stereochemistry of the C-1−C-5 fragment was confirmed in a study by Oikawa *et al.*[105] who used degradation studies and Mosher ester analysis to confirm that the stereochemistry at C-2 was *S*. Synthesis of model compounds of the right half of the toxin and comparative analysis of the ^{13}C and ^{1}H NMR spectra of the model compounds and natural toxin allowed for the assignment of the absolute configuration at C-4 (*S*) and C-5 (*R*), confirming the result obtained by Boyle *et al.*[26] In the same studies the stereochemistry of the tricarballylic ester fragment was found to be identical to that of the tricarballylic ester of the fumonisins, establishing the configuration of the fragment for the fumonisins.

The known structures of the AAL-toxins are summarised in **Figure 16** and **Table 5**.

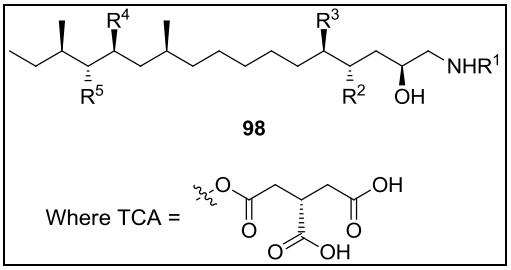

Figure 16: Basic structure of the AAL-toxins.

[105] Oikawa, H., Matsuda, I., Ichihara, A., Kohmoto, K. *Tetrahedron Lett*. **1994**, *35*, 1223.

Table 5: AAL-toxin analogues.

Analogue	R^1	R^2	R^3	R^4	R^5
AAL-toxin TA_1	H	OH	OH	TCA	H
AAL-toxin TA_2	H	OH	OH	OH	TCA
AAL-toxin TB_1	H	OH	H	TCA	H
AAL-toxin TB_2	H	OH	H	OH	TCA
AAL-toxin TC_1	H	H	H	TCA	H
AAL-toxin TC_2	H	H	H	OH	TCA
AAL-toxin TD_1	$COCH_3$	OH	H	TCA	H
AAL-toxin TD_2	$COCH_3$	OH	H	H	TCA
AAL-toxin TE	$COCH_3$	H	H	TCA	H
AAL-toxin E_2	$COCH_3$	H	H	H	TCA

1.2.2. Synthetic Studies

After the elucidation of the structure of the AAL-toxins, the mode of action of the toxins was of interest, especially since the fumonisins seemed to exhibit a broader spectrum of activity, while having a structure remarkable similar to that of the AAL-toxins. In order to study the mode of action, it is required to know the role that the structural features of the toxin play in the observed toxicity. To do this, a structure-activity relationship (SAR) study is required. In this interest, AAL-toxin TA_1 was synthesised by Oikawa *et al.*[106] by a route which could easily give access to analogues of the left half of the toxin. As with the synthetic studies on the fumonisins, the approach involved retrosynthetically dividing AAL-toxin TA_1 into three fragments: the left- and right-side, and the tricarballylic fragment, which were then each synthesised separately, and coupled at a late stage of the synthesis.

Their synthesis of the left fragment (**Scheme 9**) began from methyl (*R*)-3-hydroxy-2-methylpropionate (**99**), which was protected as the *t*-butyldiphenylsilyl ether before being reduced to the aldehyde by DIBALH. The aldehyde was subjected to a Grignard reaction with vinylmagnesium bromide, and the allylic alcohol produced was protected as the benzyl ether. This allowed for separation of the two diastereomers formed as a result of the Grignard reaction, giving **100** as a single enantiomer. The alkene (**100**) was then subjected to an osmium-catalysed dihydroxylation, which proceeded stereoselectively, giving **101** as a 6:1 mixture which was separated by column chromatography. The vicinal diol was converted into the epoxide via the acetoxonium ion method described by Kolb and Sharpless,[107] and this epoxide was opened by reaction with the lithium acetylide derived from ethyl ethynyl ether.

[106] Oikawa, H.; Yamawaki, D.; Kagawa, T.; Ichihara, A. *Tetrahedron Lett*. **1999**, *40*, 6621.
[107] Kolb, H.C.; Sharpless, K.B. *Tetrahedron* **1992**, *48*, 10515.

The ether was cleaved by mercury(II) chloride hydrolysis, and the product converted into lactone (**102**). The backbone was extended by a single carbon atom by deprotection of the silyl ether by TBAF, oxidation to the aldehyde by the Swern protocol, and a Wittig reaction with methyltriphenylphosphonium bromide. Reduction of the alkene, accompanied by hydrogenolysis of the benzyl ether gave alcohol (**103**), which was reprotected as the benzyl ether by benzyl trichloroacetimidate and triflic acid. Stereoselective α-methylation of the lactone by methyl iodide in the presence of lithium bis(trimethylsilyl)amide gave **104** as the target for the left side of the toxin after separation of the 8.7:1 mixture obtained.

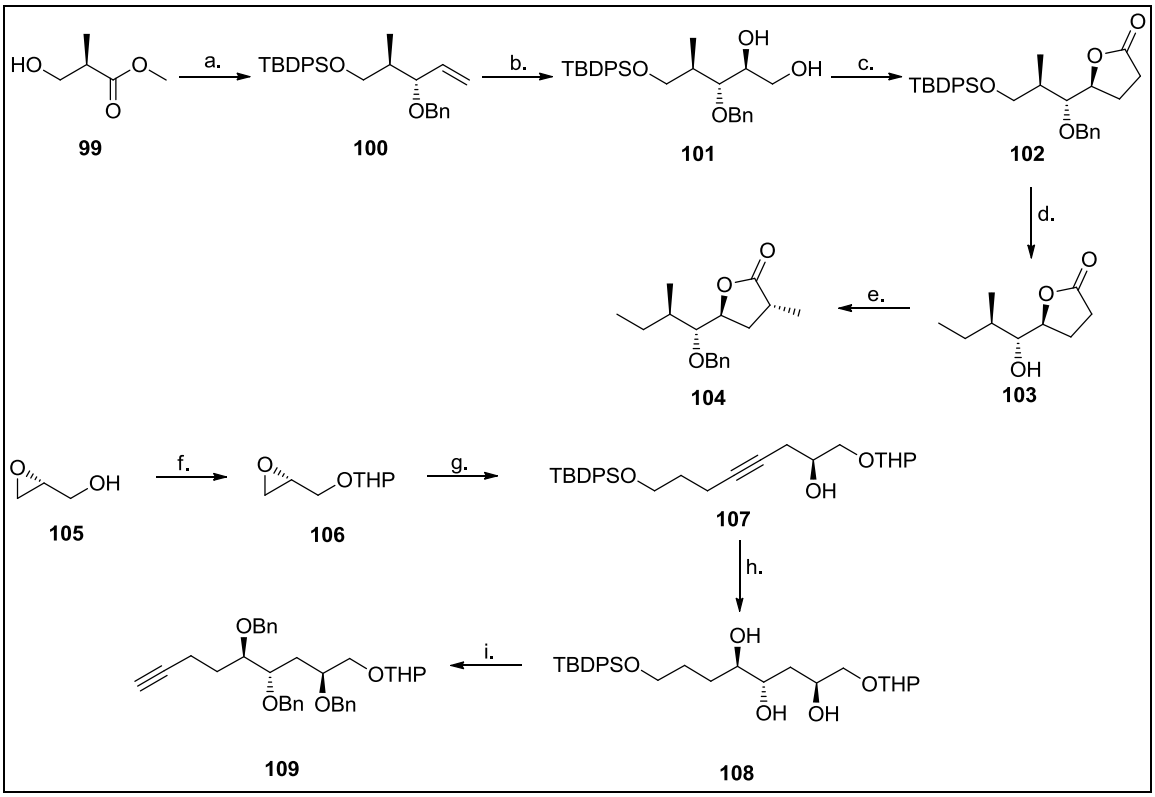

Scheme 9: Synthesis of targets for the left- and right-sides of AAL-toxin TA_1.

> *Reagents*: a. i). TBDPSCl, Imidazole, ii). DIBALH, iii). vinyl-MgBr, iv). NaH, BnBr, separation; b. OsO_4, NMO; c. i). $MeC(OMe)_3$, PPTS, ii). AcBr, K_2CO_3, iii). Ethyl ethynyl ether, *n*-BuLi, $BF_3.Et_2O$, iv). $HgCl_2$, v). K_2CO_3, HCl; d. i). TBAF, ii). $(COCl)_2$, DMSO, Et_3N, iii). CH_3PPh_3Br, *n*-BuLi, iv). H_2, Pd/C; e. i). $CCl_3C(NH)OBn$, TfOH, ii). LiHMDS, MeI; f. dihydropyran; g. $HCC(CH_2)_4OTPDPS$, $BF_3.Et_2O$; h. i). H_2, Pd-$BaSO_4$, quinoline, ii). OsO_4, DHQD-IND, $K_3Fe(CN)_6$, K_2CO_3; i. i). BnBr, NaH, TBAI, ii). TBAF, iii). CBr_4, PPh_3, *i*Pr_2NEt, iv). *n*-BuLi, $BF_3.Et_2O$.

Synthesis of the right-side of the toxin began by the protection of (*R*)-glycidol (**105**) as the tetrahydropyranyl ether (**106**), and reaction of the epoxide with lithium acetylide of TBDPS-protected but-3-yn-1-ol to give alcohol (**107**) as product. Partial hydrogenation of the alkyne in the presence of $Pd/BaSO_4$ and quinoline gave the *cis*-allylic alcohol which was subjected to Sharpless asymmetric dihydroxylation to give diol (**108**). Benzylation by benzyl bromide and

sodium hydride in the presence of tetrabutylammonium iodide gave the perbenzylated product. The silyl ether was removed by treatment with TBAF, and the alcohol converted into the target alkyne (**109**) by a Corey-Fuchs procedure after Swern oxidation.

The tricarballylic fragment was synthesised from racemic dimethyl 2-benzylsuccinate (**110**) as shown in **Scheme 10** using enzymatic kinetic resolution by porcine pancreatic lipase (PPL) to generate the required stereochemistry. Enzymatic hydrolysis of the terminal methyl ester of the (*S*)-enantiomer gave monoester (**111**) in 82% ee. Methylation of this mixture with diazo-methane followed by a second enzymatic resolution gave the monoester in 95% ee. The remaining ester was cleaved by base hydrolysis before the free carboxylic acid groups were protected as trimethylsilylethyl ethers. Free acid (**112**) was produced by ruthenium tetroxide oxidation of the benzyl group.

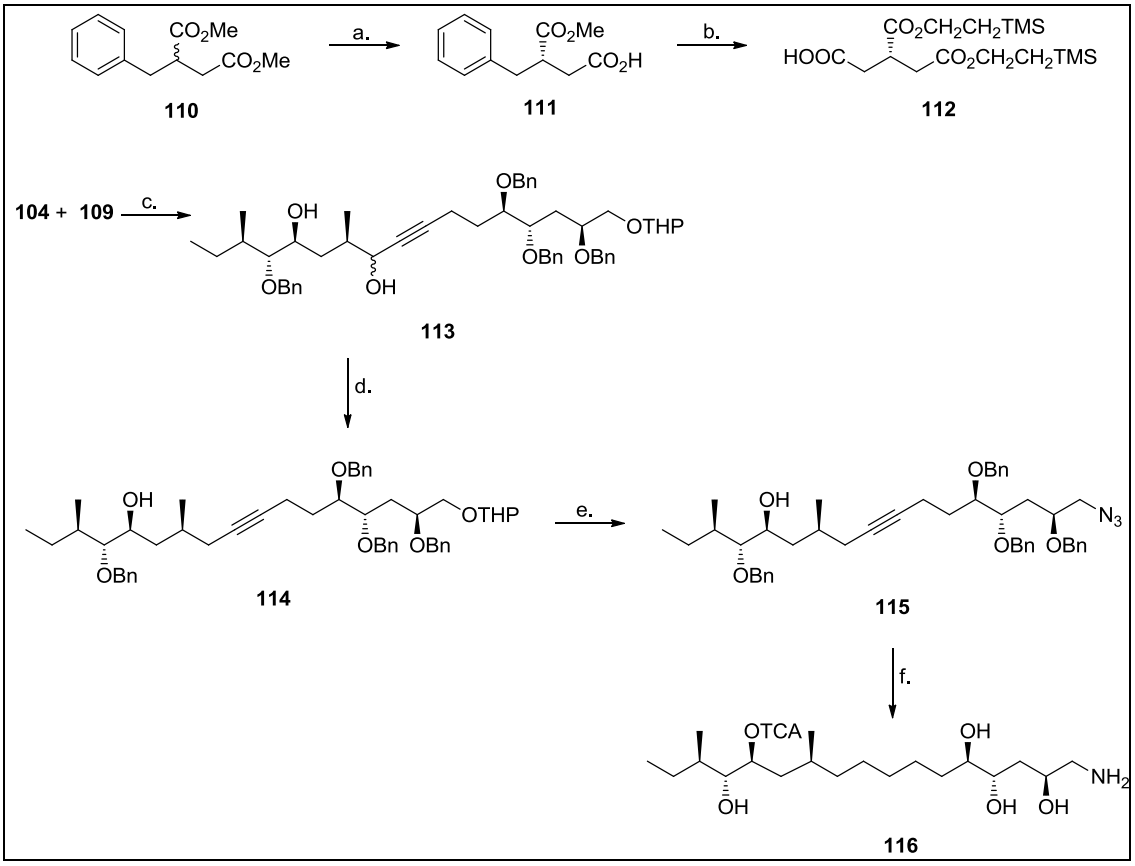

Scheme 10: Synthesis of the TCA fragment and coupling to give AAL-toxin TA_1.

Reagents: a. i). PPL, 0.1M KH_2PO_4 (pH 7.2), ii). CH_2N_2, iii). PPL, 0.1M KH_2PO_4 (pH 7.2); b. i). NaOH, ii). $TMS(CH_2)_2OH$, EDCI, Et_3N, DMAP, iii). $RuCl_2$, $NaIO_4$; c. i). *n*-BuLi, ii). $NaBH_4$, $CeCl_3$; d. i). Ac_2O, HCO_2H, ii). $Pd(OAc)_2$, *n*-Bu_3P, iii). $LiAlH_4$; e. i). PPTS, ii). PPh_3, DEAD, HN_3; f. i). *m*-$NO_2C_6H_4COCl$, Et_3N, DMAP, **110**, ii). TBAF, iii).H_2, Pd/C.

Lithiated alkyne (**109**) was coupled to lactone (**104**) and the resulting ketone reduced under Luche conditions giving a diastereomeric mixture of **113**. Formylation of the free hydroxyl

groups by formic acid in the presence of acetic anhydride and reduction of the formyl ester alpha to the alkyne by $Pd(OAc)_2$ and $(n\text{-}Bu)_3P$ gave the alkane. The second formyl ester was reduced by $LiAlH_4$ giving alcohol (**114**). Hydrolysis of the tetrahydropyranyl ether by pyridinium *p*-toluenesulfonate in ethanol, and azide substitution at the primary hydroxyl group under Mitsunobu conditions gave azidoalcohol (**115**). Alcohol (**115**) was coupled to acid (**112**) in the presence of triethylamine, DMAP and *m*-nitrobenzoyl chloride. Removal of the silyl protection by TBAF, followed by hydrogenation over Pd/C gave target AAL toxin TA_1 (**116**).

This synthesis represents the first total synthesis of an AAL toxin. Oikawa *et al.*[105] demonstrated that a number of C-14 and C-15 diastereomers of the toxin could be synthesised by stereoselective crotylation of an L-glutamate derivative to give (after hydrogenation) diastereomers of alcohol (**103**) which after use to synthesise the complete toxin, could then be used in SAR studies. There have been no reports of SAR studies on these compounds however.

1.2.3. Biological Effects

With a structure so similar to that of the fumonisins, it could easily be expected that the AAL-toxins would exhibit very similar effects on biological systems. This however has not been observed, with the AAL toxins only affecting a single cultivar of tomatoes, though there is evidence that the toxins do affect other plants,[108] as well as mammalian cells.[109]

The AAL-toxins are thought to target ceramide synthase (as do the fumonisins) in animal models,[110] though their target in plants has not been definitively proven. It has been proven however, that AAL-toxins disrupt sphingolipid biosynthesis in plant systems, producing increased concentrations of free sphingoid bases such as phytosphingosine (**80**) and sphinganine (**87**).[111] The AAL-toxins are also known to cause apoptosis in susceptible tomato cultivars,[112] and it is known that sphingolipids play a role in maintaining cellular homeostasis.[113] From this data, it could be suggested that the AAL-toxins, by their disruption

[108] Abbas, H.K.; Duke, S.O.; Merrill, A.H.; Wang, E.; Shier, W.T. *Phytochemistry* **1998**, *47*, 1509.
[109] Abbas, H.K.; Tanaka, T.; Shier, W.T. *Phytochemistry* **1995**, *40*, 1681.
[110] Merrill, A.H.; Wang, E.; Gilchrist, D.G.; Riley, R.T. *Adv. Lipid Res.* **1993**, *26*, 215.
[111] Abbas, H.K.; Tanaka, T.; Duke, S.O.; Porter, J.K.; Wray, E.M.; Hodges, L.; Sessions, A.E.; Wang, E.; Merrill, A.H.; Riley, R.T. *Plant Physiol.* **1994**, *106*, 1085.
[112] Witsenboer, H.M.A.; van Schaik, C.E.; Bino, R.J.; Loffler, H.J.M.; Nijkamp, H.J.J.; Hille, J. *Plant Sci.* **1988**, *56*, 253.
[113] Hannun, Y.A.; Luberto, C.; Argraves, K.M. *Biochemistry* **2001**, *40*, 4893.

of sphingolipid metabolism, cause changes in sphingolipid levels within the cell, resulting in apoptosis.

The tomato plants susceptible to the AAL toxins have been shown to be homozygous recessive at the *Asc-1* locus, having the genotype *asc/asc*.[114] Homozygous dominant *Asc/Asc* varieties of tomato have been shown to be much more resistant to the effects of AAL toxins in studies where leaflets of both varieties were treated with AAL-toxins, though they do show elevated sphingolipid levels, though not to the same degree as the *asc/asc* varieties.[115] In another study whereby the *Asc-1* was cloned and introduced into the *asc/asc* variety, resistance to the toxins, as well as to infection by the pathogen was acquired. The data showed that only a single functional copy of the gene is required for resistance.[116]

1.3. CONCLUSION

Due to the fumonisins and AAL-toxins being highly biologically active, and that there are a number of individual toxins within each class whose structure and activity have not been well studied, there is scope for further research into these toxins. Examination of the structure of the toxins reveals that the gross structure of the C-11–C-20 fragment of the fumonisins and the C-10–C-17 fragment of the AAL toxins is conserved across all members of the classes, while in those members whose absolute configuration has been determined, this too remains highly conserved. Most of the variation in the members in each class is in the pattern of substitution of the backbone as well as stereochemistry of the C-1–C-10 fragment of the fumonisins and the C-1–C-9 fragment of the AAL-toxins.

The most efficient way to establish the absolute configuration of those toxins whose configurations are unknown would be to synthesise a fragment representing the conserved C-11–C-20 fragment of the fumonisins and the C-10–C-17 fragment of the AAL-toxins which could then be coupled to numerous possible stereoisomers of the C-1–C-10 and C-1–C-9 fragments, respectively. Comparison of spectroscopic and physical data of the newly synthesised compounds with those of the natural products would allow for both structure confirmation and absolute configuration assignment.

[114] Clouse, S.D.; Gilchrist, D.G. *Phytopathology* **1987**, *77*, 80.
[115] Spassieva, S.D.; Markham, J.E.; Hille, J. *Plant J. Cell Molec. Biol.* **2002**, *32*, 561.
[116] Brandwagt, B.F.; Kneppers, T.; Nijkamp, H.J.; Hille, J. *J. Mol. Plant–Microbe Interact*. **2002,** *15*, 35.

With this in mind, it was decided to devise an efficient stereoselective synthetic route to provide access to large amounts of very pure fragments representing the conserved C-11–C-20 fragment of the fumonisins and the C-10–C-17 fragment of the AAL toxins.

2. RETROSYNTHESIS

Before the development of retrosynthetic analysis, the predominant method of design of a synthetic pathway was by choosing a starting material bearing some structural resemblance to the target, and subjecting this starting material to synthetic transformations until the desired target was achieved. E.J. Corey (amongst others) realised that although synthetic chemists were interested in the synthesis of *targets*, the starting point of the design of a synthetic pathway was guided and directed by features in *starting materials*. It was proposed that the process of synthetic design should start from the *target*, and the synthetic route be thought of in a reverse sense, guided by features in the target rather than a starting material and from this, the idea of retrosynthesis was born.[1]

Retrosynthetic analysis is a tool used by synthetic chemists by which targets are systematically deconstructed into ever simpler components (or synthons) by a retrosynthetic transform (which is opposite to a known transformation in the synthetic direction). Each of the synthons generated by a retrosynthetic transform is then subjected to the same process until the target molecule has been deconstructed into either simple or commercially available starting materials.[2] Since the target (and each of the identified synthons) can potentially be produced by more than one transform, retrosynthetic analysis produces a "tree" of possible synthetic routes. The various pathways available are then evaluated based on literature precedent, identifying the best option which is then executed in the synthetic direction.

There are number of distinct strategies which can be used to direct retrosynthetic planning, including transform-based strategies–which make use of a single transform which greatly reduces complexity of the strategy as a whole; structure-goal strategies–which are based on the structure of potential starting materials; topological strategies–disconnections at strategic bonds; stereochemical strategies–which are based on stereochemical simplifications controlled either by the transform or the substrate; and functional group strategies–which involve transformation of functional groups to facilitate the synthetic process.[2] In most cases, a combination of these strategies is used to simplify a target.

[1] Corey, E.J. *Angew. Chem., Int. Ed. Engl*. **1991**, *30*, 455.
[2] Corey, E.J.; Cheng, X.-M. *The Logic of Chemical Synthesis*. John Wiley & Sons, New York, 1989.

The aim of this project was to identify and execute a short, stereoselective synthesis of a fragment representing the left-side of the fumonisins and AAL-toxins, containing the four stereocentres which remain highly conserved among the individual fumonisins and AAL-toxins whose structures have been elucidated to date. The ultimate goal would be to use this left-side fragment in the determination of the absolute configuration of fumonisins and AAL-toxins whose absolute configurations have not yet been established. Since the configuration of the left-side appears to be conserved, coupling the left-side fragment with different stereoisomers of the right-side, and subsequent comparison of spectroscopic data and physical properties of the synthetic compounds with that of the natural toxins would allow for absolute configuration assignment for the compounds with undefined stereochemistry (as well as offering a route for their total synthesis).

2.1. RETROSYNTHETIC ANALYSIS OF FUMONISINS

2.1.1. Disconnection of the tricarballylic fragment and backbone

Examination of the fumonisin toxins leads to the identification of two distinct structural units, which could be coupled at a late stage of the synthesis. These structural units are the C_{20} polyhydroxyamino backbone, and the tricarballylic acid fragment. The general structure of the fumonisins can be disconnected at the ester bonds between the tricarballylic acid fragments and the backbone of the toxins. This retrosynthetic disconnection is of the topological type, and leads to synthons **117** and **118** as targets as shown in **Scheme 1** (with fumonisin B_2 used as an example). The presence of both free and esterified hydroxyl groups, carboxylic acid groups and amino groups in the fumonisins implies that an appropriate protecting group strategy would be required to ensure regioselectivity of the site of esterification, as well as to limit interference of these relatively reactive functional groups in the synthetic transformations.

Further analysis of the backbone clearly identifies two distinct halves, defined by the clusters of stereocentres separated by a six carbon alkyl chain (in the case of fumonisin B_2), which could be retrosynthetically disconnected at any bond along the alkyl chain. The strategic choice of a disconnection of the C-10–C-11 bond was made, as by varying the methodology used to couple the two fragments, it would allow for generation of either the unfunctionalised C-10 or the hydroxylated C-10 as required by the target. The synthon representing the left-half of the backbone (**119**) was the target for this project, and further analysis of this fragment now follows.

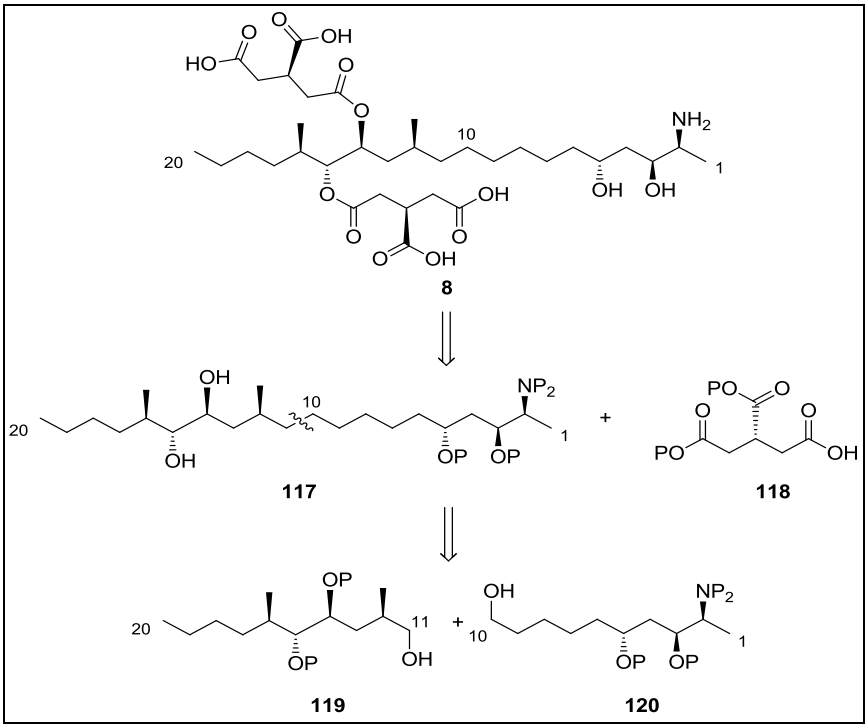

Scheme 1: Retrosynthetic analysis of fumonisin B_2, showing the target for the left-side.

2.1.2. Retrosynthetic analysis of the left synthon

The left synthon, containing three hydroxyl groups requires a protecting group strategy which would allow selective deprotection of the primary alcohol at C-11 to allow coupling to the right-side synthon (**120**) after its successful synthesis. This requires that the protecting group used at the C-11 hydroxyl (P^1) be orthogonal to that used in the protection of the hydroxyl groups at C-14 and C-15 (P^2). There are numerous combinations of protecting groups which could be used, though the final choice will depend on the reaction conditions expected to be used in the synthetic procedure.

Rotation around the C-15–C-16 bond reveals a *syn* relationship between a hydroxyl and alkyl group, which, when present with the methyl group at C-16, represents a structural unit which could conceivably be derived through an asymmetric aldol reaction. The Evan's chiral auxiliaries are known for their reliance in producing *syn* products, with the absolute configuration being controlled by the choice of auxiliary. This transformation is a stereochemical based strategy and allows for a great simplification in the synthetic route, as two of the stereocentres present are introduced simultaneously. With this goal in mind, synthon (**119**) was retrosynthetically analysed (as shown in **Scheme 2**) with the aim of using an asymmetric aldol reaction for the generation of the stereochemistry at C-15 and C-16.

Synthon (**119**) can be derived from the primary alcohol (**120**) by reductive functional group

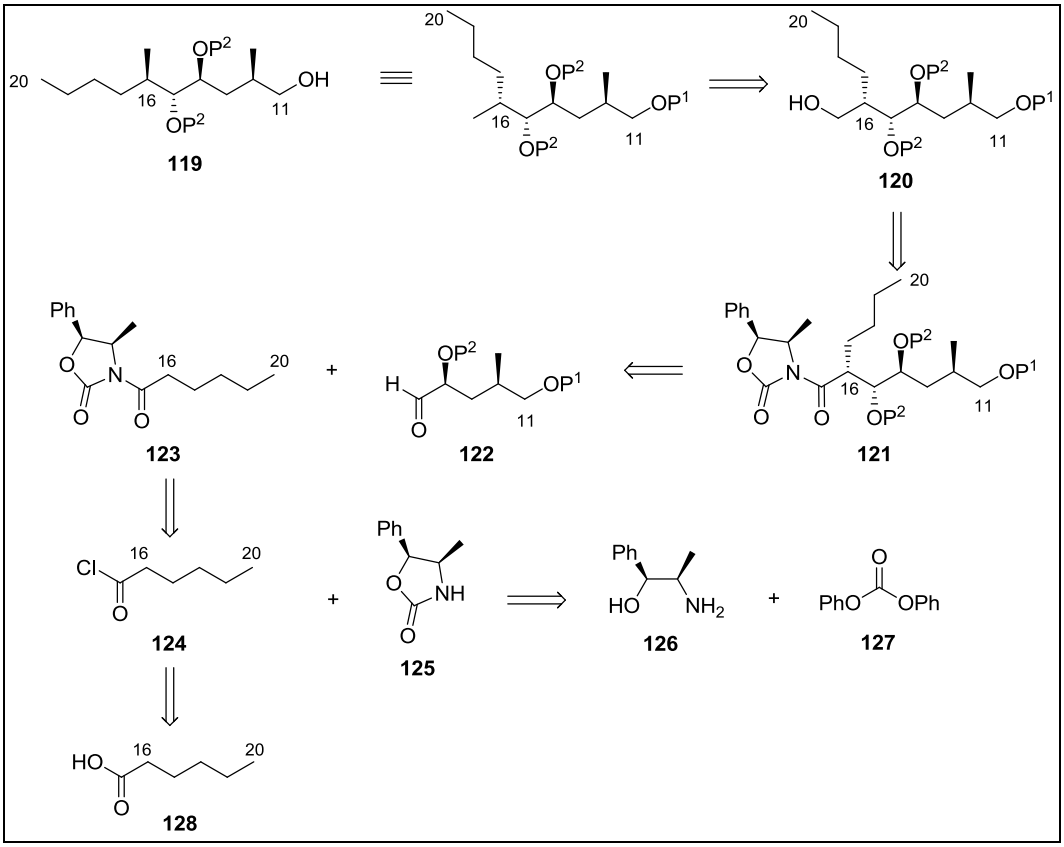

Scheme 2: Retrosynthetic analysis of the left synthon for the fumonisins (**119**).

transformation. The primary alcohol synthon (**120**) is a product of the reduction of imide (**121**), representing the protected product of an aldol reaction whose stereochemistry is controlled by the (+)-norephedrine based Evan's auxiliary. In the synthetic direction synthon (**121**) can be converted into the target by simple functional group transformations, including reduction of the imide, conversion of the primary alcohol into a leaving group, and a nucleophillic substitution by hydride.

Removal of protection at the hydroxyl group at C-15 reveals the aldol retron (O=C-C-OH), which is retrosynthetically derived from the carbonyl (imide) synthon (**123**) and the aldehyde synthon (**122**). The imide (**123**) can be disconnected to reveal the acyl chloride (**124**) and the oxazolidinone (**125**) as precursors, which are derived from hexanoic acid (**128**) and (+)-norephedrine (**126**), respectively. In the synthetic direction, the acyl chloride (**124**) is prepared from hexanoic acid and $SOCl_2$, and the oxazolidinone (**125**) from (+)-norephedrine and diphenyl carbonate (**127**). Metallation of the oxazolidinone by *n*-BuLi and nucleophillic acyl substitution at the activated carbonyl would give the imide synthon (**123**) as shown in **Scheme 2**.

Aldehyde synthon (**122**) can be produced from primary alcohol (**129**), which contains a terminal 1,2-diol motif at C-14 and C-15 in which the secondary alcohol is protected as

shown in **Scheme 3**. Protection of a secondary alcohol in a terminal 1,2-diol motif is usually achieved by the formation of a benzylidene acetal, and reductive ring opening at the less hindered carbon (C-15) by a bulky reducing agent such as DIBALH giving rise to synthon (**129**). There are numerous stereoselective reactions which can be used in the stereoselective generation of the diol motif either directly by Sharpless dihydroxylation of an alkene, or the resolution of racemic terminal epoxides using Jacobsen methodology with the epoxide derived from the same terminal alkene. Indirect methods also exist whereby Sharpless asymmetric epoxidation (SAE) of the appropriate allylic alcohol could stereoselectively give the 2,3-epoxy alcohol which could be opened to give the desired motif. From this point it is clear that the retrosynthetic pathway could have a number of branches based on these different methodologies. The pathway involving Sharpless asymmetric epoxidation was chosen as the preferred pathway due to the high selectivity generally observed in the reaction.

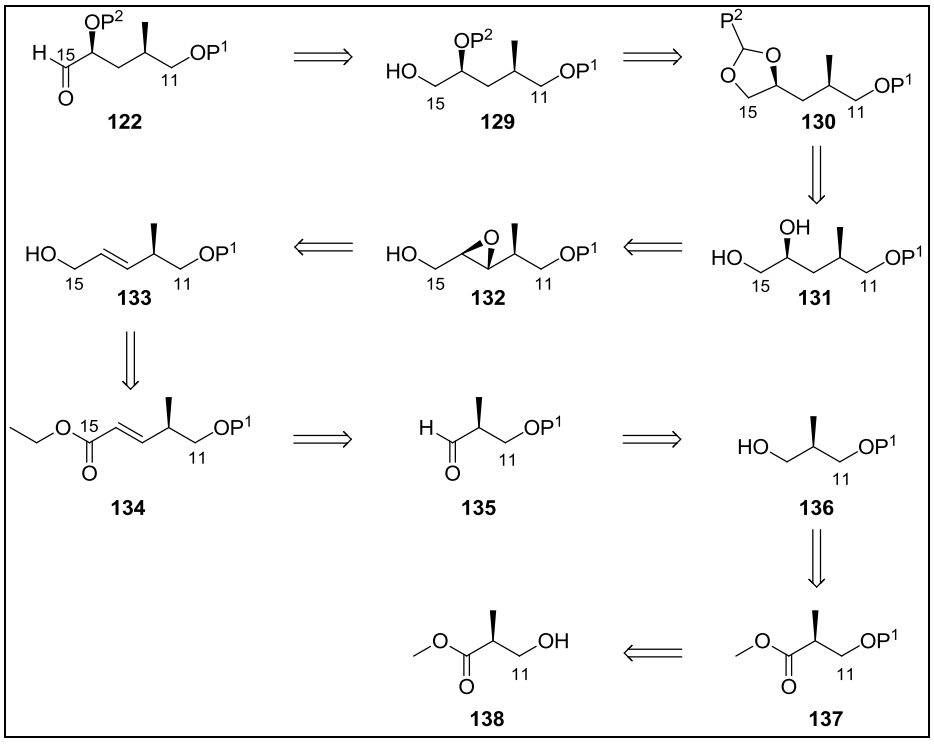

Scheme 3: Retrosynthetic analysis of aldehyde synthon (**122**).

Diol (**131**) could be obtained by regioselective opening of the 2,3-epoxy alcohol (**132**) which could be produced from the allylic alcohol (**133**) by SAE. This sequence of a regioselective and stereoselective transform produces the allylic alcohol which is available by reduction of an α,β-unsaturated ester (**134**). The latter can itself be generated by the well-known Horner-Wadsworth-Emmons (HWE) reaction. The aldehyde synthon (**135**) for the HWE reaction can be produced by a sequence of functional group transformations from commercially available methyl (*S*)-3-hydroxy-2-methylpropionate (**138**) by an oxidative transform to synthon (**136**),

followed by a reductive transform to synthon (**137**) and protection to give **138** as shown in **Scheme 3**.

Examination of the conditions predicted for the synthetic sequence shows that there are no strongly oxidising, acidic or basic reaction conditions predicted for the sequence. The silyl protecting groups, and orthogonal benzyl and benzyl derivative-type protecting groups would be appropriate for the synthesis (*e.g.* P^1 = silyl and P^2 = *p*-methoxybenzyl, or P^1 = benzyl and P^2 = *p*-methoxybenzyl). The ethers are attractive options due to their tolerance for a wide range of reaction conditions, though caution must be exercised not to employ strongly acidic or basic conditions, as the *p*-methoxybenzyl ether is acid sensitive, while silyl groups are both acid and base sensitive.

2.2. RETROSYNTHETIC ANALYSIS OF AAL-TOXINS

2.2.1. Disconnection of the Tricarballylic Acid Fragment and Backbone

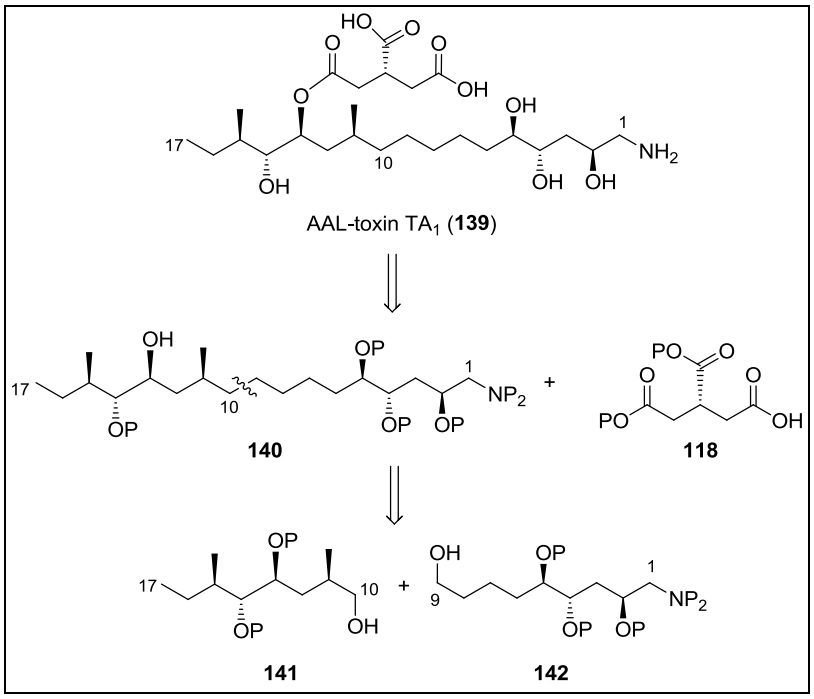

Scheme 4: Retrosynthetic analysis of AAL-Toxin TA_1, showing the target for the left side.

The AAL-toxins can be disconnected using the same principles applied to the fumonisins, in that the first strategic disconnection, the ester bond, can be made between the C_{17} polyhydroxyamino backbone, and the single tricarballylic acid fragment. This disconnection, followed by a disconnection of the C-9–C-10 bond again gives a left and right fragment by the application of a suitable protecting group strategy. The left fragment of the AAL-toxins (**141**) appears almost identical to fragment (**119**) of the fumonisins, save for the length of the

alkyl chain: all the stereocentres are in the same relative positions and absolute configurations, as shown in **Scheme 4** using AAL-toxin TA_1 as an example.

2.2.2 Retrosynthetic Analysis of the Left Synthon

The left hand synthon identified for the AAL-toxins contains the same structural features as those identified for the fumonisins, therefore a similar retrosynthetic analysis can be performed on this synthon. By rotation around the C-14–C-15 bond the same *syn* relationship between a hydroxyl and an alkyl (in this case ethyl) group is evident indicating that this motif could be derived from an asymmetric aldol reaction controlled by the appropriate Evan's chiral auxiliary. Further disconnections follow that of the fumonisins, eventually identifying the use of butanoic acid (**147**) as a starting material, in place of hexanoic acid, as shown in **Scheme 5**. In the synthetic direction, the oxazolidinone (**125**) is synthesised in the same manner as for the fumonisins, and acylated with butanoyl chloride giving imide (**145**). This imide when reacted with aldehyde (**122**) (identical to that of the fumonisins) in an aldol reaction, would be expected to give **144** which by a series of functional group transformations and protection identical to that of the fumonisins would be expected to give the target for the left-side of the AAL-toxins.

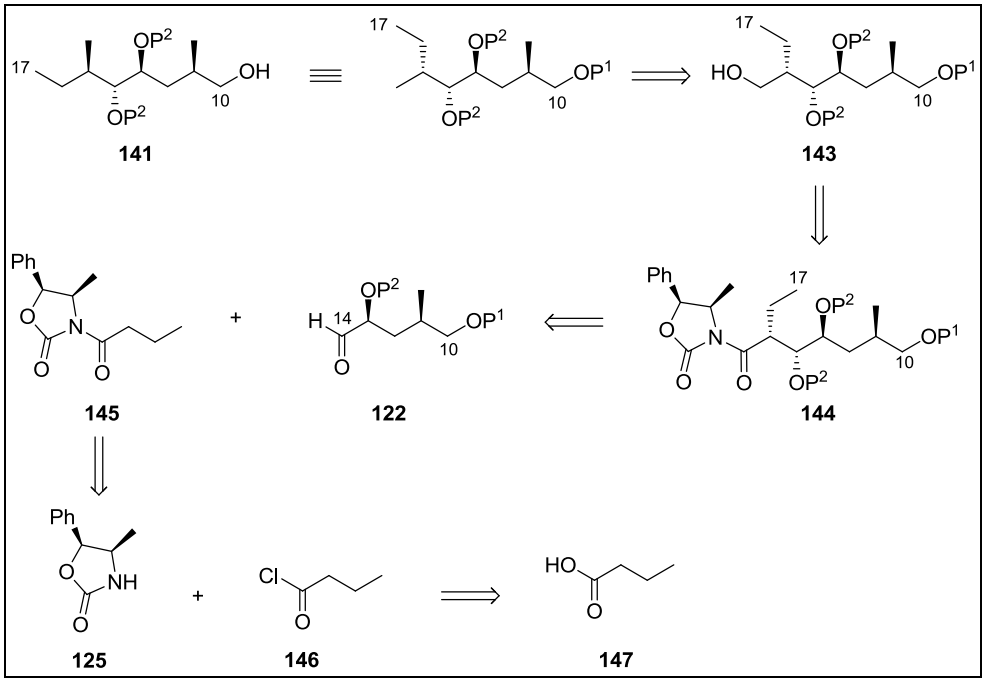

Scheme 5: Retrosynthesis of the left synthon for the AAL-toxins (**141**).

The aim of this project was therefore to attempt and optimise the identified synthetic routes for the left-side of both the fumonisins and AAL-toxins. This would provide access to these fragments in large quantities for coupling to the right-side fragments of selected fumonisins or AAL-toxins for absolute structure elucidation and total synthesis.

3. SYNTHETIC DISCUSSION

As stated in Chapter 2, the primary goal of this project was to synthesise a fragment representing the left side of both the fumonisins and AAL toxins for use in the elucidation of the absolute configuration of those toxins which have not yet been fully characterised. Retrosynthetic analysis of the toxins as illustrated in Chapter 2 identified **119** and **141** as targets, which could be synthesised from the common intermediate aldehyde (**122**) which could in turn be derived from methyl (*S*)-3-hydroxy-2-methylpropionate (**138**) (**Scheme 1**). In order to accomplish the synthesis, a suitable protecting group strategy had to be developed due to the presence of multiple hydroxyl functionalities in the final product, as well as the expected reaction conditions in which hydroxyl groups would interfere.

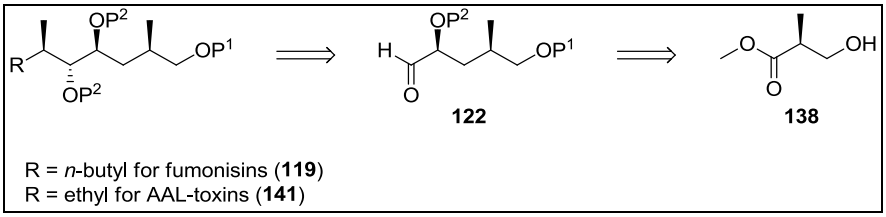

Scheme 1: Retrosynthetic analysis of left side fragment.

The proposed synthetic route is illustrated in **Scheme 2**. The protecting group strategy used in the scheme is discussed below.

3.1. PROTECTING GROUP STRATEGY

The proposed synthetic pathway required the protection of two hydroxyl groups, one being a primary hydroxyl group present in the starting material, requiring protection throughout the synthetic sequence and the other secondary which is introduced later in the synthetic pathway as part of a 1,2-diol system. The literature offers numerous protecting groups for primary hydroxyl groups, including alkyl ethers, aromatic and substituted aromatic ethers, silyl ethers, esters and ester derivatives. The ester derivatives are not practical due to their reactivity under reductive conditions employed numerous times in the proposed synthetic pathway. Of the ethers, the silyl ethers are the most attractive of the options, due to their relative stability under most reaction conditions, including mildly acidic and basic conditions and reductive and oxidative conditions. The silyl ethers undergo highly selective cleavage in the presence of

fluoride, leaving other protecting groups intact and thus allowing for the selective deprotection of the primary hydroxyl group as required for the coupling of the left and right fragments of the fumonisins and AAL toxins.

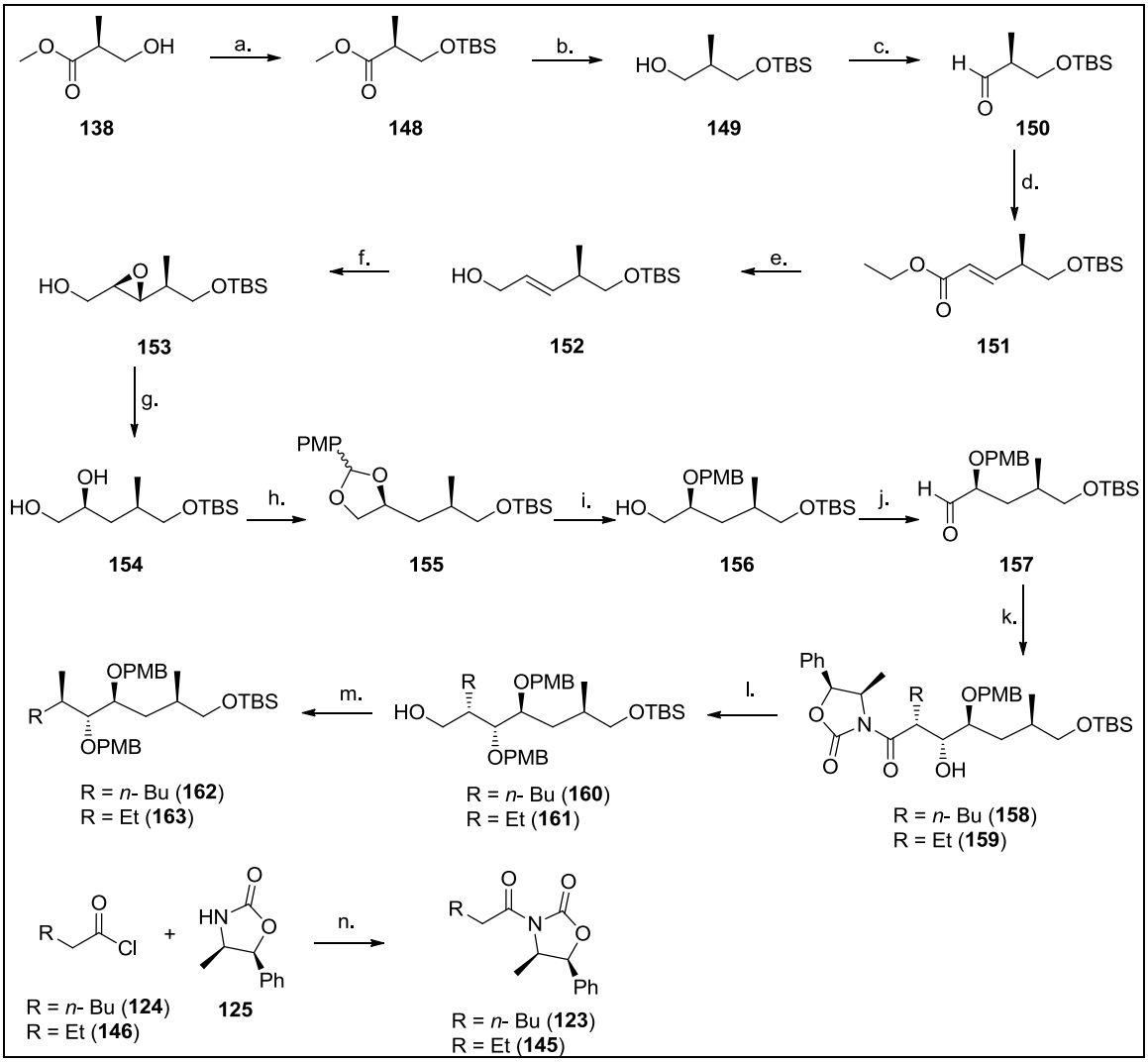

Scheme 2: Proposed synthetic route for the left-side fragment.

> *Reagents*: a. TBSCl, imidazole (96%); b. DIBALH (79%); c. DMSO, $(COCl)_2$, Et_3N (90%); d. ^{t}BuOK, $(^i PrO)_2P(O)CH_2COOEt$ (80%); e. DIBALH (85%); f. (*S*,*S*)-DIPT, $Ti(O^iPr)_4$, TBHP (30%); g. DIBALH (66%); h. $(OMe)_2CHC_6H_4OMe$, PPTS (33%); i. DIBALH (53%); j. DMSO, $(COCl)_2$, Et_3N; k. **123** or **145**, Bu_2BOTf, Et_3N; l. i). NaH, $MeOC_6H_4CH_2Br$, ii). $LiAlH_4$; m. i). TsCl, pyridine, ii). $LiAlH_4$; k. *n*-BuLi.

Another ubiquitous ether-based protecting group is the *O*-benzyl group. The *O*-benzyl group is stable to a host of reaction conditions including reductions, oxidations, acidic and basic conditions, and is orthogonal to many other protecting groups. Cleavage is most often performed by hydrogenolysis over Pd-C, and is another potential protecting group that could be considered for protection of the primary hydroxyl group in the first step of the proposed synthesis.

The selective protection of a secondary hydroxyl group in the presence of a primary hydroxyl group presents more of a challenge, as the primary hydroxyl group is less sterically hindered and consequently more reactive to protection than a secondary hydroxyl group. This effect would be expected to be more pronounced the larger the protecting group employed. Thermodynamic effects most likely control the process, favouring reaction at the less hindered position; however, if the secondary hydroxyl does react, migration of the protecting group would have to be considered, as has been observed for silyl groups.[1] Methods are known for the selective introduction of a protecting group at a primary hydroxyl group in the presence of a secondary hydroxyl group. However, if this strategy is employed, followed by the protection of the secondary hydroxyl group with an orthogonal protecting group, two additional steps are added to the synthetic process, and this is undesired.

An alternative to this approach is to make use of the benzylidene acetals, which can be selectively cleaved to give either the benzyl ether of the primary hydroxyl group, or of the secondary hydroxyl group depending on the choice of reagent. DIBALH is expected to reductively cleave at the least hindered position, giving the primary hydroxyl group. This would give access to an intermediate whose primary hydroxyl function is free for reaction while its secondary hydroxyl function is protected, as required by the synthetic plan.

3.1.1. Silyl Ethers

The silyl ethers are one of the most ubiquitous protecting groups used for hydroxyl groups in the literature.[2] This has been attributed to their ease of both introduction and selective removal, and the ability to control their properties by modifying the substituents at the silicon atom, affecting both the steric and electronic properties of members of this class. Two of the more commonly employed silyl ethers are the *tert*-butyldimethylsilyl (TBS) ether and *tert*-butyldiphenylsilyl (TBDPS) ether.

TBS ethers are more susceptible to acid than TBDPS ethers but both are equally sensitive to base.[3] The difference in acid sensitivity is likely due to differences in electronic effects between the methyl and phenyl substituents on the silicon atom.

TBS ethers and TBDPS ethers are both most commonly introduced at hydroxyl groups under the same reaction conditions, using TBSCl[4] or TBDPSCl,[5] imidazole as both base and acid

[1] Mulzer, J.; Schollhorn, B. *Angew. Chem. Int. Ed. Engl.* **1990**, *29*, 431.
[2] Van Look, G.; Simchen, G.; Heberle, J. *Silylating Agents*. Fluka Chemie AG, 1995.
[3] Wuts, P.G.M.; Greene, T.W. *Greene's Protective groups in organic synthesis.* John Wiley & Sons; New Jersey, 2007.
[4] Clark, J.H. *Chem. Rev.* **1980**, *80*, 429.

scavenger in DMF or DCM. Hydroperoxides, phenols and hydroxylamines are also silylated by TBSCl under these conditions, but other functional groups such as carboxylic acids, thiols and amines remain unreacted. The use of imidazole has been associated with an increased migration rate of silyl groups during selective protections. Altering the reaction conditions allows for the selective introduction of the protecting group at a primary hydroxyl group rather than a secondary hydroxyl group using TBSCl[6] or TBDPSCl,[7] DMAP (catalyst), Et_3N (base) in DMF or DCM. Imidazole is a stronger base than Et_3N, and therefore able to deprotonate the less acidic secondary hydroxyl groups, allowing for migration of the silyl group, which is undesired.

The chemoselective cleavage of most silyl ethers, including TBS and TBDPS ethers by the fluoride ion is one of the most appealing aspects of their application in organic synthesis. Cleavage is carried out in the presence of tetrabutylammonium fluoride (TBAF) in THF at room temperature.[5,8] The basicity of the fluoride ion can cause complications for base-sensitive substrates, and in such cases, ammonium fluoride is used to buffer the basicity,[9] or the reaction can be run in the presence of acetic acid.[10] Other fluoride sources commonly used include KF in 18-crown-6, aqueous HF in acetonitrile and HF.pyridine in THF. Both the TBS and TBDPS ethers can be selectively cleaved in the presence of one another, with selective TBS cleavage occurring with $(BF_3.Et_2O)$-Bu_4NF,[11] whereas selective TBDPS cleavage occurs with NaH and hexamethylphosphoramide.[12]

Fluoride-based cleavage of silyl ethers is thought to be as a consequence of the larger Si-F bond enthalpy compared to the Si-O bond enthalpy, implying that silicon has a higher affinity for fluorine than oxygen, resulting in cleavage of silyl ethers in the presence of fluoride.[3]

Methods do exist for the cleavage of silyl ethers which are not based on fluoride. These methods are less selective in nature, and can therefore be used to both deprotect silyl ethers, and accomplish other transformations in a single step, with most of these methods exploiting the acid sensitivity of the silyl ethers. Methods for the cleavage of TBS ethers using protic acids include the use of acetic acid in water and THF (cleaving primary hydroxyl TBS ethers

---

[5] Hanessian, S.; Lavallee, P. *Can. J. Chem*. **1975**, *53*, 2975.
[6] Ogilvie, K.K.; Shifman, A.L.; Penney, C.L. *Can. J. Chem.* **1979**, *57*, 2230.
[7] Guindon, Y.; Yoakim, C.; Bernstein, M.A.; Morton, H.E. *Tetrahedron Lett.* **1985**, *26*, 1185.
[8] Corey, E.J.; Venkateswarlu, A. *J. Am. Chem. Soc.* **1972**, *94*, 6190.
[9] Furstner, A.; Weintritt, H. *J. Am. Chem. Soc.* **1998**, *120*, 2817.
[10] Higashibayashi, S.; Shinko, K.; Ishizu, T.; Hashimoto, K.; Shirahama, H.; Nakata, M. *Synlett*. **2000**, 1306.
[11] Kawahara, S.I.; Wada, T.; Sekine, M. *Tetrahedron Lett*. **1996**, *37*, 509.
[12] Sheckhani, M.S.; Kahn, K.M.; Mahmood, K.; Shah, P.M.; Malik, S. *Tetrahedron Lett.* **1990**, *31*, 1669.

only),[8] *p*-TsOH acid in water and THF,[13] pyridinium *p*-toluenesulfonate in EtOH,[14] conc. HCl in EtOH,[15] sulfuric acid[16] and trifluoroacetic acid.[17] TBS ethers can also be cleaved under both reductive and oxidative conditions, for example using DIBALH in DCM at room temperature,[18] BH_3.DMS, TMSOTf in DCM,[19] or ceric ammonium nitrate in MeOH.[20]

3.1.2. Benzylidene Acetal Derivatives

Numerous protecting groups exist for the protection of 1,2-and 1,3-diols, with the largest and most prevalent class being the acetals, giving dioxolanes and dioxanes. The development of this class of protecting groups was a result of the large number of diol systems observed in natural products (including carbohydrates and oligonucleotides), which are often used as starting materials due to their availability.

When the protection of a diol system is required, the isopropylidene acetals are the most frequently used. The system (prepared from the diol, acetone and an acid catalyst) is used extensively in sugar chemistry, where the formation of 1,3-dioxolanes is favoured over the formation of 1,3-dioxanes. Cleavage is facilitated by addition of acid, whether through an acidic Dowex 50-W resin,[21] or the use of 1M HCl in THF,[22] though methods exist for the cleavage of selected systems (such as the cleavage of an *anti* acetonide in the presence of a *syn* acetonide), [23] by altering the cleavage conditions.

Benzylidene acetals and derivatives thereof (such as the *p*-methoxybenzylidene, and dimethoxybenzylidene derivatives) are also popular protecting groups for diol systems. They are synthesised by a number of routes, including acid catalysed reaction with the appropriate aldehyde,[24,25] or acid catalysed acetal exchange, with the dimethyl acetal of the appropriate aldehyde.[26,27] Cleavage is performed under reductive conditions (H_2/Pd-C in AcOH for

[13] Thomas, E.J.; Williams, A.C. *J. Chem. Soc., Chem. Comm.* **1987**, 992.
[14] Prakash, C.; Saleh, S.; Blair, I.A. *Tetrahedron Lett.* **1989**, *30*, 19.
[15] Wetter, H.; Oertle, K. *Tetrahedron Lett.* **1985**, *26*, 5515.
[16] Franke, F.; Guthrie, R.D. *Aust. J. Chem.* **1978**, *31*, 1285.
[17] Baker, R.; Cummings, W.J.; Hayes, J.F.; Kumar, A. *J. Chem. Soc., Chem. Comm.* **1986**, 1237.
[18] Corey, E.J.; Jones, G.B. *J. Org. Chem.* **1992**, *57*, 1028.
[19] Hunter, R.; Bartels, B.; Michael, J.F. *Tetrahedron Lett.* **1991**, *32*, 1095.
[20] DattaGupta, A.; Singh, R.; Singh, V.K. *Synlett*, **1996**, 69.
[21] Ho, P.T. *Tetrahedron Lett.* **1978**, *19*, 1623.
[22] Angyal, S.J.; Beveridge, R.J. *Carbohydr. Res.* **1978**, *65*, 229.
[23] Bode, S.E.; Muller, M.; Wolberg, M. *Org. Lett.* **2002**, *4*, 619.
[24] Fletcher, H.G. *Methods Carbohydr. Chem.* **1963**, *II*, 307.
[25] Smith, M.; Rammler, D.H.; Goldberg, I.H.; Khorana, H.G. *J. Am. Chem. Soc.* **1962**, *84*, 430.
[26] Albert, R.; Dax, K.; Pleshko, R.; Stutz, A. *Carbohydr. Res.* **1985**, *137*, 282.
[27] Kloosterman, M.; Slaghek, T.; Hermans, J.P.G.; Van Boom, J.H. *Recl. Trav. Chim. Pays-Bas* **1984**, *103*, 335.

benzylidenes,[28] $Pd(OH)_2/H_2$ for *p*-methoxybenzylidenes),[29] or their acid sensitivity can be exploited with cleavage being effected in 80% AcOH.[25]

Though useful in their own right, these protecting groups have an additional advantage in that one of the C-O bonds can be selectively reduced, giving a free hydroxyl group, and an *O*-benzyl (or *O*-*p*-methoxybenzyl) protected hydroxyl group. The choice of reducing agent (as well as steric and electronic properties of the substrate) allows control over which of the C-O bonds are reduced. Use of DIBALH usually gives the product that has been reduced at the least sterically hindered position[27,30] (in this case, giving the free primary hydroxyl group), though in substrates where coordination to an adjacent oxygen atom is possible, reduction can occur at the more hindered position. Use of some borane-derived reagents such as $NaBH_3CN$-HCl in THF,[31] $BH_3.NMe_3$-$AlCl_3$ in THF[32] or triethylsilane and trifluoroacetic acid[33] allows for the reduction to occur at the more hindered position, giving access to a substrate where the less hindered primary hydroxyl group is protected as the respective ether, and the more hindered secondary hydroxyl group is free for further reaction.

3.1.3. Benzyl Ethers

O-Benzyl ethers are used in the protection of hydroxyl groups due to their remarkable stability and tolerance to a wide range of reaction conditions. The benzyl ethers undergo few side reactions, and can be introduced into molecules under acidic, basic or neutral conditions, depending on the reactivity of the substrate, making this an attractive option for pH sensitive substrates.

O-Benzyl ethers are most frequently synthesised under basic conditions, using the traditional Williamson ether synthesis. Reagents employed include NaH or KOH as base, with either benzyl bromide or benzyl chloride.[34,35] There have been numerous modifications to this procedure to allow for introduction of the benzyl group to more unique substrates, such as the addition of Bu_4NI, generating benzyl iodide *in situ* allowing for the *O*-benzylation of sterically hindered hydroxyl groups.[36] Benzylation of base sensitive substrates can be

[28] Hartung, W.H.; Simonhoff, R. *Org. React.* **1953**, *7*, 263.
[29] Toshima, K.; Murkaiyama, S.; Yoshida, T.; Tamai, T.; Tatsuta, K. *Tetrahedron Lett.* **1991**, *32*, 6155.
[30] Ito, Y.; Ohnishi, Y.; Ogawa, T.; Nakahara, Y. *Synlett.* **1998**, 1102.
[31] Garegg, P.J.; Hultberg, H.; Waolin, S. *Carbohydr. Res.* **1982**, *108*, 97.
[32] Ek, M.; Garegg, P.J.; Hultberg, H.; Oscarson, S. *J. Carbohydr. Res.* **1983**, *2*, 305.
[33] De Ninno, M.P.; Etienne, J.B.; Duplantier, K.C. *Tetrahedron Lett.* **1995**, *36*, 1179.
[34] Fletcher, H.G. *Methods Carbohydr. Chem.* **1963**, *2*, 166.
[35] Fukuzawa, A.; Sato, H.; Masamune, T. *Tetrahedron Lett.* **1987**, *28*, 4303.
[36] Czernecki, S.; Georgoulis, C.; Provelenghiou, C. *Tetrahedron Lett.* **1976**, *17*, 3535.

achieved using benzyl bromide, in the presence of silver oxide in DMF,[37] or by using Dudley's reagent (2-benzyloxy-1-methylpyridinium triflate) and magnesium oxide.[38] These conditions avoid the use of strong bases, but rather use weakly basic, sparingly soluble metal oxides. Benzyl ethers can also be synthesised under acidic conditions, making use of benzyl 2,2,2-trichloroacetimidate in the presence of either *p*-TsOH[39] or trimethylsilyl triflate.[40] This variety of conditions for the introduction of the benzyl group makes it a popular choice of protecting group as the reaction conditions can be modified to suit a number of substrates, unlike the conditions for the introduction of many other protecting groups.

The most common method for cleavage of benzyl ethers is by hydrogenolysis over Pd-C in EtOH,[41] though through careful manipulation of the reaction conditions, benzyl ethers can be preserved, while other functionalities (such as double bonds and benzyl esters) within a substrate are reduced. The use of transfer hydrogenation (with formic acid,[42] ammonium formate,[43] cyclohexene[44] or cyclohexadiene[45]) to effect the cleavage of benzyl ethers allows for the preservation of functional groups (such as *p*-methoxybenzyl ethers[46] and benzylidene acetals[43]) which would otherwise be susceptible to hydrogenation.

Other methods for the cleavage of benzyl ethers include cleavage by Lewis acids (such as Me_3SiI,[47] Me_2BBr[48] or $FeCl_3$[49]), dissolving metal reductions utilising Na in liquid ammonia[50] or other metals in the presence of ammonia and other solvents, or by oxidative methods using CrO_3/AcOH and generating the benzyl ester which can be cleaved by hydrolysis giving the deprotected product.[51] As the cleavage conditions become harsher, fewer functional groups would be expected to survive the cleavage conditions limiting the use of these methods.

From the above, the protecting group strategy shown in **Scheme 2** was used, where the *O*-TBS ether was used for protection of the hydroxyl group in the starting material, and the *p*-methoxybenzylidene acetal, and consequently the *p*-methoxybenzyl group was used for the

[37] Kuhn, R.; Low, I.; Trishmann, H. *Chem. Ber.* **1957**, *90*, 203.
[38] Poon, K.W.C.; Dudley, G.B. *J. Org. Chem.* **2006**, *71*, 3923.
[39] Wessel, H.P.; Iverso, T.; Bundle, D.R. *J. Chem. Soc., Perkin Trans 1*, **1985**, 2247.
[40] Xuesong, C.; Yu-Lin, W.; Dihhua, C. *Tetrahedron Lett.* **2002**, *43*, 3529.
[41] Heathcock, C.H.; Ratcliffe, R. *J. Am. Chem. Soc.* **1971**, *93*, 1746.
[42] El Amin, B.; Anantharamaiah, G.M.; Royer, G.P.; Means, G.E. *J. Org. Chem*. **1979**, *44*, 3442.
[43] Bieg, T.; Szeja, W. *Synthesis* **1985**, 76.
[44] Anantharamaiah, G.M.; Sivanandaiah, K.M. *J. Chem. Soc., Perkin Trans. 1*, **1977**, 490.
[45] Felix, A.M.; Heimer, E.P.; Lambros, T.J.; Tzougraki, C.; Meinholder, J. *J. Org. Chem.* **1978**, *43*, 4194.
[46] Evans, D.A.; Rippin, D.H.B.; Halstead, D.P.; Campos, K.R. *J. Am. Chem. Soc.* **1999**, *121*, 6816.
[47] Jung, M.E.; Lyster, M.A. *J. Org. Chem*. **1977**, *42*, 3671.
[48] Guindon, Y.; Yoakim, C.; Morton, H.E. *Tetrahedron Lett.* **1983**, *24*, 2969.
[49] Kartha, K.P.R.; Dasgupta, F.; Singh, P.P.; Srivastava, H.C. *J. Carbohydr. Chem*. **1986**, *5*, 437.
[50] McCloseky, C.M. *Adv. Carbohydr. Chem*. **1957**, *12*, 137.
[51] Angyal, S.J.; James, K. *Carbohydr. Res.* **1970**, *12*, 147.

hydroxyl groups at C-14 and C-15 in the final target. These protecting groups are able to withstand the reaction conditions expected in the synthetic route, and also allow for the selective deprotection of the silyl ether with the view to coupling fragments **119** and **120** to synthesise the complete fumonisin toxin backbone and fragments **141** and **142** to synthesise the complete AAL toxin backbone.

3.2. SHARPLESS ASYMMETRIC EPOXIDATION ROUTE

The proposed synthetic route makes use of Sharpless asymmetric epoxidation reaction as a key transformation for introducing the OH-bearing stereocentre at C-14 in target (**119**). This key transformation was chosen due to its wide applicability and reliance in producing epoxides of high enantiopurity.[52]

3.2.1. Theoretical Aspects

The Sharpless (also Sharpless-Katsuki) epoxidation was first reported in 1980, and involved the use of a stoichiometric quantity of $Ti(O^iPr)_4$, diethyl tartrate (DET) and *t*-butyl hydroperoxide to synthesise highly enantiopure epoxy alcohols from allylic alcohols.[53] Since then, the reaction has undergone only a single major modification, in that a catalytic version of the reaction, utilising as little as 5-10 % of the active catalyst was developed, by the introduction of 4Å molecular sieves in the reaction mixture.[52]

The epoxide is a valuable functional group for the synthetic chemist, due to its versatility and wide range of transformations that the group undergoes. Naturally occurring epoxides, especially chiral epoxides, are limited in availability from the chiral pool, therefore methods for the synthesis of enantiopure epoxides would be highly valuable.

Transition metal-catalysed epoxidations offer mild reaction conditions for the introduction of an epoxide to a double bond in both cyclic and acyclic substrates. Transition metals are useful as catalysts in many reactions due to their ability to coordinate with substrates, offering an additional degree of control over the mechanism of the reaction. Transition metal-catalysed epoxidations of cyclic substrates bearing allylic or homoallylic hydroxyl groups is of particular interest due to the degree of stereocontrol observed in such reactions. $VO(acac)_2$ is a common catalyst used in epoxidations, and the ability of the vanadium centre to coordinate to hydroxyl groups is exploited in epoxidations of cyclic substrates, as shown in **Scheme 3**.

[52] Gao, Y.; Klunder, J.M.; Hanson, R.M.; Masamune, H.; Ko, S.Y.; Sharpless, K.B. *J. Am. Chem. Soc.* **1987**, *109*, 5765.
[53] Katsuki, T.; Sharpless, K.B. *J. Am. Chem. Soc.* **1980**, *102*, 5974.

Coordination of the vanadium centre to the hydroxyl oxygen and oxidising agent, forces the delivery of the epoxide oxygen on the same face as the hydroxyl group, giving a product whose relative stereochemistry is *syn*. In this case, the stereochemical outcome of the reaction is controlled by structural features in the starting material, in a substrate controlled pathway. This application is most useful for conformationally rigid cyclic substrates, though stereocontrol has been observed in acyclic substrates, though is less reliable.[54]

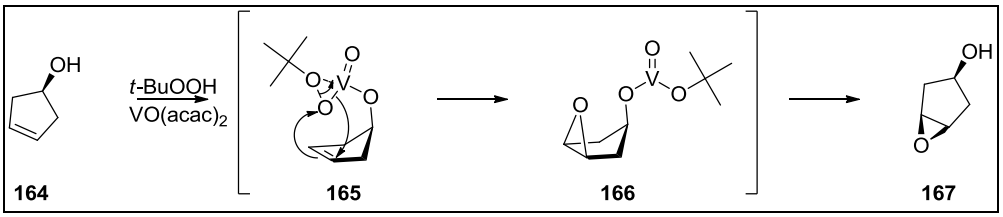

Scheme 3: Mechanism of $VO(acac)_2$ epoxidation of 4-hydroxycyclopentene showing origin of stereoselectivity.[55]

In the above case stereoselectivity originates from the substrate. Reagent controlled stereoselectivity would have a far larger scope as the desired stereochemical relationship would not be a function of the substrate (potentially giving unwanted products), but rather that of the reagent, which can be controlled as desired. This reagent would require some source of chirality, though still maintaining the coordination controlled mechanism of epoxidation. Sharpless and Katsuki developed such a reaction, by which the metal centre was titanium, and the source of chirality was a tartrate ester, either diethyl- or diisopropyl tartrate (DET or DIPT, respectively), maintaining *t*-BuOOH as the oxidant in the reaction.

The Sharpless epoxidation is based on the generation of a chiral pocket through the complexation of $Ti(O^iPr)_4$ and the chiral tartrate species, into which the allylic alcohol coordinates. The delivery of the oxygen atom to a specific face of the alkene is controlled by the stereochemistry of the tartrate species. The face of attack can be predicted by the mnemonic shown in **Figure 1**, published in Sharpless and Katsuki's original report.

Consensus is yet to be reached about the absolute structure of the catalytic complex and mechanism of stereoinduction, though most studies indicate that the active and major species is a bridged-octahedral dimeric titanium complex, with two molecules of tartrate bridging the two titanium centres (2:2 complex), though a number of additional titanium-tartrate species have been shown to exist in the reaction mixture.[56] A possible pathway for the generation of

[54] Pereira, C.L.; Chen, Y.H.; McDonald, F.E. *J. Am. Chem. Soc*. **2009**, *131*, 6066.
[55] Clayden, J.; Greeves, N.; Warren, S.; Wothers, P. *Organic Chemistry*. Oxford University Press: Oxford, **2004**, 877, 1239.
[56] Finn, M.G.; Sharpless, K.B. *J. Am. Chem. Soc*. **1991**, *113*, 113.

epoxy alcohols is shown in **Scheme 4**.

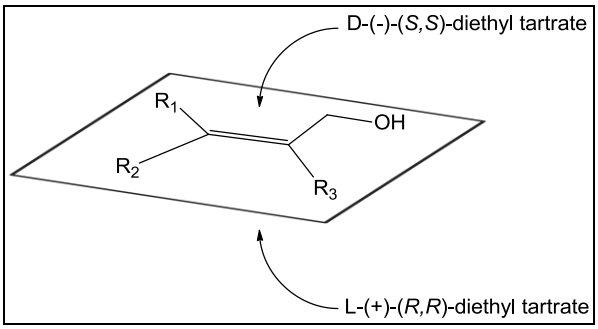

Figure 1: Mnemonic for prediction of enantioselectivity of Sharpless epoxidation.

A mixture of $Ti(O^iPr)_4$ and a slight excess of diethyl tartrate is allowed to stir in DCM generating the dimeric complex (**168**) after displacement of two labile isopropoxide ligands from each titanium centre. Evidence of this displacement comes from changes in chemical shifts of isopropoxide and ester carbonyl resonances in ^1H and ^{13}C NMR spectroscopic studies of titanium-tartrate mixtures.[56] This dimeric complex has been shown to be both temperature and moisture sensitive, and formation of the complex is only achieved at temperatures below 0 °C.

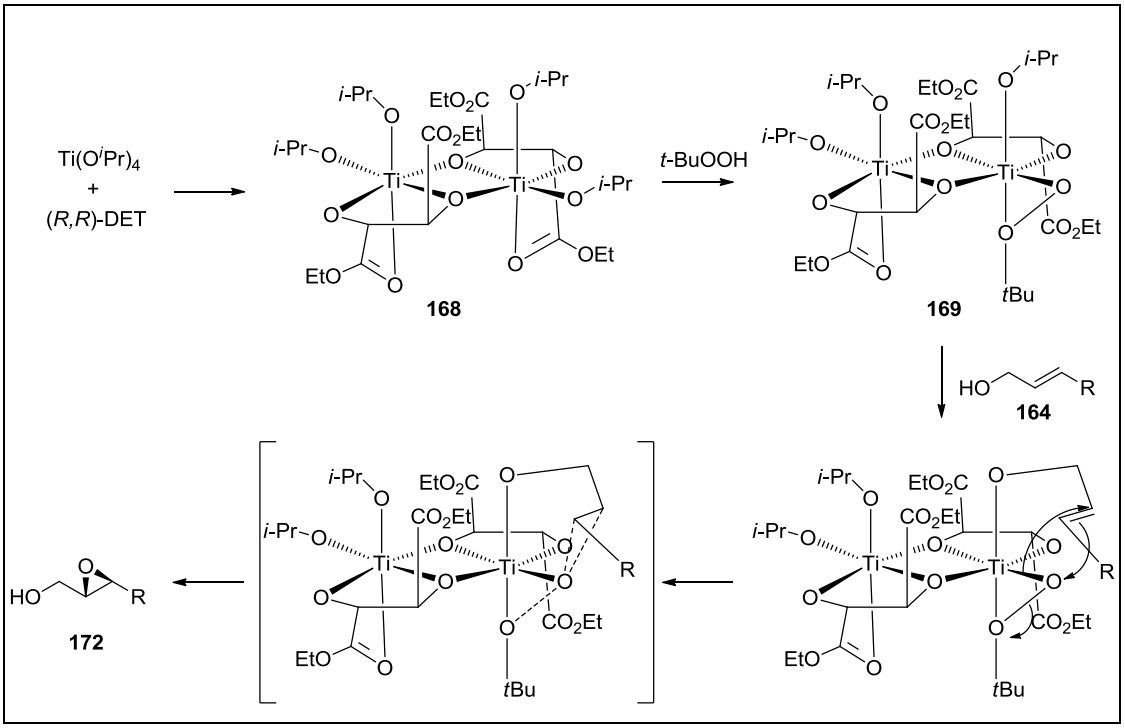

Scheme 4: Proposed mechanism for Sharpless asymmetric epoxidation.[55]

Addition of the bulky *t*-butyl hydroperoxide leads to the displacement of a third isopropoxide ligand from the equatorial position of the titanium centre, leading to the bidentate

coordination of the peroxide to the titanium centre. Evidence of this bidentate coordination is provided by the extreme broadening of signals in both ^{1}H and ^{13}C NMR spectra, as well as significant changes in the IR spectrum which could not be attributed to monodentate binding. Displacement of the fourth isopropoxide on the same titanium centre by the addition of the allylic alcohol generates the active complex delivering the epoxide oxygen to the face of the double bond as shown due to the pseudo-C_2 symmetric complex forcing a specific orientation of the double bond and peroxy-oxygen. Using deuterium isotope labelling studies, it has been shown that the bond at C-3 (alkene carbon furthest from the –OH) forms slightly earlier than that at C-2 (evidenced by a marginally larger isotope effect), however the difference in rate is not significant.[52]

The reaction was first developed using stoichiometric quantities of the chiral catalyst, but it was later realised that upon addition of 4 Å molecular sieves, the mole equivalents of tartrate ester and $Ti(O^{i}Pr)_4$ could be reduced to as little as 5 % of the quantity of allylic alcohol, and that the effectiveness of the procedure on transforming some otherwise problematic substrates was increased significantly. Molecular sieves were found to both increase the rate of reaction, and remove any water (either present in reagents or solvents, or produced in side reactions) from the reaction medium. Addition of water to a reaction mixture not containing molecular sieves was found to slow the reaction significantly and destroyed the catalyst reducing the enantioselectivity of the epoxidation to 4 % e.e. Addition of molecular sieves to an identical reaction mixture containing the same amount of water increased the e.e. to 80 %, though the reaction was significantly slower than that of the control containing molecular sieves and no water. This data indicated that the active catalyst reacts reversibly with water but a significant quantity of the catalyst is irreversibly destroyed.[52]

This versatility of the reaction was demonstrated by Sharpless himself, when the used the method to synthesise a number of intermediates used in the synthesis of natural products, including intermediates for the total synthesis of methymycin (**172**), erythromycin (**173**), leukotriene C-1 (**174**) and (+)-disparlure (**175**), shown in **Figure 2**.[57]

Since then, the reaction has found application in the total synthesis of a number of natural products, including the potential anti-cancer agent laulimalide,[58] L-hexoses,[59] the antiviral venustatriol,[60] the polyether antibiotic aferensimycin B,[61] the diterpene (–)-7-

[57] Rossiter, B.E.; Katsuki, T.; Sharpless, K.B. *J. Am. Chem. Soc*. **1981**, *103*, 464
[58] Wender, P.A.; Hegde, S.G.; Hubbard, R.D.; Zhang, L. *J. Am. Chem. Soc*. **2002**, *124*, 4956.
[59] Ko, S.Y.; Lee, A.W.M.; Masamune, S.; Reed III, L.A.; Sharpless, K.B.; Walker, F.J. *Tetrahedron* **1990**, *46*, 245.
[60] Corey, E.J.; Ha, D.-C. *Tetrahedron Lett.* **1988**, *29*, 3171.

deacetoxyalcyonin acetate,[62] and the chromophore of the antitumour antibiotic (+)-neocarzinostatin.[63]

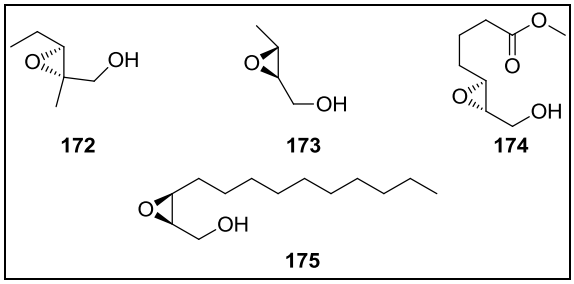

Figure 2: Synthetic intermediates synthesised by Sharpless epoxidation.

The Sharpless epoxidation has also found application in the kinetic resolution of allylic secondary alcohols. Kinetic resolution involves the separation of enantiomers based on differences in the rate of reaction of the two enantiomers with a chiral reagent.[64] In this case, one enantiomer of the allylic alcohol reacts with the titanium-tartrate complex more rapidly than the other, producing an excess of one diastereomer of the 2,3-epoxy alcohol, while the slow-reacting enantiomer remains unreacted, as shown in **Scheme 5**. The process is kinetically controlled, and if left long enough, conversion of the slow-reacting enantiomer would also occur. For this reason, the reaction is often stopped before the maximum 50 % conversion has occurred so as to ensure the e.e. remains high (>99 %).[52] The same mnemonic for the standard Sharpless epoxidation can be used to predict the rapid-reacting enantiomer during kinetic resolution by placing the –OH in the plane of the double bond, and examining which of the enantiomers offers the least steric hindrance to the approach of the oxidant.

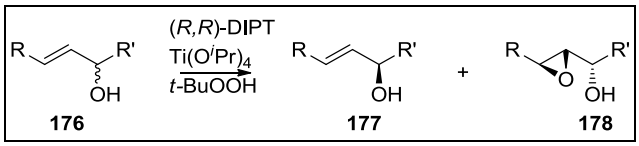

Scheme 5: Kinetic resolution of secondary allylic alcohols.[52]

The kinetic resolution process allows access to two different compounds both of high enantiomeric excess, with the drawback being that maximum yield is only 50 %.

When the reaction was developed, it was one of very few reliable stereoselective reactions, so

[61] Evans, D.A.; Polniaszek, R.P.; DeVries, K.M.; Guinn, D.E.; Mathre, D.J. *J. Am. Chem. Soc.* **1991**, *113*, 7613.
[62] MacMillan, D.W.C.; Overman, L.E. *J. Am. Chem. Soc.* **1995**, *117*, 10391.
[63] Myers, A.G.; Liang, J.; Hammond, M.; Harrington, P.M.; Yusheng, W.; Kuo, E.Y. *J. Am. Chem. Soc.* **1998**, *120*, 5319.
[64] Solomons, T.W.G.; Fryhle, C.B. *Organic Chemistry*. John Wiley & Sons: New Jersey, **2004**.

numerous transformations of 2,3-epoxy alcohols were developed in order to utilise the reaction in the synthesis of natural products. The epoxide moiety can be opened reductively with DIBALH to give the 1,2-diol, with Red-Al to give the 1,3-diol,[65] or opened by another nucleophile, with N, C and O nucleophiles attacking at C-3 whereas cuprates favour attack at C-2.[66] Substitution at C-1 can also be performed via a base-catalysed Payne rearrangement followed by attack of the 1,2-epoxy-3-alcohol at C-1 (least hindered position) by a nucleophile. Alternatively, the free hydroxyl group can be converted into a leaving group (e.g. tosylate), and nucleophilic substitution can give a C-1 substituted 2,3-epoxide derivative.[66]

3.2.2. Experimental Aspects

The synthetic route illustrated in **Scheme 2a** was the first synthetic route attempted to synthesise targets **162** and **163** via the common intermediate aldehyde (**157**). The synthesis began by protection of the hydroxyl group of methyl (*S*)-3-hydroxy-2-methylpropionate (**138**) as the TBS ether, by deprotonation with imidazole in DCM and addition of TBSCl giving the protected compound (**148**) in high yield (96%) through a nucleophilic substitution at silicon. The most common procedure for this reaction employs DMF as a solvent; however, the polar nature of the solvent coupled with its high boiling point can make its removal difficult.[8] Substitution of DMF with DCM led to longer reaction times (10 h vs. 48 h) but offered similar yields. DMF being a polar aprotic solvent would facilitate the nucleophilic substitution better than the less polar DCM, resulting in the longer reaction times as observed when DCM is used as a solvent.

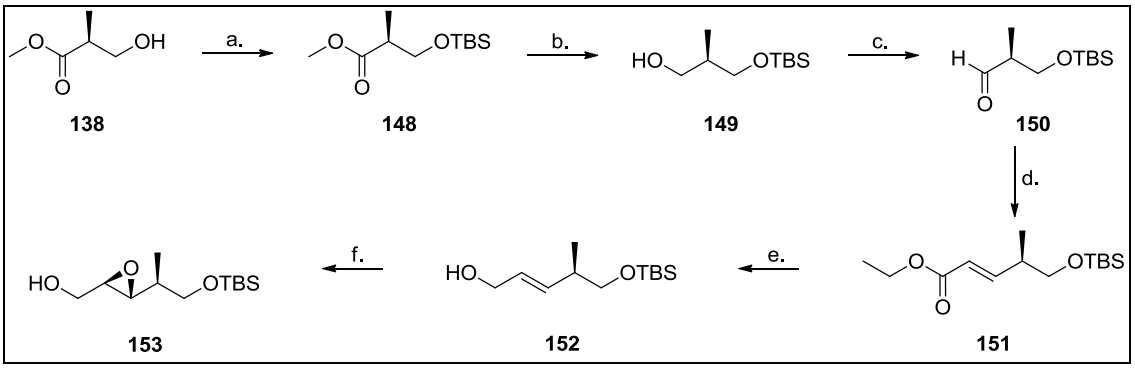

Scheme 2a: Synthetic route utilising Sharpless asymmetric epoxidation.

Reagents: a. TBSCl, imidazole (96%); b. DIBALH (79%); c. DMSO, $(COCl)_2$, Et_3N (90%); d. ^tBuOK, $(^iPrO)_2P(O)CH_2COOEt$ (80%); e. DIBALH (85%); f. (*S*,*S*)-DIPT, $Ti(O^iPr)_4$, TBHP (30%).

[65] Suzuki, T.; Saimoto, H.; Tomioka, H.; Oshima, K.; Nozaki, H. *Tetrahedron Lett.* **1982**, *23*, 3597.
[66] Sharpless, K.B.; Behrens, C.H.; Katsuki, T.; Lee, A.W.M.; Martin, V.S.; Takatani, M.; Viti, S.M.; Walker, F.J.; Woodard, S.S. *Pure Appl. Chem.* **1988**, *55*, 589.

The TBS group gave a characteristic set of resonances in both the ^{1}H and ^{13}C NMR spectra: the silyl methyl groups at δ_H 0.00 and δ_C −5.53 and the *t*-butyl methyl group at δ_H 0.84 and δ_C 18.18, with the upfield shifts reflecting the electropositive nature of carbons bonded to weakly electronegative carbon and silicon. The spectroscopic data and physical properties correlated well with those published in the literature.[67]

Reduction of the ester functionality of **148** to the alcohol (**149**) was accomplished using DIBALH in DCM at −78 °C. DIBALH is a mild reducing agent with reduction happening in a stepwise manner – from the ester to the aldehyde with the first equivalent of DIBALH,[68] and from the aldehyde to the alcohol (**149**) with the second equivalent of DIBALH.[69] Though the corresponding aldehyde was a target and could be produced from the ester directly by addition of just one equivalent of DIBALH, this reaction mixture could conceivably contain a mixture of unreacted ester, aldehyde, and alcohol, which would be produced by DIBALH reacting with the aldehyde as it is formed. As a consequence DIBALH is most often used to fully reduce the ester to the alcohol, which is then oxidised to the aldehyde.[67,70,71] Lithium aluminium hydride can be used for this transformation, though experience in our laboratories, and those of others,[72] indicated that deprotection of TBS ethers is possible during LAH reductions of esters. In order to accomplish this transformation two equivalents of DIBALH would be required according to the stoichiometry of the reaction; however, it was found that the reaction gave highest yields when 2.5–2.7 equivalents of DIBALH were used. After hydride transfer an aluminium alkoxide bond is formed which is then cleaved during the work-up process. DIBALH is thought to exist as a dimer with bridging hydride ligands,[73] so there is the possibility that unreacted DIBALH molecules remain bridged to the aluminium bound to the alkoxide, trapping the reagent so that it cannot react, as illustrated in **Scheme 6**. This would then mean additional equivalents of DIBALH would be required to force the reaction to completion as was observed experimentally.

During the work-up procedure excess hydride was quenched by addition of MeOH at −78 °C. This liberated hydrogen gas, and resulted in the formation of a gelatinous aluminium complex. The second component of the work-up procedure was usually accomplished by the

[67] Kalesse, M.; Chary, K.P.; Quitschalle, M.; Burzlaff, A.; Kasper, C.; Scheper, T. *Chem. Eur. J.* **2003**, *9*, 1129.
[68] Winterfeldt, E. *Synthesis* **1975**, 617.
[69] Yoon, N.M.; Gyoung, Y.S. *J. Org. Chem.* **1985**, *50*, 2243.
[70] Organ, M.G.; Wang, J. *J. Org. Chem*. **2003**, *68*, 5568.
[71] De Lemos, E.; Porée, F.-H.; Commerçon, A.; Betzer, J.-F.; Pancrazi, A.; Ardisson, J. *Angew. Chem. Int. Ed. Engl.* **2007**, *46*, 1917.
[72] Glushka, J.N.; Perlin, A.S. *Carbohydr. Res.* **1990**, *205*, 305.
[73] Self, M.F.; Pennington, W.T.; Robinson, G.H. *Inorg. Chim. Act.* **1990**, *175*, 151.

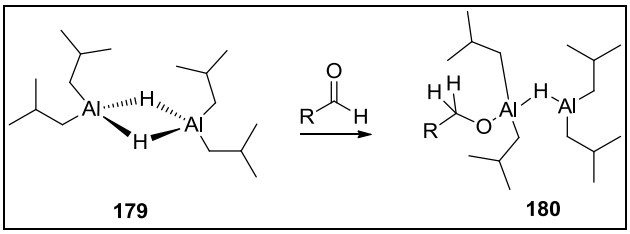

Scheme 6: Trapping of DIBALH reagent due to the dimeric nature of the reagent.

addition of excess acid which hydrolysed the Al-O bond and dissolved the complex.[69] The presence of an acid-sensitive TBS group in the compound precluded the use of excess acid to hydrolyse the Al-O bond and effect dissolution of the complex, therefore an alternate work-up procedure was used. After the addition of MeOH, saturated ammonium chloride was added, which is weakly acidic in nature, allowing for cleavage of the Al-O bond. As the solution warmed there was a vigorous evolution of gas, most likely dissolved hydrogen and isobutene, and the formation of a gelatinous precipitate. This was followed by dropwise addition of 3M HCl with vigorous stirring, until the gelatinous aluminium complex had dissolved. If extractions were performed before the complex was completely dissolved, yields of the alcohol were significantly lower, implying that dissolution of the complex is necessary for complete hydrolysis of the Al-O bond. Since the yields for this reaction were always moderate (60-79%), the HCl-based work-up most likely leads to some deprotection, yielding water soluble 2-methyl-1,3-propanediol, and negatively affecting the yield of the reaction.

The ^{1}H NMR spectrum of **149** showed the presence of a hydroxyl group by a broad signal at δ_H 2.79 while in the ^{13}C NMR spectrum the carbonyl carbon signal was absent and was replaced by a signal at δ_C 68.20T representing the carbon bearing the free hydroxyl group.

Transformation of alcohol (**149**) to the aldehyde (**150**), the substrate for the Horner-Wadsworth-Emmons (HWE) reaction, was accomplished by the Swern protocol using DMSO, oxalyl chloride and Et_3N.[74] The aldehyde was obtained in high yield as evidenced by the presence of a doublet signal in the ^{1}H NMR spectrum at δ_H 9.71 (*J* 1.6 Hz) which correlated with a resonance at δ_C 204.67 in the ^{13}C NMR spectrum. The aldehyde (**150**) was then reacted with the ethyl diisopropylphosphonoacetate in a HWE reaction, which gave a 9:1 mixture of *E:Z* alkene (**151**), in good yield (80 %).

The HWE reaction proceeds with high *E* selectivity due to the reaction occurring under thermodynamic control, with a number of equilibria being established in the reaction medium. Deprotonation of the phosphonate was achieved using ^{t}BuOK, to which the aldehyde was

[74] Omura, K.; Swern, D. *Tetrahedron*, **1978**, *34*, 1651.

added. Nucleophilic addition of the resonance stabilised phosphonate (**181**) to the aldehyde occurs as a reversible process, with the adduct in equilibrium with an oxaphosphetane intermediate.[75] The two possible geometries of the oxaphosphetane intermediate differ significantly in energy with the oxaphosphetane with the two large substituents *anti* on the 4-membered ring (**182**) being thermodynamically much more stable than that of its *syn* isomer (**183**) as shown in **Scheme 7**. The collapse of the ring with *anti* arrangement of substituents, driven by the presence of the electron withdrawing group gives the *E* isomer of the alkene (**184**). Due to the two oxaphosphetanes existing in equilibrium any *syn* isomer formed rapidly converts into the more stable *anti* isomer leading to a predominance of the *E* over the *Z* isomer.[76]

In this case a 9:1 ratio of *E:Z* isomers was obtained. In the ^{1}H NMR spectrum the resonances of the protons of the double bond (δ_H 6.89 and 5.79) showed a coupling constant of $^{3}J_{HH}$ 15.8 Hz which is characteristic for a disubstituted *E* alkene. The minor component showed a coupling constant of $^{3}J_{HH}$ 11.6 Hz characteristic of a *Z* alkene. The product was obtained as a mixture of isomers, but the abundance of the *Z* isomer was deemed low enough to continue with the synthesis. The *Z* isomer is formed by the collapse of the *syn* oxaphosphetane, which although thermodynamically unstable, must form to some extent in the reaction. Since the reaction was performed at low temperature (–78 °C), addition of the aldehyde at higher temperatures (0° C) would be expected to favour the thermodynamic product and increasing the yields of the desired *E* alkene. This modification should be investigated further.

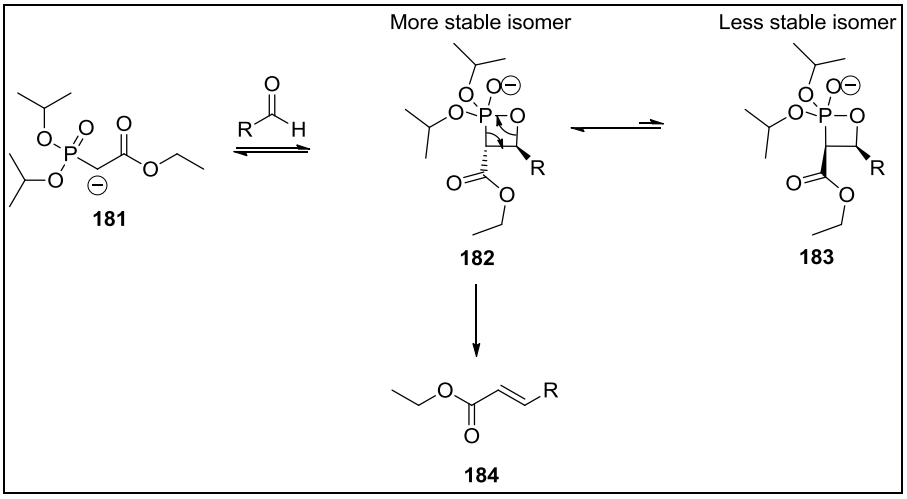

Scheme 7: Equilibrium of the oxaphosphetanes and formation of ester.

The α,β-unsaturated ester (**151**) was efficiently reduced to allylic alcohol (**152**), the substrate

[75] Larsen, R.O.; Aksnes, G. *Phosphorus Sulfur* **1983**, *15*, 219.
[76] Lefèbvre, G.; Seyden-Penne, J. *J. Chem Soc., Chem. Commun.* **1970**, 1308.

for the Sharpless epoxidation, by DIBALH.[77] Other common reducing agents such as LAH, and $NaBH_4$ reduce both the ester and the double bond to the alkanol due to their nucleophilic nature.[78,79] DIBALH is extremely effective in the reduction of the ester, with this reaction being complete in 20 min at −78 °C. After one equivalent of DIBALH had been added reduction to the aldehyde stage was indicated by the solution changing colour from clear to yellow, and this was reversed upon addition of the second equivalent of DIBALH as the reduction progressed to the alcohol stage. This reduction, though rapid and efficient, offered the same problematic work-up procedure. Hydrolysis of the Al-O bond was effected in the same manner as described previously by the addition of saturated NH_4Cl solution, followed by dropwise addition of 3M HCl solution until the gelatinous precipitate dissolved. Yields obtained by this method were good being in the region of 65-85%, with longer reaction times resulting in lower yields, probably due to some reductive cleavage of the O-Si bond.[80]

The appearance of a broad signal at δ_H 1.60 in the ^1H NMR spectrum indicated the presence of the –OH group, which when considered with resonances at δ_H 5.65 and 5.59 for the protons of the double bond, indicated the presence of an allylic alcohol. There was no indication of the presence of the *Z* isomer of the allylic alcohol in the ^1H and ^{13}C NMR spectra of the product after column chromatography.

Allylic alcohol (**152**) was then subjected to the Sharpless asymmetric epoxidation with the aim of producing epoxide (**153**). Application of the mnemonic shown in **Figure 1** indicates that the (*S*,*S*) enantiomer of tartrate should be used to oxidise the allylic alcohol to generate epoxide (**153**) with the required stereochemistry. The first attempt at epoxidation used the procedure described by Sharpless in his *Organic Syntheses* preparation of (2*S*,3*S*)-2,3-epoxyhexan-1-ol employing a semi-stoichiometric quantity of titanium catalyst.[81] $Ti(O^iPr)_4$ and diethyl (*S*,*S*)-tartrate were mixed at −20 °C in DCM in the presence of 4Å molecular sieves. This mixture was allowed to stir for 20 min to allow for the formation of Ti-tartrate complex (**168**). It has been found that the allylic alcohol or the TBHP can be added after complex formation, both methods giving similar yields, provided the catalyst is allowed to "age" prior to the addition of the final reagent. Omitting this aging period has been found to reduce the e.e. to 50 % for some substrates.[52] Preference is given to the method in which the TBHP is added after the aging of the complex, as there is the risk of an uncontrolled exothermic reaction upon addition of TBHP, especially if the reaction is performed on a large

[77] Martin, R.; Islas, G.; Moyano, A.; Pericas, M.; Riera, A. *Tetrahedron* **2001**, *57*, 6367.
[78] Evans, D.A.; Andrews, G.C.; Fujimoto, T.T.; Wells, D. *Tetrahedron Lett.* **1973**, 1389.
[79] Brown, M.S.; Rapoport, H. *J. Org. Chem.* **1963**, *28*, 3261.
[80] Corey, E.J.; Jones, G.B. *J. Org. Chem.* **1992**, *57*, 1028.
[81] Hill, J.G.; Sharpless, K.B.; Exon, C.M.; Regenye, R. *Org. Syn. Coll*. **1990**, *7*, 461.

scale. This reaction was on small scale, so this was not a concern; allyl alcohol (**152**) was therefore added to the titanium-tartrate mixture and the solution stirred for 30 min to allow the complex to age. One equivalent of anhydrous TBHP as a 4.9M solution in toluene was added slowly and the reaction was stirred for 72 h at –20 °C. After quenching and work-up it was found that the starting material and product had very similar R_f values on TLC using hexanes-Et_2O (1:1) and were consequently isolated together.

^{1}H NMR spectroscopic analysis of the product showed that these conditions produced a mixture of starting material and the two diastereomers of the epoxide. Two downfield resonances at δ_H 3.00 and 2.97 (each a ddd) were present representing H-2 for both diastereomers, while two upfield resonances at δ_H 2.91 and 2.80 (each a dd) represented H-3 for the two diastereomers. The resonances at δ_H 3.00 and 2.80 and those at δ_H 2.97 and 2.91 were shown to be coupled in a 2-D COSY experiment and assigned each of them to a specific diastereomer. Integration of the two lowfield resonances showed a ratio of *ca*. 1:1 which indicated that there was no selectivity in the Sharpless epoxidation. Resonances for the double bond protons were also observed in the spectrum and integration established that the amount of starting material was equivalent to the quantities of the two diastereomers of epoxide present.

This result seemed to indicate that some factor was overriding the preference that the Sharpless catalyst has for epoxidation of the *Si* face of the double bond and that in using the (*S*,*S*)-tartrate derived catalyst both the required (2*R*,3*R*)- and unwanted (2*S*,3*S*)-epoxides were formed in equal quantities during the reaction. This factor must have been responsible for both faces of the double bond being equally favoured as epoxidation sites.

There are two possible causes for the lack of stereoselectivity in this reaction. The first is simply that the chiral titanium-tartrate catalyst was not formed in the early stages of the reaction; therefore no stereocontrol would be observed during the epoxidation resulting in reaction on either face of the double bond to an equal extent. If this were the case the presence of the methyl group at C-4 would be expected to have some effect on the stereochemical outcome of the reaction with the *Re* face expected to be favoured, which would not produce a 1:1 ratio of products. The second reason would be due to substrate-reagent interactions reducing the energy difference between the two reaction pathways. This could be expected to give a 1:1 diastereomeric ratio of products.

Since the Sharpless reaction is a reagent controlled process and is known for producing epoxides in high e.e.'s, the observed ratio is more likely due to some contribution that the substrate makes to the structure and energy of the transition state complex. A number of

substrate specific factors such as the methyl group present at C-4 in the structure, which is *syn* to the *Si* face of the alkene being epoxidised, and the bulky TBS ether could have affected the outcome of the reaction, indicating that substrate control (as for the vanadium catalysed epoxidation of 4-hydroxycyclopentene in **Scheme 3**) potentially played an important role in this reaction. The opposing effect of these two factors, the reagent control of the Sharpless catalyst and substrate control of allylic alcohol (**152**), could combine to produce a 1:1 ratio of products.

The proposed mechanism of the reaction involves the delivery of the oxygen atom onto a specific face of the alkene, relying on a favourable interaction of the chiral catalyst with one face of the alkene, and consequently, this transition state must be energetically favoured (lower energy) compared to the transition state formed if epoxidation were to occur on the opposite face. Due to the large e.e.'s observed for other substrates,[52] it can be assumed that there is usually a large energy difference between these two states. If some factor were to increase the energy of the transition state lower e.e.'s would be expected. It is plausible then that the low e.e.'s obtained in this reaction was a result of the steric interactions of the catalyst with the substrate, most likely attributed to the methyl group at C-4, and the sterically demanding TBS group. This is a case of stereochemical mismatch between the chiral catalyst and the chiral substrate, whereby the desired transformation is energetically unfavourable due to the steric demands of the interaction.

Further evidence for this second pathway was provided by the achiral epoxidation of allylic alcohol (**152**) using MCPBA in DCM to give (2*RS*,3*RS*)-**153**. Analysis of the crude product by ^{1}H NMR spectroscopy indicated a diastereomeric ratio of 5:8 with the H-2 and H-3 resonances of the major diastereomer at δ_H 2.95 (ddd, *J* 2.5, 2.5, 4.8 Hz) and 2.88 (dd, *J* 2.5, 7.0 Hz), respectively. This result showed that the methyl group at C-4 and the alkene both contributed to the stereofacial selectivity observed in the reaction products.

Due to the steric mismatch between the catalyst and the substrate, the reaction was performed again but this time using diisopropyl (*S*,*S*)-tartrate to generate the chiral catalyst. In order to ensure that the reaction went to completion 1.5 equivalents of TBHP in toluene was used while the quantities of Ti($O^{i}Pr$)$_4$ and diisopropyl (*S*,*S*)-tartrate were increased to 0.84 and 1.0 equivalents, respectively. This combination of reagents gave mixtures which showed near complete reaction and a d.r. of 9:1 after purification by column chromatography. The H-2 and H-3 resonances of the major diastereomer appeared at δ_H 3.00 and 2.80, respectively which is the opposite finding to that obtained for the product from the reaction with MCPBA. The results further support the conclusion that MCPBA produced the epoxide product with the *anti* relative stereochemistry, whereas the Sharpless method as predicted favoured the *syn*

product. It appeared then that the chirality of the catalyst complex overrode, to some extent, the inherent stereofacial selectivity of the substrate.

Repetition of the reaction with catalytic quantities of titanium-tartrate complex (0.05, 0.10, 0.20 equivalents $Ti(O^iPr)_4$) resulted in all cases in the crude product having a d.r. in the range of 4:1–5:1 with overall yields between 65–80%. It therefore appeared that the optimum ratio of catalyst to substrate using 0.84 and 1.0 equivalents of $Ti(O^iPr)_4$ and (*S*,*S*)-diisopropyl tartrate gave the best results. When the reaction was repeated under these conditions a 4:1 d.r. was obtained for the crude product which, when combined with the results of the catalytic studies, indicated that the first result of a 9:1 d.r. must have been due to diastereomeric enrichment as a result of separation of the two diastereomers during the chromatography process.

This was indeed the case. Thin layer chromatography (TLC) of the mixture of diastereomers on silica gel using hexane-Et_2O (1:1) as eluent established a slightly greater R_f value for the major diastereomer than the minor diastereomer (0.18 vs. 0.16). Since these diastereomers were separable by TLC an attempt was made to purify the 4:1 mixture, obtained from the reaction employing 10 % catalyst, using flash column chromatography with hexane-Et_2O (1:1). Some degree of separation was achieved giving a 9:1 mixture of diastereomers. A second flash column with the same solvent afforded epoxide (**153**) as a 97:3 mixture (as determined by ^{1}H NMR spectroscopy) which was of sufficient purity to continue the synthesis. The yield of the reaction, however, at only 30% was low due to loss of product during the separation process.

As a result of the low yields, and the low diastereoselectivity observed in this reaction, it was decided to investigate other methods for the introduction of the stereocentre under study. Diol (**154**) as shown in **Scheme 2** was chosen as the target, as two stereoselective reactions known to produce diols in high e.e.'s are known: Sharpless asymmetric dihydroxylation,[82] and Jacobsen's hydrolytic kinetic resolution.[83] Sharpless dihydroxylation required a terminal alkene as a substrate and Jacobsen's method involves kinetic resolution of a terminal racemic epoxide also synthesised from a terminal alkene. The modified pathway, using the same chiral ester as starting material is shown in **Scheme 8**.

3.3 VINYL ADDITION ROUTE

3.3.1 Theoretical Aspects

[82] Hentges, S.G.; Sharpless, K.B. *J. Am. Chem. Soc*. **1980**, *102*, 4263.
[83] Tokunaga, M.; Larrow, J.F.; Kakiuchi, F.; Jacobsen, E.N. *Science* **1997**, *277*, 936.

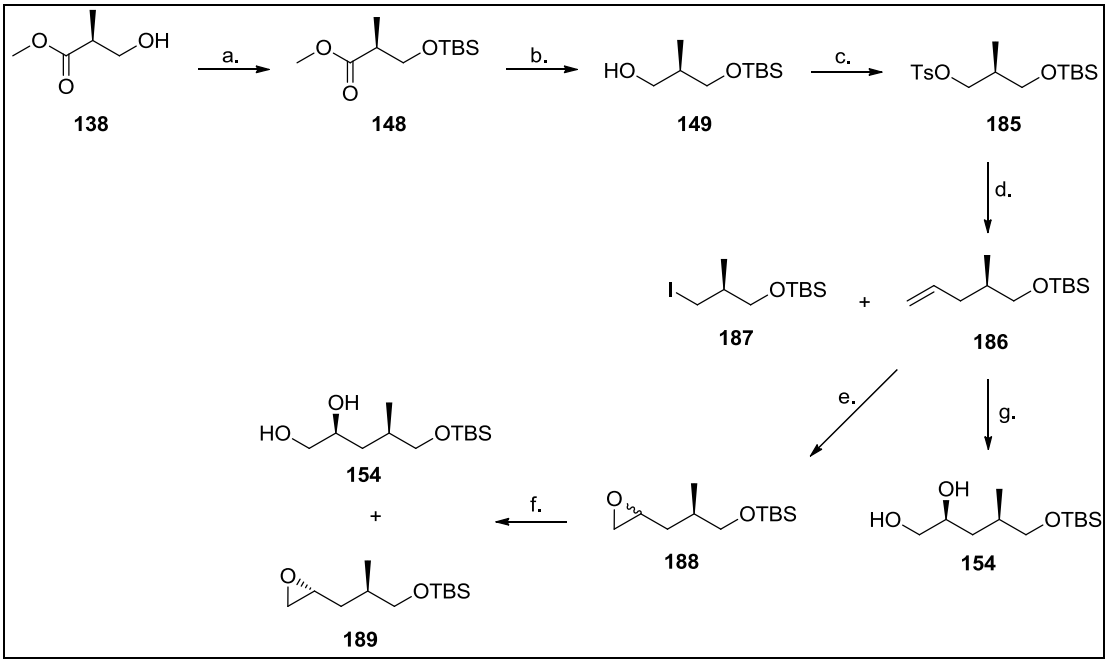

Scheme 8: Proposed synthesis of diol (**154**) using Sharpless dihydroxylation and hydrolytic kinetic resolution methodology.

Reagents: a. TBSCl, imidazole (96%); b. DIBALH (79%); c. TsCl, DMAP (67%); d. H_2C=CHMgBr, Cu(I)I (15% for **187**, 0% for **186**); e. MCPBA; f. (*R*,*R*)-Co(salen), H_2O, TsOH; g. K_2OsO_4, K_2CO_3, $(DHQ)_2PYR$, $K_3Fe(CN)_6$.

Organocopper and organolithium reagents have found many uses in organic synthesis as reagents for the formation of C-C bonds, and in the case of organolithiums also as strong bases, and as a result these reagents have been extensively studied. Organocopper reagents have found application in natural product synthesis and have been used in notable syntheses and critical coupling steps as in the synthesis of prostaglandin E_2 (**192**) which utilised a copper-mediated conjugate addition as a key step as shown in **Scheme 9**.[84,85]

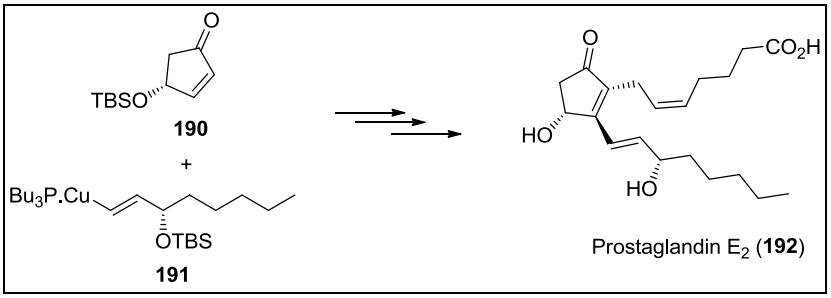

Scheme 9: Use of organocopper reagents in the synthesis of prostaglandin E_2.

[84] Suzuki. M.; Yanagissawa, A.; Noyori, R. *J. Am. Chem. Soc.* **1985**, *107*, 3348.
[85] Suzuki. M.; Yanagissawa, A.; Noyori, R. *J. Am. Chem. Soc.* **1988**, *110*, 4718.

Organolithium reagents (R-Li) are used predominantly as nucleophiles and bases in organic chemistry due to their behaviour as "R^-". These reagents can be used for the formation of C-C bonds by their reaction with either carbonyl electrophiles, generating alcohols, or with leaving groups (OTs, I, Br, Cl) giving alkylated products.

Organolithium reagents are produced predominantly by two methods: oxidative insertion using Li metal and the appropriate alkyl/aryl/vinyl halide, and through lithium-halogen exchange with *n*-BuLi and the appropriate alkyl/aryl/vinyl halide.[55]

Organocopper reagents are used for five key C-C bond formation reactions: conjugate addition, conjugate addition with enolate trapping, acylation, alkylation and arylation, and alkyne carbocupration trapping.[86] Probably the best known application of the organocopper reagents is in the conjugate addition of cuprates to the appropriate substrates. An application of this reaction is evident when α,β-unsaturated carbonyl compounds are subjected to Grignard reagents: the Grignard reagent, being a hard nucleophile, attacks the carbonyl carbon of the system rather than the alkene carbon due to the hard electrophilic nature of the carbonyl centre, giving the carbonyl adduct (**193**) as the major product. Addition of 1% CuCl generates the cuprate *in situ*, which, being a soft nucleophile attacks the soft electrophilic carbon centre of the alkene, giving the conjugate addition adduct (**195**) as the major product, as illustrated in **Scheme 10**.[55] Some dehydration products are also observed.

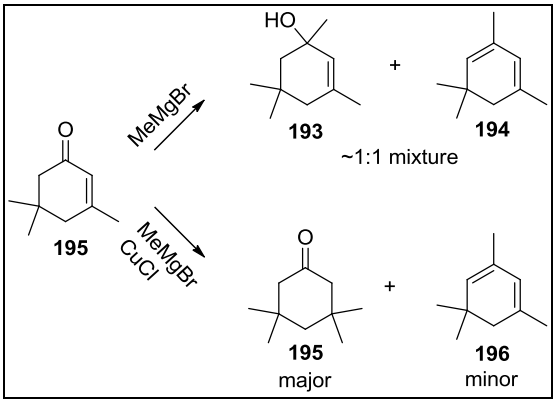

Scheme 10: Effect of addition of CuCl on a Grignard reaction with an α,β-unsaturated ketone.

Of particular interest of these copper-mediated reactions are the alkylation reactions. Alkylations with organocopper reagents use reagents derived from simple halides, negating the need to use complex functional group transformations to accomplish the desired reaction. The general alkylation reaction making use of organocopper reagents is shown in **Scheme 11**,

[86] Taylor, R.J.K. *Organocopper Chemistry: an overview*. Organocopper Reagents. Taylor, R.J.K (ed.). Oxford University Press, Oxford, p. 1.

with the organocopper reagent shown as "RCu".

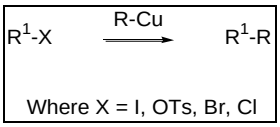

Scheme 11: General copper-mediated alkylation.

There are several classes of organocopper reagents which can be used in alkylations, including the copper-catalysed Grignard reagents, mono-organocopper reagents, Gilman reagents and higher order (HO) heterocuprates.[86] All of these reagents can be employed as the "RCu" species shown in **Scheme 11** with minor modifications to the reaction conditions.

Copper-catalysed Grignard reagents rely upon a transmetallation reaction between Mg and Cu to generate the organocopper reagent *in situ* by the reaction of R-MgX with a catalytic quantity of CuX where X = Cl, Br, I or CN. The exact structure of this organocopper reagent is unknown. As stated before, the softer Cu nucleophile enhances the reactivity of the reagent, allowing for alkylation reactions to proceed through a substitution-type mechanism with the suitable alkyl halide or alkyl sulfonate as evidenced by the inversion of configuration observed with secondary bromides and sulfonates.86 The primary advantage of using these reagents is their ease of preparation due to the commercial availability of many Grignard reagents.

Most other organocopper reagents can be produced from either the Grignard reagent, or from its lithiated equivalent as both Mg and Li are more active metals than copper and react to displace copper from the halide or cyanide salt, generating the organocopper reagent. When one equivalent of CuX is combined with one equivalent of R-M (M = Li or MgX), a mono-organocopper species is produced. The active species is thought to be the oligomeric/polymeric cuprate RCuX, which can then react as a nucleophile with the appropriate substrate in an alkylation reaction.[87] A major drawback of these reagents is their instability with most mono-copper reagents decomposing above –15 °C.

Gilman reagents (R_2CuM) are the major reactive species when two equivalents of R-M are used, and show enhanced nucleophilicity and stability and are therefore generally preferred. These reagents also do not seem to be polymeric and as a consequence, transformations are more reproducible due to the increased homogeneity of the reagent. During the reaction only a single "R" group of the Gilman reagent is transferred, which is problematic if R-M is not a cheap/commercially available species but has rather been synthesised by a complex synthesis.

[87] Posner, G.H. *Org. React.* **1975**, *22*, 253.

A method using mixed cuprates (R′RCuM) where R is the group for transfer and R′ is an alkynyl ligand overcomes this problem as alkynyl ligand transfer is slow compared to alkyl transfer, affording the desired product in high yields.[88] The use of two equivalents of R-Li and one equivalent of CuCN generates a higher-order heterocuprate, where CN acts as a "dummy ligand" and R is transferred during the reaction, while offering increased nucleophilicity and thermal stability.[89]

3.3.2 Experimental Aspects

The target for the vinyl addition reaction was tosylate (**185**), which could be synthesised from alcohol (**149**), derived from ester (**138**) as previously described, utilising protection of the free hydroxyl group of the ester (**138**) as the TBS ether, followed by DIBALH reduction of the ester to the primary alcohol, as shown in **Scheme 8a**. Tosylation of the alcohol (**149**) was performed in DCM by the addition of TsCl and DMAP as the base giving *O*-tosylate (**185**) in moderate yield.[90] Yields were only moderate due to the formation of a tosyl by-product, which had a similar R_f value to that of the tosylate product (**185**), which complicated product isolation due to co-elution of some fractions during column chromatography. Characteristic resonances between δ_H 7.3 and 7.8 were observed for the aromatic protons of the tosyl group, with a singlet observed at δ_H 2.42 in the ^{1}H NMR spectrum representing the resonance of the aromatic methyl group as well as the typical resonances of the TBS-ether, indicating that the desired product had indeed been formed.

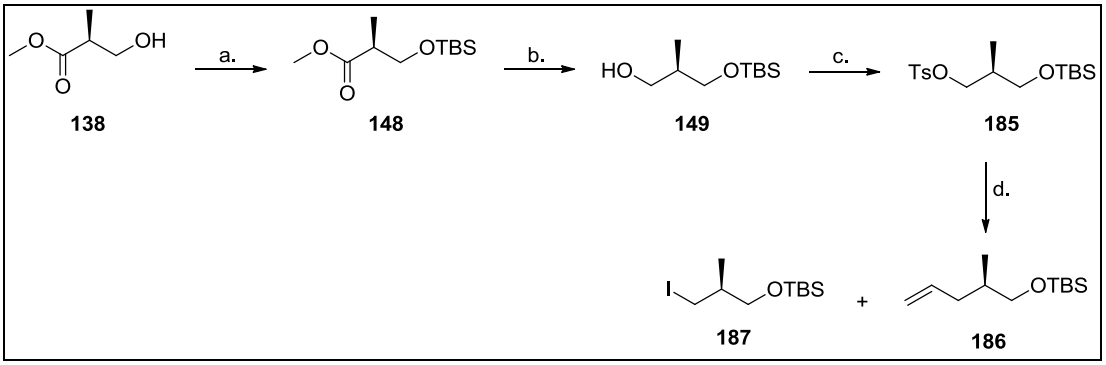

138 **148** **149** **185** **187** **186**

Scheme 8a: Synthesis of the alkene (**186**) the substrate for the Sharpless dihydroxylation reaction and hydrolytic kinetic resolution methodology.

Reagents: a. TBSCl, imidazole (96%); b. DIBALH (79%); c. TsCl, DMAP (67%); d. H_2C=CHMgBr, Cu(I)I (15% for **187**, 0% for **186**).

[88] Corey, E.J.; Beames, D.J. *J. Am. Chem. Soc.* **1972**, *94*, 7210.
[89] Lipshutz, B.H.; Wilhelm, R.S.; Floyd, D.M. *J. Am. Chem. Soc.* **1981**, *103*, 7672.
[90] Jung, M.E.; Nishimura, N. *Org. Lett.* **2001**, *3*, 2113.

The *O*-tosylate (**185**) was then subjected to the vinyl addition reaction utilising one equivalent of purified CuI[86] and 2.5 equivalents of vinyl-MgBr to generate the Gilman reagent. The CuI was added to a solution of the *O*-tosylate (**185**) in DCM at −50 °C followed by the dropwise addition of 2.5 equivalents of vinyl-MgBr, as a 1M solution in THF.[90] Upon warming, the solution became black and after 18 h, a significant quantity of starting material was still evident by TLC though a second spot had appeared with a higher R_f than the starting material as would be expected for the vinyl product. However, after isolation and spectroscopic analysis it was found that the vinyl product had not formed, but the iodo-substituted product (**187**) had been formed instead as was evident from the characteristic resonances at δ_H 3.28 (dd, *J* 4.3, 7.9 Hz, H-1a) and 3.23 (dd, *J* 4.3, 7.6 Hz, H-1b) and δ_C 13.81 for the carbon bearing the iodine atom. This is explained by a simple nucleophilic substitution of the tosylate group by iodide, a relatively good nucleophile.

Since this reaction did not appear to work, synthesis of the higher order (HO) heterocuprate was attempted as CuCN is known to be more stable than CuI, and these reagents show increased stability and nucleophilicity. Vinyllithium was prepared from vinyl bromide by metal-halogen exchange with 2 equivalents of 1.6M *n*-BuLi in hexanes at −78 °C, followed by addition of CuCN to produce an orange solution and a copper coloured precipitate to which the *O*-tosylate (**185**) in THF was added.[91] TLC analysis of this reaction showed that all starting material remained and no conversion to the vinyl product had occurred. Since HO cuprates are known to work well in the literature, it was postulated that the problem lay in the synthesis of the vinyllithium, and that the halogen-metal exchange reaction had not proceeded to completion, possibly due to a second metal-halogen exchange (between the vinyllithium and butyl bromide) occurring in the solution.

Preparation of vinyllithium by oxidative insertion between lithium metal and vinyl bromide was also attempted, followed by direct reaction with the *O*-tosylate with the aim of using vinyllithium directly as the nucleophile.[92] After the reaction only starting material was isolated while some decomposition of the starting material was observed. There are other methods available for the preparation of vinyllithium including the use of methyllithium and tetravinyltin,[93] or phenyllithium and tetravinyllead, or lithium metal and tetravinyltin,[94] however, these reagents were not available so these routes were not pursued.

[91] Lipshutz, B.H.; Parker, D.A.; Kozlowski, J.A.; Miller, R.D. *J. Org. Chem.* **1983**, *48*, 3334.
[92] Whitesides, G.M.; Casey, C.P.; Krieger, J.K. *J. Am. Chem. Soc.* **1971**, *95*, 1379.
[93] Liu, H.; Tomooka, C.S.; Xu, S.L.; Yerxa, B.R.; Sullivan, R.W.; Xiong, Y.; Moore, H.W. *Org. Syn. Coll.* **2004**, *10*, 178.
[94] Juenge, E.C.; Seyferth, D. *J. Org. Chem.* **1961**, *26*, 563.

Since these routes were unsuccessful alternative routes for the synthesis of alkene (**186**) were sought. One reliable method for the generation of alkenes is through the use of Wittig methodology so this route was investigated further.

3.3.3 Alternative Experimental Approach

Using Wittig methodology to generate the terminal alkene requires the use of two one-carbon addition reactions. Retrosynthetic analysis (**Scheme 12**) of the aldehyde required for the Wittig reaction (**198**) leads to nitrile (**199**) produced from tosylate (**200**) by an S_N2 reaction with cyanide. This procedure therefore adds three steps to the synthetic route but is a reliable method based on simple functional group transformations.

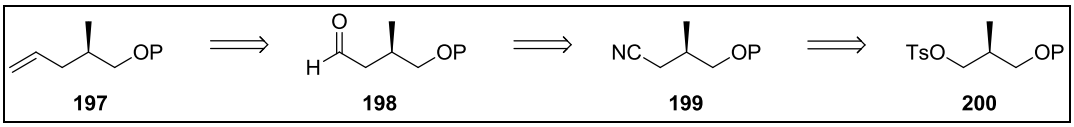

Scheme 12: Retrosynthetic analysis using Wittig methodology.

The protecting group strategy for this method was changed and instead of using the silyl ether as the protecting group, the benzyl ether was used. The change of protecting group allowed for the reduction of the ester to be performed with LAH instead of DIBALH and hopefully increasing the yields of the reduction with the synthetic strategy shown in **Scheme 13**.

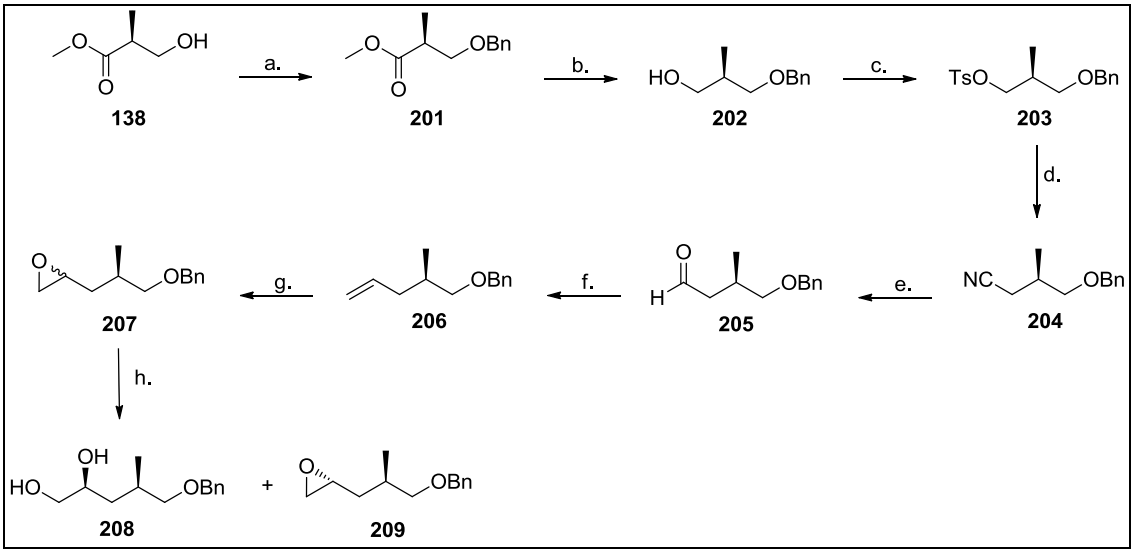

Scheme 13: Modified alkene approach using Wittig methodology.

Reagents: a. i). Benzyl 2,2,2-trichloroacetimidate, TfOH (96%); b. LAH (94%); c. TsCl, DMAP, pyridine (98%); d. NaCN, DMF (92%); e. DIBALH (69%); f. CH_3PPh_3I, *n*-BuLi (83%); g. MCPBA (50%); h. (*R*,*R*)-Co(salen), H_2O, TsOH (21%).

The ester (**138**) was benzylated under acidic conditions using benzyl 2,2,2-trichloro-acetimidate and catalytic TfOH. The solid 2,2,2-trichloroacetamide by-product is filtered from the reaction medium before concentration and column chromatography gave the benzyl ether (**201**) in 96% yield.[95] Acidic conditions were preferred over basic conditions for the benzylation reaction to prevent elimination of the hydroxyl group. The characteristic AB spin system of the benzylic protons was observed at δ_H 4.51 and 4.50 with $^2J_{HH}$ 12.6 Hz in the ^{1}H NMR spectrum while the corresponding carbon resonance appeared at δ_C 71.83T in the ^{13}C NMR spectrum.

The ester function in (**201**) was reduced by dropwise addition of a solution of the ester in Et_2O to a suspension of LAH in Et_2O.[95] The alcohol (**202**) was obtained in 94% yield after column chromatography – an improvement over the yield for the DIBALH reduction. Tosylation of the alcohol was performed by addition of alcohol (**202**) to a solution of pyridine and catalytic DMAP in DCM, before *p*-TsCl was added. The *O*-tosylate (**203**) was isolated in 98% yield and showed the aromatic methyl resonance at δ_H 2.39 in the ^{1}H NMR spectrum. The *O*-tosylate (**203**) was subjected to a nucleophilic substitution with NaCN in DMF at 90 °C for 24 h. After work-up of the reaction the nitrile (**204**) was obtained as a clear oil in 92% yield after distillation. The nitrile carbon resonance appeared at δ_C 118.44 in the ^{13}C NMR spectrum, with the characteristic nitrile stretching frequency was observed at 2334 cm^{-1} in the IR spectrum.

The nitrile (**204**) was then reduced to the aldehyde by addition of DIBALH at 0 °C, generating the imine, which was hydrolysed to the aldehyde (**205**) (69% yield) upon work-up of the reaction with aqueous sodium potassium tartrate solution.[96] The tartrate solution forms a complex with aluminium ions preventing the formation of the gelatinous aluminium complex and emulsion, which had complicated previous work-up procedures. The NMR spectra of the aldehyde (**205**) were characterised by the aldehyde proton resonance in the ^{1}H NMR spectrum as a double doublet (*J* 2.0, 2.2 Hz) at δ_H 9.69, as a result of coupling with the adjacent diastereotopic methylene protons, and the carbonyl carbon resonance at δ_C 202.35D in the ^{13}C NMR spectrum.

Subsequent Wittig olefination of the aldehyde (**205**) was accomplished by reaction with the ylid prepared by deprotonation of methyltriphenylphosphonium iodide with *n*-BuLi in THF[97] to give the alkene (**206**) in 83% yield. The carbon atoms of the newly-formed terminal double

[95] White, J.D.; Johnson, A.T. *J. Org. Chem.* **1994**, *59*, 3347.
[96] Reid, J.G.; Debiak-Krook, T. *Tetrahedron Lett*. **1990**, *31*, 3669.
[97] Mandel, A.L.; Bellosta, V.; Curran, D.P.; Cossy, J. *Org. Lett*. **2009**, *11*, 3282.

bond appeared at δ_C 136.92D and 115.90T in the ^{13}C NMR spectrum. The protons of the terminal double bond appeared at δ_H 5.78 (ddt, *J*, 17.0, 10.2, 6.8 Hz) and 5.04 – 4.97 (m).

Although the use of this alternative route (as outlined in **Scheme 13**) required additional steps, the reactions were accomplished in good yields to provide the terminal alkene required for synthesis of the diol (**208**). Attention now turned to the conversion of the double bond to a 1,2-diol system with the concomitant formation of a new stereocentre.

3.4 JACOBSEN ROUTE

3.4.1 Theoretical aspects

Although Sharpless had developed an efficient catalyst system for the asymmetric epoxidation of allylic alcohols the methodology cannot be used for the stereoselective epoxidation of unfunctionalised alkenes.

This problem was solved when a chiral salen ligand was developed by Jacobsen and co-workers in the 1990's, and its associated Mn(III) complex shown in **Figure 3** was shown to be an efficient chiral catalyst for the epoxidation of conjugated unfunctionalised alkenes.[98] The complex was based on either of the two enantiomers of 1,2-diaminocyclohexane from which the sterically bulky Schiff-base complex is derived.

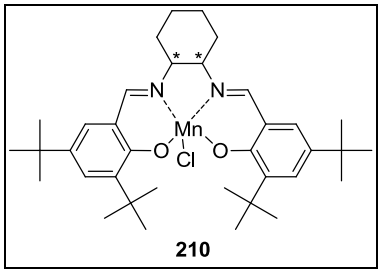

210

Figure 3: Jacobsen's asymmetric salen-Mn(III) catalyst.

The catalyst employs an oxidant (either NaOCl or MCPBA) as well as a co-oxidant such as 4-phenylpyridine *N*-oxide or *N*-morpholine oxide to give an active oxo-species which stereoselectively epoxidises a specific face of the alkene. The mechanism of the reaction giving rise to the stereoselectivity is not fully understood, though it is thought that the active complex adopts a specific conformation giving rise to a chiral pocket which then interacts with the alkene. The additives are thought to prevent the formation of unreactive μ-oxo dimers by binding to the monomeric manganese centres, thereby inhibiting dimer formation.[98]

[98] Canali, L.; Sherrington, D.C. *Chem. Soc. Rev.* **1999**, *28*, 85.

Insight into the potential application of such a reaction was demonstrated by Jacobsen when the catalyst was used to synthesise the *N*-benzoyl-3-phenylisoserine side-chain of the anti-cancer compound taxol.[99]

While developing a similar catalyst based on the same ligand for the desymmetrization of *meso* epoxides, Jacobsen serendipitously discovered that a cobalt complex had stereoselectively hydrolysed 1,2-epoxyhexane, which after some study, was found to be co-catalysed by residual acetic acid present in the 1,2-epoxyhexane.[100] This reaction and catalyst were developed further into a system widely applicable for the hydrolytic kinetic resolution of racemic terminal epoxides using relatively cheap, safe starting materials including water as summarised in **Scheme 14**.

The chiral salen-Co(III) complex selectively hydrolyses one enantiomer (diastereomer) of the epoxide due to the structural features conferred by the 1,2-diamino moiety of the catalyst. The reaction therefore produces one enantiomer of a 1,2-diol while the other enantiomer of the epoxide remains unreacted. Although originally developed as a route for the stereoselective synthesis of terminal epoxides, the 1,2-diols produced as side-products in the reaction are also potentially synthetically useful as these too are produced stereoselectively in the reaction.

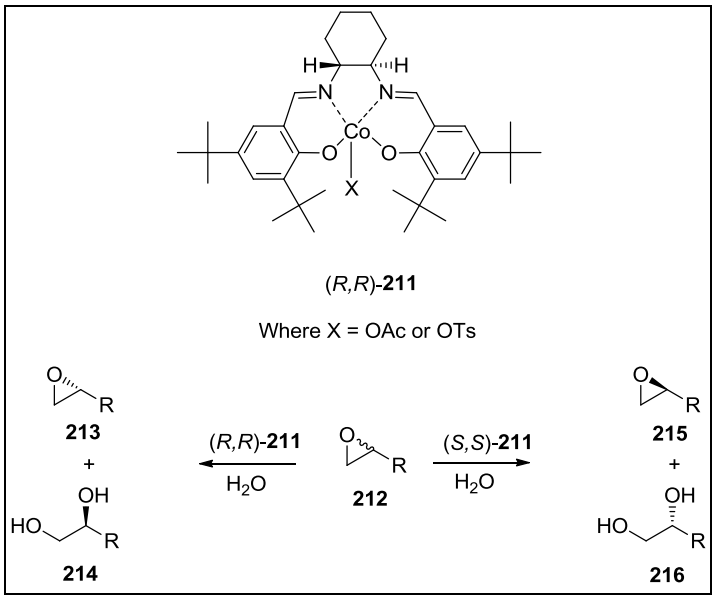

Scheme 14: Jacobsen's hydrolytic kinetic resolution catalyst and prediction of products.[101]

[99] Deng, L.; Jacobsen, E.N. *J. Org. Chem.* **1992**, *57*, 4320.
[100] Jacobsen, E.N. *Acc. Chem. Res.* **2000**, *33*, 421.
[101] Schaus, S.E.; Brandes, B.D.; Larrow, J.F.; Tokunaga, M.; Hansen, K.B.; Gould, A.E.; Furrow, M.E.; Jacobsen, E.N. *J. Am. Chem. Soc.* **2002**, *124*, 1307.

This reaction, being a kinetic resolution, relies on the more rapid reaction of one enantiomer (diastereomer) of a substrate to resolve the stereoisomers. The most useful method to characterise kinetic resolution processes involves the comparison of the rates of reaction of the fast-reacting stereoisomer (k_{fast}) and that of the slow-reacting stereoisomer (k_{slow}), which, by division gives the k_{rel} value for the process. This method is favoured over comparison of e.e.'s for the two products due to the e.e. being a function of conversion for kinetic resolution processes. For any kinetic resolution process the larger the k_{rel} value, the more efficient the kinetic resolution, with highly selective processes having k_{rel} values >50. This reaction has been shown to have k_{rel} values of >100 for most substrates, with some substrates having k_{rel} values of >500.[101] These values indicate an extremely selective process and this represents one of the most stereoselective reactions known.

The salen-Co(II) complex is available commercially, or can be synthesised from cobalt(II) acetate and the salen ligand, which itself can be prepared from relatively cheap starting materials including L-tartaric acid (resolving agent), 1,2-diaminocyclohexane and 2,4-di-*t*-butylphenol.[102] The Co(II) complex is inactive and must first be oxidised to the Co(III) complex to be catalytically active. Oxidation is achieved by addition of AcOH or TsOH (or any mild Bronsted acid), and stirring in the presence of oxygen (air is sufficient), resulting in a colour change from red to brown- indicating the completion of the oxidation. This activated complex is then used directly with no further purification. The complex is added to a solution of the epoxide followed by the addition in most cases of 0.55 equivalents of water and stirring for 12 h, though for some substrates 0.7 equivalents of water and reaction times >40 h have been shown to be optimal. The catalyst has been found to be effective at producing epoxides of high e.e. with as little as 0.5-2 % catalyst. An additional benefit of this reaction is that the catalyst can be recycled in cases were the products can be easily removed from the reaction mixture (*e.g.* by distillation). The catalyst residue can be reactivated by reaction with the appropriate Bronsted acid in the presence of air with little to no loss of selectivity observed in cycles of catalyst use and regeneration.[101]

The origin of stereoselectivity has yet to be proven; however, from the data currently available, a mechanism for the reaction has been postulated by Jacobsen and co-workers.[103] Kinetic studies have shown a second order rate dependence on the Co-catalyst concentration, which seems to indicate that the reaction process involves two molecules of Co-catalyst

[102] Larrow, J.; Jacobsen, E.N. *Org. Syn.* **1998**, *75*, 1.
[103] Nielsen, L.P.C.; Stevenson, C.P.; Blackmond, D.G.; Jacobsen, E.N. *J. Am. Chem. Soc.* **2004**, *126*, 1360.

(bimetallic mechanism),[83] while other studies have shown that the anion present (OAc vs OTs, Cl etc.) also affects the rate of the reaction.[104]

Based on this evidence, Jacobsen proposed a mechanism by which the reaction was thought to work. Though predicting the products it does not explain the origin of stereoselectivity. The kinetic data seem to indicate that the catalytic cycle begins with the generation of a hydroxo-complex by the irreversible reaction with the activated Co(III) catalyst using water and one equivalent of the matched epoxide to form the epoxide addition product (**217**) which is lost as shown in **Scheme 15**. The hydroxo-complex (**218**) then reacts with a Lewis base (thought most likely to be water) generating complex (**220**). At the same time a second activated Co(III) catalyst molecule binds to the epoxide oxygen of the matched epoxide. The hydroxo-Lewis base complex then reacts as a nucleophile with the epoxide-complex with the opening of the epoxide ring by nucleophilic attack of the hydroxo group in the rate determining step of the reaction. The adduct (**221**) is hydrolysed upon reaction with water giving the free diol (**214**), activated Co(III) complex (**211**), and the hydroxo-complex (**220**) which are free to perform a second catalytic cycle.

The simplified rate expression for the addition of Co-OH complex (**220**) to epoxide is given in **Equation 1** (where f is a function of the concentration of water, matched epoxide and mismatched epoxide), and reflects the dependence of the rate of the reaction on the concentration of the two Co species in the reaction.[103] From this rate law the rate of the reaction will be greatest when the concentration of Co-X (**211**) and Co-OH (**218**) are approximately equal in the reaction mixture, and from the mechanism shown in **Scheme 15**, it can be seen that the concentration of the Co-OH species is in turn controlled by the rate of irreversible addition of counter ion X to the epoxide, implying that the identity of the counter ion can play a significant role in the overall rate of catalysis.

$$\text{rate} = k'_{\text{cat}} f\,[\text{Co}-\text{OH}]_{\text{tot}}[\text{Co}-\text{X}]_{\text{tot}} \qquad (1)$$

Counter ion X plays two important roles in the reaction. Its identity governs how quickly Co-OH is formed, as this process involves the addition of X to the epoxide, and it also affects the binding of the epoxide to the Co-X complex, with more electronegative X ligands being expected to increase the rate of addition of Co-X to the epoxide due to its ability to stabilise the negative charge formed on Co-X during the addition.

If counter ion X adds rapidly to the epoxide (as observed when X = Cl), most of the catalyst exists in the Co-OH mode, while the concentration of Co-X becomes low. This results in a

[104] Kim, G.-J.; Lee, H.; Kim, S.-J. *Tetrahedron Lett.* **2003**, *44*, 5005.

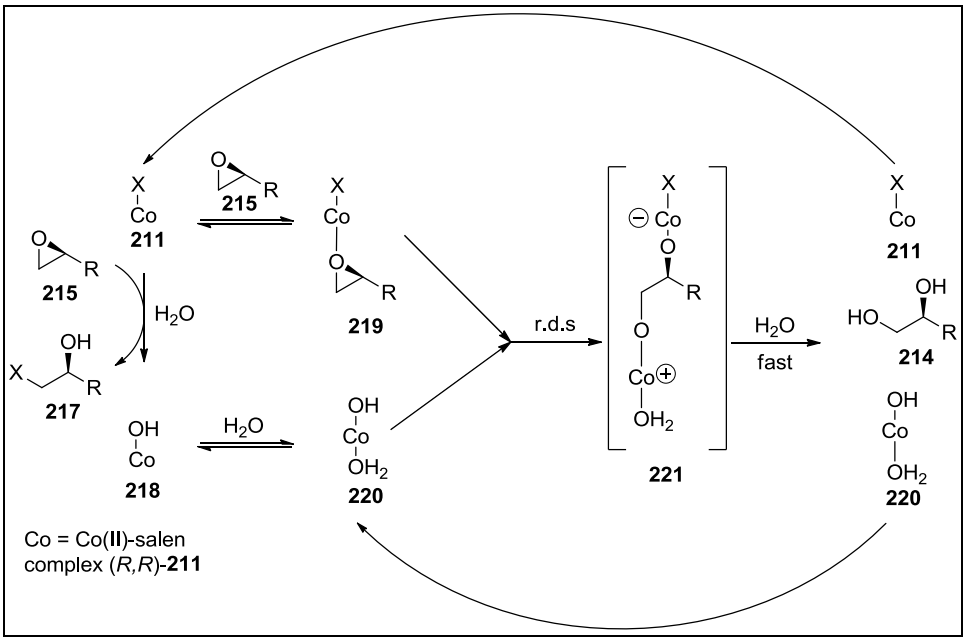

Scheme 15: Mechanism of hydrolytic kinetic resolution.[103]

slow rate of reaction (or in this case resolution), as predicted by **Equation 1**, however the e.e.'s observed remain high. When X = OAc the resolution process occurs rapidly at first, but slows significantly as conversion approaches 100 % for the matched epoxide. This effect is due to the acetate ion reacting more slowly with epoxide to generate Co-OH, meaning concentrations of Co-OH and Co-X remain at near optimal 50:50 ratio for a longer time period and resulting in reduced times for resolution. Most of the catalyst is converted to the Co-OH form when the conversion approaches 100 % for the matched epoxide resulting in lower yields. It was found by experiment that optimal conversion occurs when X = OTs. Addition of X to the epoxide generating Co-OH occurs at such a rate that when conversion approaches 100 %, the Co-OH: Co-X catalyst ratio is approximately 50:50, meaning shorter reaction times and increased yields.[103]

The origin of the selectivity of the resolution is still debated. However, a proposal has been made after studying various complexes using NMR spectroscopic techniques and density functional theory (DFT) calculations.[105] Using pulsed field gradient NMR spectroscopic techniques, it was shown that both stereoisomers of the epoxide bind with equal affinity to the Co-X species in the reaction, indicating that the observed stereoselectivity is not as a result of epoxide binding, but is due to the stereoselective attack of the nucleophilic species (Co-OH). Using data generated from paramagnetic chemical shifts for the complex in titration experiments, as well as data from chemical shift and structure calculations using DFT,

[105] Kemper, S.; Hrobárik, P.; Kaupp, M.; Schlörer, N.E. *J. Am. Chem. Soc.* **2009**, *131*, 4172.

allowed for the calculation of a proposed structure of the catalytic, bimetallic complex. This calculated structure of the complex showed that the nucleophilic species (Co-OH) adopted a twisted conformation where the aromatic rings of the salen ligand are not co-planar. As a result the *t*-butyl groups on the aromatic rings could be predicted to preclude the approach of the nucleophilic species to the mismatched stereoisomer of the epoxide bound to Co-X, most likely through a steric interaction. As a result of this steric interaction, this epoxide is not opened by the nucleophile and remains unreacted, providing the means for kinetic resolution.

3.4.2 Experimental Aspects

The synthetic route based on the hydrolytic kinetic resolution methodology shown in **Scheme 13a** used the benzyl protected alkene (**206**) synthesised as discussed earlier.

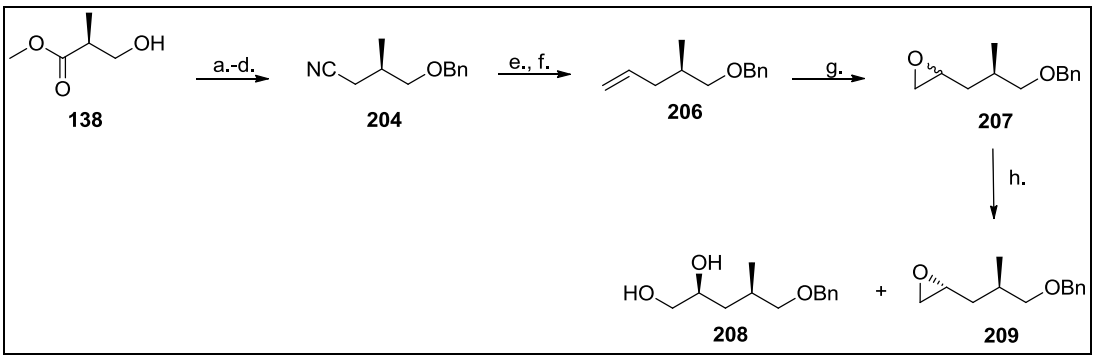

Scheme 13a: Wittig methodology and the hydrolytic kinetic resolution approach to the diol (**208**).

Reagents: a. i). Benzyl 2,2,2-trichloroacetimidate, TfOH (96%); b. LAH (94%); c. TsCl, DMAP, pyridine (98%); d. NaCN, DMF (92%); e. DIBALH (69%); f. CH_3PPh_3I, *n*-BuLi (83%); g. MCPBA (50%); h. (*R*,*R*)-Co(salen), H_2O, TsOH (21%).

In order to generate the benzyl protected epoxide (**207**) for use in the hydrolytic kinetic resolution reaction using the salen-Co(II) complex, the alkene (**206**) was treated with MCPBA in DCM for 48 h to give the epoxide (**207**) in 50% yield. The integration of the signals for the epoxide protons between δ_H 3.00 and 2.40 in the ^{1}H NMR spectrum of the epoxide (**207**) established the d.r. as *ca*. 1:1 for the mixture of diastereomeric epoxides formed in the reaction. During the reaction it was noted that significant quantities of by-products were forming in the reaction (up to 0.4 g from 1.0 g of alkene) indicating that side reactions were most likely the cause of the low yields. These by-products appear to be *m*-chlorobenzoate esters, but their identity could not be unambiguously assigned.

The epoxide obtained was then subjected to a hydrolytic kinetic resolution, using Jacobson's

method. (*R*,*R*)-Co(II)-salen (13 mol%) was dissolved in DCM and *p*-TsOH was added. The mixture was stirred open to the air for 2 h, during which time the colour changed from red to brown, indicating that the oxidation process had occurred and the (*R*,*R*)-Co(III)-salen-OTs complex had formed. After dissolving the catalyst in THF the racemic epoxide (**207**) was added and the solution cooled to 0 °C before three equivalents of water were added dropwise, and stirred at room temperature for 3 h. TLC analysis showed two distinct spots, one with the R_f value which matched that of the epoxide and another with a much lower R_f value, which was assumed to be the diol. Separation of these products by column chromatography, followed by characterization showed that the diol had been produced, in 21% yield with a d.r. of *ca*. 1:1 with the one diastereomer present in a slight excess as estimated from the signal intensities of the hydroxyl bearing carbons in the ^{13}C NMR spectrum at δ_C 68.15D (major) and 67.02D (minor) for C-2.

Much of the epoxide remained unreacted (150 mg isolated from 257 mg), indicating that the hydrolysis was occurring very slowly, with little to no selectivity or preference for one of the diastereomers. Slow hydrolysis is usually due to the effect of the counter ion; however, the tosylate has been shown to be one of the most efficient catalysts for the reaction, indicating that another factor was responsible for the slow reaction.

In order to ensure the counter ion was not responsible for the slow reaction and lack of resolution, the procedure was repeated with glacial acetic rather than *p*-TsOH during the activation step. This experiment had the same result as the experiment where the counter ion was *p*-TsOH in that conversion after 40 h was very low (12 %), and the diol had a diastereomeric ratio again of approximately 1:1; but in this case, the other diastereomer was in slight excess, as estimated from the ^{13}C NMR spectrum, with most of the starting material recovered.

During the kinetic resolution process, the mismatched substrate is also expected to react, but the rate of this reaction is expected to be significantly slower than that of the matched substrate (as given by k_{rel}). Since the conversion rate was slow for the reaction, it could be concluded that the rate of the reaction of the matched substrate had been slowed to match that of the mismatched substrate, most likely due to a feature or property of the substrate. Structural features of the substrate which could potentially interfere with the reaction include the methyl group, projecting onto the same face as that which is reacting in this case, or potentially the benzene ring, which could be involved in π-π stacking interactions with the two salen ligands in the active complex and thus affect the stereochemical outcome of the reaction. These interactions could have prevented the approach of the nucleophilic Co-OH species, as the nucleophilic species is required to approach the catalyst-bound matched

epoxide along a specific orientation to minimize steric interactions between the epoxide- and nucleophile-bearing cobalt complexes participating in the reaction. If the approach of the nucleophile bearing complex is hindered in any significant way it could be predicted that the rate of the reaction would be significantly slowed.

Since this reaction also failed to provide diol (**208**) in sufficient enantiomeric excess, it was decided to attempt the direct asymmetric dihydroxylation of the alkene using Sharpless' method based on quinine derivatives. The protecting group strategy was again altered, and a silyl ether (TBDPS) was used for the protection of the primary hydroxyl of starting material (**138**), as summarised in **Scheme 16**.

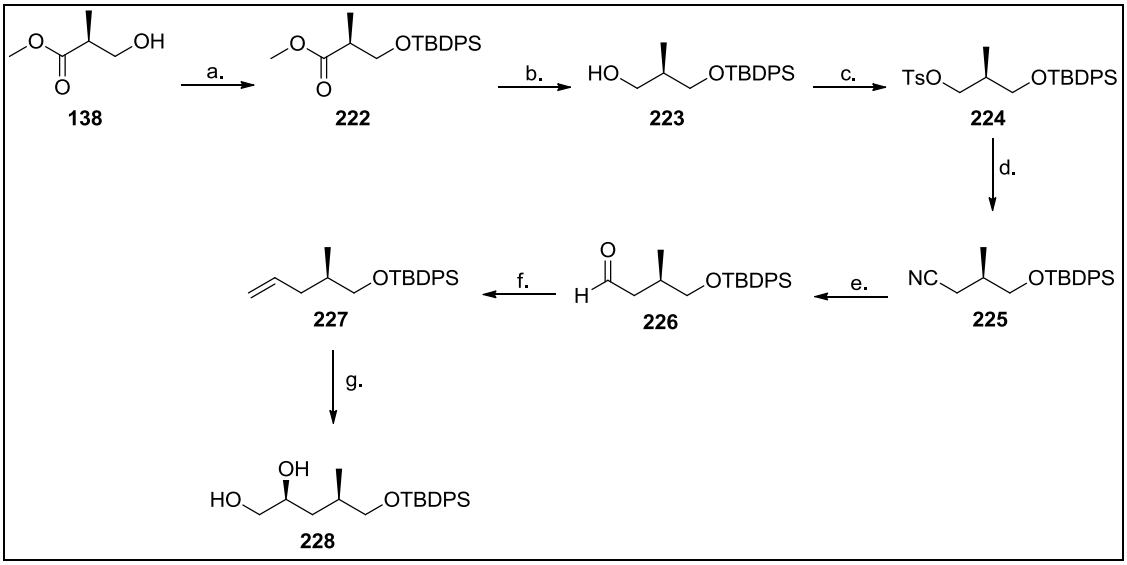

Scheme 16: Sharpless asymmetric dihydroxylation route, using TBDPS as the protecting group.

Reagents: a. TBDPSCl, imidazole (99%); b. DIBALH (77%); c. TsCl, DMAP (91%); d. NaCN, DMF (94%); e. DIBALH (66%); f. CH_3PPh_3I, *n*-BuLi (67%); g. K_2OsO_4, K_2CO_3, $(DHQ)_2PYR$, $K_3Fe(CN)_6$ (92%).

3.5 Sharpless Asymmetric Dihydroxylation Route

3.5.1 Theoretical Aspects

Before the discovery of catalytic *syn* dihydroxylation, vicinal diols were most commonly synthesised from alkenes using stoichiometric quantities of the highly toxic osmium tetroxide (OsO_4) in pyridine, followed by a reductive work-up to cleave the osmate ester and obtain the diol.[106] This procedure is mild and applicable to a number of substrates and was therefore

[106] Crigee, R. *Justus Liebigs Ann. Chem*. **1936**, *45*, 3329.

popular despite the toxicity of the reagent. The versatility of the reaction led to a drive to discover a stereoselective version of the same reaction based on the same principles described above: using coordination of a chiral ligand to the active metal centre with the hope of introducing stereoselectivity during the reaction mechanism.

The basis for the modification came from the idea that pyridine, the solvent for the general reaction, was thought to coordinate to the osmium centre via the nitrogen atom during the reaction and consequently increasing the rate of the dihydroxylation. Sharpless and Hentges theorised that by introducing a chiral nitrogen-containing ligand, the reaction could potentially be made stereoselective.[82] They found that the cinchona alkaloid derived diastereomers dihydroquinidine acetate (**229**) and dihydroquinine acetate (**230**) (**Figure 4**) when added to the stoichiometric reaction in toluene, gave products in moderate enantiomeric excesses (highest being for stilbene, at around 80% e.e.), with improvements obtained at low temperatures. The face of the alkene involved in the hydroxylation was predicted by the choice of ligand. The stereochemistry of the product is predicted with the mnemonic shown in **Figure 4** and is based on assigning the relative sizes of the substituents around the double bond.

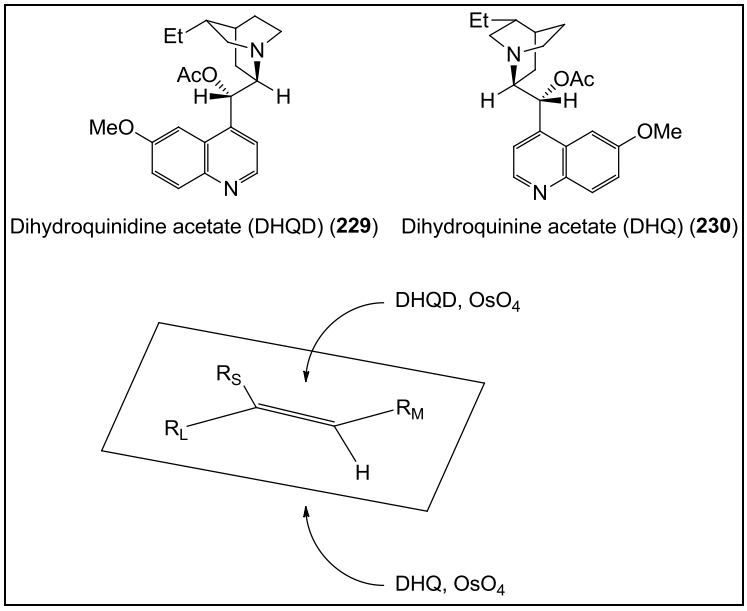

Figure 4: Ligands investigated for introduction of chirality during dihydroxylation.

These initial conditions underwent a number of modifications, each of which resulted in increased e.e.'s. The first of these modifications involved the addition of a co-oxidant, such as *N*-morpholine oxide, allowing the reaction to proceed with catalytic amounts of OsO_4, while

using the *p*-chlorobenzoate derivatives rather than the acetate derivatives.[107] The co-oxidant oxidised osmate (OsO_4^{2-}) back to OsO_4 regenerating the active reagent – thus reducing possible exposure to large amounts of OsO_4 and significantly reducing the cost of the procedure. The alkaloid amine derivatives were shown to dramatically increase the reaction rate, where $t_{1/2}$ for the reaction in the absence of chiral tertiary amine ligands was 108 min, while in the presence of the ligands it was 4.5 min, indicating that the process of ligand accelerated catalysis was important. In the presence of achiral tertiary amine ligands, $t_{1/2}$ increased substantially to over 30 h.

In experiments to determine the reaction mechanism, stepwise addition of reagents (alkene, oxidant, then either additional alkene, or water) led to the inference of the catalytic mechanism.[108] Observations in these stepwise addition experiments led to a proposed mechanism where two catalytic cycles operated concurrently: one which produces products with high enantioselectivity, and the other which did not, which was inferred from observations that could not be explained by a single cycle. At the conjunction of these two proposed catalytic cycles lay a trioxoglycolate species which could undergo two possible reactions: either a hydrolysis giving the diol and osmium catalyst (in the cycle producing high e.e's) or addition of a second equivalent of alkene to give a bisglycolate ester (in the cycle producing low e.e.'s). The second cycle was shown to produce very low e.e.'s, and in some cases the opposite diastereomer to what is predicted.

Probably the most significant improvement to the catalytic reaction was the introduction of potassium hexacyanoferrate as the co-oxidant, in a biphasic *t*-BuOH-water reaction medium as described by Minato *et al.*[109] This process was also found to overcome the decreased reaction rate as observed for achiral tertiary amine ligands. The substitution of *N*-morpholine oxide with potassium hexacyanoferrate was shown to significantly increase the e.e.'s obtained during the reactions and was thought to be due to suppression of the second e.e. reducing catalytic cycle as a result of the formation of a biphasic system by a salting-out effect.[110]

Subsequent modifications to the reaction in order to increase both the e.e. and scope of substrate involved substitution of various groups in place of the *p*-chlorobenzoate ester. Various aryl ether derivatives were shown to increase the selectivity of the reaction, with some aryl ethers shown to give higher e.e.'s for aliphatic substrates, with 9-*O*-phenyl, 9-*O*-

[107] Jacobsen, E.N.; Marko, I.; Mungall, W.S.; Schroder, G.; Sharpless, K.B. *J. Am. Chem. Soc.* **1988**, *110*, 1968.
[108] Wai, J.S.M.; Marko, I.; Svendsen, J.S.; Finn, M.G.; Jacobsen, E.N.; Sharpless, K.B. *J. Am. Chem. Soc.* **1989**, *111*, 1123.
[109] Minato, M.; Yamamoto, K.; Tsuji, J. *J. Org. Chem.* **1990**, *55*, 766.
[110] Kwong, H.-L.; Sorato, C.; Ogino, Y.; Chen, H.; Sharpless, K.B. *Tetrahedron Lett.* **1990**, *31*, 2999.

(1′-naphthyl) and 9-*O*-(9′-phenanthryl) ethers showing the greatest selectivity.[111,112] Even with these modifications, there was still room for the general improvement of the procedure as the e.e.'s for some substrates remained relatively low (especially for terminal alkenes, such as 1-decene where maximum e.e. was 74%). Further ligand development led to the discovery of the phthalazine ligand class (**Figure 5**), which showed improved results and is now the most common catalyst for all non-terminal alkenes.[113]

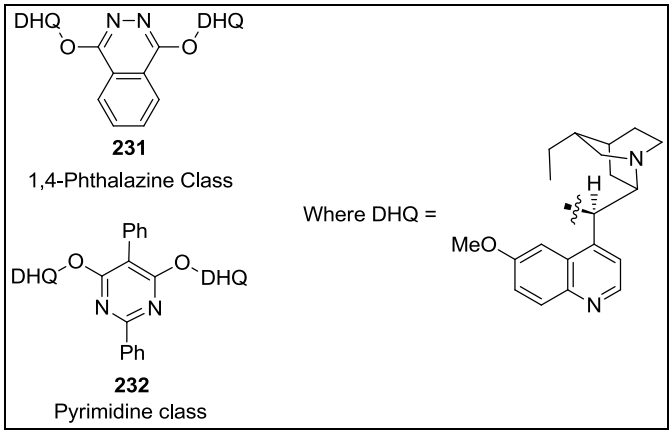

Figure 5: Phthalazine and pyrimidine class of ligands, showing $(DHQ)_2$-PHAL and $(DHQ)_2$-PYR.

In addition to the discovery of the new class of ligands, it was found that organic sulfonamides, and methane sulfonamide in particular, greatly reduced reaction times, thought to be a product of the increased rate of hydrolysis of osmate esters facilitated by the sulfonamide. The sulfonamide was, however, found to slow the reaction rate of terminal alkenes, which had proven problematic in that lower e.e.'s (though still useful) were obtained in most cases for terminal alkenes compared to di-, tri- and tetra substituted alkenes.[111,112,113] A new ligand class (the pyrimidine derivatives) was discovered which showed markedly improved results with terminal alkenes. The pyrimidine derivatives as shown in **Figure 5** showed a marked improvement of the e.e.'s for the reaction with terminal alkenes. This result meaned that efficient and stereoselective procedures for the synthesis of diols from all classes of alkenes was now available.[114] One interesting aspect worth noting is that the use of DHQ ligands usually results in lower e.e.'s than when DHQD ligands are used for an identical

[111] Sharpless, K.B.; Amberg, W.; Beller, M.; Chen, H.; Hartung, J.; Kawanami, Y.; Lubben, D.; Manoury, E.; Ogino, Y.; Shibata, T.; Ukita, T. *J. Org. Chem.* **1991**, *56*, 4585.
[112] Ogino, Y.; Chen, H.; Manoury, E.; Shibata, T.; Beller, M.; Lubben, D.; Sharpless, K.B. *Tetrahedron Lett*. **1991**, *32*, 5761.
[113] Sharpless, K.B.; Amberg, W.; Bennani, Y.L.; Crispino, G.A.; Hartung, J.; Jeong, K.S.; Kwong, H.-L.; Morikawa, K.; Wang, Z.M.; Xu, D.; Zhang, X.-L. *J. Org. Chem*. **1992**, *57*, 2768.
[114] Crispino, G.A.; Jeong, K.S.; Kolb, H.C.; Wang, Z.M.; Xu, D.; Sharpless, K.B. *J. Org Chem*. **1993**, *58*, 3785.

substrate, regardless of which ligand class is employed.[115]

3.5.2 Experimental Aspects

As discussed previously, TPDPS was chosen as a more appropriate protecting group, and using this strategy, TBDPS protected alkene (**227**) was synthesised from methyl (*S*)-3-hydroxy-2-methylpropionate (**138**) using a similar strategy to that of the synthesis of the benzyl protected alkene and is outlined in **Scheme 16**.

The hydroxyl group in (**138**) was converted in 99% yield to the *O*-TBDPS ether (**222**) using TBDPSCl and imidazole. The *O*-TBDPS ether was identified by the distinct peaks of the TBDPS group at δ_H 1.03 and δ_C 26.74 and 19.26 for the *t*-butyl group and the aromatic protons between δ_H 7.66 and 7.36 in the ^{1}H NMR spectrum. Reduction of the ester functionality of (**222**) using DIBALH gave the primary alcohol (**223**) which was converted to the *O*-Ts derivative (**224**) by treatment with *p*-TsCl and DMAP. The methyl group of the tosylate resonated as a singlet at δ_H 2.41 in the ^{1}H NMR spectrum, correlating with a peak at δ_C 21.59 in the ^{13}C NMR spectrum.

A one-carbon chain extension was carried out by subjecting the *O*-Ts (**224**) to an S_N2 reaction using cyanide ion as nucleophile in refluxing DMSO to give after 18 h the nitrile (**225**) (94% yield) as a colourless oil. The characteristic nitrile resonance appeared at δ_C 118.84S in the ^{13}C NMR spectrum. DIBALH reduction of the nitrile (**225**) led to the formation of an imine which was hydrolysed upon work-up to the TBDPS-protected aldehyde (**226**). The aldehyde proton appeared as a triplet (*J* 2.1 Hz) at δ_H 9.78 and the carbonyl carbon atom at δ_C 202.63D in the ^{13}C NMR spectrum. The second one-carbon chain extension leading to the C_5 alkene (**227**) was carried out by a Wittig olefination reaction with the ylide obtained from the reaction of methyltriphenylphosophonium iodide and *n*-BuLi in hexanes, giving alkene (**227**), with the alkene protons appearing at δ_H 5.75 (dddd, *J* 6.9, 7.6, 10.1, 17.0 Hz, H-2), 4.99 (ddd, *J* 1.4, 2.3, 10.1 Hz, H-1a), 4.96 (ddd, *J* 1.4, 2.3, 17.0 Hz, H-1b), and the alkene carbons resonating at δ_C 137.27D and 115.70T. The alkene (**227**) was then subjected to Sharpless asymmetric dihydroxylation under a variety of conditions.

Since it had been shown by Sharpless and his co-workers[114] that the most effective catalyst for the asymmetric dihydroxylation of terminal alkenes were the pyrimidine (PYR) derivatives, this class was chosen as the catalyst for the reaction. Using the mnemonic derived by Sharpless *et al.*,[82] the dihydroquinine pyrimidine derivative $(DHQ)_2PYR$ was selected as the

[115] Becker, H.; Sharpless, K.B. *Angew. Chem. Int. Ed. Engl.* **1996**, *35*, 448.

asymmetric catalyst for the reaction as this catalyst favours reaction on the *Re* face of the alkene and thus should afford the 2*S* configuration of the 1,2-diol product. The reactions were carried out using potassium osmate dihydrate ($K_2OsO_4.2H_2O$) as a pre-catalyst which was then oxidised *in situ* to active osmium tetroxide by the oxidant, potassium ferricyanide. Potassium osmate dihydrate is preferred over the use of osmium tetroxide due to the relatively high volatility (and vapour pressure) and toxicity associated with osmium tetroxide.

The reaction was first attempted in the absence of methane sulfonamide which has been shown to slow the dihydroxylation of terminal alkenes. The reaction was performed at 0 °C, by addition of potassium ferricyanide, potassium carbonate and $(DHQ)_2PYR$ in 8 mL of 1:1 *t*-BuOH-water solution, before the osmate was added. The alkene (**227**) was added and the reaction allowed to proceed for 48 h at 0 °C with continuous monitoring using TLC. The reaction proceeded slowly with only partial conversion observed after 48 h. The reaction was, however, quenched at this time by reducing the osmium tetroxide to osmate using sodium sulphite solution. Purification of the crude product gave the 1,2-diol (**228**) as a 4:1 mixture (estimated from intensities of the peaks of C-2 (δ_C 70.66 (minor) and 69.97(major)) in the ^{13}C NMR spectrum, with the major product assumed to be that predicted by the mnemonic shown in **Figure 4**.

In an effort to improve the diastereoselectivity of the Sharpless asymmetric dihydroxylation reaction it was decided to repeat the reaction in the presence of 1 equivalent of methanesulfonamide at 0 °C. The reaction proceeded at an increased rate with no trace of starting material observed after 22 h of reaction. ^{13}C NMR spectral analysis of the product showed again that the 1,2-diol had been produced; however, the diastereomeric ratio was still 4:1, but the yield of the reaction had increased significantly. Next the temperature dependence of the reaction was investigated. The reaction was performed at −10 °C (lowest temperature achievable with this solvent system) and quenched after 18 h to give once again the 1,2-diol (**228**) in 92% yield with a d.r. of 4:1.

The above results indicate that catalyst-substrate interactions are the main factor in determining the stereochemical outcome of the reaction and that the production of the undesired diastereomer is not as a result of a kinetic effect, but rather that of a thermodynamic (and most likely binding interaction) effect.

When the initial mechanism of the reaction was proposed, a dual-cycle mechanism was proposed, as discussed earlier and as shown in **Scheme 17**. It is thought that the first cycle produces the desired product in high e.e.'s, while the second cycle contributes to low e.e.'s. It is thought that the use of potassium ferricyanide supresses the second cycle thus reducing the

amount of product produced through the pathway offering low enantioselectivity. The poor levels of diastereoselectivity observed for the alkene (**227**) are most likely as a result of the displacement of the chiral ligand from the osmium centre by the binding of a second molecule of the alkene. The concurrent loss of the chiral ligand from the osmium centre and oxidation of alkene means that the stereoinduction in this complex would be as a result of the departing chiral ligand and the 1st molecule of alkene. In contrast to the situation where the bound chiral ligand directs the approach of the alkene, the departing nature of the ligand would therefore be partially responsible for reduced ee's as observed in this reaction. One possible reason for the reactivation of the second cycle could be an increased affinity between the osmate ester (**236**) and the terminal alkene (**234**) which would result in an increased amount of product being produced by the second cycle and thus contributing to the low d.r. obtained.

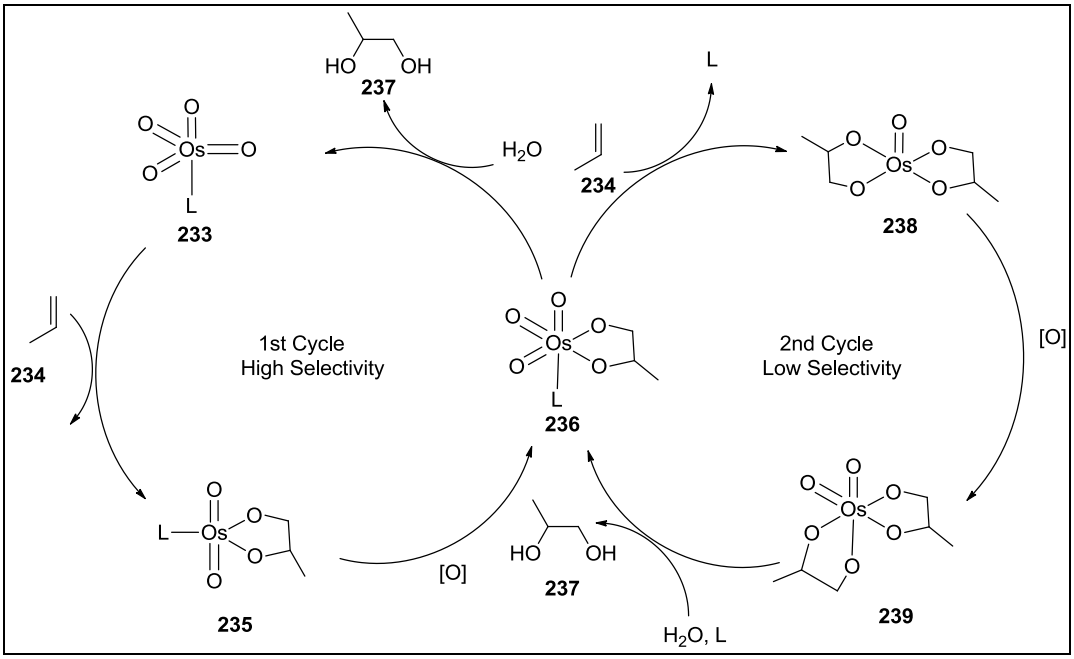

Scheme 17: Catalytic cycles operating during Sharpless asymmetric dihydroxylation.[108]

The low d.r.'s observed were most likely due to a combination of effects, many of which have been observed in isolation, but are all present for this particular substrate. As stated, terminal alkenes have proved problematic in the past most likely due to the mechanism of binding of the catalyst to the alkene, which is thought to make use of the steric bulk of the alkene to orientate one of the faces of the alkene with the active catalyst by its interactions with the chiral ligand. Since terminal alkenes lack bulk on the one side of the double bond, stereoinduction has proved more problematic. The use of the DHQ ligand derivative as the chiral catalyst is also a likely contributor to the lower selectivity observed, as this trend has been observed for almost all substrates tested during the development of the reaction. These factors, combined with substrate specific factors, such as the methyl group at C-4, which

could conceivably affect the binding of the substrate to the catalyst, all contribute to produce a reaction with selectivity lower than expected.

Since none of the changes to the reaction conditions appeared to increase the diastereomeric ratio obtained, and the diastereomeric reaction products could not be separated, it was decided to pursue the original route as shown in **Scheme 2b** using Sharpless asymmetric epoxidation to generate the epoxide (**153**) as a 4:1 ratio of diastereomers which could be separated by flash column chromatography giving the desired epoxide albeit in low yields but with sufficiently high ee. This epoxide then gives access to diol (**154**), from which point the synthetic route can continue as planned to give targets (**162**) and (**163**).

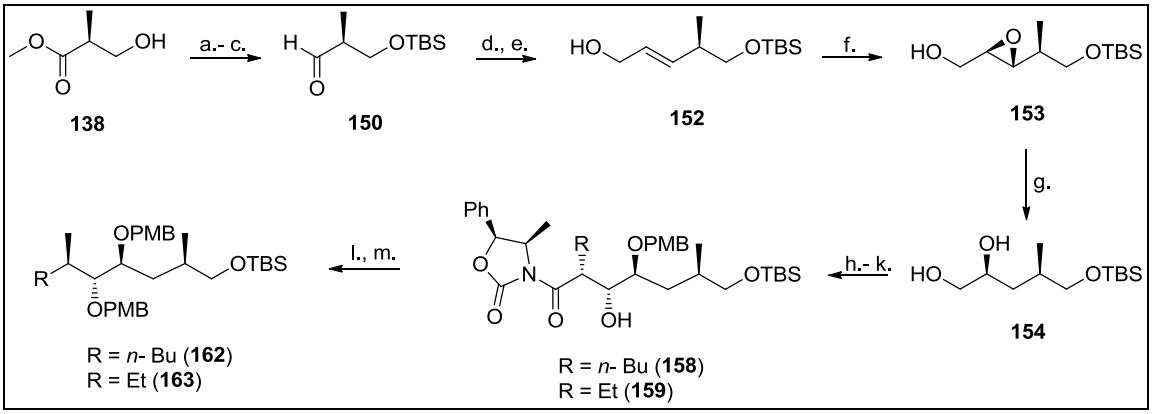

Scheme 2b: Synthetic route for the left-side fragment giving diol (**154**) with highest selectivity.

Reagents: a. TBSCl, imidazole (96%); b. DIBALH (79%); c. DMSO, $(COCl)_2$, Et_3N (90%); d. ^{t}BuOK, $(^i PrO)_2P(O)CH_2COOEt$ (80%); e. DIBALH (85%); f. (*S*,*S*)-DIPT, $Ti(O^iPr)_4$, TBHP (30%); g. DIBALH (66%); h. $(OMe)_2CHC_6H_4OMe$, PPTS (33%); i. DIBALH (53%); j. DMSO, $(COCl)_2$, Et_3N; k. **123** or **145**, Bu_2BOTf, Et_3N; l. i). NaH, $MeOC_6H_4CH_2Br$, ii). $LiAlH_4$; m. i). TsCl, pyridine, ii). $LiAlH_4$; k. *n*-BuLi.

3.6 Evans Auxiliary Route

3.6.1 Theoretical Aspects

The aldol reaction is one of the most powerful and widely used reactions in organic synthesis due to its versatility in the formation of C-C bonds and generation of new stereocentres. The aldol reaction is generalised in **Scheme 18** and involves the reaction of an enolate (**240**) with a carbonyl compound (**241**), with the enolate being also being derived from a carbonyl compound. The enolate acts as a nucleophile attacking the electrophilic carbon of the carbonyl compound leading to the addition product (**242**), which can undergo dehydration to give the α,β-unsaturated carbonyl compound as the aldol condensation product.

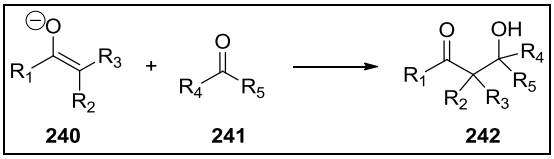

Scheme 18: General aldol addition reaction.

When the enolate is substituted, four possible diastereomers can be produced as a result of the aldol reaction: two *syn* enantiomers, and two *anti* enantiomers. Since most organic methodology is directed towards the synthesis of enantiopure compounds (either natural products or derivatives thereof), there was a search for a means to control the stereochemical outcome of the reaction.

The enolate is formed by the deprotonation at the α-carbon to the carbonyl group generating a resonance stabilised enolate. There are two possible geometries for the enolate when the enolate is substituted: either the *Z*- or the *E*-enolate can be formed. It was observed for substrates that could only form *E* enolates (such as cyclopentanone) that the major product of an aldol reaction was the *anti* product, while that of *Z* enolates (formed from sterically hindered carbonyl compounds such as 2,2-dimethyl-pentan-3-one) predominantly gave *syn* aldol products.[42,116] This result is due to the Zimmerman-Traxler chair-like transition state postulated for aldol reactions where the aldehyde and enolate are both coordinated to a Lewis acid (most often lithium or boron), with the aldehyde having its R substituent in the more energetically favoured (due to fewer steric interactions) pseudoequatorial position, as shown in **Scheme 19**.

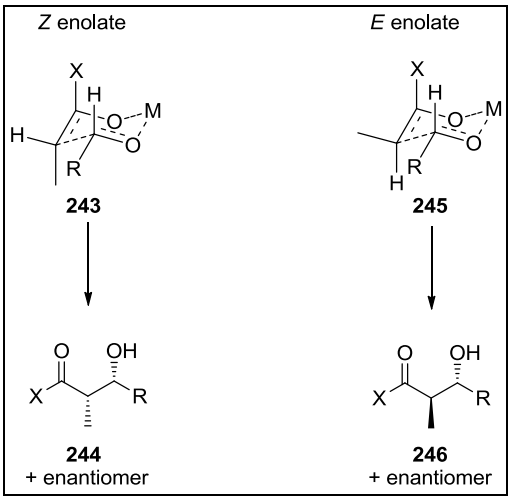

Scheme 19: Stereocontrol in aldol reactions.

[116] Dubois, J.E.; Fellman, P. *C. R. Acad. Sc. Paris, Ser. C.* **1972**, *274*, 1307.

When boron is used as the co-ordinating species (M in **Scheme 19**), changing the substituents attached to the trivalent boron atom can allow for the better control of enolate geometry- possibly due to the shorter B-O bond versus the O-Li bond, leading to a "tighter" transition state, and consequently a higher degree of control.[117] When bulky alkyl groups (such as cyclohexyl groups) are attached to boron, the *E*- enolate is favoured when triethylamine is used as the base, giving rise to *anti* products.[118] When less sterically demanding alkyl groups are employed (such as in 9-borabicyclononane triflate or di-*n*-butylboron triflate), *Z*-enolates are the predominant products that give rise to *syn* products.[119]

This offers a route for the control of the relative stereochemistry of the products but does not establish the absolute stereochemistry in that there is no control offered as to which of the two possible *syn* or *anti* enantiomers is formed.

The most frequently used asymmetric aldol reagents are the Evans auxiliaries based on chiral 2-oxazolidinones derived from amino acids (such as phenylalanine or valine) or other widely available chiral biological derivatives (such as norephedrine). These reagents were introduced by Evans *et al*. in 1981 and were shown to offer a high degree of enantioselectivity in aldol reactions with a wide variety of substrates.[120] These reagents gave predominantly *Z* enolates after deprotonation (in ratios >100:1), and consequently *syn* products with the enantioselectivity derived from the configuration of the chiral auxiliary. Representative examples are shown in **Scheme 20**.

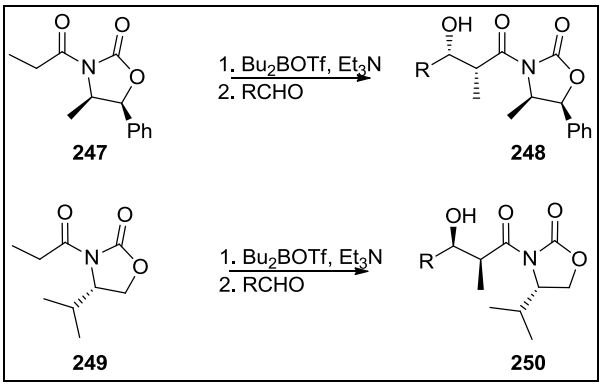

Scheme 20: Enantioselectivity in aldol reactions using the Evans auxiliaries.

The chiral auxiliaries are derived from chiral 1,2-aminoalcohols which can be derived from

[117] Evans, D.A.; Nelson, J.V.; Vogel. E.; Taber, T.R. *J. Am. Chem. Soc.* **1981**, *103*, 3099.
[118] Brown, H.C.; Dhar, R.K.; Bakshi, R.K.; Pandiarajan, P.K.; Singaram, B. *J. Am. Chem. Soc.* **1989**, *111*, 3441.
[119] Von Horn, D.E.; Masamune, S. *Tetrahedron Lett.* **1979**, 2229.
[120] Evans, D.A.; Bartroli, J.; Smith, T.L. *J. Am Chem. Soc*. **1981**, *103*, 2127.

amino acids by borane reduction. Reaction of the aminoalcohol with either phosgene, diethyl carbonate or diphenyl carbonate gives the 2-oxazolidinone. Acylation of the oxazolidinone with the appropriate acyl chloride gives an acyl oxazolidinone that can be deprotonated to generate the chiral enolate for the aldol reaction.[120]

Stereocontrol in the aldol reaction is thought to be the result of the reaction proceeding through a Zimmerman-Traxler-like cyclic transition state in which the chiral auxiliary sterically blocks the one face of the *Z*-enolate, preventing approach of the aldehyde on this face. The result is a face-specific attack of the *Z*-enolate on the aldehyde resulting in only a single enantiomer of the *syn* product being formed. **Scheme 21** illustrates this approach.

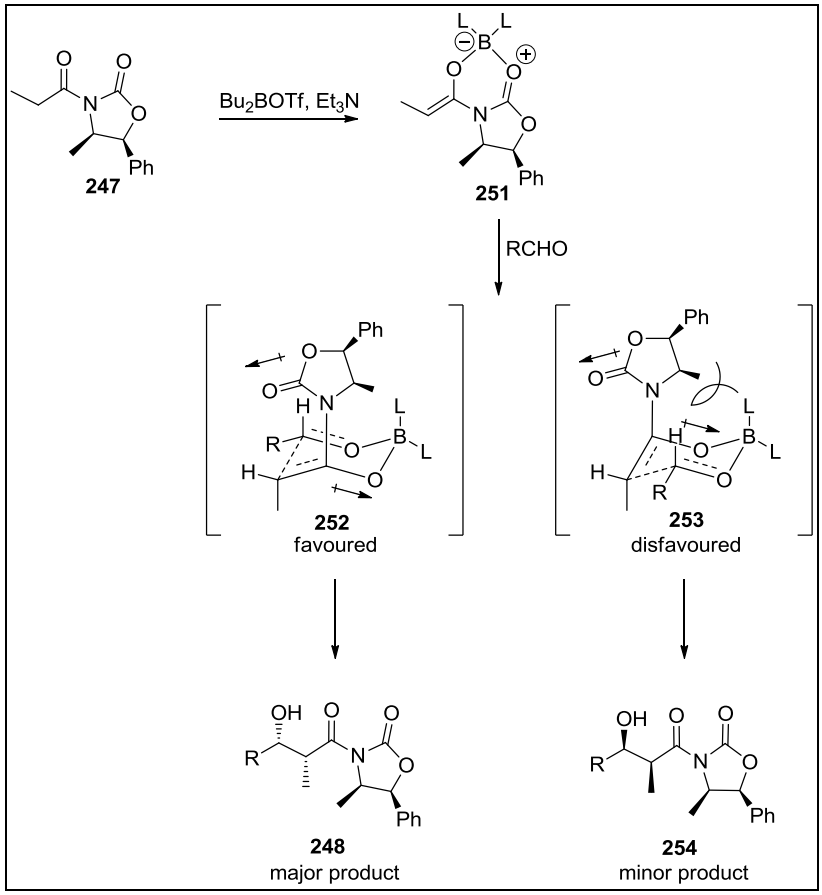

Scheme 21: Origin of enantioselectivity using the Evans auxiliaries.[121]

It is accepted that the oxazolidinone orientates itself in such a way that the dipole of the oxazolidinone carbonyl group opposes the dipole of the enolate carbon-oxygen bond. This conformation of the enolate results in the steric blocking of the *Re* face of the enolate by the methyl and phenyl groups [as shown for intermediate (**253**)], forcing the aldehyde to approach the enolate's *Si* face to give transition state (**252**) as shown in **Scheme 21**. The enolate has

[121] Arya, P.; Qin, H. *Tetrahedron* **2000**, *56*, 917.

been shown to have an extremely high stereofacial selectivity as chiral GC analysis of products has shown that the ratio of the major (known as the Evans *syn* product) to minor (known as the non-Evans *syn* product) product is usually in the region of 500:1 for most substrates.[120] It has also been shown that when the corresponding lithium enolates are used in place of the boron enolates, the selectivity diminishes greatly, which is thought to be as a result of the chelation-controlled coordination of the lithium cation to the enolate, imide and aldehyde oxygens, giving a transition state which is not as selective as that formed when boron derivatives are used.[120]

Minor modifications to the reaction procedure can lead to the formation of the non-Evans *syn* product as the major diastereomer produced and can also give rise to the *anti* product. Non-Evans *syn* products can be obtained by addition of 2-3 equivalents of triisopropoxytitanium chloride to the lithium enolate; however, this method is less selective than that producing the Evans *syn* product.[122] The *anti* products can also be produced by the addition of excess dibutylboron triflate, which is thought to activate the aldehyde by a Lewis acid-mediated process, allowing the first equivalent of dibutylboron to remain coordinated to the imide oxygen, affording a transition state which gives rise to *anti* products.[123]

The Evans auxiliaries also offer the added benefit in that after their use, they can be cleaved, recovered and reused. The simplest cleavage of the auxiliary uses base hydrolysis (4 equivalents aqueous 4M potassium hydroxide in methanol) and gives the corresponding acid, while direct esterification can be accomplished using sodium methoxide in anhydrous methanol. Reductive cleavage using $LiAlH_4$ or $LiBH_4$ gives the corresponding alcohol that can in turn be used for a number of functional group transformations.[120]

3.6.2 Experimental Aspects

Since the alternate approaches to synthesise diol (**154**) in sufficiently high e.e.'s had failed, it was decided to pursue the Sharpless asymmetric epoxidation route (**Scheme 2c**) as the two diastereomeric products formed in a 4:1 d.r. could be separated, giving access to epoxide (**153**) in sufficiently high d.e.'s. Epoxide (**153**) was subjected to a regioselective reductive ring opening reaction with DIBALH as the reducing agent, which had been shown previously to selectively give 1,2-diols by nucleophilic attack at C-3.[124] In contrast Red-Al [$NaAlH_2(OCH_2CH_2OCH_3)_2$] is known to selectively give 1,3-diols.[125] Three equivalents of

[122] Nerz-Stormes, M.; Thornton, E.R. *Tetrahedron Lett.* **1986**, *27*, 897.
[123] Walker, M.A.; Heathcock, C.H. *J. Org. Chem.* **1991**, *55*, 173.
[124] Suzuki, T.; Saimoto, H.; Tomioka, H.; Oshima, K.; Nozaki, H. *Tetrahedron Lett.* **1982**, *23*, 3597.
[125] Minami, N.; Ko, S.S.; Kishi, Y. *J. Am. Chem. Soc.* **1982**, *104*, 1109.

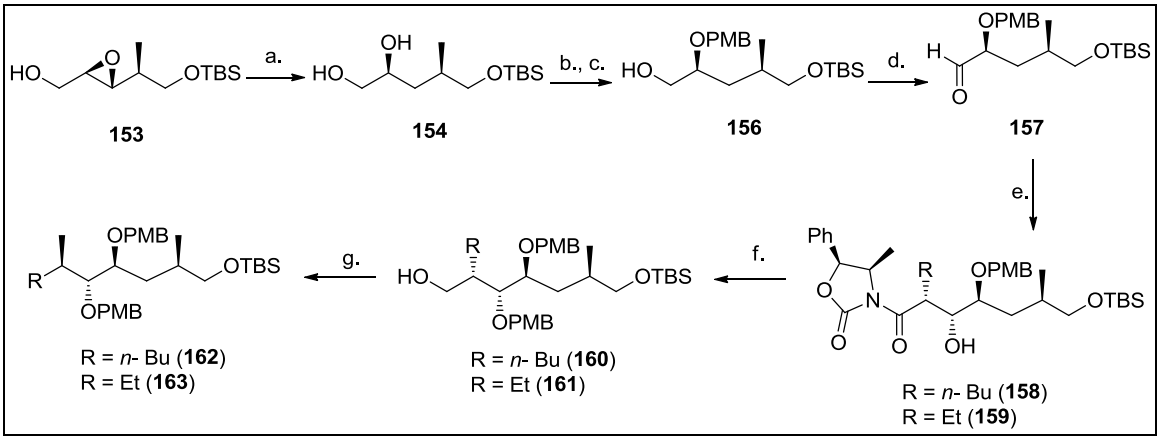

Scheme 2c: Proposed path from epoxide (**153**) to targets (**162**) and (**163**).

> *Reagents*: a. DIBALH (66%); b. $(MeO)_2CHC_6H_4OMe$, PPTS (33%); c. DIBALH (53%); d. DMSO, $(COCl)_2$, Et_3N; e. **123** or **145**, Bu_2BOTf, Et_3N; f. i). NaH, $MeOC_6H_4CH_2Br$, ii). $LiAlH_4$; g. i). TsCl, pyridine, ii). $LiAlH_4$.

DIBALH were added to a solution of epoxide (**153**) in DCM at 0°C, which afforded an inseparable 8:1 mixture of 1,2-diol (**154**) and 1,3-diol (66% overall yield) as indicated by the signal intensities in the ^{13}C NMR spectrum. The 1,2-diol (**154**) was determined as the major product of the reaction by the correlations observed in the HSQC spectrum for the C$\underline{H}_2$OH [δ_H 3.55 (dd) and 3.41 (dd)] and C$\underline{H}$OH [δ_H 3.81 (broad signal)] protons, which were absent in the spectrum of the minor isomer.

Since these isomers were inseparable, the mixture was used in the next step, which involved the protection of the 1,2-/1,3-diol as the *p*-methoxybenzaldehyde acetal. The protection was achieved using an acetal exchange approach utilising anisaldehyde dimethylacetal and a catalytic quantity of pyridinium *p*-toluenesulfonate at 0 °C. The reaction produced a mixture of two dioxolane derivatives (**155**), epimeric at C-2 of the dioxolane ring, and the dioxane derivative as indicated by the characteristic peaks in the ^{13}C NMR spectrum. In the study of benzylidene acetal derivatives of sugars it was noted that the acetal carbon resonance in the dioxolane appeared between δ_C 101.9–104.0, whereas that of the dioxane derivatives appeared between δ_C 100.6–101.4 or from δ_C 93.7–94.9 in the ^{13}C NMR spectrum.[126]

In the present case the single resonance at δ_C 100.98 was assigned to the acetal derived from the 1,3-diol produced as a by-product in the previous step. Although the acetal derivative contains an additional stereocentre the single peak observed in the NMR spectrum indicated that only a single diastereomer [(**255**) in **Figure 6**] had been produced with all equatorial

[126] Grindley, T.B.; Gulasekharam, V. *Carbohydr. Res*. **1979**, *74*, 7.

substituents of the six-membered ring, thus avoiding unfavourable 1,3-diaxial interactions between the substituents.

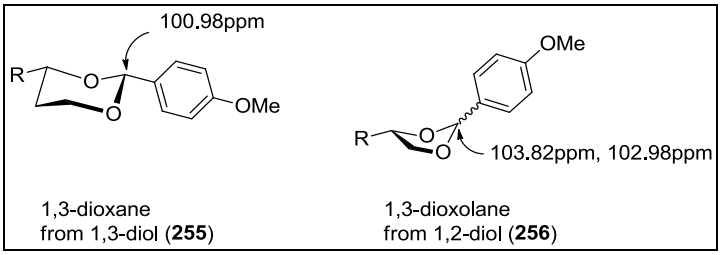

Figure 6: Dioxane and dioxolane produced in the reaction.

Two signals are observed in the 13C NMR spectrum for the acetal carbon of the dioxolane product, one at δ_C 103.82 and a second at δ_C 102.98 in a ratio of 2:1. The signals are due to the two possible diastereomers of the five-membered ring (**256**) with the diastereomer with the equatorial *p*-methoxyphenyl group favoured over the one with the pseudo-axial group in order to minimise steric interactions. However, the steric effect is less pronounced in the dioxolane ring when compared to the dioxane ring and hence both diastereomers are produced. The mixture of dioxane and dioxolane diastereomers was inseparable at this stage of the synthesis and the next transformation was performed on the mixture in the hope that the products could be separated.

The acetal mixture was subjected to a reductive acetal cleavage to give the *p*-methoxybenzyl protected secondary alcohol and free primary alcohol. This was accomplished using DIBALH which opens the acetal at the least sterically hindered position due to the bulky nature of the reducing agent.[30] In the reduction the acetal stereocentre created during the previous step is destroyed and the 1,2-diol and 1,3-diol derivatives could be easily separated by column chromatography to give the *p*-methoxybenzyl protected secondary alcohol (**156**) in 53 % yield as a colourless oil. The hydroxyl proton was found as a broad signal at δ_H 1.90 (1H), while the methyl signal of the *p*-methoxybenzyl group was found at δ_H 3.78 in the ^{1}H NMR spectrum, and at δ_C 55.24Q in the ^{13}C NMR spectrum. The protons of the newly-formed benzylic group appeared as an AB spin system (J = 11.2 Hz) at δ_H 4.53 and 4.45 in the ^{1}H NMR spectrum and the carbon atom at δ_C 70.88T in the ^{13}C NMR spectrum.

Attention now turned to the synthesis of the chiral auxiliary required for the aldol reaction, as shown in **Scheme 22**. (4*R*,5*S*)-4-Methyl-5-phenyloxazolidin-2-one (**125**) was synthesised by refluxing a mixture of (1*S*,2*R*)-(+)-norephedrine (**126**) and diphenyl carbonate (**127**) for 18 h at 110 °C, which after work-up and recrystallization from toluene gave **125** as a white crystalline compound with $[\alpha]_D^{20}$ +169.6 (*c* 1.03, $CHCl_3$) [lit.,[120] +163.7 (*c* 1.0, $CHCl_3$)]. The

oxazolidinone was acylated by reacting the anion of the oxazolidinone (generated by reaction with *n*-BuLi) with the appropriate acyl chloride – either butanoyl chloride for **145**, or hexanoyl chloride for **123**. The acyl chlorides were in turn synthesised from the corresponding acid by refluxing with thionyl chloride and a catalytic amount of DMF. These imides could then be used in the Evans aldol reaction with aldehyde (**157**) producing intermediates which could be transformed either into target (**163**) for the left-side of the AAL toxins or target (**162**) for the left-side of the fumonisins.

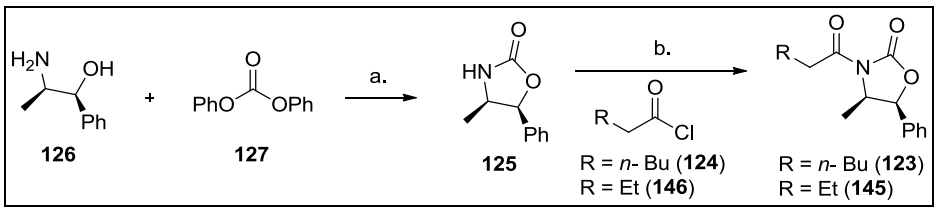

Scheme 22: Synthesis of the chiral auxiliaries.

Reagents: a. Heat (88%); b. *n*-BuLi (87% for **145,** 90% for **123**).

In order to optimise the reaction conditions for the aldol reaction, a series of test reactions using benzaldehyde as the electrophile and the enolates derived from **145** and **123** were performed, as shown in **Scheme 23**.

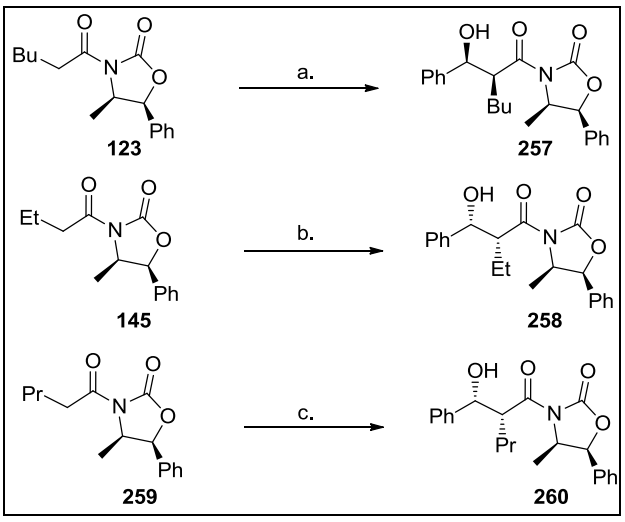

Scheme 23: Evan's aldol reactions with benzaldehyde and various imides.

Reagents: a. Bu_2BOTf, Et_3N, PhCHO (39%); b. Bu_2BOTf, Et_3N, PhCHO (38%); c. Bu_2BOTf, Et_3N, PhCHO (34%).

The aldol reactions were performed according to the procedure described by Heathcock.[127] The enolate was generated at 0 °C by addition of 1M di-*n*-butylboron triflate to a solution of

[127] Heathcock, C.H. Modern Enolate Chemistry in *Modern Synthetic Methods 1992;* Scheffold, R. (Ed.); VCH Publishers Inc., New York, 1992; p 70.

the imide in DCM, followed by the addition of Et_3N. The mixture was stirred for 15 min before being cooled to −78 °C, when freshly distilled benzaldehyde was added dropwise. The reaction was allowed to proceed for 30 min at this temperature and was then warmed to 0 °C and stirred for an additional hour before quenching. The yields for the aldol reactions were all relatively low, possibly due to the formation of by-products due to decomposition of the enolate or its incomplete reaction, as well as loss of product during the purification process. After column chromatography, however, the products of these two aldol reactions were found to be crystalline with the C-2′ ethyl derivative (**258**) forming needle-shaped crystals whereas the C-2′ butyl derivative (**257**) appeared as large, block-shaped crystals. Both products produced crystals which were suitable for single crystal X-ray diffraction studies (XRD) and the results of the XRD experiment were highly unexpected.

It was found that the C-2′ butyl derivative (**257**) was the non-Evans *syn* product, an unexpected result, while the C-2′ ethyl derivative (**258**) was the expected *syn* Evans product. The crystal structures are shown in **Figure 7** and **Figure 8**, respectively. Due to the reliability of the aldol reaction to form the Evans *syn* product, the generation of the non-Evans *syn* product required further investigation.

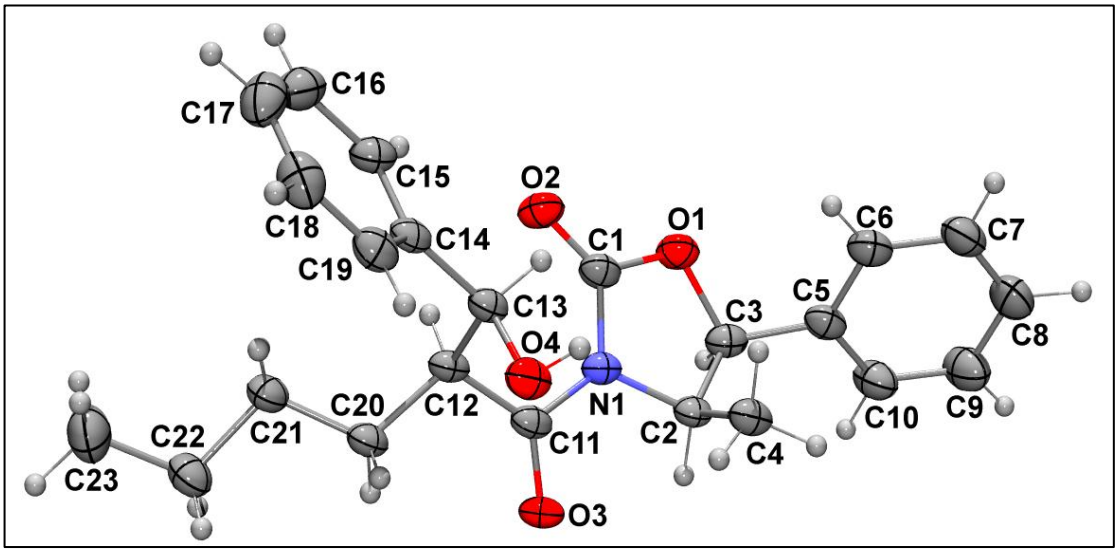

Figure 7: Aldol product (**257**) with the C-2′ butyl side-chain.

The *syn* relative configuration for both the aldol products (**257**) and (**258**) established that the *Z*-enolate was involved in the reaction. It can be assumed that the reaction of the *Z*-enolate of the butanoyl derivative (**145**) with benzaldehyde proceeds through the favoured low energy transition state (**252**) as shown in **Scheme 21** in which the dipole of the oxazolidinone carbonyl group opposes the dipole of the enolate carbon-oxygen bond. However, an explanation for the formation of the non-Evans product is more elusive. The transition state

(**253**), giving the non-Evans product as depicted in **Scheme 21** results in a disfavoured high-energy transition state as a result of steric hindrance. An alternative conformation for the transition state (**253**), but with the two dipoles aligned is also disfavoured. Since these reactions were both carried out at the same time, using the same reagents, it is unlikely that a contaminant was present which could affect the outcome of the reaction in one of the reaction vessels.

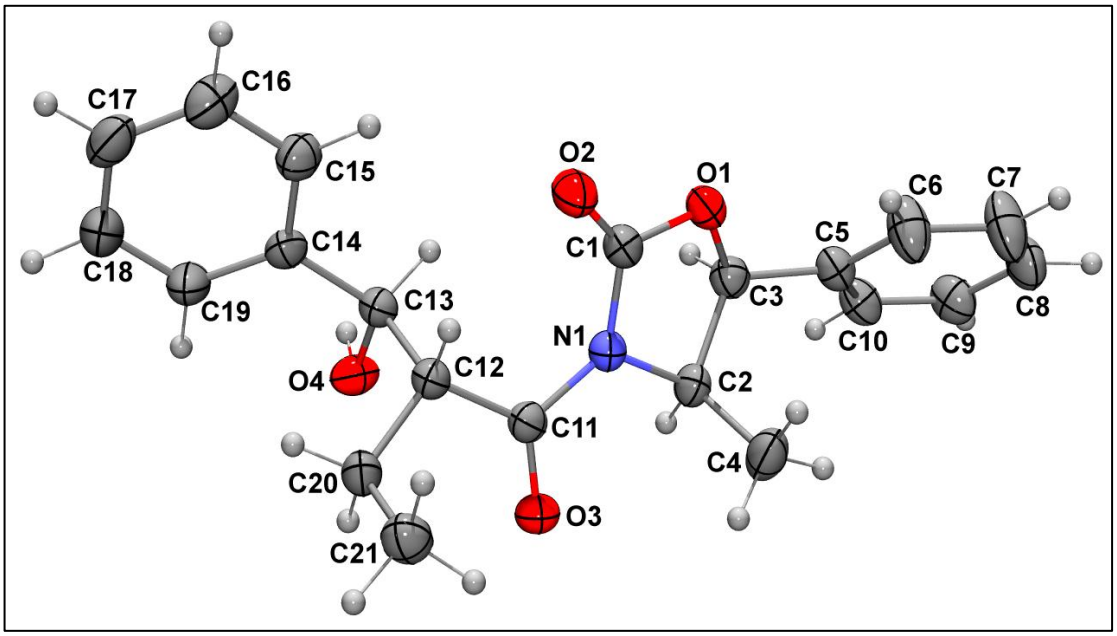

Figure 8: Aldol product (**258**) with the C-2′ ethyl side-chain.

The most plausible explanation for the observed result could be that the reaction proceeds through a mechanism similar to that of the asymmetric alkylation reactions with enolates derived from Evans chiral auxiliaries. The reaction possibly proceeded through an open-chain transition state with stereocontrol arising through the conformation of the enolate, which governed which face of the enolate was available for attack by the electrophile. This reaction pathway requires that the boron atom remains coordinated to the imide oxygen atom, as well as the enolate oxygen, giving rise to the intermediate (**261**) shown in **Scheme 24**. The *Si* face of the enolate is then blocked by the substituents on the oxazolidinone ring leaving the *Re* face open for approach of the electrophile. In this case, the bulky R group (phenyl in this case) of the aldehyde is oriented away from the oxazolidinone ring and the *Si* face of the aldehyde is attacked by the enolate. Reaction through this transition state does produce the non-Evans *syn* product (**257**), as illustrated in **Scheme 23**.

This mechanism offers an explanation for the formation of the unexpected aldol product, it does not provide a reason as to why the *N*-butanoyl derivative (**145**) follows the expected

reaction pathway, while the *N*-hexanoyl derivative (**123**) of the oxazolidinone follows an alternate pathway. The only significant difference between the two *Z*-enolates is the two-carbon difference in the alkyl chains which has a profound effect on the outcome of the aldol reaction. Further investigations into the reason for this difference are required in order to explain the exact cause of the unexpected result.

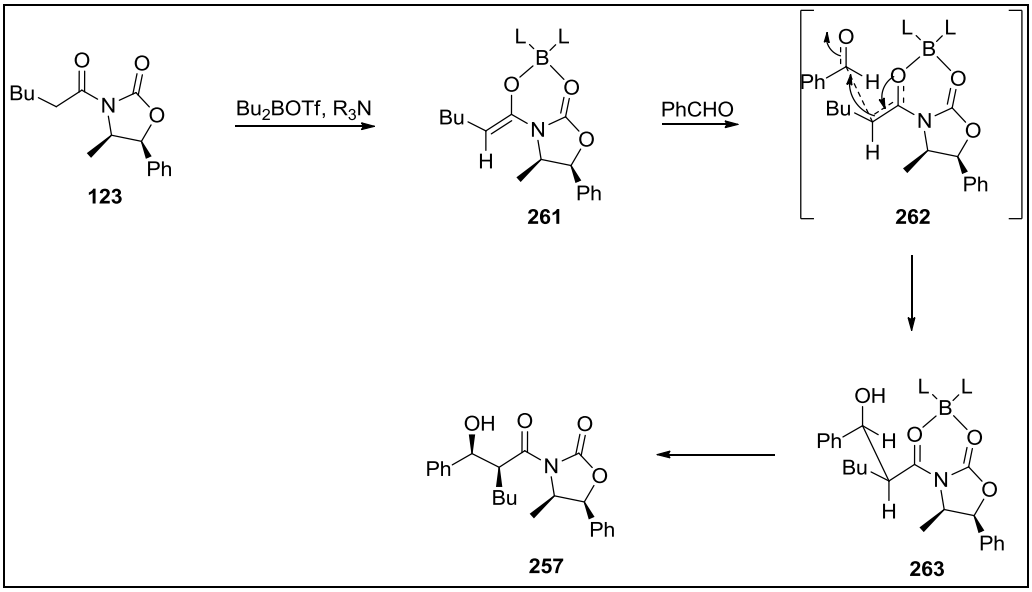

Scheme 24: Possible origin of the non-Evans *syn* aldol product.

Since the *N*-butanoyl (**145**) and *N*-hexanoyl (**123**) derivatives behave differently, it was decided to investigate the behaviour of the *N*-pentanoyl derivative. The oxazolidinone (**125**) was treated with *n*-BuLi and the lithiated species reacted with pentanoyl chloride, derived from the reaction between pentanoic acid and thionyl chloride, to give the *N*-pentanoyl derivative (**259**). The compound was isolated in moderate yield as yellow crystals, which were shown to be pure by NMR spectroscopy. The reaction of **259** with dibutylboron triflate and triethylamine generated the corresponding *Z*-enolate which on addition of benzaldehyde gave the aldol product (**260**) as a white, foamy solid after column chromatography. The *syn* relative configuration for **260** followed from the 6.2 Hz coupling constant between C-2′ and C-3′ protons in the ^{1}H NMR spectrum which is comparable to the values of 6.3 and 5.7 Hz for the aldol products (**258**) and (**257**), respectively.

All attempts at recrystallization of aldol product (**260**) failed, though numerous recrystallization techniques were employed. This precluded the use of XRD as a method to determine the absolute configuration of the aldol product (**260**) and to establish whether the compound was the Evans *syn* or non-Evans *syn* product. Other means were therefore required to establish which of the *syn* products had been formed. The H-2′–H-3′ coupling constant of

6.2 Hz correlates more closely with that of C-2′ ethyl derivative (**258**) than that of the C-2′ butyl derivative (**257**), indicating that the product is possibly the predicted Evans *syn* product. Examination of the proton chemical shifts for the three derivatives also seemed to indicate a higher degree of correlation between the C-2′ ethyl and propyl derivatives with the chemical shifts of the protons on the oxazolidinone ring of the C-2′ butyl derivative (**257**) being significantly different by as much as 0.47 ppm to those of the other two aldol products. This data (summarised in **Table 1**) seemed to indicate that **260** was indeed the predicted Evans *syn* product as shown in **Scheme 23**.

Table 1: Chemical shifts of selected protons of the aldol products.

	Chemical Shift (δ_H)		
Proton	2′-ethyl (**258**)	2′-propyl (**260**)	2′-butyl (**257**)
H-4	4.47	4.46	4.71
H-5	5.14	5.12	5.59
Me-H	0.82	0.81	0.56
H-2′	4.30	4.37	4.40
H-3′	4.89	4.88	4.96

The final piece of evidence that established the absolute configuration of the C-2′ propyl aldol product (**260**) and its identity as the Evans *syn* product were the specific rotations for the three aldol compounds shown in **Table 2**. The C-2′ ethyl derivative (**258**) and the propyl derivative (**260**) had specific rotations of the same sign and magnitude as would be expected for two compounds with identical absolute stereochemistry with the only difference being a single methylene group. The C-2′ butyl derivative (**257**) showed a specific rotation in the opposite direction to that of the other two compounds, and of significantly greater magnitude indicating that this compound had a different stereochemical relationship to the other two compounds, supporting the conclusion that the C-2′ propyl compound is indeed the Evans *syn* product (**260**).

Table 2: Specific rotations of the three aldol products.

Compound	**Specific Rotation, $[\alpha]_D^{20}$**
2′-ethyl (**258**)	–2.4 (0.95, $CHCl_3$)
2′-propyl (**260**)	–3.5 (1.02, $CHCl_3$)
2′-butyl (**257**)	+23.5 (1.21, $CHCl_3$)

The results obtained in the above aldol reactions of benzaldehyde with *N*-acyl oxazolidinone derivatives of different chain lengths raised a number of questions. Is the non-Evans *syn* product using the *N*-hexanoyl derivative an isolated case or is the trend continued with the *N*-heptanoyl and *N*-octanoyl derivatives? What is the effect of using branched *N*-acyl derivatives with different number of carbon atoms? Such experiments would perhaps provide more

evidence as to the exact reason why the *N*-hexanoyl derivative favours the production of the non-Evans *syn* aldol product. The results also raised some concerns about the outcome of the aldol reaction of the *N*-hexanoyl derivative (**123**) with other aldehydes and especially with aldehyde (**157**) in the synthetic route to the target compound (**162**).

The aldol model experiments using benzaldehyde indicated that the aldol reaction of the aldehyde (**157**) with the *N*-butanoyl derivative (**145**) should give the desired aldol product (**159**) leading to the AAL-target (**163**). The primary alcohol (**156**) was thus oxidised to the aldehyde (**157**) under Swern conditions utilising DMSO, $(COCl)_2$ and Et_3N. The aldehyde was then used directly (no purification) for the aldol reaction out of concern for the stability of the aldehyde on a silica gel column and the possibility of racemisation of the α-stereocentre.

The aldol reaction was performed according to the procedure described above. The enolate was prepared at 0 °C by addition of 1M di-*n*-butylboron triflate to a solution of the imide (**145**) in DCM followed by the addition of Et_3N. The mixture was stirred for 15 min before being cooled to −78 °C when the aldehyde (**157**) was added dropwise. The reaction was allowed to proceed for 30 min at this temperature and was then warmed to 0 °C and stirred for an additional hour. The NMR spectra of the compound isolated from this aldol reaction lacked the signals of the *O*-TBS group present in the aldehyde (**157**) as well as the expected signals for the protons of an ethyl group. No aldol product had been formed in the reaction. Analysis of the ^{1}H and ^{13}C NMR spectra of the isolated compound established the structure as a mixture of the α- and β-anomers of lactol (**265**) shown in **Scheme 25**. The signals at δ_H 5.16 (d, $J_{2,3}$ 3.2 Hz, H-2) and δ_C 90.19D (C-2) were assigned to the α-anomer, whereas the signals of the β-anomer appeared at δ_H 4.55 (d, $J_{2,3}$ 7.4 Hz, H-2) and δ_C 99.06D (C-2). The complete proton-proton connectivity pattern of both the α- and β-anomers was established from the COSY spectrum and analysis of the coupling constants of the multiplets in the ^{1}H NMR spectrum. The coupling constants established the $^{1}C_4$ conformation for lactol (**265**) in which both substituents are in the equatorial position.

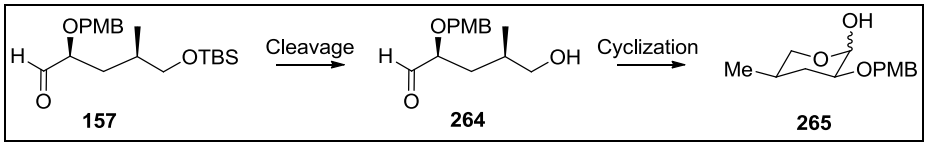

Scheme 25: Lactol production during the aldol reaction.

Formation of lactol (**265**) occurred as a result of the cleavage of the *O*-TBS protecting group under the reaction conditions employed during the aldol reaction. The presence of a hydroxyl

group leads to an intramolecular cyclization with the aldehyde to form the lactol. Lewis acid triflates (Sc, Ce, Bi) have been used previously to cleave *O*-TBS ethers and it is possible that a similar process occurs upon addition of the aldehyde to the reaction mixture containing dibutylboron triflate.[128,129,130] The cleavage of the TBS ether must occur rapidly in the reaction medium as the aldehyde does not have a chance to react with the enolate, but instead reacts rapidly with the newly-formed hydroxyl group.

Since the *O*-TBS ether is unstable under the reaction conditions employed a more robust protecting group would be required.

3.7 FUTURE WORK

In conclusion, a short and elegant synthetic route to synthesise the left side of the backbone of both the fumonisins and AAL toxins was devised, with the intention of using Sharpless asymmetric epoxidation and an Evans aldol reaction as the key transformation in producing targets **162** and **163** from the common intermediate aldehyde **157**, which is in turn derived from methyl (*S*)-3-hydroxy-2-methylpropionate (**138**).

In practice, it was found that the Sharpless asymmetric epoxidation produced the desired epoxide in low enantiomeric excess, but the two diastereomers produced could be separated by two consecutive flash chromatography silica gel columns. In pursuit of a more efficient method for the synthesis of diol **154**, other synthetic routes and key transformations were explored. It was desired to use Jacobsen's kinetic resolution of terminal racemic epoxides and in order to synthesise the racemic epoxide, a terminal alkene was required. It was though that the terminal alkene could be synthesised from the appropriate tosylate, and a vinyl-containing reagent, mediated by copper (I) salts. However, all attempts at this method failed. The synthetic route was redesigned, and the terminal alkene was synthesised by two one-carbon additions: the first a nucleophilic substitution with cyanide, and the second a Wittig olefination giving the terminal alkene. The resolution of the terminal epoxide was also unsuccessful, with no significant kinetic resolution occurring. The synthesis of diol (**228**) using Sharpless asymmetric dihydroxylation was also attempted, but this reaction too failed to produce the required diol in sufficiently high enantiomeric excess, with the best ratio obtained being 4:1. As a consequence, it was decided to pursue the asymmetric epoxidation route, as the diastereomeric products could at least be separated.

[128] Oriyama, T.; Kobayashi, Y.; Noda, K. *Synlett*. **1998**, 1047.
[129] Bartoli, G.; Cupone, G.; Dalpozzo, R.; De Nino, A.; Maiuolo, L.; Procopio, A.; Sambri, L.; Tagarelli, A. *Tetrahedron Lett.* **2002**, *43*, 5945.
[130] Firouzabadi, H.; Mohammadpoor-Baltork, I.; Kolagar, S. *Synth. Commum.* **2001**, *31*, 905.

The second key transformation, being the Evans aldol reaction, also provided an interesting result. When the aldol reaction was attempted with benzaldehyde and enolates derived from **123** and **145**, the butanoyl derivative was found to give the expected Evans *syn* product, while the hexanoyl derivative was found to give the non-Evans *syn* product, with proof provided by single crystal XRD analysis. It was proposed that the aldol reaction with the hexanoyl derivative does not proceed through the expected Zimmerman-Traxler-type transition state, but rather through an open chain transition state, similar to that seen for asymmetric alkylation reactions. By synthesising the pentanoyl derivative, and subjecting it to the same aldol reaction, it was inferred that the aldol product of this reaction resembles that of the butanoyl derivative, by comparison of spectroscopic properties. This seemed to indicate that the hexanoyl derivative interfered with the formation of the Zimmerman-Traxler-type transition state, causing the reaction to proceed through an open chain transition state. Further study of this reaction is required to be able to propose a reason as to why the hexanoyl derivative leads to this anomalous result.

When the aldol reaction was attempted with aldehyde (**157**) and enolate (**145**), it was found that the dibutylboron triflate in the reaction medium caused the cleavage of the *O*-TBS ether protection, resulting in the formation of lactol (**265**), before the aldehyde could undergo the aldol reaction. In order to avoid this problem, a more robust protecting group, stable to Lewis acids could be substituted for the *O*-TBS group.

The benzyl ether derivative of aldehyde (**157)** would not be expected to be cleaved under the aldol reaction conditions, and would be an appropriate protecting group for the reaction, and should circumvent the formation of the lactol, and allow the aldol reaction to proceed as predicted. There are two possible points for the introduction of the benzyl group: it could either be introduced in the first step in the reaction pathway, and the use of the TBS ether could be avoided completely, or the TBS ether could be cleaved by reaction of the benzylidene acetal intermediate (**155**) with TBAF, followed by the introduction of the benzyl ether under basic reaction conditions. Introduction of the benzyl ether at the start of the reaction pathway would mean that all reaction conditions would need to be re-optimised; however, it could have the benefit of increasing yields. More importantly, there can be no guarantee that the diastereomeric products of the Sharpless asymmetric epoxidation (**153**) could be separated. Introduction of the benzyl ether at the benzylidene acetal stage would mean that an additional two reaction steps would be added to the synthetic pathway, but avoids the need to re-optimise the reaction conditions of all of the other steps completed. With this in mind, **Scheme 26** shows the proposed route for generation of the target for the AAL

toxins (**272**) and fumonisins (**271**), where an *O*-TBS group is used in the initial steps of the synthesis, which is then replaced by an *O*-Bn group at the acetal stage.

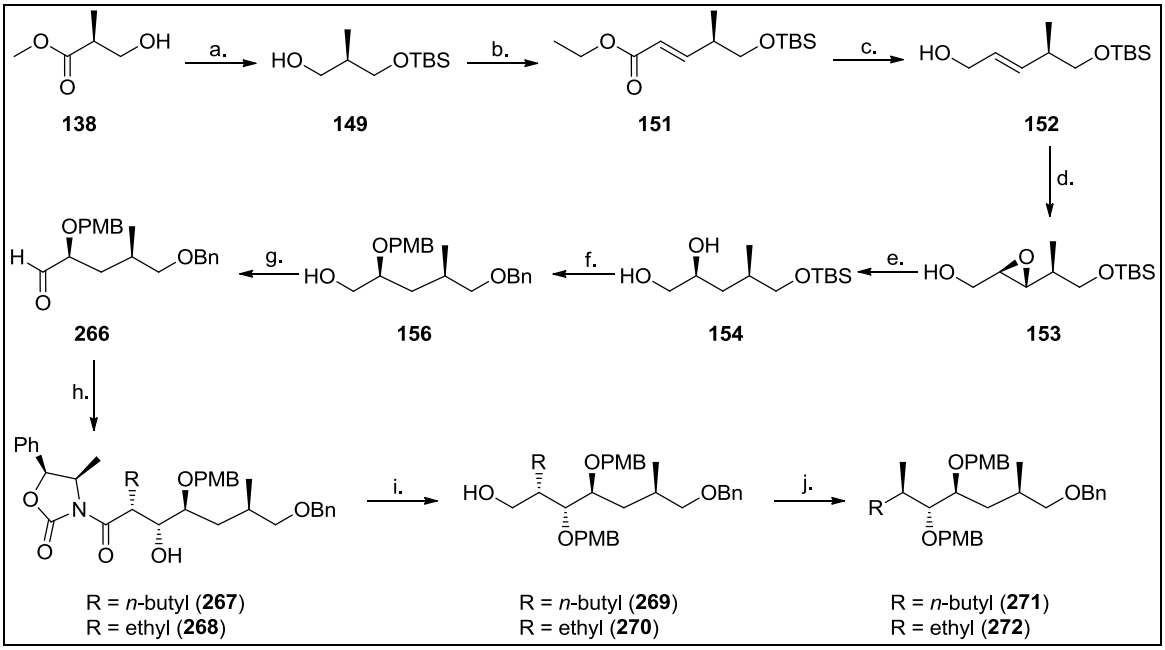

Scheme 27: Proposed optimal synthetic route, showing introduction of alternate protection.

> *Reagents*: a. i). TBSCl, imidazole, ii). DIBALH; b. i). DMSO, $(COCl)_2$, Et_3N, ii). ^{t}BuOK, $(^i PrO)_2P(O)CH_2COOEt$; c. DIBALH; d. (*S*,*S*)-DIPT, $Ti(O^iPr)_4$, TBHP; e. DIBALH; f. i). $(OMe)_2CHC_6H_4OMe$, PPTS, ii). TBAF, iii). NaH, BnBr, TBAI, iv). DIBALH; g. DMSO, $(COCl)_2$, Et_3N; h. **123** or **145**, Bu_2BOTf, Et_3N; i. i). NaH, $MeOC_6H_4CH_2Br$, ii). $LiAlH_4$; j. i). TsCl, pyridine, ii). $LiAlH_4$.

This proposed route should provide access to targets (**271**) and (**272**), and overcomes the problems encountered in this synthetic study. These targets could then be used in coupling reactions after removal of the *O*-Bn group, and used in the synthesis of various fumonisin and AAL toxin analogues.

4. EXPERIMENTAL

4.1. GENERAL

Air and moisture sensitive reactions were carried out under an atmosphere of argon in glassware dried at 100 °C. Room temperature (rt) refers to 18-25 °C. All evaporations and concentrations were performed under reduced pressure. All reagents were of synthetic grade and were used without further purification, unless stated otherwise. When necessary, solvents and reagents were dried prior to use according to standard methods.[1]

The course of reactions was followed by thin-layer chromatography (TLC) using aluminium plates coated with silica gel ($60F_{245}$ Merck). TLC plates were examined under UV (254 nm and 266 nm) before being visualised with ammonium heptamolybdate, anisaldehyde – sulfuric acid or ceric sulfate – sulfuric acid. Column chromatography was performed on Merck silica gel 60 (70-230 mesh or 250-400 mesh).

Nuclear magnetic resonance (NMR) spectra were measured in $CDCl_3$ solutions on Bruker AMX-300 (7.0 T), AVANCE III-400 (9.4 T) or AVANCE-500-DXR (11.7 T) spectrometers. All chemical shifts are reported as δ (ppm) values downfield from tetramethylsilane using $CHCl_3/CDCl_3$ as an internal standard (δ_H 7.24 and δ_C 77.00 respectively). Proton coupling constants (*J*) are given in Hz. Coupling patterns are designated as follows: s/S: singlet; d/D: doublet, t/T: triplet; q/Q: quartet; m: multiplet; br: broad signal.

The assignments of the signals in the ^{1}H NMR spectra are based on first-order analysis of the spin systems and when required, confirmed by two-dimensional (2-D) (^{1}H-^{1}H) homonuclear chemical shift correlation (COSY) experiments. The ^{13}C shifts were obtained from proton-decoupled ^{13}C NMR spectra. The multiplicities of the signals were determined from the proton-decoupled DEPT-135 spectra. The signals of the proton-bearing carbon atoms were correlated with specific proton resonances in 2D (^{13}C-^{1}H) heteronuclear single-quantum coherence (HSQC) experiments utilising one-bond spin-spin couplings. Standard Bruker pulse programs were used in the experiments.

[1] Perrins, D.D.; Armarego, W.L.F. *Purification of laboratory chemicals*. 3rd Ed., Pergamon Press, Oxford, **1992**.

Optical rotations were measured with a Perkin Elmer 341 polarimeter in a 10.0 cm cell at the wavelength of the sodium D-line (λ = 589 nm). Specific rotations are given in units of 10^{-1}deg cm^2 g^{-1} and concentrations are given in g/100 mL. Mass spectra were recorded at the University of Stellenbosch on a Waters API Q-TOF Ultima spectrometer using the electrospray ionisation (ESI) technique, and detection of positive ions with *m/z* > 99. FTIR spectra were measured on a Perkin Elmer RX I spectrometer fitted with a PIKE Technologies ATR accessory using the reflectance technique. Melting points are uncorrected.

XRD data were collected at the University of Cape Town on a Siemens P4 diffractometer with a Nonius Kappa CCD detector using graphite monochromated, MoKα radiation at 173 K by means of phi and omega scans. Structures were solved by direct methods using SHELXS-97 and refined by full-matrix least squares techniques using SHELXL-97.

4.2. PREPARATION OF REAGENTS

4.2.1. Visualising Reagents

Ammonium heptamolybdate

A solution was prepared by dissolving ammonium heptamolybdate (5 g) in EtOH (50 mL). Compounds on the TLC plate were visualised after dipping in the solution and heating with a heat gun until blue spots appeared on a yellow-green background.

Anisaldehyde – sulfuric acid

A solution of anisaldehyde (5 g) in EtOH (50 mL) was prepared, and concentrated sulfuric acid was added slowly (2.5 mL). Compounds on the TLC plate were visualised after dipping in the solution and heating with a heatgun until dark blue spots appeared on a pink background.

Ceric sulfate – sulfuric acid

Ceric sulphate was dissolved in 15 % aqueous sulfuric acid until the solution was saturated. Compounds on the TLC plate were visualised after dipping in the solution and heating with a heatgun until brown spots appeared on a pale background.

4.2.2. General Reagents

Methyltriphenylphosphonium iodide

Triphenylphosphine (10.0 g, 38.1 mmol) was dissolved in toluene (50 mL) and methyl iodide (3.2 mL, 51.4 mmol) was added dropwise and the mixture stirred for 18 h at rt. The reaction was cooled to 0 °C and the solids collected by vacuum filtration. The off-white solid material

was washed with cold toluene (2×30 mL) and dried under reduced pressure at 50 °C to give methyltriphenylphosphonium iodide as an off-white powder (14.8 g, 96%) which was used without further purification.

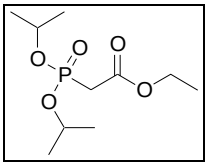

Ethyl diisopropylphosphonoacetate

A mixture of triisopropyl phosphite (20.7 g, 99.6 mmol) and ethyl 2-chloroacetate (12.5 g, 102 mmol) was refluxed at 130 °C for 18 h. The crude product was purified by vacuum distillation (2 mmHg, 150 °C) giving a colourless oil as product (16.2 g, 65%).

δ_H: 4.67-4.76 (m, 2H, isopropyl CH); 4.15 (q, 2H, *J* 7.2, ester CH_2); 2.88 (d, 2H, $J_{H,P}$ 21.6, P-CH_2); 1.30 (d, 12H, *J* 6.1, isopropyl CH_3); 1.11 (d, 3H, *J* 7.1, ester CH_3).

δ_C: 165.90 (S, carbonyl C); 71.37 (DD, isopropyl CH); 61.36 (T, ester CH_2); 35.47 (TD, $J_{P,C}$ 134.9, P-CH_2); 23.89 (QD, J_{CP} 26.4, isopropyl CH_3); 14.06 (Q, ester CH_3).

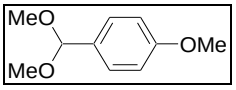

Anisaldehyde dimethylacetal

Anisaldehyde (33.5 mL, 276 mmol) was dissolved in MeOH (200 mL), and trimethyl orthoformate (30.0 mL, 274 mmol) and *p*-TsOH (1.01 g, 5.30 mmol) were added. The mixture was heated to 50 °C for 48 h. The reaction mixture was quenched by pouring into a saturated $NaHCO_3$ solution (300 mL), before the phases were separated, and the aqueous phase was extracted with Et_2O (3×300 mL). The Et_2O solution was concentrated and the residue dissolved in EtOAc (200 mL) and washed with a 1:1 5 % KOH-brine solution (3 × 100 mL). The organic phase was dried over anhydrous $MgSO_4$, concentrated, and evaporated. The residual liquid was distilled under vacuum (100 °C, 2 mmHg) to give anisaldehyde dimethyl acetal as colourless oil (24.5 g, 49%) which was used without further purification.

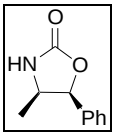

(4*R*,5*S*)-4-Methyl-5-phenyl-oxazolidin-2-one (125)

A mixture of (1*S*,2*R*)-(+)-norephedrine (56.4 g, 373 mmol) and diphenyl carbonate (79.9 g, 373 mmol) were heated to 110 °C for 18 h before being cooled and diluted with DCM (1 L). The organic phase was washed with 2M NaOH (3×500 mL), 1M HCl (200 mL) and saturated brine (200 mL), before being dried over anhydrous Na_2SO_4, and concentrated. The crude product was purified by recrystallization from toluene to give **125** as a white solid (58.1 g, 88%). R_f = 0.04 (1:1 hexanes-EtOAc); $[\alpha]_D^{20}$ +169.6 (*c* 1.03, $CHCl_3$) [lit.,[2] $[\alpha]_D^{20}$ +163.7 (*c* 1.0, $CHCl_3$)]; ν_{max} 1760, 2357 cm^{-1}.

δ_H: 7.37-7.26 (m, 5H, Ar-H); 6.62 (br s, 1H, N-H); 5.68 (d, 1H, *J* 8.0, H-5); 4.19 (qd, 1H, *J* 6.5, 8.0, H-4); 0.78 (d, 3H, *J* 6.5, 4-methyl).

δ_C: 159.77 (S, C-2); 134.88, 128.41, 128.37, 125.87 (Ar-C); 80.96 (D, C-5); 52.37 (D, C-4); 17.41 (Q, 4-methyl).

HRMS (ESI): *m/z* 178.0859 $[M+H]^+$; Calculated for $C_{10}H_{12}NO_2$: 178.0868. *m/z* 200.0687 $[M+Na]^+$; Calculated for $C_{10}H_{11}NO_2Na$, 200.0687.

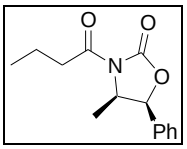

(4*R*,5*S*)-3-Butanoyl-4-methyl-5-phenyl-oxazolidin-2-one (145)

The (4*R*,5*S*)-oxazolidinone (**125**) (21.2 g, 120 mmol) was dissolved in THF (180 mL) and cooled to −78 °C, before 1.56M *n*-BuLi in hexanes (81.0 mL, 126 mmol) was added over 30 min, until the orange colour of the dianion just persisted. Butanoyl chloride (14.4 mL, 135 mmol) was added in a single portion, and the reaction mixture warmed to 0 °C and stirred for 3 h. The reaction was quenched by addition of 1M K_2CO_3 solution (200 mL), and the volatiles were removed. The residue was extracted with DCM (3×150 mL) and the combined organic phases were washed with saturated K_2CO_3 solution (200 mL) and brine (200 mL) before being dried over anhydrous Na_2SO_4, and concentrated. Column chromatography on silica gel (4:1 hexanes-EtOAc) gave **145** as a colourless oil which was recrystallized from Et_2O-pentane (25.8 g, 87%). R_f = 0.53 (4:1 hexanes-EtOAc); $[\alpha]_D^{20}$ +53.8 (*c* 0.60, $CHCl_3$) [lit.,[3] $[\alpha]_D^{20}$ +40.2 (*c* 1.5, CH_2Cl_2)]; ν_{max} 1780, 1690 cm^{-1}.

δ_H: 7.40–7.26 (m, 5H, Ar-H); 5.64 (d, 1H, *J* 7.3, H-5); 4.74 (dq, 1H, H-4); 2.94

[2] Evans, D.A.; Bartroli, J.; Smith, T.L. *J. Am. Chem. Soc.* **1981**, *103*, 2127.
[3] Brimble, M.A. *Aust. J. Chem*. **1990**, *43*, 1035.

(ddd, 1H, *J* 6.9, 8.0, 16.9, H-2′a); 2.70 (ddd, 1H, *J* 7.0, 7.8, 16.9, H-2′b); 1.74-1.63 (m, 2H, H-3′), 0.97 (dd, 3H, *J* 7.5, 7.5, H-4′); 0.87 (d, 3H, *J* 6.5, 4-methyl).

δ_C: 172.94 (S, C-1′); 153.01 (S, C-2); 133.34, 128.68, 128.64, 125.60 (Ar-C); 78.90 (D, C-5); 54.66 (D, C-4); 37.40 (T, C-2′); 17.69 (T, C-3′); 14.51 (Q, 4-methyl); 13.59 (Q, C-4′).

HRMS (ESI): *m/z* 248.1286 $[M+H]^+$; Calculated for $C_{14}H_{18}NO_3$: 248.1287. *m/z* 270.1103 $[M+Na]^+$; Calculated for $C_{14}H_{17}NO_3Na$: 270.1106.

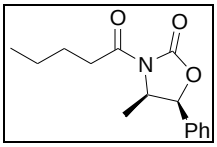

(4*R*,5*S*)-4-Methyl-3-pentanoyl-5-phenyl-oxazolidin-2-one (259)

Valeric acid (2.80 g, 27.4 mmol) was added to a flask with 2 drops of dimethyl formamide, before $SOCl_2$ (5.40 mL, 74.0 mmol) was added in a single portion. The mixture was refluxed for 1 h, before being cooled and diluted with benzene (50 mL). The benzene and excess $SOCl_2$ were removed under reduced pressure. The residue was diluted with benzene (50 mL) and evaporated twice, leaving crude valeryl chloride which was used without further purification.

(4*R*,5*S*)-Oxazolidinone (**125**) (3.00 g, 16.9 mmol) was dissolved in THF (50 mL) and cooled to −78 °C, before 1.6M *n*-BuLi in hexanes (11.9 mL, 19.0 mmol) was added dropwise, until the orange colour of the dianion just persisted. The crude valeryl chloride was added in a single portion, and the reaction mixture warmed to 0 °C and stirred for 2 h. The reaction was quenched by addition of 1M K_2CO_3 solution (50 mL), and the volatiles were removed. The residue was diluted with EtOAc and the phases separated. The aqueous phase was extracted with EtOAc (2×50 mL) and the combined organic phases were dried over anhydrous $MgSO_4$, and concentrated. Column chromatography on silica gel (1:1 hexanes-EtOAc) gave **259** as a yellow solid (2.56 g, 58%). R_f = 0.46 (1:1 hexanes: EtOAc); $[\alpha]_D^{20}$ +43.3 (*c* 0.60, $CHCl_3$) [lit.,[4] $[\alpha]_D^{20}$ +43.3 (*c* 4.9, $CHCl_3$)]; ν_{max} 1780, 1682, 738 cm^{-1}.

δ_H: 7.36-7.19 (m, 5H, Ar-H); 5.58 (d, 1H, *J* 6.6, H-5); 4.68 (dq, 1H, *J* 6.6, 7.3, H-4); 2.97-2.75 (m, 2H, H-2′); 1.63-1.47 (m, 2H, H-3′); 1.39-1.25 (m, 2H, H-

[4] Zelle, R.E.; DeNinno, R.P.; Selnik, H.G.; Danishefsky, S.J. *J. Org. Chem.* **1986**, *56*, 5032.

4′); 0.86 (dd, 3H, *J* 7.3, 7.3, H-5′); 0.81 (d, 3H, *J* 6.6, 4-methyl).

δ_C: 173.04 (S, C-1′); 152.94 (S, C-2); 133.32, 128.60, 128.57, 125.55 (Ar-C); 78.82 (D, C-5); 54.60 (D, C-4); 35.23 (T, C-2′); 26.28 (T, C-3′); 22.13 (T, C-4′); 14.44 (Q, 4-methyl); 13.75 (Q, C-5′).

HRMS (ESI): *m/z* 262.1432 $[M+H]^+$; Calculated for $C_{15}H_{20}NO_3$: 262.1443; *m/z* 284.1249 $[M+Na]^+$; Calculated for $C_{15}H_{19}NO_3Na$: 284.1262.

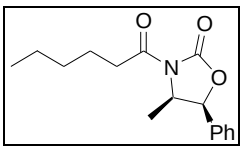

(4*R*,5*S*)-3-Hexanoyl-4-methyl-5-phenyl-oxazolidin-2-one (123)

Hexanoic acid (7.66 g, 65.9 mmol) was dissolved in benzene (100 mL) and $SOCl_2$ (9.60 mL, 132 mmol) was added in a single portion. The mixture was refluxed for 1 h, before being cooled and excess $SOCl_2$ and benzene removed under reduced pressure. The residue was diluted with benzene (50 mL) and evaporated leaving crude hexanoyl chloride which was used without further purification.

(4*R*,5*S*)-Oxazolidinone (**125**) (10.6 g, 60.0 mmol) was dissolved in THF (100 mL) and cooled to −78 °C, before 1.56M *n*-BuLi in hexanes (40.0 mL, 62.4 mmol) was added dropwise until the orange colour of the dianion just persisted. The solution was stirred for 15 min before the crude hexanoyl chloride was added in a single portion, and the reaction mixture warmed to 0 °C and stirred for 3 h. The reaction was quenched by addition of 1M K_2CO_3 solution (100 mL), and the volatiles were removed. The residue was diluted with DCM and the phases separated. The aqueous phase was extracted with DCM (2×50 mL) and the combined organic phases were being dried over anhydrous Na_2SO_4, and concentrated. Column chromatography on silica gel (4:1 hexanes-EtOAc) gave **123** as a clear oil, which was recrystallized from pentane-Et_2O (14.9 g, 90%). R_f = 0.43 (1:1 hexanes-Et_2O); $[\alpha]_D^{20}$ +42.6 (*c* 1.30, $CHCl_3$); ν_{max} 1780, 1695 cm^{-1}.

δ_H: 7.39-7.26 (m, 5H, Ar-H); 5.63 (d, 1H, *J* 7.3, H-5); 4.73 (dq, 1H, *J* 6.8, 7.3, H-4); 2.94 (ddd, 1H, *J* 6.7, 8.4, 16.8, H-2′a); 2.85 (ddd, 1H, *J* 7.0, 8.2, 16.8, H-2′b); 1.68-1.61 (m, 2H, H-3′); 1.34-1.29 (m, 4H, H-4′, H-5′); 0.88 (dd, 3H, *J* 6.8, 6.8, H-6′); 0.85 (d, 3H, *J* 6.8 , 4-methyl).

δ_C: 173.08 (S, C-1′); 152.95 (S, C-2); 133.33, 128.62, 128.58, 125.56 (Ar-C); 78.83 (D, C-5); 54.61 (D, C-4); 35.48 (T, C-2′); 31.17 (T, C-4′), 24.02 (T, C-

3′); 22.32 (T, C-5′); 14.46 (Q, 4-methyl), 13.82 (Q, C-6′).

HRMS (ESI): *m/z* 276.1589 $[M+H]^+$; Calculated for $C_{16}H_{22}NO_3$: 276.1600; *m/z* 298.1407 $[M+Na]^+$; Calculated for $C_{16}H_{21}NO_3Na$: 298.1419.

4.3. PROCEDURES

4.3.1. Sharpless Asymmetric Epoxidation Route

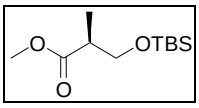

Methyl (*S*)-3-(*tert*-Butyldimethylsilanyloxy)-2-methylpropionate (148)

A stirred solution of methyl (*S*)-3-hydroxy-2-methylpropionate (4.47 g, 37.8 mmol) in DCM (250 mL) was cooled to 0 °C and imidazole (3.86 g, 56.7 mmol) was added. When the imidazole was completely dissolved, TBSCl (6.52 g, 43.5 mmol) was added and the mixture stirred for 48 h at rt. The reaction was quenched by addition of saturated NH_4Cl solution (100 mL), and stirred for 20 min. The phases were separated, and the aqueous phase was extracted with EtOAc (3×150 mL). The combined organic phases were washed with saturated brine solution (200 mL), before being dried over anhydrous $MgSO_4$, and concentrated. Column chromatography on silica gel (4:1 hexanes-EtOAc) gave **148** as a colourless oil (8.44 g, 96%). R_f = 0.58 (4:1 hexanes-EtOAc); $[\alpha]_D^{20}$ +19.0 (*c* 0.86, $CHCl_3$) [lit.,[5] $[\alpha]_D^{20}$ +20.7 (*c* 1.0, CCl_4)]; ν_{max} 1736, 1090 cm^{-1}.

δ_H: 3.74 (dd, 1H, *J* 6.8, 9.6, H-3a); 3.64 (s, 3H, ester methyl); 3.62 (dd, 1H, *J* 6.0, 9.6, H-3b); 2.62 (ddq, 1H, *J* 6.0, 6.8, 7.1, H-2); 1.11 (d, 3H, *J* 7.1, 2-methyl); 0.84 (s, 9H, $SiC(C\underline{H}_3)_3$); 0.01 (s, 6H, $Si(C\underline{H}_3)_2$).

δ_C: 175.46 (S, C-1); 65.22 (T, C-3); 51.47 (Q, ester methyl); 42.51 (D, C-2); 25.75 (Q, $SiC(\underline{C}H_3)_3$); 18.18 (S, $Si\underline{C}(CH_3)_3$); 13.43 (Q, 2-methyl); –5.53, –5.53 (Q, $Si(\underline{C}H_3)_2$).

HRMS (ESI): *m/z* 233.1562 $[M+H]^+$; Calculated for $C_{11}H_{25}O_3Si$: 233.1562; *m/z* 201.1302 $[M-OCH_3]^+$; Calculated for $C_{10}H_{21}O_2Si$: 201.1311.

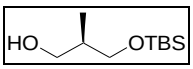

[5] Gaucher, A.; Ollivier, J.; Marguerite, J.; Paugam, R.; Salaun, J. *Can. J. Chem.* **1994**, *72*, 1312.

(*R*)-3-(*tert*-Butyldimethylsilanyloxy)-2-methylpropan-1-ol (149)

148 (4.37 g, 18.8 mmol) was dissolved in DCM (250 mL) and cooled to −78 °C under argon, and DIBALH (9.1 mL, 51 mmol) was added dropwise over 5 min with thorough stirring. The mixture was allowed to warm to rt over 1.5 h at which point the reaction was quenched by the dropwise addition of MeOH (10 mL), followed by the addition of saturated NH_4Cl (50 mL), and 3M HCl dropwise until the precipitate dissolved. This was stirred for 15 min, the phases were separated, and the aqueous phase extracted with Et_2O (3×150 mL). The combined organic phases were washed with saturated brine solution (100 mL), before being dried over anhydrous $MgSO_4$, and concentrated. Column chromatography on silica gel (1:1 hexanes: Et_2O) gave **149** as a colourless oil (3.0 g, 79%). R_f = 0.35 (4:1 hexanes: EtOAc); $[\alpha]_D^{20}$ +6.4 (*c* 0.80, $CHCl_3$) [lit.,[6] $[\alpha]_D^{20}$ +5.7 (*c* 1.1, $CHCl_3$)]; ν_{max} 3349, 1084 cm^{-1}.

δ_H: 3.70 (ddd, 1H, *J* 0.7, 4.5, 9.9, H-3b), 3.61 (ddd, 1H, *J* 0.7, 4.4, 10.7, H-1b); 3.56 (dd, 1H, *J* 7.2, 10.7, H-1a); 3.51 (dd, 1H, *J* 7.9, 9.9, H-3a); 2.79 (br s, 1H, OH); 1.90 (ddddq, 1H, *J* 4.4, 4.5, 7.2, 7.9, 6.9, H-2); 0.87 (s, 9H, $SiC(C\underline{H}_3)_3$); 0.84 (d, 3H, *J* 6.9, 2-methyl); 0.04 (s, 6H, $Si(C\underline{H}_3)_2$).

δ_C: 68.66 (T, C-3), 68.20 (T, C-1); 37.20 (D, C-2); 25.82 (Q, $SiC(\underline{C}H_3)_3$); 18.14 (S, $Si\underline{C}(CH_3)_3$); 13.05 (Q, 2-methyl); −5.58 (Q, $Si(\underline{C}H_3)_2$); −5.64 (Q, $Si(\underline{C}H_3)_2$).

HRMS (ESI): *m/z* 205.1615 $[M+H]^+$; Calculated for $C_{10}H_{25}O_2Si$: 205.1614; *m/z* 187.1509 $[(M+H)-H_2O]^+$; Calculated for $C_{10}H_{23}O_1Si$: 187.1518.

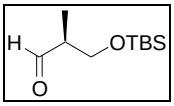

(*S*)-3-(*tert*-Butyldimethylsilanyloxy)-2-methylpropanal (150)

DMSO (2.6 mL, 36 mmol) was added dropwise to a solution of $(COCl)_2$ (1.6 mL, 18 mmol) in DCM (200 mL) under argon at −78 °C. This was stirred for 30 min, at which point alcohol (**149**) (3.03 g, 14.8 mmol) dissolved in DCM (100 mL) was added dropwise over 10 min. This was stirred for 1 h, at which point Et_3N (10.4 mL, 74.7 mmol) was added slowly, and the reaction mixture allowed to warm slowly to rt over 1 h. Water (100 mL) was added and the phases were separated. The aqueous phase was extracted with Et_2O (3×50 mL) and the combined organic phases were dried over anhydrous $MgSO_4$, and concentrated. Column chromatography on silica gel (3:1 hexanes-Et_2O) gave **150** as a colourless oil (3.0 g, 90%). R_f

[6] Pemp, A.; Seifert, K. *J. Prakt. Chem.* **1999,** *341*, 65.

= 0.52 (4:1 hexanes-EtOAc); $[\alpha]_D^{20}$ +21.8 (*c* 0.70, CCl_4) [lit.,[5] $[\alpha]_D^{20}$ +25.4 (*c* 1.0, CCl_4)].

δ_H: 9.71 (d, 1H, *J* 1.6, H-1); 3.83 (dd, 1H, *J* 5.2, 10.2, H-3a); 3.78 (dd, 1H, *J* 6.3, 10.2, H-3b); 2.50 (dddq, 1H, *J* 1.2, 5.2, 6.3, 7.0, H-2); 1.06 (d, 3H, *J* 7.0, 2-methyl); 0.85 (s, 9H, $SiC(C\underline{H}_3)_3$); 0.03 (s, 6H, $Si(C\underline{H}_3)_2$).

δ_C: 204.67 (D, C-1); 63.42 (T, C-3); 48.79 (D, C-2); 25.75 (Q, $SiC(\underline{C}H_3)_3$); 18.19 (S, $Si\underline{C}(CH_3)_3$); 10.26 (Q, 2-methyl); −5.54 (Q, $Si\underline{C}(CH_3)_3$); −5.57 (Q, $Si\underline{C}(CH_3)_3$).

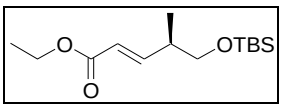

Ethyl (2*E*,4*R*)-5-(*tert*-butyldimethylsilanyloxy)-4-methylpent-2-enoate (151)

t-BuOK (3.00 g, 26.8 mmol) was added to a stirred solution of ethyl diisopropyl-phosphonoacetate (6.70 g, 26.6 mmol) in THF (100 mL) at 0 °C. This mixture was stirred for 90 min, before being cooled to −78 °C. Aldehyde (**150**) (2.67 g, 13.2 mmol) was dissolved in THF (50 mL) and added dropwise to the phosphonate-base mixture, and stirred at this temperature for 90 min, before being allowed to warm to rt. The reaction was quenched by addition of saturated NH_4Cl solution (50 mL), stirring for 10 min, and dilution with water (50 mL). Volatiles were then removed by rotary evaporation, and the resultant slurry diluted with Et_2O (100 mL). The phases were separated, and the aqueous phase was extracted with Et_2O (3×50 mL). The combined organic phases were washed with saturated brine solution (100 mL), before being dried over anhydrous $MgSO_4$, and concentrated. Column chromatography on silica gel (3:1 hexanes-Et_2O) gave an inseparable 9:1 mixture of the *E* and *Z* isomers of **151** (2.88 g, 80%). R_f = 0.60 (4:1 hexanes-EtOAc); ν_{max} 2855, 1718, 1471 cm^{-1}.

δ_H: 6.89 (dd, 1H, *J* 7.2, 15.8, H-2); 5.79 (dd, 1H, *J* 1.3, 15.8, H-3); 4.15 (q, 2H, *J* 7.1, ethyl CH_2); 3.51 (dd, 1H, *J* 6.5, 9.8, H-5a); 3.47 (dd, 1H, *J* 6.5, 9.8, H-5b); 2.46 (dddq, 1H, *J* 1.3, 6.5, 7.2, 6.7, H-4); 1.25 (t, 3H, *J* 7.1, ethyl CH_3); 1.01 (d, 3H, *J* 6.7, 4-methyl); 0.85 (s, 9H, $SiC(C\underline{H}_3)_3$); 0.00 (s, 6H, $Si(C\underline{H}_3)_2$).

δ_C: 166.69 (S, C-1); 151.35 (D, C-3); 120.86 (D, C-2); 66.86 (T, C-5); 60.11 (T, ethyl CH_2); 39.11 (D, C-4); 25.81 (Q, $SiC(\underline{C}H_3)_3$); 18.25 (S, $Si\underline{C}(CH_3)_3$); 15.46 (Q, 4-methyl); 14.21 (Q, ester CH_3); −5.46 (Q, $Si(\underline{C}H_3)_2$).

HRMS (ESI): *m/z* 273.1873 $[M+H]^+$; Calculated for $C_{14}H_{29}O_3Si$: 273.1886; *m/z* 295.1694 $[M+Na]^+$; Calculated for $C_{14}H_{28}O_3SiNa$: 295.1705; *m/z* 227.1454 $[M-OEt]^+$; Calculated for $C_{12}H_{23}O_2Si$, 227.1467.

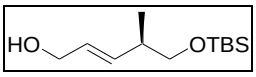

(2*E*,4*R*)-5-(*tert*-Butyldimethylsilanyloxy)-4-methylpent-2-en-1-ol (152)

A solution of ester (**151**) (2.10 g, 7.70 mmol) in DCM (250 mL) was cooled to −78 °C and DIBALH (3.50 mL, 19.3 mmol) was added dropwise over 15 min. After 20 min the reaction was warmed to rt before being quenched by the addition of MeOH (10 mL), followed by saturated NH_4Cl (100 mL), and 3M HCl until the precipitate dissolved. The phases were separated, and the aqueous phase was extracted with Et_2O (3×100 mL). The combined organic phases were dried over anhydrous $MgSO_4$, and concentrated. Column chromatography on silica gel (1:1 hexanes-Et_2O) gave **152** as a colourless oil (1.50 g, 85%). R_f = 0.31 (1:1 hexanes-Et_2O); ν_{max} 1652, 1398 cm^{-1}.

δ_H: 5.65 (dt, 1H, *J* 15.6, 4.9, H-2); 5.59 (dd, 1H, *J* 5.7, 15.6, H-3); 4.96 (d, 2H, *J* 4.9, H-1); 3.46 (dd, 1H, *J* 6.3, 9.8, H-5a); 3.38 (dd, 1H, *J* 6.9, 9.8, H-5b); 2.31 (dddq, 1H, J 5.7, 6.3, 6.9, 6.8, H-4); 1.60 (br s, 1H, OH); 0.97 (d, 3H, *J* 6.7, 4-methyl); 0.86 (s, 9H, SiC($C\underline{H}_3$)$_3$); 0.01 (s, 6H, Si($C\underline{H}_3$)$_2$).

δ_C: 135.47 (D, C-3); 128.66 (D, C-2); 67.87 (T, C-5); 63.82 (T, C-1); 38.94 (D, C-4); 25.89 (Q, SiC($\underline{C}H_3$)$_3$); 18.33 (S, Si$\underline{C}$(CH_3)$_3$); 16.35 (Q, 4-methyl); −5.34 (Q, Si($\underline{C}H_3$)$_2$).

HRMS (ESI): *m/z* 213.1667 $[M+H-H_2O]^+$; Calculated for $C_{12}H_{25}OSi$: 213.1675; *m/z* 253.1597 $[M+Na]^+$; Calculated for $C_{12}H_{25}O_2SiNa$: 253.1600.

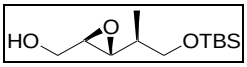

(2*R*,3*R*,4*S*)-5-(*tert*-Butyldimethylsilanyloxy)-2,3-epoxy-4-methylpentan-1-ol (153)

Activated 4 Å molecular sieves (0.8 g) were suspended in DCM (50 mL) and cooled to −20 °C. (*2S*,*3S*)-Diisopropyl tartrate (254 µl, 1.56 mmol), titanium(IV) isopropoxide (326 µl, 1.30 mmol) and *tert*-butyl hydroperoxide (4.93M,[7] 3.30 mL, 16.3 mmol) were added and the mixture stirred for 45 min. **152** (1.50 g, 6.65 mmol) was dissolved in DCM (10 mL), and added slowly. The reaction mixture was stirred at −20 °C for 18 h. The reaction was warmed to 0 °C and quenched by addition of H_2O (30 mL), followed by 30% NaOH in brine (10 mL). This was stirred vigorously for 40 min, however no phase separation was observed. The mixture was vacuum filtered, and the filtrate diluted with DCM (100 mL) and the resulting

[7] Concentration of TBHP in toluene solution was determined using the method described in "Hill, J.G.; Sharpless, K.B.; Exon, C.M.; Regenye, R. *Org. Syn. Coll.* **1990**, *7*, 461."

phases separated. The aqueous phase was then extracted with Et_2O (3×50mL). The combined organic phases were dried over anhydrous $MgSO_4$, and concentrated. Flash column chromatography on silica gel (1:1 hexanes-Et_2O) gave a 9:1 mixture of diastereomers. A second flash column in the same solvent gave **153** as a colourless oil (0.450 g, 30%). R_f = 0.22 (1:1 hexanes-Et_2O); ν_{max} 1251, 1091 cm^{-1}.

δ_H: 3.86 (dd, 1H, *J* 2.5, 12.6, H-1a); 3.53 (dd, 1H, *J* 4.7, 12.6, H-1b); 3.53 (dd, 1H, *J* 5.4, 10.2, H-5a); 3.47 (dd, 1H, *J* 7.8, 10.2, H-5b); 3.00 (ddd, 1H, *J* 2.4, 2.5, 4.8, H-2); 2.80 (dd, 1H, *J* 2.4, 7.1, H-3); 2.28 (br s, 1H, OH); 1.57 (dddq, 1H, *J* 5.4, 7.1, 7.8, 6.8, H-4); 0.93 (d, 3H, *J* 6.8, 4-methyl); 0.85 (s, 9H, $SiC(C\underline{H}_3)_3$); 0.00 (s, 6H, $Si(C\underline{H}_3)_2$).

δ_C: 65.26 (T, C-5); 61.85 (T, C-1); 58.71 (D, C-2); 58.25 (D, C-3); 38.29 (D, C-4); 25.84 (Q, $SiC(\underline{C}H_3)_3$); 18.21 (S, $Si\underline{C}(CH_3)_3$); 13.18 (Q, 4-methyl); –5.51, -5.52 (Q, $Si(\underline{C}H_3)_2$).

HRMS (ESI): *m/z* 247.1719 $[M+H]^+$; Calculated for $C_{12}H_{27}O_3Si$: 247.1729; *m/z* 269.1537 $[M+Na]^+$; Calculated for $C_{12}H_{26}O_3SiNa$, 269.1549.

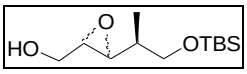

(2*RS*,3*RS*)-5-(*tert*-Butyldimethylsilanyloxy)-2,3-epoxy-4-methylpentan-1-ol (153)

Allylic alcohol (**152**) (500 mg, 2.17 mmol) was dissolved in DCM (50 mL) and MCPBA (70%, 1.60 g, 6.51 mmol) was added. The mixture was stirred for 48 h at rt. The reaction was quenched by addition of saturated Na_2SO_3 solution (50 mL), and stirred for 1 h. The phases were separated, saturated $NaHCO_3$ solution (50 mL) was added to the organic phase and stirred for 1 h. The phases were separated and the aqueous phase was extracted with EtOAc (3×50 mL). The combined organic phases were dried over anhydrous $MgSO_4$, and concentrated. Column chromatography on silica gel (1:1 hexanes-Et_2O) gave (2*RS*,3*RS*)-**153** as a colourless oil (338 mg, 63%), which was found to be a 5:8 mixture of diastereomers (by ^1H NMR spectroscopy). R_f = 0.22 (1:1 hexanes-Et_2O); ν_{max} 1251, 1091 cm^{-1}.

Major diastereomer:

δ_H: 3.86 (dd, 1H, *J* 2.6, 12.6, H-1a); 3.59-3.45 (m, 3H, H-1b, H-5, major and minor); 2.95 (ddd, 1H, *J* 2.5, 2.5, 4.8, H-2); 2.88 (dd, 1H, *J* 2.5, 7.0, H-3); 2.22 (br s, 1H, OH, major and minor); 1.63-1.52 (m, 1H, H-4, major and minor); 0.91 (d, 3H, *J* 6.9, 4-methyl); 0.85 (s, 9H, $SiC(C\underline{H}_3)_3$); 0.00 and 0.01 (s, 6H, $Si(C\underline{H}_3)_2$).

δ_C: 65.43 (T, C-5); 61.98 (T, C-1); 57.56 (D, C-2); 57.13 (D, C-3); 37.77 (D, C-4); 25.83 (Q, SiC($\underline{C}H_3)_3$); 18.24 (S, Si$\underline{C}(CH_3)_3$); 12.70 (Q, 4-methyl); –5.54(Q, Si($\underline{C}H_3)_2$).

Minor diastereomer:

δ_H: 3.88 (dd, 1H, *J* 2.5, 12.6, H-1a); 3.59-3.45 (m, 3H, H-1b, H-5, major and minor); 3.01 (ddd, 1H, *J* 2.5, 2.5, 4.8, H-2); 2.80 (dd, 1H, *J* 2.5, 7.1, H-3), 2.22 (br s, 1H, OH, major and minor); 1.63-1.52 (m, 1H, H-4, major and minor); 0.93 (d, 3H, *J* 6.7, 4-methyl); 0.85 (s, 9H, SiC($C\underline{H}_3)_3$); 0.00 (s, 6H, Si($C\underline{H}_3)_2$).

δ_C: 65.60 (T, C-5); 61.84 (T, C-1); 58.71 (D, C-2); 58.27 (D, C-3); 38.29 (D, C-4); 25.80 (Q, SiC($\underline{C}H_3)_3$); 18.17 (S, Si$\underline{C}(CH_3)_3$); 13.14 (Q, 4-methyl); –5.52 (Q, Si($\underline{C}H_3)_2$).

HRMS (ESI): *m/z* 247.1719 $[M+H]^+$; Calculated for $C_{12}H_{27}O_3Si$: 247.1729; *m/z* 269.1537 $[M+Na]^+$; Calculated for $C_{12}H_{26}O_3SiNa$, 269.1549.

4.3.2. Vinyl Addition Route

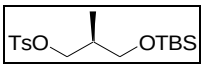

(*S*)-3-(*tert*-Butyldimethylsilanyloxy)-2-methylpropan-1-ol tosylate (185)

Alcohol (**149)** (2.60 g, 12.7 mmol) and DMAP (2.02 g, 16.5 mmol) were dissolved in DCM (150 mL) and cooled to 0 °C under argon. *p*-TsCl (2.48 g, 13.0 mmol) was added and the mixture was allowed to warm to rt over 18 h at which point the reaction was quenched by the addition of water (150 mL) and the mixture stirred for 30 min. The phases were separated, and the aqueous phase extracted with Et_2O (2×30 mL) and DCM (30 mL). The combined organic phases were dried over anhydrous $MgSO_4$, and concentrated. Column chromatography on silica gel (9.5:0.5 to 2:1 hexanes-Et_2O gradient) gave **185** as a colourless oil (3.07 g, 67%). R_f = 0.14 (9.5:0.5 hexanes-Et_2O); $[\alpha]_D^{20}$ +3.5 (*c* 0.81, $CHCl_3$) [lit.,[6] $[\alpha]_D^{20}$ +2.6 (*c* 0.99, $CHCl_3$)]; ν_{max} 1176, 793 cm^{-1}.

δ_H: 7.76 (d, 2H, *J* 8.3, Ar-H); 7.31 (d, 2H, *J* 8.3, Ar-H); 3.99 (dd, 1H, *J* 5.8, 9.2, H-3a); 3.89 (dd, 1H, *J* 5.9, 9.2, H-3b); 3.47 (dd, 1H, *J* 5.0, 10.0, H-1a); 3.38 (dd, 1H, *J* 6.5, 10.0, H-1b); 2.42 (s, 3H, Ar-methyl); 1.92 (ddddq, 1H, *J* 5.0, 5.8, 5.9, 6.5, 6.9, H-2); 0.85 (d, 3H, *J* 6.9, 2-methyl); 0.79 (s, 9H, SiC($C\underline{H}_3)_3$); –0.05 (s, 6H, Si($C\underline{H}_3)_2$).

δ_C: 144.57, 133.02, 129.75, 127.89 (Ar-C); 72.10 (T, C-3); 63.68 (T, C-1); 35.59 (D, C-2); 25.74 (Q, SiC($\underline{C}H_3)_3$); 21.58 (Q, tosyl methyl); 18.13 (S, Si$\underline{C}(CH_3)_3$); 13.26 (Q, 2-methyl); –5.61, –5.63 (Q, Si($\underline{C}H_3)_2$).

HRMS (ESI): *m/z* 359.1703 $[M+H]^+$; Calculated for $C_{17}H_{31}O_4SSi$:, 359.1712; *m/z* 381.1524 $[M+Na]^+$; Calculated for $C_{17}H_{30}O_4SSiNa$: 381.1532.

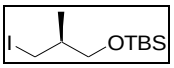

(*S*)-3-(*tert*-Butyldimethylsilanyloxy)-1-iodo-2-methylpropane (187)

Tosylate (**185**) (3.00 g, 8.37 mmol) in THF (150 mL) was added to purified Cu(I)I (1.60 g, 8.40 mmol) and the solution cooled to –50 °C. Vinylmagnesium bromide (1M, 21.0 mL, 21.0 mmol) was added dropwise and the solution warmed to 0 °C and stirred at this temperature for 5 h, before being warmed to rt and stirred for a further 18 h. The reaction was quenched by the addition of MeOH (20 mL) and volatiles were removed. The slurry was diluted with hexane (100 mL) and filtered through a pad of celite and the filtrate concentrated. Column chromatography on silica gel (9:1 to 1:1 hexanes-Et_2O gradient) gave starting material (1.90 g) and **187** as a yellow oil (0.390 g, 15%). R_f = 0.81 (9:1 hexanes-Et_2O).

δ_H: 3.50 (dd, 1H, *J* 4.0, 8.0, H-3a); 3.38 (dd, 1H, *J* 5.4, 8.0, H-3b); 3.28 (dd, 1H, *J* 4.3, 7.9, H-1a); 3.23 (dd, 1H, *J* 4.3, 7.6, H-1b); 1.65-1.59 (m, 1H, H-2); 0.93 (d, 3H, *J* 5.3, 2-methyl); 0.88 (s, 9H, SiC($\underline{C}H_3)_3$); 0.04 (s, 6H, Si($\underline{C}H_3)_2$).

δ_C: 66.69 (T, C-3); 37.78 (D, C-2); 25.88 (Q, SiC($\underline{C}H_3)_3$); 18.26 (S, Si$\underline{C}(CH_3)_3$); 17.24 (Q, 2-methyl); 13.81 (T, C-1); –5.38 (Q, Si($\underline{C}H_3)_2$).

4.3.3. Jacobsen Route

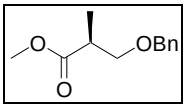

Methyl (*S*)-3-benzyloxy-2-methylpropionate (201)

Benzyl 2,2,2-trichloroacetimidate (27.8 g, 110 mmol) followed by trifluoromethanesulfonic acid (1.0 mL, 11 mmol), was added to a stirred solution of methyl (*S*)-3-hydroxy-2-methylpropionate (**138**) (11.8 g, 100 mmol) in cyclohexane (100 mL) and DCM (50 mL). After 12 h the reaction mixture was filtered to remove the formed 2,2,2-trichloroacetamide, and the solid washed with 2:1 cyclohexane-DCM (50 mL). The combined filtrates were washed with saturated aqueous $NaHCO_3$ solution (50 mL), water (50 mL), dried over Na_2SO_4 and concentrated. Column chromatography on silica gel (9:1 hexanes-EtOAc) gave the *O*-

benzyl derivative (**201**) (20 g, 96%) as a colourless oil. R_f = 0.50 (4:1 hexanes-EtOAc); $[\alpha]_D^{20}$ +11.2 (*c* 3.40, $CHCl_3$), [lit.,[8] $[\alpha]_D^{20}$ +11.3 (*c* 3.80, $CHCl_3$)]; ν_{max} 1732 cm^{-1}.

δ_H: 7.32-7.28 (m, 5H, Ar-H); 4.51 and 4.50 (AB system, 2H, *J* 12.6, benzylic H); 3.68 (s, 3H, methyl ester); 3.65 (dd, 1H, *J* 7.3, 9.2, H-3a); 3.49 (dd, 1H, *J* 5.7, 9.2, H-3b); 2.78 (ddq, 1H, J 5.7, 7.3, 7.1, H-2); 1.18 (d, 3H, *J* 7.1, 2-methyl).

δ_C: 175.08 (Q, C-3), 138.06, 128.19, 127.47 (Ar-H); 72.94 (T, C-3); 71.83 (T, benzylic C); 51.51 (Q, ester methyl); 40.04 (D, C-2); 13.82 (Q, 2-methyl).

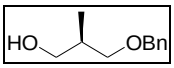

(*R*)-3-Benzyloxy-2-methylpropan-1-ol (202)

A solution of the benzyl ether (**201**) (16.7 g, 80.0 mmol) in Et_2O (50 mL) was added dropwise to a stirred suspension of $LiAlH_4$ (3.03 g, 80.0 mmol) in Et_2O (150 mL) at 0 °C. The mixture was warmed to rt and after 2 h the excess $LiAlH_4$ was quenched by careful addition of 2M NaOH. The reaction mixture was diluted with Et_2O (150 mL) and anhydrous Na_2SO_4 (20 g) was added. After 15 min the mixture was filtered, and the solids were washed with Et_2O, and the combined filtrates concentrated. Column chromatography on silica gel (3:1 hexane-EtOAc) gave the alcohol (**202**) (13.6 g, 94%) as a colourless oil. R_f = 0.52 (1:1 hexanes-EtOAc); $[\alpha]_D^{20}$ +16.4 (*c* 1.26, $CHCl_3$), [lit.,[8] $[\alpha]_D^{20}$ +16.8 (*c* 3.80, $CHCl_3$)].

δ_H: 7.36-7.25 (m, 5H, Ar-H); 4.51 and 4.50 (AB system, 2H, *J* 12.1, benzylic H); 3.58 (d, 2H, H-1); 3.52 (dd, 1H, *J* 2.0, 9.1, H-3a); 3.41 (dd, 1H, *J* 7.8, 9.1, H-3b); 2.45 (s, 1H, OH); 2.11-1.95 (m, 1H, H-2); 0.87 (d, 3H, *J* 7.0, 2-methyl).

δ_C: 137.96, 128.21, 127.45, 127.38 (Ar-H); 74.57 (T, C-3); 73.01 (T, benzylic C); 66.78 (T, C-1); 35.51 (D, C-2); 13.41 (Q, 2-methyl).

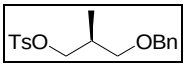

(*S*)-3-Benzyloxy-2-methylpropan-1-ol tosylate (203)

Pyridine (4.74 g, 60.0 mmol) and DMAP (1.22 g, 10.0 mmol) were added to a solution of alcohol (**202**) (10.8 g, 60.0 mmol) in DCM (100 mL) and the solution cooled to 0 °C. *p*-TsCl (14.3 g, 75.0 mmol) was added and the reaction mixture stirred at rt for 6 h. The reaction was quenched by addition of water (30 mL). The phases were separated and the organic phase

[8] White, J.D. *J. Org. Chem.* **1994**, *59*, 3347.

washed with 6 M HCl (100 mL) and water (100 mL), and then dried over anhydrous $NaSO_4$ and concentrated. Column chromatography on silica gel (9:1 hexane-EtOAc) gave the *O*-tosylate (**203**) (19.7 g, 98 %) as a colourless oil. R_f = 0.30 (9:1 hexanes-EtOAc).

δ_H: 7.78 (d, 2H, *J* 8.3, Ar-H); 7.33-7.21 (m, 7H, Ar-H); 4.39 (s, 2H, benzylic H); 4.05 (dd, 1H, *J* 5.7, 9.4, H-1a); 3.99 (dd, 1H, *J* 5.7, 9.4, H-1b); 3.35 (dd, 1H, *J* 5.4, 9.3, H-3a); 3.31 (dd, 1H, *J* 6.7, 9.3, H-3b); 2.39 (s, 3H, methyl); 2.14-2.02 (m, 1H, H-2); 0.94 (d, 3H, *J* 7.0, 2-methyl).

δ_C: 149.93, 144.51, 138.06, 129.63, 127.69, 127.31 (Ar-H); 72.83 (T, benzylic C); 72.08 (T, C-3); 72.06 (T, C-1); 33.47 (D, C-2); 21.89 (Q, methyl); 13.42 (Q, 2-methyl).

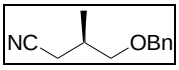

(*R*)-4-Benzyloxy-3-methylbutanenitrile (204)

NaCN (24.5 g, 500 mmol) was dissolved in DMF (500 mL) by heating to 70 °C. A solution of tosylate (**203**) (16.7 g, 50.0 mmol) in DMF (50 mL) was then added and the reaction mixture stirred at 90 °C for 24 h. The reaction mixture was cooled and diluted with saturated aqueous $NaHCO_3$ (200 mL) and brine (800 mL). The aqueous layer was extracted with Et_2O (3×250 mL). The combined Et_2O solutions were diluted with hexane (150 mL) and washed with brine (4×200 mL) to remove any DMF present. The Et_2O solution was dried over Na_2SO_4, filtered and concentrated. The product was purified by Kugelrohr distillation (150 °C, 0.1 mmHg) to give nitrile (**204**) (8.70 g, 92%), as a clear oil. R_f = 0.46 (4:1 hexanes-EtOAc); $[\alpha]_D^{20}$ +5.2 (*c* 1.05, $CHCl_3$) [lit.,[9] $[\alpha]_D^{23}$ +9.6 (*c* 2.09, $CHCl_3$)]; ν_{max} 2334 cm^{-1}.

δ_H: 7.37–7.26 (m, 5H, Ar-H); 4.51 (s, 2H, benzylic H); 3.45 (dd, 1H, *J* 4.9, 9.5, H-4a); 3.30 (dd, 1H, *J* 7.7, 9.5, H-4b); 2.48 (dd, 1H, *J* 5.4, 16.6, H-2a); 2.37 (dd, 1H, *J* 6.9, 16.6, H-2b); 2.20-2.10 (m, 1H, H-3); 1.07 (d, 3H, *J* 6.9, 3-methyl).

δ_C: 137.81; 128.19; 127.48; 127.35 (Ar-C); 118.44 (S, C-1); 73.04 (T, benzylic C); 72.94 (T, C-4); 30.84 (D, C-3); 21.09 (T, C-2); 15.96 (Q, 3-methyl).

HRMS (ESI): *m/z* 190.1220 $[M+H]^+$; Calculated for $C_{12}H_{16}NO$: 190.1232; *m/z* 212.1028 $[M+Na]^+$; Calculated for $C_{12}H_{15}NONa$: 212.1051.

[9] Ghosh, AK.; Wang, Y.; Kim, J.T. *J. Org. Chem.* **2001**, *66*, 8973.

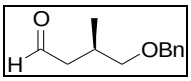

(*R*)-4-Benzyloxy-3-methylbutanal (205)

A stirred solution of nitrile (**204**) (2.55 g, 13.5 mmol) in DCM (100 mL) was cooled to 0 °C and DIBALH (4.50 mL, 25.3 mmol) was added dropwise and the mixture stirred for 2.5 h. The reaction was quenched by dropwise addition of MeOH (5 mL), followed by saturated sodium potassium tartrate solution (150 mL) and Et_2O (150 mL), and the mixture stirred for 1 h. The phases were separated, and the aqueous phase was extracted with Et_2O (3×50mL) and DCM (50mL). The combined organic phases were dried over anhydrous $MgSO_4$, and concentrated. Column chromatography on silica gel (1:1 hexanes-EtOAc) gave **205** as a colourless oil (1.79 g, 69%). R_f = 0.54 (1:1 hexanes: EtOAc).

δ_H: 9.69 (dd, 1H, *J* 2.0, 2.2, H-1); 7.30-7.18 (m, 5H, Ar-H); 4.42 (s, 2H, benzylic H); 3.35 (dd, 1H, *J* 5.2, 9.1, H-4a); 3.19 (dd, 1H, *J* 7.6, 9.1, H-4b); 2.48 (ddd, 1H, *J* 2.0, 6.9, 16.1, H-2a); 2.35 (ddddq, 1H, *J* 5.2, 6.3, 6.9, 7.6, 6.8, H-3); 2.21 (ddd, 1H, *J* 2.2, 6.3, 16.1, H-2b); 0.92 (d, 3H, *J* 6.8, 3-methyl).

δ_C: 202.35 (D, C-1); 138.19, 128.31, 127.53, 127.49 (Ar-C); 74.84 (T, C-4); 72.98 (T, benzylic C); 48.40 (T, C-2); 29.05 (D, C-3); 17.08 (Q, 3-methyl).

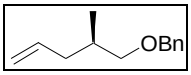

(4*R*)-5-Benzyloxy-4-methylpent-1-ene (206)

Methyltriphenylphosphonium iodide (6.97 g, 17.2 mmol) was suspended in THF (100 mL) and cooled to 0°C before 1.6M *n*-BuLi in hexanes (11.5 mL, 18.4 mmol) was added dropwise and the mixture stirred for 45 min and warmed to rt. Aldehyde (**205**) (1.33 g, 6.90 mmol) was dissolved in THF (50 mL), and added dropwise to the ylid solution. The reaction was stirred at rt for 20 h after which the reaction was quenched by dropwise addition of saturated NH_4Cl solution (30 mL). Volatiles were removed under reduced pressure and the slurry diluted with saturated NH_4Cl (100 mL) and EtOAc (100 mL). The phases were separated, and the aqueous phase filtered to remove the solid triphenylphosphine oxide, after which it was extracted with EtOAc (3×50 mL). The combined organic phases were dried over anhydrous $MgSO_4$, and concentrated. Column chromatography on silica gel (9:1 hexanes-Et_2O) after dry-loading the crude product gave **206** as a pale yellow oil (1.09 g, 83%). R_f = 0.64 (9:1 hexanes-Et_2O); $[\alpha]_D^{20}$ –2.1 (*c* 1.21, $CHCl_3$) [lit.,[10] $[\alpha]_D^{22}$ –1.6 (*c* 2.21, CH_2Cl_2]; ν_{max} 1683 cm^{-1}.

[10] Jones, T.K.; Reamer, R.A.; Desmond, R.; Mills, S.G. *J. Am. Chem. Soc.* **1990**, *112*, 2998.

δ_H: 7.37-7.24 (m, 5H, Ar-H); 5.78 (ddt, 1H, *J* 17.0, 10.2, 6.8, H-2); 5.04-4.97 (m, 2H, H-1); 4.50 (s, 2H, benzylic H); 3.33 (dd, 1H, *J* 6.2, 9.0, H-5a); 3.28 (dd, 1H, *J* 6.2, 9.0, H-5b); 2.26-2.18 (m, 1H, H-3a); 1.96-1.90 (m, 1H, H-3b); 1.88-1.80 (m, 1H, H-4); 0.94 (d, 3H, *J* 6.6, 4-methyl).

δ_C: 138.72, 128.29, 127.50, 127.41 (Ar-C); 136.92 (D, C-2); 115.90 (T, C-1); 75.27 (T, C-5); 72.96 (T, benzylic C); 38.01 (T, C-3); 33.42 (D, C-4); 16.73 (Q, 4-methyl).

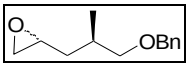

(2*RS*,4*R*)-5-Benzyloxy-1,2-epoxy-4-methylpentane (207)

The alkene (**206**) (1.09 g, 5.70 mmol) was dissolved in DCM (30 mL) and MCPBA (60%, 2.06 g, 7.17 mmol) was added and the mixture stirred for 48 h. The reaction was quenched by addition of saturated Na_2SO_3 solution (50 mL), and the mixture was stirred for 30 min. The phases were separated, and saturated $NaHCO_3$ solution (50 mL) was added to the organic phase, and the mixture was stirred for 90 min. The phases were separated, and the aqueous phases combined and extracted with EtOAc (3×50 mL). The combined organic phases were dried over anhydrous $MgSO_4$, and concentrated. Column chromatography on silica gel (9:1 hexanes-Et_2O) gave **207,** a pale yellow oil (0.59 g, 50%) as a 1:1 mixture of diastereomers. R_f = 0.15 (9:1 hexanes-Et_2O); ν_{max} 1357 cm^{-1}.

δ_H: 7.35-7.25 (m, 10H, Ar-H); 4.50 (s, 2H, benzylic H); 3.38 (dd, 1H, *J* 5.2, 7.3, H-5a); 3.36 (dd, 1H, *J* 4.0, 7.2, H-5a′); 3.33 (dd, 1H, *J* 5.3, 7.2, H-5b′); 3.32 (dd, 1H, *J* 5.2, 7.3, H-5b); 2.98-2.93 (m, 2H, H-2); 2.75 (dd, 1H, *J* 3.5, 4.0, H-1a); 2.72 (dd, 1H, *J* 4.0, 5.2, H-1a′); 2.44 (dd, 1H, *J* 2.2, 4.0, H-1b); 2.41 (dd, 1H, *J* 2.2 ,4.0, H-1b′); 2.07-1.97 (m, 2H, H-4); 1.72 (ddd, 1H, *J* 4.0, 4.9, 11.1, H-3a); 1.66 (ddd, 1H, *J* 5.0, 5.0, 11.4, H-3a′); 1.38 (ddd, 1H, *J* 4.3, 6.6, 11.1, H-3b); 1.36 (ddd. 1H, *J* 5.7, 5.7, 11.4, H-3b′); 1.03 (d, 3H, *J* 5.6, 4-methyl); 1.02 (d, 3H, *J* 5.5, 4′-methyl).

δ_C: 138.56, 138.54, 128.31, 127.51, 127.48, 127.46 (Ar-H); 75.47 and 75.30 (T, C-5); 73.04 and 72.98 (T, benzylic C); 51.16 and 50.84 (D, C-2); 47.40 and 46.92 (T, C-1); 36.82 and 36.73 (T, C-3); 32.12 and 31.90 (D, C-4); 17.48 and 17.10 (Q, 4-methyl).

HRMS (ESI): *m/z* 229.1221 $[M+Na]^+$; Calculated for $C_{13}H_{18}O_2Na$: 229.1205.

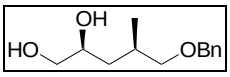

(2*S*,4*R*)-5-Benzyloxy-4-methylpentane-1,2-diol (208)

(*R*,*R*)-Co(II)-(salen) (99 mg, 0.16 mmol) was dissolved in DCM (8 mL) and *p*-TsOH (46 mg, 0.24 mmol) was added, and the resulting solution stirred open to the atmosphere for 2 h. The solution was concentrated, and diluted with THF (5 mL), before being concentrated again, to give the active catalyst.

The crude catalyst was dissolved in THF (5 mL) and epoxide (**207**) (257 mg, 1.25 mmol) was added before the reaction mixture was cooled to 0 °C and water (66 µL, 3.7 mmol) was added dropwise. The reaction was stirred for 24 h and during which it was allowed to warm to RT. The solvent was removed under reduced pressure to give the crude product, which was purified by column chromatography on silica gel (1:1 hexanes-Et_2O) giving **208** as an oil (29 mg, 21 %) as a 1:1 mixture of diastereomers. R_f = 0.15 (1:1 hexanes-Et_2O).

Only distinguishable peaks are given:

Major diastereomer:

δ_H: 0.91 (d, 3H, *J* 7.4, 4-methyl).

δ_C: 76.16 (T, C-5); 73.96 (T, C-1); 73.20 (T, benzylic C); 68.16 (D, C-2); 38.74 (T, C-3); 31.29 (D, C-4); 17.74 (Q, 4-methyl).

Minor diastereomer:

δ_H: 0.89 (d, 3H, *J* 7.1, 4-methyl).

δ_C: 75.59 (T, C-5); 73.54 (T, C-1); 73.27 (T, benzylic C); 67.02 (D, C-2); 37.98 (T, C-3); 29.81 (D, C-4); 17.76 (Q, 4-methyl).

4.3.4. Sharpless Asymmetric Dihydroxylation Route

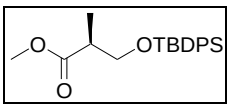

Methyl (*S*)-3-(*tert*-butyldiphenylsilanyloxy)-2-methylpropionate (222)

Imidazole (1.23 g, 18.0 mmol) was added to a stirred solution of methyl (*S*)-3-hydroxy-2-methylpropionate (**138**) (1.71 g, 14.8 mmol) in DCM (150 mL). When the imidazole was completely dissolved, TBDPSCl (3.85 mL, 14.8 mmol) was added and the mixture stirred for 18 h at rt. The reaction was quenched by addition of saturated NH_4Cl solution (100 mL) and

stirred for 20 min. The phases were separated and the aqueous phase was extracted with Et_2O (3×100 mL). The combined organic phases were dried over anhydrous $MgSO_4$ and concentrated. Column chromatography on silica gel (9:1 hexanes-Et_2O) gave **222** as a colourless oil (5.10 g, 99%). R_f = 0.60 (9:1 hexanes-Et_2O); $[\alpha]_D^{20}$ +13.0 (*c* 0.36, $CHCl_3$) [lit.,[11] $[\alpha]_D^{20}$ +23 (*c* 7.0, MeOH)]; ν_{max} 1818, 1112 cm^{-1}.

δ_H: 7.66-7.36 (m, 10H, Ar-H); 3.83 (dd, 1H, *J* 7.0, 9.8, H-3a); 3.72 (dd, 1H, *J* 5.8, 9.8, H-3b); 3.68 (s, 3H, ester methyl); 2.72 (ddq,1H, *J* 5.8, 7.0, 7.0, H-2); 1.15 (d, 3H, *J* 7.0, 2-methyl); 1.03 (s, 9H, $SiC(C\underline{H}_3)_3$).

δ_C: 175.41 (S, C-1); 135.60, 133.56, 133.50, 129.69, 127.69 (Ar- C); 65.94 (T, C-3); 51.57 (Q, ester methyl); 42.42 (D, C-2); 26.74 (Q, $SiC(\underline{C}H_3)_3$); 19.26 (S, $Si\underline{C}(CH_3)_3$); 13.50 (Q, 2-methyl).

HRMS (ESI): *m/z* 379.17040 $[M+Na]^+$; Calculated for $C_{21}H_{28}O_2SiNa$: 379.1705; *m/z* 279.1419 $[M-C_6H_5]^+$; Calculated for $C_{15}H_{23}O_3Si$, 279.1416.

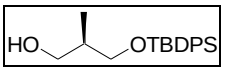

(2*R*)-3-(*tert*-Butyldiphenylsilanyloxy)-2-methylpropan-1-ol (223)

A stirred solution of ester (**222**) (5.10 g, 14.3 mmol) in DCM (350 mL) was cooled to −78 °C and DIBALH (6.50 mL, 36.4 mmol) was added. The mixture was stirred for 2.5 h while warming to rt. The reaction was quenched by dropwise addition of MeOH (5 mL), followed by saturated NH_4Cl solution (100 mL), and stirred for 20 min. Hexane (100 mL) and Et_2O (100 mL) were added and the phases were separated (after warming gently), and the aqueous phase was extracted with Et_2O (4×100 mL). The combined organic phases were dried over anhydrous $MgSO_4$, and concentrated. Column chromatography on silica gel (1:1 hexanes-Et_2O) gave **223** as a colourless oil (3.65 g, 77%). R_f = 0.36 (1:1 hexanes-Et_2O); $[\alpha]_D^{20}$ +3.6 (*c* 0.69, $CHCl_3$) [lit.,[11] $[\alpha]_D^{20}$ +6.3 (*c* 1.0, $CHCl_3$)]; ν_{max} 1112, 739 cm^{-1}.

δ_H: 7.68-7.64; 7.45-7.34 (m, 10H, Ar-H); 3.72 (dd, 1H, *J* 4.5, 10.1, H-3a); 3.65 (d, 2H, *J* 6.5 H-1); 3.59 (dd, 1H, *J* 7.7, 10.1, H-3b); 2.04-1.94 (m, 1H, H-2); 1.05 (s, 9H, $SiC(C\underline{H}_3)_3$); 0.82 (d, 3H, *J* 6.9, 2-methyl).

[11] Ley, S.V.; Anthony, N.J.; Armstrong, A.; Brasca, M.G.; Clarke, T.; Culshaw, D.; Greck, G.; Grice, P.; Jones, A.B.; Lygo, B.; Madin, A.; Sheppard, R.N.; Slawin, A.M.Z.; Williams, D.J. *Tetrahedron* **1989**, *45*, 7161.

δ_C: 135.57, 135.55, 133.14, 133.12, 129.77, 127.74 (Ar-C); 68.70 (T, C-3); 67.64 (T, C-1); 37.27 (D, C-2); 26.81 (Q, SiC($\underline{C}H_3)_3$); 19.12 (S, Si$\underline{C}(CH_3)_3$); 13.13 (Q, 2-methyl).

HRMS (ESI): *m/z* 351.1748 $[M+Na]^+$; Calculated for $C_{20}H_{28}O_2SiNa$, 351.1756.

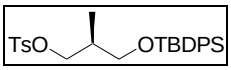

(*S*)-3-(*tert*-Butyldiphenylsilanyloxy)-2-methylpropan-1-ol tosylate (224)

Alcohol (**223**) (3.65 g, 11.1 mmol) was dissolved in DCM (350 mL), and DMAP (1.89 g, 15.5 mmol) was added. The solution was cooled to 0 °C and *p*-TsCl (2.37 g, 12.2 mmol) was added. The mixture stirred for 18 h while warming to rt. The reaction was quenched by addition of water (100 mL) and stirred for 30 min. The phases were separated and the aqueous phase was extracted with Et_2O (3×100 mL). The combined organic phases were dried over anhydrous $MgSO_4$ and concentrated. Dry loaded column chromatography on silica gel (1:1 hexanes-Et_2O) gave **224** as a colourless oil (4.87 g, 91%). R_f = 0.48 (1:1 hexanes-Et_2O); ν_{max} 1358, 1175 cm^{-1}.

δ_H: 7.77 (d, 2H, *J* 8.3), 7.59-7.55, 7.44-7.27 (Ar-H); 4.12 (dd, 1H, *J* 5.8, 9.3, H-3a); 3.99 (dd, 1H, *J* 6.1, 9.3, H-3b); 3.54 (dd, 1H, *J* 4.8, 10.2, H-1a); 3.99 (dd, 1H, *J* 6.6, 10.2, H-1b); 2.41 (s, 3H, methyl); 2.05-1.93 (m,1H, H-2); 0.97 (s, 9H, SiC($C\underline{H}_3)_3$); 0.88 (d, 3H, *J* 6.9, 2-methyl).

δ_C: 144.56, 135.49, 135.48, 133.33, 133.30, 133.03, 129.77, 129.67, 127.90, 127.66 (Ar-H); 72.08 (T, C-3); 67.47 (T, C-1); 35.61 (D, C-2); 26.72 (Q, SiC($\underline{C}H_3)_3$); 21.59 (Q, methyl); 19.17 (S, Si$\underline{C}(CH_3)_3$); 13.26 (Q, 2- methyl).

HRMS (ESI): *m/z* 483.2029 $[M+H]^+$; Calculated for $C_{27}H_{35}O_4SSi$: 483.2025; *m/z* 505.1845 $[M+Na]^+$; Calculated for $C_{27}H_{34}O_4SSiNa$, 505.1845.

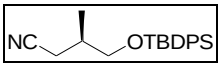

(3*R*)-4-(*tert*-Butyldiphenylsilanyloxy)-3-methylbutanenitrile (225)

p-Tosylate (**224**) (4.87 g, 10.1 mmol) was dissolved in DMSO (40 mL), and NaCN (1.49 g, 30.3 mmol) dissolved in DMSO (40 mL) was added in one portion. The mixture was heated to 90 °C for 18 h, after which the reaction mixture was cooled, diluted with water (50 mL) and Et_2O (100 mL). The phases were separated, and the aqueous phase was extracted with Et_2O (3×100 mL). The combined organic phases were washed with brine (150 mL) dried over anhydrous $MgSO_4$, and concentrated. Column chromatography on silica gel (1:1 hexanes-

Et_2O) gave **225** as a colourless oil (3.21 g, 94%). R_f = 0.50 (1:1 hexanes-Et_2O); $[\alpha]_D^{20}$ +9.9 (*c* 0.27, $CHCl_3$) [lit.,[12] $[\alpha]_D^{20}$ +14 (*c* 3, $CHCl_3$)].

δ_H: 7.66-7.62, 7.46-7.36 (m, 10H, Ar-H); 3.63 (dd, 1H, *J* 4.7, 10.3, H-4a); 3.46 (dd, 1H, *J* 7.4, 10.3, H-4b); 2.55 (dd, 1H, *J* 5.3, 16.6, H-2a); 2.37 (dd, 1H, *J* 7.4, 16.6, H-2b); 2.12–2.01 (m, 1H, H-3); 1.06 (s, 9H, $SiC(C\underline{H}_3)_3$); 1.03 (d, 3H, *J* 6.4, 3-methyl).

δ_C: 135.52, 135.49, 133.18, 133.12, 129.81, 127.76 (Ar-C); 118.84 (S, C-1); 66.82 (T, C-4); 33.27 (D, C-3); 26.81 (Q, $SiC(\underline{C}H_3)_3$); 21.06 (D, C-2); 19.25 (S, $Si\underline{C}(CH_3)_3$); 15.87 (Q, 3-methyl).

HRMS (ESI): *m/z* 338.1933 $[M+H]^+$; Calculated for $C_{21}H_{28}NOSi$, 338.1940; *m/z* 360.1754 $[M+Na]^+$; Calculated for $C_{21}H_{27}NOSiNa$: 360.1760.

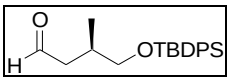

(3*R*)-4-(*tert*-Butyldiphenylsilanyloxy)-3-methylbutanal (226)

A stirred solution of nitrile (**225**) (3.21 g, 9.52 mmol) in DCM (350 mL) was cooled to 0 °C and DIBALH (2.2 mL, 12 mmol) was added dropwise and the mixture stirred for 2.5 h. The reaction was quenched by dropwise addition of MeOH (5 mL), followed by water (150 mL) the mixture stirred for 30 min. The phases were separated, and the aqueous phase was extracted with Et_2O (3×100 mL). The combined organic phases were dried over anhydrous $MgSO_4$, and concentrated. Column chromatography on silica gel (1:1 hexanes-Et_2O) gave **226** as a pale yellow oil (2.1 g, 66%). R_f = 0.62 (1:1 hexanes-Et_2O).

δ_H: 9.78 (t, 1H, *J* 2.1, H-1); 7.66-7.61, 7.45-7.34 (m, 10H, Ar-H); 3.58 (dd, 1H, *J* 5.0, 10.0, H-4a); 3.43 (dd, 1H, *J* 7.0, 10.0, H-4b); 2.60 (ddd, 1H, *J* 2.1, 5.6, 15.7, H-2a); 2.39-2.28 (m, 1H, H-3); 2.26 (ddd, 1H, *J* 2.1, 7.3, 15.7, H-2b); 1.05 (s, 9H, $SiC(C\underline{H}_3)_3$); 0.93 (d, 3H, *J* 6.7, 3-methyl).

δ_C: 202.63 (D, C-1); 135.56, 135.44, 133.45, 133.43, 129.66, 127.67 (Ar-C); 66.34 (T, C-4), 43.11 (D, C-3), 31.24 (T, C-2); 26.54 (Q, $SiC(\underline{C}H_3)_3$); 19.21 (S, $Si\underline{C}(CH_3)_3$); 16.74 (Q, 3-methyl).

[12] Keyling-Bilger, F.; Schmitt, G.; Beck, A.; Luu, B. *Tetrahedron* **1996**, *52*, 14891.

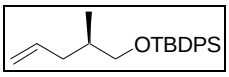

(4*R*)-5-(*tert*-Butyldiphenylsilanyloxy)-4-methylpent-1-ene (227)

Methyltriphenylphosphonium iodide (6.48 g, 15.7 mmol) was suspended in THF (200 mL) and cooled to 0 °C before 1.6M *n*-BuLi in hexanes (10.6 mL, 17.0 mmol) was added dropwise and the mixture stirred for 45 min and warmed to rt. Aldehyde (**226**) (2.14 g, 6.28 mmol) was dissolved in THF (30 mL), and added dropwise over 30 min to the ylid solution. The reaction was stirred at rt for 20 h after which the reaction was quenched by dropwise addition of saturated NH_4Cl solution (20 mL). Volatiles were removed under reduced pressure and the slurry diluted with saturated NH_4Cl (100 mL) and Et_2O (200 mL). The phases were separated, and the aqueous phase filtered to remove the solid triphenylphosphine oxide, and extracted with Et_2O (3×100 mL). The combined organic phases were dried over anhydrous $MgSO_4$, and concentrated. Column chromatography on silica gel (9:1 hexanes-Et_2O) after dry-loading the crude product gave **227** as an oil (1.37 g, 67%). R_f = 0.65 (9:1 hexanes-Et_2O); $[\alpha]_D^{20}$ +2.6 (*c* 1.03, $CHCl_3$) [lit.,[13] $[\alpha]_D^{20}$ +3.1 (*c* 1.14, $CHCl_3$)]; ν_{max} 1639, 1426, 1104 cm^{-1}.

δ_H: 7.68-7.67, 7.44-7.35 (m, 10H, Ar-H), 5.75 (dddd, 1H, *J* 6.9, 7.6, 10.1, 17.0, H-2); 4.99 (ddd, 1H, *J* 1.4, 2.3, 10.1, H-1a); 4.96 (ddd, 1H, *J* 1.4, 2.3, 17.0, H-1b), 3.51 (dd, 1H, *J* 6.1, 9.8, H-5a); 3.41 (dd, 1H, *J* 6.0, 9.8, H-5b); 2.25 (ddddd, 1H, *J* 1.4, 1.4, 5.5, 6.9, 13.8, H-3a); 1.90 (ddddd, 1H, *J* 1.4, 1.4, 7.6, 7.6, 13.8, H-3b); 1.75 (ddddq, 1H, J 6.0, 6.1. 6.9, 7.6, 6.7, H-4); 1.05 (s, 9H, $SiC(C\underline{H}_3)_3$); 0.91 (d, 3H, *J* 6.7, 4-methyl).

δ_C: 137.27 (D, C-2); 135.61, 134.03, 134.01, 129.49, 127.76 (Ar-C), 115.70 (T, C-1); 68.34 (T, C-5); 37.26 (T, C-3); 35.71 (D, C-4); 26.86 (Q, $SiC(\underline{C}H_3)_3$); 19.32 (S, $Si\underline{C}(CH_3)_3$); 16.41 (Q, 4-methyl).

HRMS (ESI): *m/z* 339.38 $[M+H]^+$; Calculated for $C_{22}H_{31}OSi$, 339.2144.

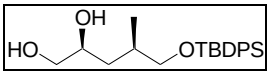

(2*S*,4*R*)-5-(*tert*-Butyldiphenylsilanyloxy)-4-methylpentane-1,2-diol (228)

Potassium ferricyanide (858 mg, 2.61 mmol), K_2CO_3 (341 mg, 2.47 mmol), methanesulfonamide (83 mg, 0.87 mmol), and $(DHQ)_2PYR$ (24 mg, 27 μmol) were dissolved in 1:1 *t*-BuOH-water (8 mL) and stirred for 30 min. Potassium osmate (3.11 mg, 9.34 μmol) was

[13] Gille, A.; Hiersemann, M. *Org. Lett.* **2010**, *12*, 5258.

added and the solution cooled to −10 °C and **227** (302 mg, 0.890 mmol) was added. The solution was stirred at this temperature for 18 h before being quenched by addition of sodium sulfite (1 g) and the slurry allowed to warm to rt and stirred for 30 min. The mixture was diluted with DCM (30 mL) and the solution washed with KOH solution (2M, 2×50 mL) and H_2SO_4 solution (1M, 2×50 mL) and brine (50 mL). The organic phase was dried over anhydrous $MgSO_4$ and concentrated. Column chromatography on silica gel (1:1 hexanes-Et_2O) gave **228** as a yellow oil, which was found to be an inseparable 4:1 mixture of the two diastereomers (by ^{13}C-NMR spectroscopy) (300 mg, 92 %). R_f = 0.12 (1:1 hexanes-Et_2O).

Only distinguishable peaks are given:

Major diastereomer:

δ_H: 0.91 (d, 3H, *J* 6.7, 4-methyl)

δ_C: 69.84 (D, C-2); 68.82 (T, C-5); 66.99 (T, C-1); 37.61 (D, C-4); 26.82 (Q, SiC($\underline{C}H_3)_3$); 17.56 (Q, 4-methyl).

Minor diastereomer:

δ_H: 0.85 (d, 3H, *J* 6.9, 4-methyl).

δ_C: 70.70 (D, C-2); 69.92 (T, C-5); 67.32 (T, C-1); 38.60 (D, C-4); 26.79 (Q, SiC($\underline{C}H_3)_3$); 17.52 (Q, 4-methyl).

4.3.5. Evans Auxiliary Route

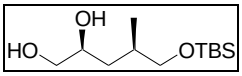

(2*S*,4*R*)-5-(*tert*-Butyldimethylsilanyloxy)-4-methylpentane-1,2-diol (154)

A solution of the (2*R*,3*R*,4*S*)-epoxy alcohol (**153**) (323 mg, 1.31 mmol) was prepared in DCM (50 mL) and cooled to 0 °C. DIBALH (0.70 mL, 3.9 mmol) was added dropwise, and the mixture stirred for 30 min. The reaction was quenched by the dropwise addition of MeOH (10 mL), before adding saturated NH_4Cl (50 mL) and 3M HCl dropwise until the precipitate dissolved. The phases were separated, and the aqueous phase was extracted Et_2O (3×50 mL). The combined organic phases were dried over anhydrous $MgSO_4$, and concentrated. Column chromatography on silica gel (1:1 hexanes-Et_2O) gave **154** as a colourless oil, which was found to be an inseparable mixture of the 1,2-diol and 1,3-diol (8:1 mixture by ^{13}C-NMR spectroscopy) (210 mg, 66%). R_f = 0.09 (1:1 hexanes: Et_2O).

NMR spectral data for the major regioisomer.

δ_H: 3.81 (m, 1H, H-2); 3.55 (dd, 1H, *J* 3.3, 11.1, H-1a); 3.53 (dd, 1H, *J* 4.2, 10.0, H-5a); 3.44 (dd, 1H, *J* 4.2, 10.0, H-5b); 3.41 (dd, 1H, *J* 3.4, 11.1, H-1b); 2.90 (br s, 2H, 1-OH, 2-OH); 1.47-1.39 (m, 2H, H-3); 0.89 (d, 3H, *J* 7.0, 4-methyl); 0.87 (s, 9H, SiC($C\underline{H}_3$)$_3$); 0.04 (s, 6H, Si($C\underline{H}_3$)$_2$).

δ_C: 69.36 (D, C-2); 68.42 (T, C-5); 66.93 (T, C-1); 38.12 (T, C-3); 32.16 (D, C-4); 25.84 (Q, SiC($\underline{C}H_3$)$_3$); 18.25 (S, Si$\underline{C}$(CH_3)$_3$); 17.24 (Q, 4-methyl); –5.55, –5.56 (Q, Si($\underline{C}H_3$)$_2$).

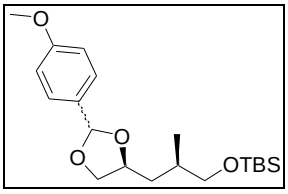

(2*S*,4*R*)-5-(*tert*-Butyldimethylsilanyloxy)-1,2-*O*-*p*-methoxybenzylidine-4-methylpentane-1,2-diol (155)

A solution of **154** (215 mg, 0.865 mmol) in DCM (20 mL) was cooled to 0 °C and anisaldehyde dimethylacetal (791 mg, 4.34 mmol) and pyridinium *p*-toluenesulfonate (21.8 mg, 0.087 mmol) were added. The mixture was stirred for 18 h while warming to rt. The reaction was quenched by addition of saturated $NaHCO_3$ solution (20 mL). The phases were separated, and the aqueous phase was extracted with DCM (3×50 mL). The combined organic phases were dried over anhydrous $MgSO_4$ and concentrated. Flash column chromatography on silica gel (19:1 hexanes-EtOAc) gave **155** as a colourless oil (104 mg, 33%), as an inseparable mixture of the dioxolane and dioxane derivatives (8:1 ratio). R_f = 0.52 (1:1 hexanes-EtOAc); ν_{max} 2854, 1246, 1085 cm^{-1}.

δ_H: 5.86 (s, 1H, dioxolane acetal, H_{ax}); 5.74 (s, 1H, dioxolane acetal, H_{eq}); 5.43 (s, 1H, dioxane acetal, H_{eq}).

δ_C: 103.83 (D, dioxolane acetal CH_{eq}); 102.84 (D, dioxolane acetal CH_{ax}); 100.99 (D, dioxane acetal CH_{eq}).

HRMS (ESI): *m/z* 389.2115 $[M+Na]^+$; Calculated for $C_{20}H_{34}O_4SiNa$: 389.2124.

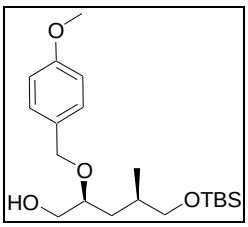

(2*S*,4*R*)-5-(*tert*-Butyldimethylsilanyloxy)-2-(4-methoxybenzyloxy)-4-methylpentan-1-ol (156)

A solution of the acetal (**155**) (531 mg, 1.39 mmol) in DCM (100 mL) was cooled to −78 °C, and DIBALH (0.75 mL, 4.2 mmol) was added dropwise. The solution was stirred for 2 h, at which point the reaction was quenched by addition of MeOH (10 mL), saturated sodium potassium tartrate solution (50 mL), water (50 mL) and HCl (3M, 20 mL). The phases were separated, and the aqueous phase was extracted with Et_2O (3×50 mL). The combined organic phases were dried over anhydrous $MgSO_4$, and concentrated. Flash column chromatography on silica gel (1:1 hexanes-Et_2O) gave **156** as a colourless oil (280 mg, 53%). R_f = 0.31 (1:1 hexanes-Et_2O); $[\alpha]_D^{20}$ +2.9 (*c* 0.93, $CHCl_3$); ν_{max} 2356, 1183 cm^{-1}.

δ_H: 7.25 (d, 2H, *J* 8.8, Ar-H); 6.86 (d, 2H, *J* 8.8, Ar-H); 4.53 and 4.45 (AB system, 2H, *J* 11.2, benzylic H); 3.78 (s, 3H, Ar-OMe); 3.68 (dd, 1H, *J* 5.2, 11.4, H-1a); 3.60-3.52 (m, 1H, H-2); 3.47 (dd, 1H, *J* 6.1, 11.4, H-1b); 3.39 (dd, 1H, *J* 5.8, 12.5, H-5a); 3.37 (dd, 1H, *J* 5.8, 12.5, H-5b); 1.90 (br s, 1H, 1-OH); 1.70-1.60 (m, 1H, H-4); 1.55 (ddd, 1H, *J* 5.6, 7.1, 13.9, H-3a); 1.41 (ddd, 1H, *J* 5.9, 7.9, 13.9, H-3b); 0.89 (d, 3H, *J* 6.7, 4-methyl); 0.87 (s, 9H, $SiC(C\underline{H}_3)_3$); 0.01 (s, 6H, $Si(C\underline{H}_3)_2$).

δ_C: 159.25, 130.50, 129.41, 113.87 (Ar-C); 77.82 (D, C-2); 70.88 (T, benzylic C); 68.09 (T, C-5); 64.39 (T, C-1); 55.24 (Q, Ar-OMe); 34.43 (T, C-3); 32.43 (D, C-4); 25.89 (Q, $SiC(\underline{C}H_3)_3$); 18.29 (S, $Si\underline{C}(CH_3)_3$); 17.33 (Q, 4-methyl); −5.43 (Q, $Si(\underline{C}H_3)_2$).

HRMS (ESI): *m/z* 391.2272 $[M+Na]^+$; Calculated for $C_{20}H_{36}O_4SiNa$: 391.2281.

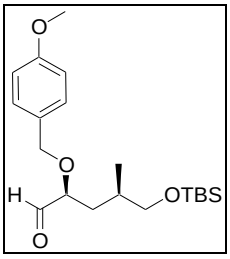

(2*S*,4*R*)-5-(*tert*-Butyldimethylsilanyloxy)-2-(4-methoxybenzyloxy)-4-methylpentanal (157)

DMSO (250 µL, 3.52 mmol) was added dropwise to a solution of $(COCl)_2$ (153 µL, 1.76 mmol) in DCM (20 mL) at −78 °C. The solution was stirred for 30 min, at which point **156** (100 mg, 0.271 mmol) dissolved in DCM (2 mL) was added dropwise over 10 min. The solution was stirred for 1 h, and Et_3N (0.82 mL, 5.9 mmol) was added slowly, and the reaction mixture allowed to warm slowly to rt over 1 h. Distilled water (20 mL) was added and the

phases were separated. The aqueous phase was extracted with Et_2O (3×15 mL) and the combined organic phases were dried over anhydrous $MgSO_4$ and concentrated giving an oil containing small needle-like crystals. The oil was dissolved in hexane, and filtered, before being concentrated to give the crude product as a yellow oil. The crude product was used directly in the next step. R_f = 0.67 (1:1 hexanes-EtOAc).

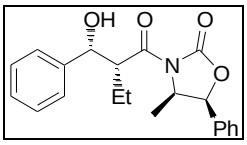

(2′*R*,3′*R*,4*R*,5*S*)-3-(2′-Ethyl-3′-hydroxy-3′-phenylpropanoyl)-4-methyl-5-phenyl-oxazolidin-2-one (258)

A stirred solution of butanoyl-oxazolidinone (**145**) (1.05 g, 4.24 mmol) in DCM (10 mL) was cooled to 0 °C and 1.0M dibutylboron triflate (5.0 mL, 5.0 mmol) was added slowly, followed by the dropwise addition of Et_3N (0.79 mL, 5.7 mmol) and the solution stirred for 15 min before being cooled to −78 °C. Freshly distilled benzaldehyde (0.500 g, 4.71 mmol) was added dropwise, and the solution stirred for 30 min, before being warmed to 0 °C and stirred for 1 h. The reaction was quenched by addition of a 3:1 MeOH-pH 7 phosphate buffer solution (5 mL) followed by dropwise addition of a 2:1 MeOH-30 % aqueous H_2O_2 solution (10 mL), and stirred for 1 h. Volatiles were removed under reduced pressure and the slurry diluted with EtOAc (50 mL). The mixture was washed with 5 % $NaHCO_3$ solution (3×50 mL) followed by saturated brine solution (50 mL). The organic phase was dried over anhydrous $MgSO_4$, and concentrated. Recrystallization from Et_2O gave **258** as white needle-shaped crystals (560 mg, 38%), mp. 130–135 °C. R_f = 0.29 (1:1 hexanes: EtOAc); $[\alpha]_D^{20}$ –2.4 (*c* 0.95, $CHCl_3$); ν_{max} 1778, 1687, 1223, 1190 cm^{-1};

δ_H: 7.41-7.15 (m, 10H, Ar-H); 5.14 (d, 1H, *J* 7.2, H-5); 4.89 (d, 1H, *J* 6.3, H-3′); 4.47 (dq, 1H, *J* 6.7, 6.7, H-4); 4.30 (ddd, 1H, *J* 4.0, 6.3, 10.2, H-2′); 2.83 (br s, 1H, OH); 1.96-1.75 (m, 2H, C-2′ ethyl CH_2); 0.88 (dd, 3H, *J* 7.4, 7.4, C-2′ ethyl CH_3); 0.82 (d, 3H, *J* 6.6, 4-methyl).

δ_C: 175.02 (S, C-1′); 152.62 (S, C-2); 141.76, 132.94, 128.69, 128.62, 128.23, 127.73, 126.31, 125.46 (Ar-C); 78.64 (D, C-5); 75.00 (D, C-3′); 54.98 (D, C-2′); 51.56 (D, C-4); 20.95 (T, C-2′ ethyl CH_2); 14.41 (Q, 4-methyl); 11.51 (Q, C-2′ ethyl CH_3).

HRMS (ESI): *m/z* 354.1690 $[M+H]^+$; Calculated for $C_{21}H_{24}NO_4$: 354.1705; *m/z* 376.1512 $[M+Na]^+$; Calculated for $C_{21}H_{23}NO_4Na$: 376.1525; *m/z* 366.1591 $[(M+H)–H_2O]^+$; Calculated for $C_{21}H_{22}NO_3$: 366.1600.

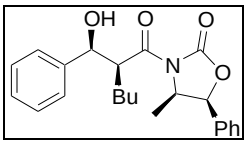

(2′*S*,3′*S*,4*R*,5*S*)-3-(2′-Butyl-3′-hydroxy-3′-phenylpropanoyl)-4-methyl-5-phenyl-oxazolidin-2-one (257)

A stirred solution of hexanoyl-oxazolidinone (**123**) (1.17 g, 4.24 mmol) in DCM (50 mL) was cooled to 0 °C and 1.0M dibutylboron triflate (5.0 mL, 5.0 mmol) was added slowly, followed by the dropwise addition of Et_3N (0.79 mL, 5.7 mmol) and the solution stirred for 10 min before being cooled to –78 °C. Freshly distilled benzaldehyde (0.500 g, 4.71 mmol) was added dropwise, and the solution stirred for 20 min before being warmed to 0 °C and stirred for 1 h. The reaction was quenched by addition of a 3:1 MeOH-pH 7 phosphate buffer solution (50 mL) followed by dropwise addition of a 2:1 MeOH-30 % aqueous H_2O_2 solution (50 mL), and stirred for 1 h. Volatiles were removed under reduced pressure and the slurry diluted with EtOAc (50 mL). The mixture was washed with 5 % $NaHCO_3$ solution (100 mL) followed by saturated brine solution (100 mL). The organic phase was dried over anhydrous $MgSO_4$, and concentrated. Column chromatography on silica gel (1:1 hexanes-EtOAc) gave **257** as a colourless oil (640 mg, 39%) which was recrystallized from 2:1 hexanes-EtOAc giving large, block-shaped crystals, mp. 121-125 °C. R_f = 0.26 (1:1 hexanes-EtOAc); $[\alpha]_D^{20}$ +23.5 (*c* 1.21, $CHCl_3$); ν_{max} 1777, 1689, 1193, 699 cm^{-1}.

δ_H: 7.43–7.19 (m, 10H, Ar-H); 5.59 (d, 1H, *J* 7.3, H-5); 4.96 (d, 1H, *J* 5.7, H-3′); 4.71 (dq, 1H, *J* 6.6, 7.2, H-4); 4.40 (ddd, 1H, *J* 3.7, 5.7, 10.4, H-2′); 2.64 (br s, 1H, OH); 1.89-1.78 (m, 1H, C-2′ butyl CH_2); 1.72-1.62 (m, 1H, C-2′ butyl CH_2); 1.32-1.15 (m, 4H, C-2′ butyl CH_2); 0.83 (dd, 3H, *J* 7.0, 7.0, C-2′ butyl CH_3); 0.56 (d, 3H, *J* 6.6, 4-methyl).

δ_C: 175.05 (S, C-1′); 152.82 (S, C-2); 141.31, 133.09, 128.77, 128.67, 128.21, 127.72, 126.60, 125.59 (Ar-C); 78.70 (D, C-5); 74.96 (D, C-3′); 54.71 (D, C-2′); 49.80 (D, C-4); 29.59 (T, C-2 butyl CH_2); 27.35 (T, C-2 butyl CH_2); 22.79 (T, C-2′ butyl CH_2); 14.03 (Q, 4-methyl); 13.87 (Q, C-2′ butyl CH_3).

HRMS (ESI): *m/z* 382.2013 $[M+H]^+$; Calculated for $C_{23}H_{28}NO_4$: 382.2018; *m/z* 404.1830 $[M+Na]^+$; Calculated for $C_{23}H_{27}NO_4Na$: 404.1838; *m/z* 364.1906 $[(M+H)-H_2O]^+$; Calculated for $C_{23}H_{26}NO_3$, 364.1913.

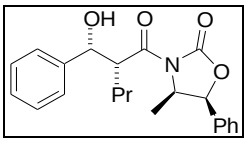

(2′*R*,3′*R*,4*R*,5*S*)-3-(3′-Hydroxy-3′-phenyl-2′-propylpropanoyl)-4-methyl-5-phenyl-oxazolidin-2-one (260)

A stirred solution of pentanoyl-oxazolidinone (**259**) (554 mg, 2.12 mmol) in DCM (20 mL) was cooled to 0 °C and 1.0M dibutylboron triflate (2.50 mL, 2.50 mmol) was added slowly, followed by the dropwise addition of Et_3N (0.39 mL, 2.8 mmol) and the solution stirred for 45 min before being cooled to −78 °C. Freshly distilled benzaldehyde (250 mg, 2.36 mmol) in DCM (10 mL) was added dropwise, and the solution stirred for 20 min before being warmed to 0 °C and stirred for 90 min. The reaction was quenched by addition of a 3:1 MeOH-pH 7 phosphate buffer solution (10 mL) followed by dropwise addition of a 2:1 MeOH-30 % aqueous H_2O_2 solution (10 mL), and stirred for 1 h. Volatiles were removed under reduced pressure and the slurry diluted with EtOAc (50 mL). The phases were separated and the aqueous phase extracted with EtOAc (3×50 mL). The organic phases were combined and dried over $MgSO_4$ and concentrated. Column chromatography on silica gel (1:1 hexanes: Et_2O) gave **260** as a foamy white solid (260 mg, 34%). R_f = 0.27 (1:1 hexanes: Et_2O); $[\alpha]_D^{20}$ – 3.5 (*c* 1.02, $CHCl_3$); ν_{max} 1775, 1686, 1194, 739 cm^{-1}.

δ_H: 7.41-7.18 (m, 10H, Ar-H); 5.12 (d, 1H, *J* 7.2, H-5); 4.88 (d, 1H, *J* 6.2, H-3′); 4.46 (dq, 1H, *J* 6.6, 6.6, H-4); 4.37 (ddd, 1H, *J* 3.7, 6.2, 10.2, H-2′); 2.63 (br s, 1H, OH); 1.93-1.80 (m, 1H, C-2′ propyl CH_2); 1.76-1.66 (m, 1H, C-2′ propyl CH_2); 1.31-1.22 (m, 2H, C-2′ propyl CH_2); 0.86 (t, 3H, *J* 7.2, C-2′ propyl CH_3); 0.81 (d, 3H, *J* 6.6, 4-methyl).

δ_C: 175.15 (S, C-1′); 152.62 (S, C-2); 141.70, 133.02, 128.74, 128.67, 128.28, 127.82, 126.34, 125.51 (Ar-C); 78.69 (D, C-5); 75.33 (D, C-3′); 55.05 (D, C-2′); 50.22 (D, C-4); 29.96 (T, C-2′ propyl CH_2); 20.95 (T, C-2′ propyl CH_2); 14.41 (Q, 4-methyl); 14.19 (Q, C-2′ propyl CH_3).

HRMS (ESI): *m/z* 368.1856 $[M+H]^+$; Calculated for $C_{22}H_{26}NO_4$: 368.1862; *m/z* 390.1674 $[M+Na]^+$; Calculated for $C_{22}H_{25}NO_4Na$: 390.1681; *m/z* 350.1747 $[(M+H)-H_2O]^+$; Calculated for $C_{22}H_{24}NO_3$: 350.1756.

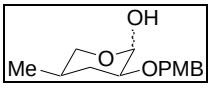

(3*S*,5*R*)-3-(4-Methoxybenzyloxy)-5-methyl-tetrahydropyran-2-ol (265)

3-Butanoyloxazolidinone (**145**) (69 mg, 0.28 mmol) was dissolved in DCM (3 mL) at 0 °C, and Et_3N (47 μL, 0.34 mmol) and Bu_2BOTf (1M, 30 μL, 0.30 mmol) were added and the solution stirred for 1 h. The solution was cooled to −78 °C and aldehyde (**157**) (100 mg, 0.28 mmol) in DCM (1 mL) was added dropwise, and the mixture stirred for 1 h, before being warmed to 0 °C and stirred for 1 h. The reaction was quenched by addition of 2:1 pH 7 phosphate buffer-MeOH (2 mL), followed by 2:1 MeOH-30 % H_2O_2 (2 mL), and the mixture stirred for 1 h at 0 °C. Volatiles were removed under reduced pressure and the residue diluted with water (10 mL) and EtOAc (50 mL) and the phases separated. The phases were separated, and the aqueous phase was extracted with EtOAc (2×50 mL). The combined organic phases were dried over anhydrous $MgSO_4$, and concentrated. Flash column chromatography on silica gel (1:1 hexanes-Et_2O) gave **265** as a colourless oil (30 mg, 43%). R_f = 0.35 (1:1 hexanes-Et_2O).

α-anomer:

δ_H: 7.27-7.21, 6.86-6.82 (m, 4H, Ar-H); 4.65 and 4.58 (AB system, 2H, *J* 11.4, benzylic H); 4.55 (d, 1H, *J* 7.4, H-2); 3.78 (s, 3H, OMe); 3.77 (ddd, 1H, *J* 2.4, 4.5, 11.0, H-6_{eq}); 3.17 (ddd, 1H, *J* 4.9, 7.4. 11.1, H-3_{ax}); 3.03 (dd, 1H, *J* 11.2, 11.2, H-6_{ax}); 2.07 (dddd, 1H, *J* 2.5, 3.9, 4.8, 12.8, H-4_{ax}); 1.86-1.66 (m, 3H, H-$5_{ax\alpha}$, H-$4_{eq\beta}$, H-$5_{ax\beta}$); 1.13 (ddd, 1H, *J* 11.1, 12.3, 12.8, H-4_{ax}); 0.83 (d, 3H, *J* 6.7, 5-methyl);

δ_C: 159.29*, 130.63^{+}, 129.37†, 113.83°, (Ar-C); 99.06 (D, C-2); 77.15 (D, C-3); 71.78 (T, C-6); 71.56 (T, benzylic C); 55.23 (Q, OMe); 37.43 (T, C-4); 29.95 (D, C-5); 16.81 (Q, 5-methyl);

β-anomer:

δ_H: 7.27-7.21, 6.86-6.82 (m, 4H, Ar-H); 5.16 (d, 1H, *J* 3.2, H-2); 4.52, 4.48 (AB system, 2H, *J* 11.5, benzylic H); 3.77 (s, 3H, OMe); 3.49 (ddd. 1H, *J* 3.2, 4.8, 11.7, H-3_{ax}); 3.48 (dd, 1H, *J* 11.0, 11.0, H-6_{ax}); 3.40 (ddd, 1H, *J* 1.8, 4.8, 11.0, H-6_{eq}); 1.86-1.66 (m, 3H, H-$5_{ax\alpha}$, H-$4_{eq\beta}$, H-$5_{ax\beta}$); 1.42 (ddd, 1H, *J* 11.8, 11.8, 11.8, H-4_{ax}); 0.81 (d, 3H, *J* 6.7, 5-methyl)

δ_C: 159.13*, 130.05^{+}, 129.34†, 113.77° (Ar-C); 90.19 (D, C-2); 74.49 (D, C-3); 70.13 (T, benzylic C); 64.96 (T, C-6); 55.23 (Q, OMe); 31.79 (T, C-4); 29.66 (D, C-5); 16.17 (Q, 5-methyl).

*, $^{+}$, †, °: Signals can be interchanged.

Addendum 1: Structure Tables for (2′*R*,3′*R*,4*R*,5*S*)-3-(2′-Ethyl-3′-hydroxy-3′-phenyl-propanoyl)-4-methyl-5-phenyl-oxazolidin-2-one (**258**)

Table 1: Crystal data and structure refinement for st06n_pub.

Identification code	st06n	
Empirical formula	C_{21} H_{23} N O_4	
Formula weight	353.40	
Temperature	173(2) K	
Wavelength	0.71073 Å	
Crystal system	Orthorhombic	
Space group	P 2_1 2_1 2_1	
Unit cell dimensions	a = 7.39550(10) Å	α= 90°.
	b = 15.7401(3) Å	β= 90°.
	c = 16.2845(2) Å	γ = 90°.
Volume	1895.61(5) $Å^3$	
Z	4	
Density (calculated)	1.238 Mg/m^3	
Absorption coefficient	0.086 mm^{-1}	
F(000)	752	
Crystal size	0.40 x 0.14 x 0.08 mm^3	
Theta range for data collection	2.50 to 27.88°.	
Index ranges	-9<=h<=9, -20<=k<=20, -21<=l<=21	
Reflections collected	4530	
Independent reflections	4530 [R(int) = 0.0000]	
Completeness to theta = 27.88°	99.8 %	
Absorption correction	None	
Max. and min. transmission	. and .	
Refinement method	Full-matrix least-squares on F^2	
Data / restraints / parameters	4530 / 0 / 304	
Goodness-of-fit on F^2	0.999	
Final R indices [I>2sigma(I)]	R1 = 0.0325, wR2 = 0.0760	
R indices (all data)	R1 = 0.0460, wR2 = 0.0805	
Absolute structure parameter	-0.6(7)	
Largest diff. peak and hole	0.108 and -0.138 $e.Å^{-3}$	

Table 2: Atomic coordinates (x 10^4) and equivalent isotropic displacement parameters ($Å^2$x 10^3) for st06n_pub. U(eq) is defined as one third of the trace of the orthogonalized U^{ij} tensor.

	x	y	z	U(eq)
O(1)	-831(1)	1858(1)	2211(1)	37(1)
C(1)	-55(2)	1430(1)	1583(1)	33(1)
N(1)	1717(1)	1714(1)	1499(1)	31(1)
C(2)	2212(2)	2279(1)	2186(1)	32(1)
C(3)	304(2)	2581(1)	2421(1)	33(1)
O(2)	-844(1)	889(1)	1207(1)	43(1)
C(4)	3235(2)	1814(1)	2853(1)	47(1)
C(5)	4(2)	2843(1)	3298(1)	34(1)
C(6)	-759(2)	2312(1)	3877(1)	53(1)
C(7)	-949(3)	2586(1)	4685(1)	60(1)
C(8)	-383(2)	3380(1)	4913(1)	47(1)
C(9)	370(2)	3914(1)	4339(1)	42(1)
C(10)	539(2)	3646(1)	3533(1)	40(1)
C(11)	3006(2)	1475(1)	909(1)	31(1)
O(3)	4556(1)	1699(1)	1022(1)	38(1)
C(12)	2386(2)	997(1)	156(1)	30(1)
C(13)	1300(2)	1616(1)	-396(1)	31(1)
O(4)	2526(1)	2266(1)	-648(1)	39(1)
C(14)	449(2)	1147(1)	-1110(1)	33(1)
C(15)	-1070(2)	648(1)	-976(1)	38(1)
C(16)	-1811(2)	172(1)	-1612(1)	46(1)
C(17)	-1056(2)	191(1)	-2384(1)	49(1)
C(18)	411(2)	710(1)	-2527(1)	61(1)
C(19)	1158(2)	1188(1)	-1895(1)	54(1)
C(20)	3985(2)	588(1)	-288(1)	35(1)
C(21)	4855(2)	-129(1)	198(1)	42(1)

Table 3: Bond lengths [Å] and angles [°] for st06n_pub.

O(1)-C(1)	1.3519(15)	C(11)-N(1)-C(2)	120.76(9)
O(1)-C(3)	1.4542(15)	N(1)-C(2)-C(4)	112.18(11)
C(1)-O(2)	1.2005(15)	N(1)-C(2)-C(3)	98.44(9)
C(1)-N(1)	1.3916(17)	C(4)-C(2)-C(3)	115.51(11)
N(1)-C(11)	1.4042(15)	N(1)-C(2)-H(2)	108.6(7)
N(1)-C(2)	1.4761(15)	C(4)-C(2)-H(2)	111.3(8)
C(2)-C(4)	1.5122(17)	C(3)-C(2)-H(2)	110.0(8)
C(2)-C(3)	1.5367(17)	O(1)-C(3)-C(5)	110.62(9)
C(2)-H(2)	0.996(15)	O(1)-C(3)-C(2)	103.30(9)
C(3)-C(5)	1.5037(17)	C(5)-C(3)-C(2)	117.15(10)
C(3)-H(3)	0.996(14)	O(1)-C(3)-H(3)	106.8(8)
C(4)-H(4A)	0.959(19)	C(5)-C(3)-H(3)	109.4(8)
C(4)-H(4B)	0.989(19)	C(2)-C(3)-H(3)	109.0(8)
C(4)-H(4C)	1.03(2)	C(2)-C(4)-H(4A)	113.9(11)
C(5)-C(10)	1.3784(19)	C(2)-C(4)-H(4B)	108.0(11)
C(5)-C(6)	1.3800(19)	H(4A)-C(4)-H(4B)	113.6(15)
C(6)-C(7)	1.391(2)	C(2)-C(4)-H(4C)	109.2(11)
C(6)-H(6)	0.994(18)	H(4A)-C(4)-H(4C)	105.0(15)
C(7)-C(8)	1.369(2)	H(4B)-C(4)-H(4C)	106.7(14)
C(7)-H(7)	0.945(19)	C(10)-C(5)-C(6)	118.87(12)
C(8)-C(9)	1.376(2)	C(10)-C(5)-C(3)	118.19(11)
C(8)-H(8)	0.982(16)	C(6)-C(5)-C(3)	122.93(12)
C(9)-C(10)	1.385(2)	C(5)-C(6)-C(7)	119.95(14)
C(9)-H(9)	0.920(17)	C(5)-C(6)-H(6)	118.7(10)
C(10)-H(10)	0.937(17)	C(7)-C(6)-H(6)	121.4(10)
C(11)-O(3)	1.2136(14)	C(8)-C(7)-C(6)	120.64(15)
C(11)-C(12)	1.5108(17)	C(8)-C(7)-H(7)	119.2(11)
C(12)-C(20)	1.5279(17)	C(6)-C(7)-H(7)	120.1(12)
C(12)-C(13)	1.5500(17)	C(7)-C(8)-C(9)	119.75(13)
C(12)-H(12)	0.956(15)	C(7)-C(8)-H(8)	121.9(10)
C(13)-O(4)	1.4267(15)	C(9)-C(8)-H(8)	118.3(10)
C(13)-C(14)	1.5149(17)	C(8)-C(9)-C(10)	119.64(14)
C(13)-H(13)	1.042(15)	C(8)-C(9)-H(9)	121.1(10)
O(4)-H(4)	0.850(18)	C(10)-C(9)-H(9)	119.3(10)
C(14)-C(19)	1.3834(19)	C(5)-C(10)-C(9)	121.13(13)
C(14)-C(15)	1.3881(18)	C(5)-C(10)-H(10)	120.1(9)
C(15)-C(16)	1.390(2)	C(9)-C(10)-H(10)	118.6(10)
C(15)-H(15)	0.988(15)	O(3)-C(11)-N(1)	117.39(11)
C(16)-C(17)	1.375(2)	O(3)-C(11)-C(12)	123.68(11)
C(16)-H(16)	0.963(17)	N(1)-C(11)-C(12)	118.86(10)
C(17)-C(18)	1.379(2)	C(11)-C(12)-C(20)	111.07(10)
C(17)-H(17)	0.980(17)	C(11)-C(12)-C(13)	108.30(10)
C(18)-C(19)	1.388(2)	C(20)-C(12)-C(13)	113.09(9)
C(18)-H(18)	1.001(19)	C(11)-C(12)-H(12)	108.3(8)
C(19)-H(19)	0.98(2)	C(20)-C(12)-H(12)	110.0(8)
C(20)-C(21)	1.5212(19)	C(13)-C(12)-H(12)	105.9(8)
C(20)-H(20A)	0.987(16)	O(4)-C(13)-C(14)	113.13(10)
C(20)-H(20B)	0.978(15)	O(4)-C(13)-C(12)	106.75(9)
C(21)-H(21A)	1.026(18)	C(14)-C(13)-C(12)	110.66(11)
C(21)-H(21B)	0.986(18)	O(4)-C(13)-H(13)	108.9(8)
C(21)-H(21C)	1.008(18)	C(14)-C(13)-H(13)	108.9(8)
		C(12)-C(13)-H(13)	108.4(7)
C(1)-O(1)-C(3)	108.80(9)	C(13)-O(4)-H(4)	102.7(11)
O(2)-C(1)-O(1)	122.26(11)	C(19)-C(14)-C(15)	118.55(12)
O(2)-C(1)-N(1)	129.38(11)	C(19)-C(14)-C(13)	121.98(11)
O(1)-C(1)-N(1)	108.33(10)	C(15)-C(14)-C(13)	119.46(11)
C(1)-N(1)-C(11)	128.41(10)	C(14)-C(15)-C(16)	120.45(13)
C(1)-N(1)-C(2)	110.60(9)	C(14)-C(15)-H(15)	120.9(9)

C(16)-C(15)-H(15)	118.6(9)	C(21)-C(20)-C(12)	113.18(10)
C(17)-C(16)-C(15)	120.59(14)	C(21)-C(20)-H(20A)	112.6(9)
C(17)-C(16)-H(16)	120.1(9)	C(12)-C(20)-H(20A)	108.4(9)
C(15)-C(16)-H(16)	119.3(9)	C(21)-C(20)-H(20B)	107.3(8)
C(16)-C(17)-C(18)	119.13(14)	C(12)-C(20)-H(20B)	109.9(8)
C(16)-C(17)-H(17)	122.2(10)	H(20A)-C(20)-H(20B)	105.1(11)
C(18)-C(17)-H(17)	118.7(10)	C(20)-C(21)-H(21A)	110.1(9)
C(17)-C(18)-C(19)	120.57(14)	C(20)-C(21)-H(21B)	107.8(11)
C(17)-C(18)-H(18)	121.2(11)	H(21A)-C(21)-H(21B)	111.8(14)
C(19)-C(18)-H(18)	118.2(11)	C(20)-C(21)-H(21C)	113.6(10)
C(14)-C(19)-C(18)	120.61(14)	H(21A)-C(21)-H(21C)	103.9(13)
C(14)-C(19)-H(19)	118.6(10)	H(21B)-C(21)-H(21C)	109.7(14)
C(18)-C(19)-H(19)	120.7(10)		

Table 4: Anisotropic displacement parameters ($Å^2 x\ 10^3$)for st06n_pub. The anisotropic displacement factor exponent takes the form: $-2\pi^2[\ h^2 a^{*2} U^{11} + ... + 2\ h\ k\ a^*\ b^*\ U^{12}\ ]$

	U^{11}	U^{22}	U^{33}	U^{23}	U^{13}	U^{12}
O(1)	32(1)	46(1)	33(1)	-5(1)	6(1)	-4(1)
C(1)	30(1)	40(1)	29(1)	0(1)	2(1)	0(1)
N(1)	28(1)	39(1)	27(1)	-3(1)	1(1)	-2(1)
C(2)	32(1)	36(1)	28(1)	-4(1)	-2(1)	0(1)
C(3)	33(1)	34(1)	32(1)	2(1)	1(1)	0(1)
O(2)	37(1)	53(1)	40(1)	-9(1)	6(1)	-12(1)
C(4)	50(1)	58(1)	33(1)	-5(1)	-9(1)	15(1)
C(5)	35(1)	34(1)	32(1)	1(1)	5(1)	1(1)
C(6)	76(1)	43(1)	39(1)	-5(1)	14(1)	-19(1)
C(7)	87(1)	55(1)	39(1)	-3(1)	21(1)	-25(1)
C(8)	54(1)	52(1)	34(1)	-7(1)	9(1)	-1(1)
C(9)	45(1)	35(1)	46(1)	-9(1)	6(1)	1(1)
C(10)	43(1)	35(1)	41(1)	2(1)	10(1)	-1(1)
C(11)	28(1)	36(1)	29(1)	4(1)	0(1)	2(1)
O(3)	27(1)	48(1)	38(1)	-3(1)	-1(1)	-2(1)
C(12)	26(1)	37(1)	28(1)	1(1)	1(1)	0(1)
C(13)	26(1)	39(1)	29(1)	1(1)	1(1)	0(1)
O(4)	29(1)	41(1)	45(1)	9(1)	-5(1)	-3(1)
C(14)	26(1)	41(1)	32(1)	2(1)	-3(1)	4(1)
C(15)	38(1)	43(1)	34(1)	6(1)	-4(1)	-4(1)
C(16)	47(1)	45(1)	47(1)	5(1)	-11(1)	-8(1)
C(17)	45(1)	58(1)	45(1)	-12(1)	-16(1)	8(1)
C(18)	39(1)	107(1)	35(1)	-14(1)	0(1)	-3(1)
C(19)	31(1)	95(1)	35(1)	-6(1)	1(1)	-14(1)
C(20)	34(1)	45(1)	28(1)	-2(1)	0(1)	5(1)
C(21)	39(1)	45(1)	44(1)	3(1)	1(1)	9(1)

Table 5: Hydrogen coordinates (x 10^4) and isotropic displacement parameters ($Å^2$x 10^3) for st06n_pub.

	x	y	z	U(eq)
H(2)	2930(20)	2764(9)	1966(8)	38
H(3)	-50(20)	3055(9)	2049(8)	39
H(4A)	4320(20)	1545(12)	2666(12)	70
H(4B)	3430(30)	2213(12)	3314(11)	70
H(4C)	2450(30)	1326(12)	3076(11)	70
H(6)	-1170(20)	1738(12)	3703(10)	64
H(7)	-1480(20)	2226(12)	5082(11)	72
H(8)	-470(20)	3579(10)	5484(10)	56
H(9)	720(20)	4457(11)	4476(9)	50
H(10)	1110(20)	4004(10)	3155(10)	47
H(12)	1547(19)	569(9)	325(8)	36
H(13)	280(20)	1890(9)	-42(8)	37
H(4)	1820(20)	2662(11)	-801(10)	58
H(15)	-1650(20)	623(10)	-430(9)	46
H(16)	-2860(20)	-176(11)	-1506(9)	56
H(17)	-1540(20)	-146(11)	-2839(10)	59
H(18)	1000(30)	736(12)	-3080(11)	73
H(19)	2240(30)	1536(11)	-1989(10)	64
H(20A)	4850(20)	1038(10)	-435(8)	43
H(20B)	3585(19)	349(9)	-812(9)	43
H(21A)	5870(20)	-403(11)	-139(10)	64
H(21B)	3900(20)	-541(12)	339(11)	64
H(21C)	5480(20)	68(11)	714(10)	64

Table 6: Torsion angles [°] for st06n_pub.

C(3)-O(1)-C(1)-O(2)	-167.95(12)
C(3)-O(1)-C(1)-N(1)	13.73(12)
O(2)-C(1)-N(1)-C(11)	4.7(2)
O(1)-C(1)-N(1)-C(11)	-177.19(11)
O(2)-C(1)-N(1)-C(2)	-169.86(12)
O(1)-C(1)-N(1)-C(2)	8.29(13)
C(1)-N(1)-C(2)-C(4)	97.43(12)
C(11)-N(1)-C(2)-C(4)	-77.57(14)
C(1)-N(1)-C(2)-C(3)	-24.62(12)
C(11)-N(1)-C(2)-C(3)	160.38(10)
C(1)-O(1)-C(3)-C(5)	-155.22(10)
C(1)-O(1)-C(3)-C(2)	-29.06(12)
N(1)-C(2)-C(3)-O(1)	30.88(11)
C(4)-C(2)-C(3)-O(1)	-88.70(12)
N(1)-C(2)-C(3)-C(5)	152.76(11)
C(4)-C(2)-C(3)-C(5)	33.18(16)
O(1)-C(3)-C(5)-C(10)	-161.34(11)
C(2)-C(3)-C(5)-C(10)	80.67(15)
O(1)-C(3)-C(5)-C(6)	19.54(17)
C(2)-C(3)-C(5)-C(6)	-98.45(16)
C(10)-C(5)-C(6)-C(7)	-1.0(2)
C(3)-C(5)-C(6)-C(7)	178.10(16)
C(5)-C(6)-C(7)-C(8)	-0.1(3)
C(6)-C(7)-C(8)-C(9)	0.5(3)
C(7)-C(8)-C(9)-C(10)	0.3(2)
C(6)-C(5)-C(10)-C(9)	1.8(2)
C(3)-C(5)-C(10)-C(9)	-177.33(13)
C(8)-C(9)-C(10)-C(5)	-1.5(2)
C(1)-N(1)-C(11)-O(3)	-168.72(12)
C(2)-N(1)-C(11)-O(3)	5.30(17)
C(1)-N(1)-C(11)-C(12)	14.23(18)
C(2)-N(1)-C(11)-C(12)	-171.74(10)
O(3)-C(11)-C(12)-C(20)	18.55(17)
N(1)-C(11)-C(12)-C(20)	-164.60(11)
O(3)-C(11)-C(12)-C(13)	-106.20(13)
N(1)-C(11)-C(12)-C(13)	70.65(13)
C(11)-C(12)-C(13)-O(4)	63.42(12)
C(20)-C(12)-C(13)-O(4)	-60.13(13)
C(11)-C(12)-C(13)-C(14)	-173.09(9)
C(20)-C(12)-C(13)-C(14)	63.36(13)
O(4)-C(13)-C(14)-C(19)	16.51(18)
C(12)-C(13)-C(14)-C(19)	-103.22(15)
O(4)-C(13)-C(14)-C(15)	-164.57(11)
C(12)-C(13)-C(14)-C(15)	75.70(14)
C(19)-C(14)-C(15)-C(16)	2.7(2)
C(13)-C(14)-C(15)-C(16)	-176.30(12)
C(14)-C(15)-C(16)-C(17)	-0.2(2)
C(15)-C(16)-C(17)-C(18)	-2.3(2)
C(16)-C(17)-C(18)-C(19)	2.2(2)
C(15)-C(14)-C(19)-C(18)	-2.8(2)
C(13)-C(14)-C(19)-C(18)	176.17(15)
C(17)-C(18)-C(19)-C(14)	0.4(3)
C(11)-C(12)-C(20)-C(21)	67.87(14)
C(13)-C(12)-C(20)-C(21)	-170.12(11)

Addendum 2: Structure Tables for (2′*S*,3′*S*,4*R*,5*S*)-3-(2′-Butyl-3′-hydroxy-3′-phenyl-propanoyl)-4-methyl-5-phenyl-oxazolidin-2-one (**257**)

Table 1: Crystal data and structure refinement for st05n_pub.

Identification code	st05n	
Empirical formula	C_{23} H_{27} N O_4	
Formula weight	381.46	
Temperature	173(2) K	
Wavelength	0.71073 Å	
Crystal system	Orthorhombic	
Space group	P 2_1 2_1 2_1	
Unit cell dimensions	a = 8.2307(9) Å	α= 90°.
	b = 9.1743(10) Å	β= 90°.
	c = 26.762(3) Å	γ = 90°.
Volume	2020.8(4) $Å^3$	
Z	4	
Density (calculated)	1.254 Mg/m^3	
Absorption coefficient	0.085 mm^{-1}	
F(000)	816	
Crystal size	0.35 x 0.28 x 0.14 mm^3	
Theta range for data collection	2.35 to 28.38°.	
Index ranges	-10<=h<=10, -11<=k<=12, -27<=l<=35	
Reflections collected	9945	
Independent reflections	5045 [R(int) = 0.0275]	
Completeness to theta = 28.38°	99.8 %	
Absorption correction	Semi-empirical from equivalents	
Max. and min. transmission	0.988 and 0.856	
Refinement method	Full-matrix least-squares on F^2	
Data / restraints / parameters	5045 / 0 / 335	
Goodness-of-fit on F^2	1.006	
Final R indices [I>2sigma(I)]	R1 = 0.0403, wR2 = 0.0808	
R indices (all data)	R1 = 0.0611, wR2 = 0.0878	
Absolute structure parameter	0.3(9)	
Extinction coefficient	0	
Largest diff. peak and hole	0.200 and -0.150 $e.Å^{-3}$	

Table 2: Atomic coordinates (x 10^4) and equivalent isotropic displacement parameters ($Å^2$x 10^3) for st05n_pub. U(eq) is defined as one third of the trace of the orthogonalized U^{ij} tensor.

	x	y	z	U(eq)
O(1)	5341(1)	9685(1)	7572(1)	36(1)
C(1)	6445(2)	9238(2)	7911(1)	31(1)
N(1)	7226(2)	8009(1)	7726(1)	29(1)
C(2)	6755(2)	7737(1)	7203(1)	28(1)
C(3)	5134(2)	8575(2)	7185(1)	32(1)
O(2)	6639(2)	9864(1)	8301(1)	40(1)
C(4)	8066(2)	8279(2)	6855(1)	33(1)
C(5)	4677(2)	9266(2)	6700(1)	33(1)
C(6)	5154(2)	10679(2)	6568(1)	37(1)
C(7)	4739(3)	11241(2)	6106(1)	44(1)
C(8)	3866(2)	10430(2)	5769(1)	49(1)
C(9)	3379(3)	9031(2)	5898(1)	51(1)
C(10)	3767(2)	8465(2)	6362(1)	43(1)
C(11)	8427(2)	7173(2)	7961(1)	29(1)
O(3)	8812(1)	6025(1)	7762(1)	36(1)
C(12)	9246(2)	7763(2)	8422(1)	28(1)
C(13)	10299(2)	9079(2)	8246(1)	27(1)
O(4)	11432(2)	8552(1)	7887(1)	37(1)
C(14)	11109(2)	9854(2)	8678(1)	29(1)
C(15)	10171(2)	10566(2)	9036(1)	35(1)
C(16)	10900(3)	11279(2)	9433(1)	45(1)
C(17)	12577(3)	11308(2)	9471(1)	49(1)
C(18)	13512(3)	10620(2)	9118(1)	45(1)
C(19)	12784(2)	9888(2)	8723(1)	35(1)
C(20)	10217(2)	6558(2)	8685(1)	31(1)
C(21)	10551(2)	6797(2)	9239(1)	36(1)
C(22)	11214(3)	5425(2)	9488(1)	40(1)
C(23)	11800(4)	5669(3)	10014(1)	58(1)

Table 3: Bond lengths [Å] and angles [°] for st05n_pub.

O(1)-C(1)	1.347(2)	C(1)-O(1)-C(3)	110.12(11)
O(1)-C(3)	1.4625(19)	O(2)-C(1)-O(1)	121.94(13)
C(1)-O(2)	1.201(2)	O(2)-C(1)-N(1)	129.43(16)
C(1)-N(1)	1.3892(18)	O(1)-C(1)-N(1)	108.63(14)
N(1)-C(11)	1.400(2)	C(1)-N(1)-C(11)	127.75(14)
N(1)-C(2)	1.475(2)	C(1)-N(1)-C(2)	110.73(13)
C(2)-C(4)	1.509(2)	C(11)-N(1)-C(2)	121.24(12)
C(2)-C(3)	1.541(2)	N(1)-C(2)-C(4)	109.98(14)
C(2)-H(2)	0.968(17)	N(1)-C(2)-C(3)	99.93(12)
C(3)-C(5)	1.491(2)	C(4)-C(2)-C(3)	115.83(13)
C(3)-H(3)	0.979(18)	N(1)-C(2)-H(2)	108.6(11)
C(4)-H(4A)	0.95(2)	C(4)-C(2)-H(2)	111.4(11)
C(4)-H(4B)	0.97(2)	C(3)-C(2)-H(2)	110.3(10)
C(4)-H(4C)	1.03(2)	O(1)-C(3)-C(5)	110.49(11)
C(5)-C(10)	1.386(3)	O(1)-C(3)-C(2)	102.96(12)
C(5)-C(6)	1.400(2)	C(5)-C(3)-C(2)	117.20(14)
C(6)-C(7)	1.382(3)	O(1)-C(3)-H(3)	104.9(11)
C(6)-H(6)	0.97(2)	C(5)-C(3)-H(3)	109.8(11)
C(7)-C(8)	1.372(3)	C(2)-C(3)-H(3)	110.6(10)
C(7)-H(7)	0.98(2)	C(2)-C(4)-H(4A)	110.5(12)
C(8)-C(9)	1.389(3)	C(2)-C(4)-H(4B)	110.3(12)
C(8)-H(8)	1.04(2)	H(4A)-C(4)-H(4B)	107.0(17)
C(9)-C(10)	1.382(3)	C(2)-C(4)-H(4C)	111.6(11)
C(9)-H(9)	0.98(2)	H(4A)-C(4)-H(4C)	108.1(16)
C(10)-H(10)	0.99(2)	H(4B)-C(4)-H(4C)	109.3(16)
C(11)-O(3)	1.2210(17)	C(10)-C(5)-C(6)	118.51(17)
C(11)-C(12)	1.507(2)	C(10)-C(5)-C(3)	118.62(14)
C(12)-C(20)	1.535(2)	C(6)-C(5)-C(3)	122.86(16)
C(12)-C(13)	1.559(2)	C(7)-C(6)-C(5)	120.16(18)
C(12)-H(12)	1.005(18)	C(7)-C(6)-H(6)	123.3(11)
C(13)-O(4)	1.4224(19)	C(5)-C(6)-H(6)	116.6(11)
C(13)-C(14)	1.513(2)	C(8)-C(7)-C(6)	120.98(17)
C(13)-H(13)	0.997(17)	C(8)-C(7)-H(7)	121.0(12)
O(4)-H(4)	0.87(2)	C(6)-C(7)-H(7)	118.0(13)
C(14)-C(19)	1.384(2)	C(7)-C(8)-C(9)	119.2(2)
C(14)-C(15)	1.394(2)	C(7)-C(8)-H(8)	122.0(12)
C(15)-C(16)	1.384(3)	C(9)-C(8)-H(8)	118.8(12)
C(15)-H(15)	0.97(2)	C(10)-C(9)-C(8)	120.3(2)
C(16)-C(17)	1.384(3)	C(10)-C(9)-H(9)	125.0(13)
C(16)-H(16)	0.99(2)	C(8)-C(9)-H(9)	114.7(13)
C(17)-C(18)	1.373(3)	C(9)-C(10)-C(5)	120.78(17)
C(17)-H(17)	0.94(2)	C(9)-C(10)-H(10)	119.0(12)
C(18)-C(19)	1.387(3)	C(5)-C(10)-H(10)	120.2(12)
C(18)-H(18)	0.94(2)	O(3)-C(11)-N(1)	117.44(15)
C(19)-H(19)	0.94(2)	O(3)-C(11)-C(12)	123.34(14)
C(20)-C(21)	1.524(3)	N(1)-C(11)-C(12)	119.11(12)
C(20)-H(20A)	1.004(19)	C(11)-C(12)-C(20)	110.50(12)
C(20)-H(20B)	1.002(18)	C(11)-C(12)-C(13)	106.18(13)
C(21)-C(22)	1.525(2)	C(20)-C(12)-C(13)	114.01(13)
C(21)-H(21A)	0.94(2)	C(11)-C(12)-H(12)	108.1(10)
C(21)-H(21B)	1.03(2)	C(20)-C(12)-H(12)	111.8(10)
C(22)-C(23)	1.505(3)	C(13)-C(12)-H(12)	106.0(9)
C(22)-H(22A)	0.98(2)	O(4)-C(13)-C(14)	112.72(12)
C(22)-H(22B)	0.99(2)	O(4)-C(13)-C(12)	107.78(11)
C(23)-H(23A)	0.94(3)	C(14)-C(13)-C(12)	112.21(13)
C(23)-H(23B)	1.01(3)	O(4)-C(13)-H(13)	108.3(10)
C(23)-H(23C)	0.93(3)	C(14)-C(13)-H(13)	107.7(10)
		C(12)-C(13)-H(13)	107.9(10)

C(13)-O(4)-H(4)	107.5(14)
C(19)-C(14)-C(15)	118.74(16)
C(19)-C(14)-C(13)	121.11(15)
C(15)-C(14)-C(13)	120.15(14)
C(16)-C(15)-C(14)	120.60(17)
C(16)-C(15)-H(15)	121.6(11)
C(14)-C(15)-H(15)	117.8(11)
C(17)-C(16)-C(15)	119.90(19)
C(17)-C(16)-H(16)	120.1(13)
C(15)-C(16)-H(16)	120.0(13)
C(18)-C(17)-C(16)	119.9(2)
C(18)-C(17)-H(17)	119.0(14)
C(16)-C(17)-H(17)	121.0(14)
C(17)-C(18)-C(19)	120.30(19)
C(17)-C(18)-H(18)	122.0(13)
C(19)-C(18)-H(18)	117.7(13)
C(14)-C(19)-C(18)	120.51(18)
C(14)-C(19)-H(19)	119.1(12)
C(18)-C(19)-H(19)	120.3(12)
C(21)-C(20)-C(12)	115.90(13)
C(21)-C(20)-H(20A)	109.4(11)
C(12)-C(20)-H(20A)	106.4(10)
C(21)-C(20)-H(20B)	109.2(10)
C(12)-C(20)-H(20B)	110.0(10)
H(20A)-C(20)-H(20B)	105.4(15)
C(20)-C(21)-C(22)	111.79(14)
C(20)-C(21)-H(21A)	111.3(12)
C(22)-C(21)-H(21A)	109.0(12)
C(20)-C(21)-H(21B)	110.4(11)
C(22)-C(21)-H(21B)	108.7(10)
H(21A)-C(21)-H(21B)	105.5(15)
C(23)-C(22)-C(21)	113.63(16)
C(23)-C(22)-H(22A)	108.8(12)
C(21)-C(22)-H(22A)	110.6(12)
C(23)-C(22)-H(22B)	111.3(12)
C(21)-C(22)-H(22B)	104.9(11)
H(22A)-C(22)-H(22B)	107.5(16)
C(22)-C(23)-H(23A)	110.7(17)
C(22)-C(23)-H(23B)	115.6(15)
H(23A)-C(23)-H(23B)	105(2)
C(22)-C(23)-H(23C)	111.1(17)
H(23A)-C(23)-H(23C)	105(2)
H(23B)-C(23)-H(23C)	108(2)

Table 4: Anisotropic displacement parameters ($Å^2 x\ 10^3$)for st05n_pub. The anisotropic displacement factor exponent takes the form: $-2\pi^2[\ h^2 a^{*2} U^{11} + ... + 2\ h\ k\ a^*\ b^*\ U^{12}\ ]$

	U^{11}	U^{22}	U^{33}	U^{23}	U^{13}	U^{12}
O(1)	35(1)	32(1)	41(1)	-6(1)	2(1)	9(1)
C(1)	30(1)	26(1)	37(1)	-1(1)	8(1)	4(1)
N(1)	31(1)	21(1)	34(1)	-3(1)	5(1)	1(1)
C(2)	33(1)	18(1)	34(1)	-1(1)	2(1)	-1(1)
C(3)	31(1)	25(1)	40(1)	-4(1)	6(1)	-2(1)
O(2)	42(1)	34(1)	44(1)	-11(1)	4(1)	8(1)
C(4)	34(1)	25(1)	41(1)	1(1)	9(1)	2(1)
C(5)	29(1)	27(1)	42(1)	0(1)	5(1)	5(1)
C(6)	35(1)	29(1)	46(1)	-3(1)	5(1)	3(1)
C(7)	50(1)	30(1)	51(1)	6(1)	4(1)	7(1)
C(8)	55(1)	42(1)	49(1)	6(1)	-3(1)	13(1)
C(9)	54(1)	40(1)	58(1)	-2(1)	-20(1)	4(1)
C(10)	46(1)	29(1)	53(1)	-1(1)	-9(1)	1(1)
C(11)	30(1)	20(1)	36(1)	2(1)	9(1)	0(1)
O(3)	45(1)	21(1)	43(1)	-5(1)	1(1)	6(1)
C(12)	30(1)	19(1)	35(1)	-1(1)	6(1)	1(1)
C(13)	29(1)	20(1)	33(1)	2(1)	6(1)	1(1)
O(4)	43(1)	29(1)	38(1)	4(1)	15(1)	2(1)
C(14)	33(1)	18(1)	35(1)	5(1)	5(1)	-2(1)
C(15)	39(1)	23(1)	43(1)	-2(1)	5(1)	-1(1)
C(16)	61(1)	33(1)	43(1)	-6(1)	8(1)	-4(1)
C(17)	60(1)	44(1)	42(1)	0(1)	-8(1)	-18(1)
C(18)	39(1)	45(1)	51(1)	10(1)	-7(1)	-9(1)
C(19)	35(1)	29(1)	41(1)	6(1)	4(1)	-2(1)
C(20)	36(1)	20(1)	36(1)	3(1)	5(1)	3(1)
C(21)	47(1)	23(1)	38(1)	3(1)	2(1)	2(1)
C(22)	45(1)	29(1)	46(1)	6(1)	-2(1)	0(1)
C(23)	72(2)	56(1)	45(1)	10(1)	-11(1)	-1(1)

Table 5: Hydrogen coordinates (x 10^4) and isotropic displacement parameters ($Å^2$x 10^3) for st05n_pub.

	x	y	z	U(eq)
H(2)	6570(20)	6703(18)	7161(7)	34
H(3)	4240(20)	7961(19)	7304(7)	38
H(4A)	8250(20)	9290(20)	6906(7)	50
H(4B)	9090(20)	7780(20)	6923(7)	50
H(4C)	7760(20)	8130(20)	6486(8)	50
H(6)	5770(20)	11220(20)	6816(7)	44
H(7)	5090(20)	12230(20)	6026(8)	52
H(8)	3570(30)	10820(20)	5416(8)	58
H(9)	2740(30)	8530(20)	5642(9)	64(6)
H(10)	3390(30)	7470(20)	6450(8)	51
H(12)	8380(20)	8183(18)	8646(7)	33
H(13)	9570(20)	9790(19)	8077(6)	33
H(4)	11590(30)	9250(20)	7669(8)	55
H(15)	9010(20)	10560(20)	8993(7)	42
H(16)	10230(30)	11760(20)	9688(8)	54
H(17)	13090(30)	11770(20)	9743(9)	59
H(18)	14660(30)	10600(20)	9137(8)	54
H(19)	13430(20)	9450(20)	8472(7)	42
H(20A)	9580(20)	5630(20)	8640(7)	37
H(20B)	11270(20)	6392(19)	8507(7)	37
H(21A)	11290(20)	7570(20)	9289(7)	43
H(21B)	9500(20)	7110(20)	9421(7)	43
H(22A)	12100(20)	5010(20)	9291(8)	48
H(22B)	10300(20)	4720(20)	9479(7)	48
H(23A)	10990(30)	6110(30)	10208(10)	86
H(23B)	12120(30)	4760(30)	10204(10)	86
H(23C)	12670(30)	6320(30)	10021(10)	86

Table 6: Torsion angles [°] for st05n_pub.

C(3)-O(1)-C(1)-O(2)	-168.68(15)
C(3)-O(1)-C(1)-N(1)	11.15(17)
O(2)-C(1)-N(1)-C(11)	1.5(3)
O(1)-C(1)-N(1)-C(11)	-178.29(13)
O(2)-C(1)-N(1)-C(2)	-172.35(16)
O(1)-C(1)-N(1)-C(2)	7.84(17)
C(1)-N(1)-C(2)-C(4)	100.62(14)
C(11)-N(1)-C(2)-C(4)	-73.72(15)
C(1)-N(1)-C(2)-C(3)	-21.68(15)
C(11)-N(1)-C(2)-C(3)	163.98(13)
C(1)-O(1)-C(3)-C(5)	-150.26(13)
C(1)-O(1)-C(3)-C(2)	-24.34(16)
N(1)-C(2)-C(3)-O(1)	26.33(14)
C(4)-C(2)-C(3)-O(1)	-91.71(17)
N(1)-C(2)-C(3)-C(5)	147.81(13)
C(4)-C(2)-C(3)-C(5)	29.8(2)
O(1)-C(3)-C(5)-C(10)	-152.17(15)
C(2)-C(3)-C(5)-C(10)	90.36(18)
O(1)-C(3)-C(5)-C(6)	29.1(2)
C(2)-C(3)-C(5)-C(6)	-88.42(18)
C(10)-C(5)-C(6)-C(7)	-1.0(2)
C(3)-C(5)-C(6)-C(7)	177.80(16)
C(5)-C(6)-C(7)-C(8)	-0.4(3)
C(6)-C(7)-C(8)-C(9)	0.8(3)
C(7)-C(8)-C(9)-C(10)	0.2(3)
C(8)-C(9)-C(10)-C(5)	-1.5(3)
C(6)-C(5)-C(10)-C(9)	1.9(3)
C(3)-C(5)-C(10)-C(9)	-176.92(17)
C(1)-N(1)-C(11)-O(3)	170.86(14)
C(2)-N(1)-C(11)-O(3)	-15.8(2)
C(1)-N(1)-C(11)-C(12)	-12.8(2)
C(2)-N(1)-C(11)-C(12)	160.50(13)
O(3)-C(11)-C(12)-C(20)	-16.8(2)
N(1)-C(11)-C(12)-C(20)	167.06(13)
O(3)-C(11)-C(12)-C(13)	107.29(16)
N(1)-C(11)-C(12)-C(13)	-68.82(16)
C(11)-C(12)-C(13)-O(4)	-59.36(16)
C(20)-C(12)-C(13)-O(4)	62.55(18)
C(11)-C(12)-C(13)-C(14)	175.96(12)
C(20)-C(12)-C(13)-C(14)	-62.14(17)
O(4)-C(13)-C(14)-C(19)	-5.8(2)
C(12)-C(13)-C(14)-C(19)	116.10(16)
O(4)-C(13)-C(14)-C(15)	173.48(13)
C(12)-C(13)-C(14)-C(15)	-64.62(18)
C(19)-C(14)-C(15)-C(16)	-0.7(2)
C(13)-C(14)-C(15)-C(16)	-179.98(15)
C(14)-C(15)-C(16)-C(17)	1.0(3)
C(15)-C(16)-C(17)-C(18)	-0.5(3)
C(16)-C(17)-C(18)-C(19)	-0.4(3)
C(15)-C(14)-C(19)-C(18)	-0.2(2)
C(13)-C(14)-C(19)-C(18)	179.11(15)
C(17)-C(18)-C(19)-C(14)	0.7(3)
C(11)-C(12)-C(20)-C(21)	-157.14(14)
C(13)-C(12)-C(20)-C(21)	83.37(19)
C(12)-C(20)-C(21)-C(22)	168.61(15)
C(20)-C(21)-C(22)-C(23)	171.19(19)